Instituto Nacional de Pesquisas da Amazônia – INPA
Programa de Pós-Graduação em Ecologia

Desvendando o desconhecido: diversidade, distribuição e diversificação de anuros no interflúvio Purus-Madeira

MIQUÉIAS FERRÃO DA SILVA JUNIOR

Manaus, Amazonas
Outubro 2018

MIQUÉIAS FERRÃO DA SILVA JUNIOR

DESVENDANDO O DESCONHECIDO: DIVERSIDADE, DISTRIBUIÇÃO E DIVERSIFICAÇÃO DE ANUROS NO INTERFLÚVIO PURUS-MADEIRA

Orientadora: Dra. Albertina Pimentel Lima
Coorientador: Dr. Igor Luis Kaefer

Tese apresentada ao Instituto Nacional de Pesquisas da Amazônia como parte dos requisitos para obtenção do título de Doutor em Biologia (Ecologia).

Manaus, Amazonas
Outubro 2018

PG·ECO·INPA
PÓS-GRADUAÇÃO EM ECOLOGIA

MINISTÉRIO DA
CIÊNCIA, TECNOLOGIA,
INOVAÇÕES E COMUNICAÇÕES

INPA
INSTITUTO NACIONAL DE PESQUISAS DA AMAZÔNIA

PROGRAMA DE PÓS-GRADUAÇÃO EM ECOLOGIA

ATA DA DEFESA PÚBLICA DA TESE DE DOUTORADO DO PROGRAMA DE PÓS-GRADUAÇÃO EM ECOLOGIA DO INSTITUTO NACIONAL DE PESQUISAS DA AMAZÔNIA

Aos 08 dias do mês de novembro do ano de 2018, às 14:00 horas, no Auditório dos PPG's ATU/CFT/ECO, Campus III, INPA/V8. Reuniu-se a Comissão Examinadora de Defesa Pública, composta pelos seguintes membros: o(a) Prof(a). Dr(a). **Camila Cherem Ribas**, do Instituto Nacional de Pesquisas da Amazônia - INPA, o(a) Prof(a). Dr(a). **Fernanda de Pinho Werneck,** do Instituto Nacional de Pesquisas da Amazônia - INPA, o(a) Prof(a). Dr(a). **Diego José Santana Silva**, da Universidade Federal de Mato Grosso do Sul - UFMS, o(a) Prof(a). Dr(a). **Marcelo Gordo**, da Universidade Federal do Amazonas - UFAM, o(a) Prof(a). Dr(a). **Tomas Hrbek,** do Instituto Nacional de Pesquisas da Amazônia - INPA, tendo como suplentes o(a) Prof(a). Dr(a). Rafael do Nascimento Leite, do Instituto Nacional de Pesquisas da Amazônia - INPA, e o(a) Prof(a). Dr(a). Renato Cintra, do Instituto Nacional de Pesquisas da Amazônia - INPA, sob a presidência do(a) primeiro(a), a fim de proceder a argüição pública do trabalho de **TESE DE DOUTORADO** de **MIQUÉIAS FERRÃO DA SILVA JUNIOR**, intitulado **"DESVENDANDO O DESCONHECIDO: DIVERSIDADE, DISTRIBUIÇÃO E DIVERSIFICAÇÃO DE ANUROS NO INTERFLÚVIO PURUS-MADEIRA"**, orientado pelo(a) Prof(a). Dr(a). Albertina Pimentel Lima, do Instituto Nacional de Pesquisas da Amazônia – INPA e coorientado pelo(a) Prof(a). Dr(a). Igor Luis Kaefer, da Universidade Federal do Amazonas – UFAM.

Após a exposição, o(a) discente foi argüido(a) oralmente pelos membros da Comissão Examinadora, tendo recebido o conceito final:

☒ APROVADO(A) ☐ REPROVADO(A)
☒ POR UNANIMIDADE ☐ POR MAIORIA

Nada mais havendo, foi lavrada a presente ata, que, após lida e aprovada, foi assinada pelos membros da Comissão Examinadora.

Prof(a). Dr(a). Camila Cherem Ribas ____________________
Prof(a).Dr(a). Fernanda de Pinho Werneck ____________________
Prof(a). Dr(a). Diego José Santana Silva ____________________
Prof(a). Dr(a). Marcelo Gordo ____________________
Prof(a). Dr(a). Tomas Hrbek ____________________
Prof(a). Dr(a).Rafael do Nascimento Leite ____________________
Prof(a). Dr(a). Renato Cintra ____________________

____
Coordenação PPG-ECO/INPA

INSTITUTO NACIONAL DE PESQUISAS DA AMAZÔNIA - INPA
PROGRAMA DE PÓS-GRADUAÇÃO EM ECOLOGIA – PPG ECO
Av. André Araújo, nº 2936, Bairro – Petrópolis, Manaus-AM, CEP: 69.067-375
Site: http://pg.inpa.gov.br e-mail: pgecologia@gmail.com

F368d Ferrão, Miquéias
Desvendando o desconhecido: diversidade, distribuição e diversificação de anuros no interflúvio Purus-Madeira / Miquéias Ferrão da Silva Junior. – 2018.
199p.

Tese (Doutorado) - INPA, Manaus, 2018.
Orientador: Albertina Pimentel Lima
Coorientador: Igor Luis Kaefer
Área de concentração: Ecologia

1. Anuros. 2. Taxonomia. 3. Ecologia . 4. Gradientes Ambientais

CDD 597.6

Sinopse

Nesta tese investigamos a diversidade e taxonomia de espécies de anuros no interflúvio entre os rios Purus e Madeira, bem como os fatores responsáveis pela distribuição e diversificação de espécies ao longo da paisagem. Foram utilizados dados morfológicos, bioacústicos e moleculares para investigar a diversidade escondida e descrever novas espécies do gênero *Scinax*. Dados de distribuição e variáveis ambientais foram utilizados para descrever associações espécie-habitat em uma espécie de *Scinax*. Por fim, foram utilizados dados genômicos de ultima geração e análises de genômica da paisagem para entender o papel de gradientes ecológicos no fluxo gênico de *Phyzelaphryne miriamae*.

Palavras-chave: 1. biodiversidade. 2. taxonomia integrativa. 3. ecologia. 4. heterogeneidade ambiental. 5. polimorfismo de nucleotídeo único. 6. genômica da paisagem. 7. fluxo gênico. 8. Amazônia.

Dedico esta tese à *Francisca Cândida de Assis Ferrão*, minha mãe e melhor amiga, por todo o amor e por ter lutado bravamente para me educar da melhor forma possível.

AGRADECIMENTOS

Esta tese de doutorado foi financiada pelo Conselho Nacional de Desenvolvimento Científico e Tecnológico (CNPq) através do Programa Ciência sem Fronteiras (processo 401327/2012–4) e pela Fundação de Amparo à Pesquisa do Estado do Amazonas (FAPEAM/CNPQ PRONEX processo 653/2009). O livre acesso aos artigos desta tese foi financiado pelo Ministério de Cultura da República Tcheca (DKRVO 2016/15, 2017/15, 2018/15).

Durante a coleta de dados e desenvolvimento desta tese, recebi bolsa de apoio técnico do CNPq (processo 573721/2008-4), bolsa de doutorada pela FAPEAM (resolução n° 007/2014 - POSGRAD 2014) e pela Coordenação de Aperfeiçoamento de Pessoal de Nível Superior (CAPES) via Programa de Excelência Acadêmica (PROEX edital 0487). Meu estágio doutoral internacional na Macquarie University (Sydney, Austrália) foi financiado pela CAPES via Programa de Doutorado Sanduíche no Exterior (edital n° 19/2016, processo 88881.131988/2016-01).

Aos meus queridos orientadores e amigos, **Albertina P. Lima** e **Igor L. Kaefer**, por terem me orientado e por estarem totalmente dispostos a transmitir seus conhecimentos. Obrigado também por terem sempre acredito em mim e por nunca terem desistido da incumbência de me formar um cientista, mesmo eu não tendo sido um orientando fácil durante o início de minha caminhada rumo ao título de doutor. <3

Obrigado especial a **Albertina**, por ser minha maior inspiração científica e por ter aberto meus olhos para o encantador mundo dos sapos quando eu só tinha olhos para o mundo dos répteis. Hoje sou totalmente apaixonado pelo meu grupo de estudo. <3

Gratidão a Jiří Moravec por ter acreditado e apoiado meu trabalho com as *Scinax*, e por ter se tornado um grande companheiro de trabalho ao longo dos últimos anos. Obrigado pelos ensinamentos taxonômicos e pelos ótimos momentos vividos em campo. <3

Ao supervisor de doutorado sanduíche e amigo Adam Stow por ter comprado meu projeto e por ter me recebido tão bem em Sydney. Além de todo o conhecimento ensinado, Adam me apresentou as paisagens mais lindas que já tive oportunidade de conhecer até aqui. <3

Obrigado Rato (Rafael de Fraga) pelos grandes momentos vividos durante as expedições de campo ao longo da BR-319. Foram muitas histórias e momentos memoráveis ao seu lado. Aproveito para agradecer nossos fiéis escudeiros de campo (Joãozinho, Pinduca, Neneco, Rubico, Phill, Jailson, Edy) por terem tornado tudo mais fácil e divertido, mesmo diante as adversidades de se coletar em locais pouco explorados e de acesso dificultado. <3

Aos amigos de laboratório que fiz ao longo dessa jornada em Manaus (Pedro I. Simões, Rafael de Fraga, Diana Rojas-Ahumada, Andresa Melo, Eveline Salvático, Rafael Jorge, Anthony Ferreira, Randolpho Dias Terceiro, Jussara Dayrell, André L. Barros, Romildo Souza, Douglas Lacerda, Kamila Xavier) e que sempre estiveram dispostos a me ajudar no que fosse possível. Obrigado também as amigas de laboratório na Macquarie University (Sonu Yadav e Sarah Reid-Anderson). Vocês me ajudaram e muito a manter a sanidade mental nesse árduo caminho da pós-graduação. Eternamente grato! <3

Obrigado a meu querido amigo, Hassam Al-Kshei, por ter estado sempre ao meu lado durante minha jornada em Sydney. Obrigado por ter me apresentado a cultura árabe e por nunca ter me deixado sentir solidão em uma terra tão distante. <3

Obrigado aos meus amigos de república, Marina Carmona, Mateus Ferreira, Derek Campos, e Malu por terem se tornado minha família manauara. Foram inúmeras alegrias vividas juntas. Vocês viverão para sempre em meu coração. Obrigado por terem me apresentado os incríveis: Dinho Heinrichs, Allana Negreiros e Susana Braz-Mota. Obrigado por tantos momentos "alucicrazy". <3

Obrigado aos amigos da casa de sementes do INPA, Geangelo P. Calvi, Neyde Martini, Aline Smychniuk, Bia Cipriani, Caio Batista e Igor Fernandes, por terem sido meu ombro amigo diário. Obrigado pelas incontáveis risadas, alegrias e por serem tão companheiros. Incontáveis foram os milhares de cafés que tomamos juntos. Os dias ao lado de vocês foram sempre mais leves. Se mantive o sorriso durante maior parte do tempo no rosto, devo a vocês. <3

Aos amigos da vida que Manaus me presenteou: Geangelo (Geysyany), Fabio Oliveira (Fabety), Felipe Pinagé (Pimba), Eduardo Sales (Duda), Fabrício Miyachi (Migota) e Marcos Baptista (Marcola). Vocês são mais que especiais e sempre estiveram ao meu lado, mesmo não estando sempre fisicamente presentes (e eu sendo um amigo ausente por conta do doc). <3

A meus amigos de Porto Velho, Lucas Oliveira (Lucaxxx) e Fernando Ribas Motas (Fefa). Obrigado por sempre me incentivarem e torcerem por mim durante esta jornada. Vocês dois são muito importantes em minha vida, cada um à sua maneira. Obrigado Lucaxxx por me apresentar o mundo dos memes e dos gifs (hahahahah). <3

Obrigado a meu companheiro amado, **Artur Melo**, por estar inquestionavelmente ao meu lado, mesmo estando a 1000 km de distância maior parte do tempo. Obrigado por ser esta pessoa maravilhosa e de um coração enorme que nunca vi igual. Obrigado por aguentar meu estresse "fim de doutorado" e por me acalmar sempre. Sem você eu teria perdido os cabelos. Obrigado pelo incentivo incondicional!!

Muito obrigado a minha mãe (Francisca Cândida), meu irmão (Leandro de Assis) e meu pai (Miquéias Ferrão) por todo o amor, pela criação, e por toda a ajuda (que não foi pouca) ao longo de minha vida acadêmica. <3

Obrigado especial **a minha mãe e melhor amiga** por diversas vezes ter abdicado de sua felicidade em nome da minha. Por ter lutado muito para que eu tivesse o menor número de preocupações possível e pudesse focar nos estudos. Obrigado por ter se desfeito de bens pessoais para me fazer chegar até aqui. Mãezinha linda, devo a você a minha vida e tudo o que tenho e sou. Você é meu exemplo de vida e minha inspiração. <3 <3

Diversas outras pessoas não citadas contribuíram para que eu chegasse aqui. Meu imenso obrigado a todas vocês e desculpem-me não mencionar vocês aqui! <3<3<3

RESUMO

O interflúvio entre os rios Purus e Madeira (IPM) compreende uma das regiões mais desconhecidas da Amazônia brasileira. Mesmo sendo uma região extremamente ameaçada pelas ações do homem, pouco se conhece sobre a identidade taxonômica dos anuros que habitam a região e os processos responsáveis por determinar padrões de distribuição e diversificação de espécies. O objetivo geral desta tese foi investigar a diversidade escondida de anuros, fornecer subsídios para estudos ecológicos e de conservação através da descrição de novos taxons, e revelar processos ecológicos responsáveis pela distribuição e diversificação de espécies no IPM. No **primeiro capítulo**, integramos dados morfológicos, bioacústicos e moleculares para investigar a existência de diversidade escondida em anuros do gênero *Scinax* ao longo de 1000 km de paisagens no IPM e áreas circunvizinhas. Análises integrativas revelaram que aproximadamente 82% da riqueza regional de espécies de *Scinax* era composta por espécies desconhecidas para a ciência. Os resultados evidenciaram o quanto o IPM é pouco conhecido do ponto de vista faunístico e a necessidade de ações conservacionistas na região. No **segundo capítulo**, descrevemos formalmente a espécie de *Scinax* com maior distribuição ao longo do IPM e investigamos se sua distribuição geográfica e abundância são influenciadas por variáveis ambientais. *Scinax ruberoculatus* é facilmente distinta das demais congêneres por caracteres morfológicos (adultos e girinos) e bioacústicos. Diferente do que se esperava para anuros de reprodução aquática, sua distribuição e abundância ao longo do IPM é influenciada positivamente pela porcentagem de silte no solo e não pela estrutura da floresta (densidade de árvores). Sugere-se que está associação espécie-habitat seja guiada pelas necessidades reprodutivas da espécie, uma vez que sítios reprodutivos em solos siltosos podem ser menos efêmeros, favorecendo assim a sobrevivência dos girinos da nova espécie. No **terceiro capítulo**, descrevemos formalmente uma nova espécie de *Scinax* com distribuição aparentemente restrita à porção central do IPM. Apesar de ser proximamente relacionada com espécies do clado *Scinax wandae*, a nova espécie se distingue de todas estas por caracteres morfológicos e de coloração, bem como por seu canto de anúncio. Sua área de ocorrência passa por forte pressão antrópica em decorrência do desmatamento influenciado pela especulação imobiliária decorrente da reconstrução da BR-319. No **quarto capítulo**, *Scinax onca* foi descrita com base em espécimes provenientes de duas populações distintas do IPM, uma distribuída em florestas densas e a outra em florestas abertas. Análises filogenéticas do primeiro capítulo mostraram que estas populações formam clados reciprocamente monofiléticos. As diferenças no padrão de coloração entre as duas populações, juntamente com suas relações evolutivas, nos levaram a levantar a hipótese de que variações ecológicas do IPM podem ser os responsáveis pela diferenciação destas duas populações. Entretanto, dados coletados ao longo de sua distribuição se fazem necessários para elucidar se a diferenciação observada é influenciada pelos gradientes ambientais. No **quinto capítulo**, utilizamos uma espécie diminuta de anuro terrícola (*Phyzelaphryne miriamae*) amplamente distribuída no IPM como modelo para testar se o fluxo gênico ao longo da paisagem pode ser explicado pela hipótese de gradientes ambientais. Pela primeira vez na Amazônia, utilizamos análises genômicas de paisagem e milhares de polimorfismos de nucleotídeos únicos (SNPs) para testar esta hipótese. Análises de estrutura genética estimaram cinco populações em *P. miriamae*. Os efeitos dos gradientes ambientais no fluxo gênico da espécie alvo foram pronunciados. Os valores de explicação das variáveis ambientais, após corrigidas pelo efeito da distância geográfica, variaram entre 24.7% (teor de silte no solo) e 30.2% (sazonalidade da temperatura). Enquanto que a distância geográfica explicou apenas 2.3–3.7% do fluxo gênico. Embora haja efeito da distância geográfica no fluxo gênico de *P. miriamae*, este se limita apenas a pequenas e longas distâncias, sendo nulo em distancias intermediarias.

ABSTRACT

The Purus-Madeira Interfluve (PMI) represents one of the less known areas of Brazilian Amazonia. Despite it is extremely threatened by anthropic actions, the knowledge about the taxonomic identity of anurans inhabiting the PMI and the processes driving their distribution and diversification are poorly known. The main goals of this thesis were to investigate the hidden diversity in anurans, provide bases to ecological and conservation studies through the description of new taxa, and illuminating the role of environment on species distribution and diversification along the PMI. In the **first chapter**, we integrated morphology, bioacoustics, and genetics to explore if there was hidden diversity in anurans of the genus *Scinax* along 1000 km of landscapes in the PMI. Integrative analyses revealed that approximately 82% of the regional richness in *Scinax* was unknown to science. Results highlighted how much the PMI faunal diversity is poorly known and its need for conservation actions. In the **second chapter**, we formally described the most widely distributed new species of *Scinax* in the PMI and tested if its geographic distribution and abundance were driven by environmental variables. *Scinax ruberoculatus* is easily distinguished from its congeners through morphological (adults and tadpoles) and bioacoustical characters. Differing from the predicted for aquatic breeding anurans, its distribution and abundance along the PMI is positively driven by silt content and not by forest structure (tree density). It is suggested that this habitat-association is driven by the species' reproductive needs once reproductive sites in silty soils may be less ephemeral, favouring the survival of tadpoles of the new species. In the **third chapter**, we described a new species of *Scinax* with distribution apparently restricted to the central portion of PMI. Despite it is close related to species of the *Scinax wandae* clade, the new species is distinguished from all other Amazonian *Scinax* through morphology and colouration, as well as by the advertisement call. The species' habitat is deeply threatened by the anthropic pressure due to property speculation as result of the reconstruction of the BR-319 highway. In the **fourth chapter**, *Scinax onca* was described based in specimens from two distinct populations in the PMI, one living in dense forests and the other in open forests. Phylogenetic analyses of the first chapter recovered these populations as reciprocally monophyletic. Differences in colour pattern, as well as its evolutionary relationship, led us to hypothesize that environmental gradients of the PMI may be responsible by observed differentiation in these populations. However, data collected along its distribution are necessary to elucidate if the observed differentiation is really

influenced by environmental gradients. In the **fifth chapter**, we used a diminutive terrestrial anuran (*Phyzelaphryne miriamae*) and widely distributed in the PMI as a model to test if the gene flow along the landscape can be explained by the ecological gradient hypothesis. For the first time in Amazonia, genomic landscape analyses and thousands of single nucleotide polymorphisms (SNPs) were used to test this hypothesis. Genetic structure analyses estimated five ancestral populations in *P. miriamae*. Results indicated that the effect of environmental gradients on gene flow of the target species was pronounced. After accounting the effect of geographic distance, the explanation of environmental variables ranges from 24.7 % (silt content) to 30.2% (temperature seasonality). On the other hand, geographic distance explained just 2.3–3.7% of the gene flow. Although there is an effect of geographic distance on gene flow in *P. miriamae*, it is restricted to short and long distances, being null in moderated distances.

SUMÁRIO

LISTA DE TABELAS

CAPÍTULO 2

CAPÍTULO 3

CAPÍTULO 4

CAPÍTULO 5

Table 2. Pairwise genetic differentiation (F_{ST}) across sampling sites (bellow diagonal) computed following Weir & Cockerham (1984) and its respective p-values (above diagonal) based on 1000 permutations. Asterisks represent p value < 0.01.

Table 3. Summary of results of maximum likelihood population effects mixed effects models (MLPE) and distance-based redundancy analyses (dbRDA) depicting the effect of isolation by resistance on gene flow of P. miriamae along the Purus-Madeira Interfluve.

LISTA DE FIGURAS

CAPÍTULO 1

Figure 1. Sampling area in the Purus-Madeira interfluve and on the east bank of the upper Madeira river, Brazilian Amazonia. (A) Vegetation cover types. (B) Soil types. Abbreviations: BR, Brazil; M1–M18, RAPELD sampling modules; Abp, lowland ombrophilous open forest with palm trees; Dbe, lowland ombrophilous dense forest with emergent canopy; Caa, Chromic-Alumic Acrisol; Ahp, Alumic-Humic Plinthosol; Hvf, Hyperdystri-Vetic Ferralsol. The small insert in each map shows part of South America and abbreviated names of countries. The transverse gray bar represents the study area and adjacent territory.

Figure 2. Maximum clade-credibility tree of *Scinax* from the Purus-Madeira interfluve and the east bank of the upper Madeira (Brazilian Amazonia) and correlated species. The 16S gene tree was recovered by Bayesian analyses in BEAST. Posterior probabilities are given near the nodes. Asterisks indicate PP > 0.95. Vertical gray bars indicate species delimitation with the molecular approach. Horizontal gray bars indicate species delimitation with the integrative approach. Colored areas in topology represent, from top to bottom, the *S. rostratus* species Group (red), *S. ruber* Clade (green), *S. wandae* Clade (blue), and *S. fuscomarginatus* Clade (yellow). Outgroup: members of Scinax rostratus species Group, plus *Julianus uruguayus* and *Ololygon berthae*. Abbreviations: ABGD, Automatic Barcoding Gap Discovery; GMYC, Generalized Mixed Yule Coalescent; CCS, Confirmed Candidate Species; UCS, Unconfirmed Candidate Species; DCL, Deep Conspecific Lineage; NS, Nominal Species.

Figure 3. Specimens of *Scinax* from the Purus-Madeira interfluve and east bank of the upper Madeira River, Brazilian Amazonia. (A) *Scinax* sp. 1, male, SVL 20.2 mm, INPA-H 34688, from M-9. (B) *Scinax* sp. 2, male, SVL 18.1 mm, INPA-H 34667, from M-11. (C) *Scinax* sp. 3, male, SVL 31.3 mm, INPA-H 34584, from M-7. (D) *Scinax* sp. 5, male, not collected, from M-8. (E) *Scinax* sp. 6, male, SVL 25.2 mm, INPA-H 35562, from M-17. (F) *Scinax* sp. 7, male, SVL 23.9 mm, INPA-H 34623, from M-8. (G) *Scinax* aff. *cruentommus* BRA, male, SVL 25.4 mm, INPA-H 34596, from M-6. (H) *Scinax ruber* PM, couple, not collected. (I) *Scinax chiquitanus* BRA, female, SVL 33.7 mm, INPA-H 35554; male, SVL 31.1 mm, INPA-H 35555, from M-14. Photographs by R. Fraga.

CAPÍTULO 2

Figure 1. Sampling area in the Purus-Madeira Rivers Interfluve and schematic representation of RAPELD sampling modules and plots. (A) Distribution of RAPELD sampling modules along a 600 km transect. Legend: green colour (M1–M9) D tropical lowland rainforest with emergent canopy; gold colour (M10–M11) D open rainforest lowlands with palm trees. (B) General configuration of each module with ten sampling plots. Open squares represent plots where environmental variables used in this study were measured. BRA, Brazil.

Figure 2. Holotype of *Scinax ruberoculatus* sp. nov. INPA-H 34665. (A) Dorsal view. (B) Ventral view. Scale D 5 mm. Photos by M Ferrão.

Figure 3. Hand and foot of the holotype of *Scinax ruberoculatus* sp. nov. INPA-H 34665. Scale = 1 mm. Photos by M Ferrão.

Figure 4. Multivariate morphometric space of *Scinax ruberoculatus* sp. nov. Principal Components Analysis of the SVL and 15 body ratios of males (N = 28) and females (N = 6). (A) Sampled by sex and (B) sampled by RAPELD sampling modules. Abbreviations: M2–5 and M7–9, RAPELD sampling modules where specimens were collected; F, females; M, males.

Figure 5. Variation in the dorsal colouration from preserved specimens of *Scinax ruberoculatus* sp. nov. (A) INPA-H 34601, male, SVL 24.1 mm. (B) INPA-H 34600, female, SVL 27.5 mm. (C) INPA-H 34609, male, SVL 24.5 mm. (D) INPA-H 34598, male, SVL 25.5 mm. (E) INPA-H 34614, male, SVL 25.5. (F) INPA-H 34611, male, SVL 23.8 mm. (G) INPA-H 34612, male, SVL 24.4 mm. (H) INPA-H 34618, male, SVL 25.2 mm. (I) INPA-H 34605, female, SVL 26.2 mm. Photos: M Ferrão.

Figure 6. Variation in the colouration of living specimens of the paratypes of *Scinax ruberoculatus* sp. nov. (A) INPA-H 34607, female, SVL 25.4 mm. (B) INPA-H 34602, male, SVL 22.6 mm. (C) INPA-H 34603, male, SVL 23.3 mm. (D) INPA-H 34604, male, SVL 25.8 mm. (E) INPA-H 34623, male, SVL 23.9 mm. (F) INPA-H 34602, male, SVL 22.6 mm. Photos: AP Lima (B, F) and R Fraga (A, C, D, E).

Figure 7. Advertisement call of *Scinax. ruberoculatus* sp. nov. (A) Waveform. (B) Audiospectrogram. Call recorded at RAPELD sampling module 9, Nascentes do Lago

Jari National Park, Beruri Municipality, Amazonas, Brazil. Male recorded: INPA-H 34665 (SVL 25.9 mm). Temperature: 25 °C.

Figure 8. Tadpole of *Scinax. ruberoculatus* sp. nov. (INPA-H 35410) in developmental stage 34. (A) Lateral view. (B) Dorsal view. (C) Ventral views. (D) Details of the opened oral disc. (E) closed oral disc. Tadpoles were collected at RAPELD sampling module 9, Nascentes do Lago Jari National Park, Amazonas, Brazil. Scales for A–C = 5 mm. Scales for D–E = 0.5 mm. Photos: M Ferrão.

Figure 9. Newly metamorphosed *Scinax. ruberoculatus* sp. nov. (INPA-H 35412). (A) Dorsolateral view. (B) Frontodorsal views. This specimen developed under our care from a typical tadpole of the new species. Photos: R de Fraga.

Figure 10. Geographic range of *Scinax. ruberoculatus* sp. nov. Numbers indicate the RAPELD sampling module. Yellow circles: RAPELD sampling modules where the new species was observed. White circles: RAPELD sampling modules where the new species was not observed. Triangles: RAPELD sampling modules outside the study area where the new species was not observed. The diameter of the yellow circles indicates the percentage of plots occupied by the new species within each sampling module (10% in 3–5; 20% in 7–8; 40% in 9; 50% in 2).

Figure 11. Relationship between the abundance of *Scinax ruberoculatus* sp. nov. and silt content in the Purus-Madeira Rivers Interfluve, Amazonas, Brazil. Model: Log (abundance + 1) = constant + log (silt content). r^2 = 0.41, F1,9 = 6.48, P = 0.031.

CAPÍTULO 3

Figure 1. Holotype of *Scinax* sp. nov. (INPA-H 34688), from Nascentes do Lago Jari National Park, Tapauá, Amazonas, Brazil. Scale bar = 5 mm.

Figure 2. Ventral view of hand (A) and foot (B) of the holotype of *Scinax* sp. nov. (INPA-H 34688), from Nascentes do Lago Jari National Park, Tapauá, Amazonas, Brazil. Scale: 2 mm.

Figure 3. Holotype of *Scinax* sp. nov. (INPA-H 34688, SVL = 20.2 mm), Nascentes do Lago Jari National Park, Tapauá, Amazonas, Brazil. Photo: Rafael de Fraga.

Figure 4. Color in preservative of the *Scinax* sp. nov. type series from Nascentes do Lago Jari National Park, Tapauá, Amazonas, Brazil. A: INPA-H 34700, female, SVL 26.5 mm. B: INPA-H 34689, male, SVL 20.7 mm. C: INPA-H 34688, male, 20.2 mm. D: INPA-H 34692, male, SVL 22.5 mm. E: INPA-H 34691, male, SVL 22.5 mm. F: INPA-H 34690, male, SVL 21.6 mm.

Figure 5. Wave form and audiospectrogram of the advertisement call type A interspersed with advertisement call type B of *Scinax* sp. nov. (INPA-H 34691, SVL 22.5 mm) from Nascentes do Lago Jari National Park, Tapauá, Amazonas, Brazil (A). Wave form and detailed audiospectrogram (B) of the advertisement call type A (C) and type B (D).

Figure 6. Bayesian 50% consensus tree inferred from mitochondrial 16S rRNA. Posterior probabilities are given above the node when ≥ 0.95. Blue area highlights the new species.

Figure 7. Geographic range of *Scinax* sp. nov. in the interfluve between the Purus and Madeira rivers, Brazilian Amazonia. Black star: type locality, border of Nascentes do Lago Jari National Park (green polygon) in contact with the federal highway BR-319, Municipality of Tapauá, Amazonas, Brazil.

CAPÍTULO 4

Figure 1. Distribution of *Scinax onca* sp. n. and *Scinax iquitorum* in Brazilian Amazonia. Yellow star: A type locality of *S. onca* sp. n., kilometre 350 of the BR-319 Highway, municipality of Beruri, State of Amazonas. Yellow circles: B paratype locality of *S. onca* sp. n., Floresta Estadual Tapauá Reserve, municipality of Tapauá, State of Amazonas C–D paratype localities of *S. onca* sp. n., municipality of Porto Velho, State of Rondônia. White triangles: E record of *S. iquitorum* near southern distribution of *S. onca* sp. n. according Melo-Sampaio and Souza (2015), municipality of Plácido de Castro, State of Acre, Brazil F record of *S. iquitorum* according Machado et al. (2015), municipality of Cruzeiro do Sul, State of Acre, Brazil.

Figure 2. Holotype of *Scinax onca* sp. n. Dorsal and ventral view of the preserved holotype of *S. onca* sp. n. INPA-H 34584 from middle Purus-Madeira Interfluve, at the kilometre 350 of the BR-319 highway, municipality of Beruri, State of Amazonas, Brazil. Scale bar 5 mm.

Figure 3. Hand and foot of holotype of *Scinax onca* sp. n. Ventral view of the hand and foot of the preserved holotype of *Scinax onca* sp. n. Scale bar 5 mm.

Figure 4. Adult specimens of *Scinax funereus* and *S. iquitorum*. A, Female specimen of *Scinax funereus* (KU221960b) from San Jacinto, Region Loreto, Peru. B, Male paratype of *Scinax iquitorum* (NMP6V 71267/1) from Puerto Almendras, Region Loreto, Peru. Photograph by W.E. Duellman (A) and Jiří Moravec (B).

Figure 5. Colour in life of *Scinax onca* sp. n. Colour variation in life of *Scinax onca* sp. n. from the Purus-Madeira Interfluve, Brazilian Amazonia. A–B, INPA-H 34584 (holotype), adult male from the kilometre 350 of the BR-319 highway, State of Amazonas. C–D, INPA-H 34591, adult female from municipality of Porto Velho, State of Rondônia. E–F, INPA-H 26625, adult female from the Floresta Estadual Tapauá Reserve, municipality of Tapauá, State of Amazonas. Photographs: A–D and F were taken after transport of the specimens to the camp, while the image of E was taken immediately in the field.

Figure 6. Colour in preservative of dorsum of *Scinax onca* sp. n. Dorsal colour variation of preserved specimens of *Scinax onca* sp. n. Specimens from middle (A−C) and southern (D−F) Purus-Madeira Interfluve, Brazilian Amazonia. A, INPA-H 34581, male, SVL 34.3 mm. B, INPA-H 34583, female, SVL 35.5 mm. C, INPA-H 34582 male, SVL 31.5 mm. D, INPA-H 34594, male, SVL 32.6 mm. E, INPA-H 34589, female, SVL 38.9 mm. F, INPA-H 34593, male, SVL 34.5 mm.

Figure 7. Colour in preservative of venter of *Scinax onca* sp. n. Ventral colour variation of preserved specimens of *Scinax onca* sp. n. Specimens from middle (A−C) and southern (D−F) Purus-Madeira Interfluve, Brazilian Amazonia. A, INPA-H 34583, female, SVL 35.5 mm. B, INPA-H 34582, male, SVL 31.5 mm. C, INPA-H 34581 male, SVL 34.3 mm. D, INPA-H 34588, male, SVL 34.1 mm. E, INPA-H 34593, male, SVL 34.5 mm. F, INPA-H 34589, female, SVL 38.9 mm.

Figure 8. Advertisement call of *Scinax onca* sp. n. Spectrogram (A) and oscillogram (B) of an advertisement call of *Scinax onca* sp. n. The specimen (INPA-H 26624, SVL 32.1 mm) was recorded in Floresta Estadual Tapauá Reserve, middle Purus-Madeira Interfluve, Amazonas, Brazil. (C) A series with eleven calls. Air temperature not measured.

Figure 9. Tadpole of *Scinax onca* sp. n. from the middle Purus-Madeira Interfluve (lot INPA-H 35411). Specimen collected at kilometre 350 of the BR-319 highway, municipality of Beruri, State of Amazonas, Brazil. From top to bottom: dorsal, ventral, and lateral views of preserved tadpole in developmental Stage 37. Scale bar 5 mm.

Figure 10. Oral disc of the tadpole of *Scinax onca* sp. n. (lot INPA-H 35411; developmental Stage 37). Left: ventrolateral and right: ventral view. The tadpole was collected in the middle Purus-Madeira Interfluve, at the kilometre 350 of the BR-319 highway, municipality of Beruri, State of Amazonas, Brazil. Scale bar 2 mm.

CAPÍTULO 5

Figure 1. Hypothetical representation of slopes of isolation by resistance (IBR) hypotheses tested for the effect of environmental variables on Fst/(1-Fst) using seven values of γ (0.01, 0.1, 0.5, 1, 5, 10, 100) and $\alpha = 1000$. Relationships between resistance and environmental variables for which high values were interpreted as restrictive (A) or permissive to gene flow (B). Numbers close to lines represent γ values. Remaining α values (0.5, 10, 100) were not shown to simplify visualization.

Figure 2. Variables used to test the effect of environmental gradients on gene flow of *P. miriamae* within the interfluve between Purus and Madeira rivers. (A) Silt content. (B) Vegetation biomass. (C) Walsh Index. (D) Temperature seasonality. Black circles: RAPELD sampling sites.

Figure 3. Genetic structure of *Phyzelaphryne miriamae* along the Purus-Madeira Interfluve. (A) Population admixture estimates ($k = 5$) as recovered by SNMF. (B) Ancestral coefficients of individuals ($k = 5$) retrieved by SNMF. (C) Posterior membership probabilities of individuals according to DAPC using $k = 5$.

Figure 4. Correlation between Fst/(1-Fst) and log(geographic distance) (A) and mantel correlogram plot depicting the spatial autocorrelation of Fst/(1-Fst) in seven classes of log(geographic distance) (B). Filled squares = distance classes with $p \leq 0.05$.

INTRODUÇÃO GERAL

A região Neotropical abriga o maior número de espécies de anuros do planeta (Duellman 1999), sendo a Amazônia a floresta tropical de terras baixas com a maior riqueza de espécies (Mittermeier et al. 2003). Aproximadamente 37% das espécies de anuros amazônicos são conhecidas por estarem distribuídas em áreas superiores a 1.000.000 km², podendo ser consideradas amplamente distribuídas (Fouquet et al. 2007a). Entretanto, a ideia de que tantas espécies possuem ampla distribuição está em desacordo com a baixa capacidade de deslocamento e alta filopatria observada em diversos grupos de anuros (Fouquet et al. 2007a). Adicionalmente, é sabido que linhagens crípticas estão ocultas dentro de espécies nominais com amplas distribuições (Angulo e Icochea 2010, Simões et al. 2010, Fouquet et al. 2014, Caminer et al. 2017, Rojas et al. 2018). Graças aos avanços recentes em diversas áreas da ciência e a integração de várias ferramentas (e.g., bioacústica, biologia molecular, morfologia, comportamento), atualmente é possível investigar de forma mais detalhada e minuciosa a diversificação evolutiva de grupos problemáticos de espécies de anuros (veja Padial et al. 2010).

Anuros amazônicos com amplas distribuições geográficas (e.g *Adelophryne* spp., *Adenomera* spp., *Allobates* spp., *Amazophrynella* spp., *Engystomops* spp., *Hypsiboas* gr. *calcaratus*, *Osteocephalus* spp., *Pristimantis fenestratus*, *Rhinella* gr. *margaritifera*, *Scinax* gr. *ruber*) estão sendo alvo de estudos que buscam investigar diversidade críptica e seus processos de diversificação evolutiva. Diversas linhagens previamente desconhecidas de *Rhinella* gr. *margaritifera* e *Scinax* gr. *ruber* foram descobertas na Guiana Francesa (Fouquet et al. 2007b). Funk et al. (2011) revelaram que duas espécies reconhecidas do grupo *Hypsiboas calcaratus* correspondem atualmente a seis espécies, e que duas espécies amazônicas de *Engystomops* correspondem a cinco espécies, um incremento de 200 e 150% na riqueza conhecida para estes grupos, respectivamente. Oito espécies de *Adenomera* ainda não descritas ocorrem na Amazônia, o que representa um incremento de 160% na riqueza conhecida para o bioma (Fouquet et al. 2014). Jungfer et al. (2013) revelou através de dados moleculares e morfológicos a existência de pelo menos nove novas espécies de *Osteocephalu*s. De forma similar, Caminer et al. (2017) investigou a existência de diversidade escondida em *Dendropsophus* gr. *leucophyllatus* através da integração de dados morfológicos, bioacústicos e moleculares, resultando na descrição de duas novas espécies. Estimativas iniciais apontavam que o número de espécies de anuros amazônicos estava subestimado em até 115% (Fouquet et al. 2007a). Entretanto, o número de espécies desconhecidas pode ser ainda maior (Funk et al. 2011).

Anuros estão passando por um drástico declínio global (Houlahan et al. 2000, Stuart et al. 2004). Paradoxalmente, o número de descrições de novas espécies de anuros encontra-se longe da estabilidade (Caramaschi 2010, Brown et al. 2011, Padial et al. 2012, Teixeira et al. 2012, Venegas e Duellman 2012, Brandão et al. 2013, Carvalho e Giaretta 2013, Caminer e Ron 2014, Peloso et al. 2014, Lima et al. 2015, Jungfer et al. 2016, Caminer et al. 2017, Rakotoarison et al. 2017, Melo-Sampaio et al. 2018), o que corrobora as predições de diversidade escondida de Fouquet et al. (2007a) e Funk et al. (2011). Apesar do contínuo incremento no número de descrições, dezenas ou talvez centenas de espécies de anuros amazônicos aguardam descrição formal.

Espécies são amplamente conhecidas como unidades fundamentais em estudos ecológicos (Gotelli 2004). Estudos taxonômicos em áreas pouco conhecidas, especialmente em florestas megadiversas como a Amazônia, são essenciais para a obtenção de padrões ecológicos. A falta de identificações precisas em nível específico pode comprometer a obtenção de padrões ecológicos, tanto em nível de espécie quanto em nível de comunidade (Isaac et al. 2004, Bortolus, 2008). Além disto, erros de identificação taxonômica empobrecem as comparações entre diferentes áreas e conclusões sobre distribuição de muitas espécies de anuros na Amazônia (Fouquet et al. 2007a, Pinheiro et al. 2012). Isto prejudica diretamente medidas de conservação com base na biodiversidade e endemismo de uma determinada área, refletindo preconceitos graves na semelhança de composição real entre áreas a serem selecionados para fins de conservação (Bickford et al. 2007). Portanto, a delimitação e descrição de espécies desempenha um papel importante no desenvolvimento de ações conservacionistas em áreas ameaçadas, além de ser fundamental para a condução de investigações ecológicas (Nair et al. 2012).

O estudo dos processos envolvidos na distribuição da biodiversidade em diferentes escalas espaciais é uma das principais questões em ecologia e biogeografia (Gaston e Blackburn 2003). Sabe-se que fatores bióticos e abióticos determinam a distribuição das espécies em diferentes escalas espaciais (Ricklefs 2004). Entretanto, para que os fatores abióticos sejam importantes preditores em modelos de distribuição e abundância de espécies, é necessário que estes atuem diretamente sobre as restrições fisiológicas das espécies. Características tais como pele permeável (Ludwig 1945), diversidade de modos reprodutivos (Silva et al. 2012), susceptibilidade dos ovos à desidratação (Duellman e Trueb 1994) e baixa habilidade de dispersão (Blaustein et al. 1994) fazem dos anuros um excelente grupo para se investigar o papel de gradientes na distribuição e abundância das espécies ao longo da paisagem na qual estas ocorrem.

Os principais fatores ambientais determinando a distribuição de anuros em grandes escalas espaciais são temperatura, precipitação, altitude e vegetação (Duellman e Thompson 1996, Duellman 1999, Silva et al. 2012). Em pequena e média escala, os principais fatores influenciando a distribuição e abundância de anuros com reprodução aquática são distância do riacho (Menin et al. 2011, Ribeiro et al. 2012, Rojas-Ahumada et al. 2012), largura (Eterovick e Barata 2009, Keller et al. 2009) e fluxo do riacho (Keller et al. 2009), disponibilidade (Ernst e Rödel 2006, Zimmerman e Bierregaard 1986) e pH de poças (Jorge et al. 2016), e por fim, a estrutura da vegetação (Parris e McCarthy 1999, Eterovick e Barata 2006, Koller et al. 2009, Ferreira et al. 2018). Os estudos correlacionando gradientes ambientais à distribuição e abundância de anuros florestais na Amazônia estão limitados a pequenas e médias escalas, e a maior parte deles foi realizada na Amazônia Central (Allmon 1991, Pearman 1997, Menin et al. 2007, Menin et al. 2011, Tsuji-Nishikido e Menin 2011, Rojas-Ahumada et al. 2012). O que se observa é que o modo reprodutivo dos anuros constitui um exemplo formidável de como as diferenças na biologia das espécies podem fornecer importantes explicações sobre seus padrões de distribuição (Menin et al. 2007, Keller et al. 2009, Menin et al. 2011, Silva et al. 2012). Novos estudos abrangendo grandes extensões da paisagem podem revelar associações espécie-habitat que de outra forma seriam impossíveis de serem observados em pequena e média escala.

Entender como a paisagem afeta o fluxo gênico de populações na natureza permanece como um dos principais interesses da biologia evolutiva e possui papel fundamental na compreensão dos fatores que promoveram a alta diversidade de espécies encontrada atualmente na Amazônia. Desde o século 19, diversas hipóteses alternativas foram criadas para tentar explicar a diversificação de espécies (Wallace 1852, Haffer 1969, Endler 1977, 1982, Räsänan et al. 1990, Ayres et al. 1992, Webb 1995, Nores 1999). Dentre estas, a mais explorada e testada nos últimos 20 anos na Amazônia é a teoria de rios como barreira (Wallace 1852). Esta teoria postula que grandes rios promovem isolamento alopático através do impedimento de fluxo gênico entre populações que habitam margem opostas de um dado rio. Apesar da diferenciação genética de várias espécies ter sido correlacionada com a presença de grandes rios Amazônicos (Funk et al. 2007, Fernandes et al. 2012, Ribas et al. 2012, Lynch Alfaro et al. 2015, Boubli et al. 2015, Fouquet et al. 2015, Ferreira et al. 2017, Maia et al. 2017, Nazareno et al. 2017, Ortiz et al. 2018, Naka & Brumfield 2018, Ribas et al. 2018), a mesma correlação não é clara ou não se aplica a outros organismos (Gascon et al. 1996, 1998, Lougheed et al. 1999; Gascon et al. 2000, Symula et al. 2003, Aleixo 2004). Com o avanço recente de técnicas analíticas e o aumento no esforço em se amostrar áreas desconhecidas da Amazônia, o teste de outras hipóteses de diversificação devem ganhar campo dentro da biologia evolutiva.

Dentre as hipóteses menos exploradas, a teoria de gradientes ambientes (Endler 1977) demonstra plausibilidade visto a heterogeneidade ambiental da paisagem Amazônica. Esta teoria prediz que diferenciação genética pode ocorrer entre populações naturais em decorrência de divergência adaptativa guiada por gradientes ambientais, como por exemple mudanças na estrutura da floresta, granulometria do solo, temperatura e pluviosidade ao longo da área de distribuição da espécie alvo. De acordo com esta hipótese, a diferenciação genética pode ocorrer mesmo diante a presença de fluxo gênico (Moritz et al. 2000). Dentre as principais dificuldades em se testar a hipótese de gradientes ambientais, a presença de potenciais barreiras físicas ao longo da área de estudo e a distância geográfica entre amostras podem enviesar fortemente os resultados de testes estatísticos. O viés associado a distância geográfica pode ser minimizado através do uso de análises que permitam condicionar esta variável, como por exemplo, análises de redundância parcial baseadas em matrizes de distância. Quanto ao viés relacionado a presença de barreiras físicas, a forma mais simples é delimitar geograficamente a área de estudo de maneira a incluir apenas amostras de um lado de potenciais barreiras, como por exemplo, restringir o esforço amostral dentro de grandes interflúvios.

Devido à heterogeneidade da paisagem (Cintra et al. 2013, Martins et al. 2015, Schietti et al. 2016, Ferreira et al. 2018) ao longo de sua extensão, sua disposição latitudinal dentro da Amazônia, o interflúvio entre os rios Purus e Madeira se mostra ideal para investigar as influências de gradientes ambientais na diferenciação genética de organismos. Recentemente, Ortiz et al. (2018) correlacionou a estrutura genética encontrada em três marcadores (um mitocondrial e dois nucleares) de um anuro arborícola com os diferentes tipos de florestas de terras baixas que compõem o interflúvio Purus-Madeira. A variação na coloração da plumagem de três espécies de aves que habitam este mesmo interflúvio foi fortemente correlacionada com a heterogeneidade ambiental existente ao longo da paisagem (Abreu et al. 2018), o que pode ser indicio indireto do efeito da variabilidade ambiental no fluxo gênico destas espécies. Ortiz et al. (2018) e Abreu et al. (2018) utilizaram apenas variáveis que representam o tipo de floresta ou a estrutura da floresta em suas associações, respectivamente. O efeito de importantes variáveis ambientais conhecidas como preditoras em anuros (e.g., temperatura, pluviosidade e granulometria do solo: Menin et al. 2007, Menin et al. 2011, Ferreira et al. 2018) na diferenciação genética permanece desconhecido na Amazônia.

A obtenção de amplas quantidades de marcadores moleculares em estudos evolutivos com grande cobertura geográfica e com grande número de indivíduos foi, durante muito tempo, uma das principais barreiras para o estudo dos efeitos da heterogeneidade ambiental no fluxo gênico de organismos. Novas técnicas moleculares (Mardis 2008), habilitadas por tecnologias de sequenciamento e facilitadas pelo rápido desenvolvimento de métodos computacionais e modelos matemáticos têm permitido que pesquisadores deixem de utilizar apenas poucas dezenas de marcadores, e passem a utilizar milhares até dezenas de milhares de sítios polimórficos únicos - SNPs (Davey et al. 2011, McCormack et al. 2013). Dentre as vantagens de se utilizar SNPs em escala genômica em estudos evolutivos, uma das mais atrativas é a possibilidade de detectar de maneira refinada os possíveis efeitos da paisagem na diversificação de espécies (Rašić et al. 2014).

OBJETIVOS

O principal objetivo desta tese foi investigar e descrever a diversidade de espécies de anuros que ocorrem no interflúvio entre os rios Purus e Madeira (IPM) e revelar o papel dos gradientes ambientais na sua distribuição e diversificação.

Capítulo 1: investigar a existência de diversidade escondida em anuros do gênero *Scinax* ao longo de 1000 km de paisagens do IPM e áreas vizinhas.

Capítulo 2: descrever uma nova espécie de *Scinax* do IPM e testar se sua distribuição e abundância estão sendo influenciados por variáveis ambientais.

Capítulo 3: descrever uma nova espécie de *Scinax* com distribuição aparentemente restrita a porção central do IPM.

Capítulo 4: descrever uma nova espécie de *Scinax* com base em duas populações divergentes e distribuídas em diferentes florestas do IPM.

Capítulo 5: testar se gradientes ambientais influenciam o fluxo gênico de *Phyzelaphryne miriamae* ao longo de paisagens heterogêneas do IPM através de abordagem genômica.

CAPÍTULO 1

High species richness of *Scinax* treefrogs (Hylidae) in a threatened Amazonian landscape revealed by an integrative approach. PLoS ONE 11(11): e0165679. doi:10.1371/journal.pone.0165679

PLOS | ONE

RESEARCH ARTICLE

High Species Richness of *Scinax* Treefrogs (Hylidae) in a Threatened Amazonian Landscape Revealed by an Integrative Approach

Miquéias Ferrão[1]*, **Olavo Colatreli**[2], **Rafael de Fraga**[1], **Igor L. Kaefer**[3], **Jiří Moravec**[4], **Albertina P. Lima**[2]

1 Programa de Pós-Graduação em Ecologia, Instituto Nacional de Pesquisas da Amazônia, Manaus, Amazonas, Brazil, **2** Coordenação de Biodiversidade, Instituto Nacional de Pesquisas da Amazônia, Manaus, Amazonas, Brazil, **3** Instituto de Ciências Biológicas, Universidade Federal do Amazonas, Manaus, Amazonas, Brazil, **4** Department of Zoology, National Museum, Prague, Czech Republic

* uranoscodon@gmail.com

Citation: Ferrão M, Colatreli O, de Fraga R, Kaefer IL, Moravec J, Lima AP (2016) High Species Richness of *Scinax* Treefrogs (Hylidae) in a Threatened Amazonian Landscape Revealed by an Integrative Approach. PLoS ONE 11(11): e0165679. doi:10.1371/journal.pone.0165679

Editor: William J. Etges, University of Arkansas, UNITED STATES

Received: August 7, 2016

Accepted: October 14, 2016

Published: November 2, 2016

Data Availability Statement: All relevant data are within the paper and its Supporting Information files.

Funding: This work was funded by PRONEX – FAPEAM/CNPq (proj. 003/2009, proc. 653/2009) and its publication was funded by Ministry of Culture of the Czech Republic (DKRVO 2016/15, National Museum, 00023272). Miquéias Ferrão had a fellowship from the Conselho Nacional de Desenvolvimento Científico e Tecnológico (CNPq – proc. 573721/2008-4), via Centro de Estudos Integrados da Biodiversidade Amazônica

Abstract

Rising habitat loss is one of the main drivers of the global amphibian decline. Nevertheless, knowledge of amphibian diversity needed for effective habitat protection is still highly inadequate in remote tropical regions, the greater part of the Amazonia. In this study we integrated molecular, morphological and bioacoustic evidence to evaluate the species richness of the treefrogs genus *Scinax* over a 1000 km transect across rainforest of the Purus-Madeira interfluve, and along the east bank of the upper Madeira river, Brazilian Amazonia. Analysis revealed that 82% of the regional species richness of *Scinax* is still undescribed; two nominal species, seven confirmed candidate species, two unconfirmed candidate species, and one deep conspecific lineage were detected in the study area. DNA barcoding based analysis of the 16s rRNA gene indicates possible existence of three discrete species groups within the genus *Scinax*, in addition to the already-known *S. rostratus* species Group. Quantifying and characterizing the number of undescribed *Scinax* taxa on a regional scale, we provide a framework for future taxonomic study in Amazonia. These findings indicate that the level to which Amazonian anura species richness has been underestimated is far greater than expected. Consequently, special attention should be paid both to taxonomic studies and protection of the still-neglected Amazonian *Scinax* treefrogs.

Introduction

Frogs achieve mega-diversity in the tropics, but this extreme species richness is under strong pressure from human disturbance, mainly via habitat loss and degradation of breeding sites [1]. Contemporaneously, it is becoming increasingly evident that the diversity of frogs has been

(CENBAM). Currently, Miquéias Ferrão receives a PhD scholarship from the Fundação de Amparo a Pesquisa do Estado do Amazonas (FAPEAM). Rafael de Fraga had a PhD scholarship from the Coordenação de Aperfeiçoamento de Pessoal de Nível Superior (CAPES). The funders had no role in study design, data collection and analysis, decision to publish, or preparation of the manuscript.

Competing Interests: The authors have declared that no competing interests exist.

severely underestimated, and that this is true in many different anuran groups. For instance, the species richness in the genus *Adenomera* Steindachner, 1867, in the subfamily *Phyzelaphryninae* Hedges, Duellman and Heinicke, 2008 and in the genus *Osteocephalus* Steindachner, 1862 increased by 116%, 100% and 37.5%, respectively [2–4]. Moreover, species richness in the genus *Engystomops* Jimenez de la Espada, 1872 and in the *Hypsiboas calcaratus–Hypsiboas fasciatus* species complex increased by at least 150% and 200%, respectively [5–6] (see S1 Appendix for cryptic diversity estimates). Finally, 11 distinct lineages of leaf-frogs of the *Rhinella margaritifera* species complex and six lineages of treefrogs of the *Scinax ruber* species complex have been identified as potentially new species [7].

Taxonomic studies of the genus *Scinax* Wagler, 1830 are very challenging due to the large number of morphologically similar species, especially those belonging to the same species complexes [8–10]. In addition to difficulties in species recognition, the high number of cryptic species [7] and the lack of information about the geographical range of many species, call for the introduction of non-morphological methods into research on the taxonomy of the genus. Such integrative taxonomic studies of Amazonian frogs have usually addressed morphological, molecular, bioacoustic and natural history data (e.g. [11–13, 6, 14–15]). The integration of different lines of evidence is a powerful tool for solving taxonomic problems (e.g. [10, 11, 13]) and understanding evolutionary relationships between taxa [16].

At present, the genus *Scinax* comprises 63 species of small and medium-sized arboreal frog (15–52 mm), and is distributed throughout the Americas from Mexico to Argentina [17]. Until 2014, 29 species of the *Scinax ruber* Clade (*sensu* [18]) were known from Amazonia (see [19]). However, *S. parkeri* (Gaige, 1929) and *S. trilineatus* (Hoogmoed and Gorzula, 1977) were recently synonymized with *S. fuscomarginatus* (Lutz, 1925), *S. madeirae* (Bokermann, 1964) was revalidated and *S. villasboasi* Brusquetti, Jansen, Barrio-Amarrós, Segalla and Haddad, 2014 was described from the eastern Brazilian Amazonia [10]. Therefore, 28 valid species of *Scinax* currently occur in Amazonia. Of these, seven species are placed in the *S. rostratus* species Group: *S. garbei* (Miranda-Ribeiro, 1926), *S. jolyi* Lescure and Marty, 2000, *S. kennedyi* (Pyburn, 1973), *S. nebulosus* (Spix, 1824), *S. pedromedinae* (Henle, 1991), *S. proboscideus* (Brongersma, 1933) and *S. rostratus* (Peters, 1863). Twenty-one species are not associated with any known species group (*sensu* [18]): *S. baumgardneri* (Rivero, 1961), *S. blairi* (Fouquette and Pyburn, 1972), *S. boesemani* (Goin, 1966), *S. chiquitanus* (De la Riva, 1990), *S. cruentommus* (Duellman, 1972), *S. danae* (Duellman, 1986), *S. exiguus* (Duellman, 1986), *S. funereus* (Cope, 1874), *S. fuscomarginatus*, *S. fuscovarius* (A. Lutz, 1925), *S. ictericus* Duellman and Wiens, 1993, *S. iquitorum* Moravec, Tuanama, Pérez and Lehr, 2009, *S. karenanneae* (Pyburn, 1992), *S. lindsayi* Pyburn, 1992, *S. madeirae*, *S. oreites* Duellman and Wiens, 1993, *S. ruber* (Laurenti, 1768), *S. sateremawe* Sturaro and Peloso, 2014, *S. villasboasi*, *S. wandae* (Pyburn and Fouquette, 1971) and *S. x-signatus* (Spix, 1824).

The number of currently-known species in the *S. ruber* Clade means it is already relatively species-rich. However, because evolutionary relationships among the species are still poorly known, addtional undescribed species may occur in this clade [7, 10, 20–21]. Our herpetological survey in southern Amazonia indicated that *Scinax* species richness has been underestimated, especially in poorly-sampled regions of the Purus-Madeira interfluve, and the east bank of the upper Madeira river, which are currently threatened by an extensive deforestation [22–24]. In this study, we investigated the species richness of *Scinax* treefrogs in the Purus-Madeira interfluve and along the eastern bank of the upper Madeira river, combining molecular, morphological and bioacoustic evidence.

Materials and Methods

Study area

The study area is located south of the Amazon river in the Brazilian states of Amazonas and Rondônia, and includes the interfluve between the Purus and Madeira rivers (PMIR) and the eastern bank of the upper Madeira (EBMR; Fig 1). It covers an area of approximately 15.4 million hectares and contains a complex network of water bodies [24]. The soil is mostly characterized as plinthosols [25], with a predominance of silt [26]. The Madeira river is the main tributary of the Amazon and its basin covers approximately 1.4 million km^2. On a regional scale, the topography of PMIR and RBMD is relatively flat, with elevation ranging from 27 to 80 m amsl. At the local scale, elevation ranges between one and three meters, promoting the occurrence of temporary ponds in lower-lying areas during the rainy season [27]. On a coarse scale, the northern portion of PMIR is covered by tropical lowland rainforest with emergent canopy, while open lowland rainforest with palm trees occurs in the southern portion of PMIR and EBMR ([28], Fig 1A).

Sampling design, collection effort and ethics

We collected data in 18 RAPELD sampling modules [29] distributed across a geographical transect of approximately 1000 km transect (15 modules in the PMIR and three modules in the EBMR; Fig 1). Each sampling module (hereafter abbreviated as M, followed by the number of each sampling unit) contained two parallel trails of 5 km each, spaced 1 km apart. Each trail contained five plots with a standardized area of 2500 m^2 (250 m in length and 10 m in wide),

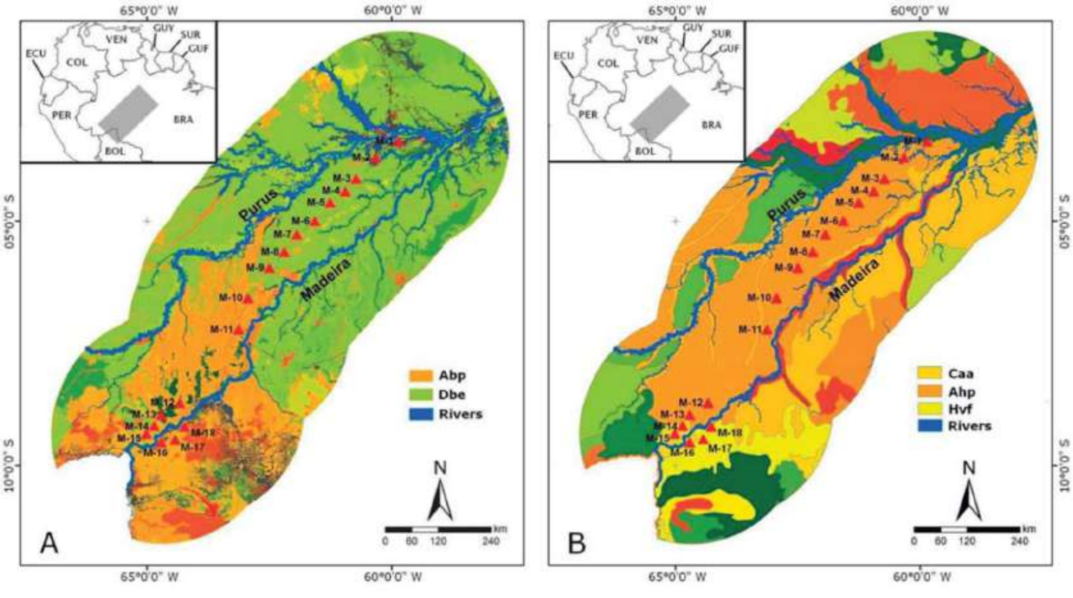

Fig 1. Sampling area in the Purus-Madeira interfluve and on the east bank of the upper Madeira river, Brazilian Amazonia. (A) Vegetation cover types. (B) Soil types. Abbreviations: BR, Brazil; M1–M18, RAPELD sampling modules; Abp, lowland ombrophilous open forest with palm trees; Dbe, lowland ombrophilous dense forest with emergent canopy; Caa, Chromic-Alumic Acrisol; Ahp, Alumic-Humic Plinthosol; Hvf, Hyperdystri-Vetic Ferralsol. The small insert in each map shows part of South America and abbreviated names of countries. The transverse gray bar represents the study area and adjacent territory.

doi:10.1371/journal.pone.0165679.g001

totaling 10 plots per module. To minimize environmental heterogeneity within each sampling unit, the outline of each plot followed local topographic contours [29].

We sampled frogs using visual search (adapted from [30]) and auditory searches for calling males. Plots from M1–M11 were sampled three times each during the rainy season (November–March) between 2013 and 2014, and the plots M12–M18 were sampled three times each during the rainy season (October–March) between 2011 and 2014. In addition, we collected adults and tadpoles when this were encountered on the individual trails and the areas surrounding the sampling modules. Adults and tadpoles were anesthetized and killed with a solution of 10% benzocaine. After death, adults were fixed in 10% formaldehyde solution and stored in 70% ethanol, tadpoles were fixed and stored in 5% formaldehyde solution. Specimens were deposited in the herpetological collection of Instituto Nacional de Pesquisas da Amazônia (INPA-H), Manaus, Amazonas, Brazil (S2 Appendix).

Specimens were collected from M12 to M18 under IBAMA/SISBIO permit number 02001.000508/ 2008–99, and from M1 to M11 under ICMBio/RAN permit number Reg. 659755 Number 13777. IBAMA and ICMBio are institutes of Ministry of Environment, Government of Brazil. These permits were subject to approval of all procedures for collecting and euthanizing frogs.

DNA extraction and sequence alignment

Genomic DNA was extracted from muscle tissue using the Wizard Genomic DNA Purification Kit (Promega Corporation, USA), following the manufacturer's protocol. We used the 16sa-L (or 16sar-L) (`CGC CTG TTT ATC AAA AAC AT`) and the 16sbr-H (`GCC GTC TGA ACT CAG ATC GCA T`) primers [31] to amplify ribosomal DNA fragments of the gene 16S. These fragments were amplified via polymerase chain reaction (PCR) using a mixture with a final volume of 15 μL, containing 5.7 μL of ddH2O, 1.5 μL of 25 mM $MgCl_2$, 1.5 μL of 10 mM dNTPs (2.5mM in each dNTP), 1.5 μL of 10X amplification buffer (75 mM Tris HCl, 50 mM KCl, 20 mM (NH4) 2SO4), 1.5 μL of 2 μM solution of each of the two primers, 0.3 μL of Taq DNA polymerase 5 U / μL (Life Technologies, USA) and 1.5μL of DNA (about 30 ng / μL). The reaction conditions had a pre-heating step at 73°C for 60 s, 35 cycles of denaturation at 92°C for 10 s, primer annealing at 50°C for 35 s, and primer extension at 72°C for 90 s, followed by a final extension step of five minutes at 72°C. Prior to the sequencing reactions, PCR products were purified with Exonuclease I and Thermosensitive Alkaline Phosphatase following manufacturer recommendations (Thermo Fisher Scientific, USA) and followed ABI BigDye Terminator Cycle Sequencing Kit protocols (Life Technologies, USA), as indicated by the manufacturer. The forward primer was used in sequencing reactions, with an annealing temperature of 50°C. The resulting single-stranded products were solved in an ABI 3130xl automatic sequencer. Base calls were verified by viewing electropherograms in Geneious [32] and sequences obtained were aligned using Clustal W algorithm [33] implemented in BioEdit [34] and checked by eye.

Candidate species delimitation

The concept of candidate species adopted in this study follows the subcategories proposed by [35]: Unconfirmed Candidate Species (UCS) corresponds to a genetically distinct lineage, for which no morphological and/or bioacoustic data are available; Deep Conspecific Lineages (DCL) represent lineages that are genetically divergent, but species cannot be differentiated by morphological and/or bioacoustic data; Confirmed Candidate Species (CCS) corresponds to a lineage that usually shows genetic divergence and can be differentiated by morphological and/or bioacoustic data, but which is not formally described as a nominal species.

Molecular approach. Unlike [35] and [36] that used genetic distance as molecular evidence in classifying genetic lineages, we opted for two automated barcoding algorithms as molecular evidence to delineate lineages of *Scinax*. When there was a discrepancy between the results from Automatic Barcoding Gap Discovery (ABGD) and Generalized Mixed Yule Coalescent (GMYC) for a set of lineages, we used the most conservative result, except in cases where morphological and/or bioacoustic evidence supported the less conservative approach.

The first algorithm used, ABGD [37], first estimates the genetic distance between pairs of aligned sequences from a matrix. It then statistically infers potential gaps as the minimum in the distribution of pairwise distances by dividing the sequences in a way that the distance between two sequences of different groups is greater than the distance between two sequences within a group [37]. The algorithm was performed via the web interface (http://wwwabi.snv.jussieu.fr/public/abgd/abgdweb.html) with the following priors: Kimura-two-parameters nucleotide substitution model—K2P [38], ten recursive steps, gap width of 1.0 and value of intraspecific divergence of 0.003 (3%). We opted for K2P distance because this is the most used method in barcoding analysis [39], as it effectiveness is similar to more complex models [40]. The use of a 3% divergence in the 16S rRNA in ABGD analysis has been recommended as an appropriate value for interspecific divergence when classifying lineages of Neotropical and Malagasy frogs as possible candidate species [41–42].

The magnitude of intraspecific differences can vary among lineages of anurans [41, 43]. The sole use of distance-based DNA barcoding methods can introduce errors in species delimitation [35]. To minimize these potential errors in our delimitation, we used GMYC [44] as additional algorithm based on branching patterns: branching patterns within clades reflect genetic neutral coalescing processes occurring within species [45], while branching among clusters reflect the timing of speciation events [46]. The GMYC algorithm assesses the difference in the degree of branching between these two modes of lineages evolution, through estimation of the point of greatest probability of transition between them by using likelihood-based analysis [44]. We used the single-threshold approach, which estimates a single point of transition between intra and interspecific coalescence rates [44, 47]. The GMYC was implemented in the SPLITS package (available http://r-forge.r-project.org/projects/splits) through the platform R [48]. Because the GMYC uses genealogical information rather than genetic distances, the algorithm requires an ultrametric genealogical tree as input.

We estimated an ultrametric genealogical tree using 16S rRNA sequences of 55 specimens of *Scinax* from PMIR and EBMR samples. Additionally, we selected 61 sequences available in Genbank but from species not previously assigned to any species group in the *S. ruber* Clade (S1 Table). As outgroup, we used seven 16S rRNA sequences from members of *Scinax rostratus* species Group, as well as *Julianus uruguayus* and *Ololygon berthae*. Ultrametric genealogical tree was estimated with BEAST software version 1.8.2 [49]. The nucleotide substitution model GTR + I + G was selected via Akaike Information Criterion [50] through jModeltest 2.1.7 [51]. The priors used for obtaining the ultrametric tree were lognormal uncorrelated relaxed clock model, substitution rate of 7.35×10^{-3} / site / Ma [median of ucld.mean parameter (95% HPD = $6.1–8.7 \times 10^{-3}$)], coalescent constant size tree and random starting tree. The substitution rate used here for the 16S rRNA was obtained from [43] which inferred Bayesian genealogical dates for 216 species of Hylidae, including species of the genus *Scinax*. Three individual runs of 100 million generations each were performed in BEAST and they were sampled every 10,000 steps, totaling a posterior distribution of 10,000 trees per running. The stationarity of the posterior distributions, the effective sample size (effective sample sizes—ESS; > 200) and the convergence between runs were examined using Tracer v1.6 [52]. We combined the files containing trees after discarding the first 10% using LogCombiner v1.8.2 [49], and we built the Maximum Clade Credibility (MCC) tree using TreeAnnotator v1.8.2 [49].

In addition, we estimated interspecific pairwise distances K2P [38] between *Scinax* from PMIR and EBMR, and related species using MEGA 6.06 [53]. The distances are summarized in S2 Table.

Morphological approach. We used morphological data to compare our specimens with described *Scinax* species. The following diagnostic characters, all classically used in *Scinax* taxonomy, were evaluated: head shape, snout shape, skin texture, toe webbing, adult body color, and adult iris color. Additionally, ten morphometric characters were measured with digital calipers in adult specimens, according to [54]: SVL (snout-vent length), HL (head length), HW (head width), ED (horizontal eye diameter), UEW (upper eyelid width) IND (internarial distance), IOD (interorbital distance), TD (horizontal tympanum diameter), TL (tibia length) and FL (foot length). The following characters were measured according to [55]: END (eye-nostril distance), 3FD (third finger disk diameter), 4TD (fourth toe disk diameter). Length of tarsus (TAL), hand (HAL) and thigh (THL) followed [56]. Webbing formulae followed [57] as modified by [58]. Color in life was described based on field observations and color photographs of live specimens. See S3 Table for morphometric data.

Bioacoustic approach. Spectral and temporal parameters used in the diagnosis of *Scinax* species were obtained from 109 recordings of advertisement calls of different *Scinax* specimens taken in the study area. As the advertisement call of *Scinax* is characterized by one note we analyzed the following acoustic characteristics: note duration (s), number of pulses per note, pulse duration (s), pulse repetition rate (pulse/s), and fundamental frequency (Hz) of the note. The calls were analyzed through oscillograms and spectrograms (Blackman window, 80 Hz of frequency resolution and 1,024 data points of Discrete Fourier Transform-DFT) generated with Raven 1.5 software [59].

Bioacoustic parameters were compared with data available in the formal descriptions of the species or descriptions of advertisement calls from (or near) the type locality of each nominal species. Differences in fundamental frequency, duration of the note and pulse repetition rate are frequently used to differentiate *Scinax* species (e.g. [60–62, 10, 63]). Therefore, as opposed to [35], and following to [36], quantitative differences between calls were considered sufficient to set the CCS lineages. The advertisement call parameters from the candidate species are available in S4 Table. Advertisement call recordings were stored in the bioacoustic library of the Research Program on Biodiversity (PPBio) from Instituto Nacional de Pesquisas da Amazônia (https://ppbio.inpa.gov.br/en/home), Manaus, Brazil.

Results

Candidate species delimitation

Barcoding analysis revealed the occurrence of 12 (GMYC) and 13 (ABGD) putative units of *Scinax* in the PMIR and EBMR samples (Fig 2). GMYC and ABGD were discordant in the definition of three sets of putative units. Unlike the GMYC, the ABGD approach delineated two distinct units under the epithet *S. chiquitanus* (*S. chiquitanus* BOL and *S. chiquitanus* BRA). However, the GMYC-based delimitation is supported by morphology and advertisement call (see next paragraph). In addition, GMYC delimited *S. ruber* specimens from the central Purus-Madeira interfluve, east bank of the Madeira river and Bolivia [36] as a unique putative unity, while ABGD divided them into two distinct units. Due to lack of morphological and bioacoustic evidence, we opted for the GMYC conservative delimitation. *Scinax ruber* PM from the northern Purus-Madeira interfluve was classified as a putative unit by ABGD, differing in this from GMYC, which delimited *S. ruber* from Peru, *S. ruber* A, *S. ruber* B, *S. x-signatus* and *S. ruber* PM as a single putative unit. We opted for the ABGD delimitation, considering that this method reconstructed the delimitation proposed by [7], which used nuclear and mitochondrial

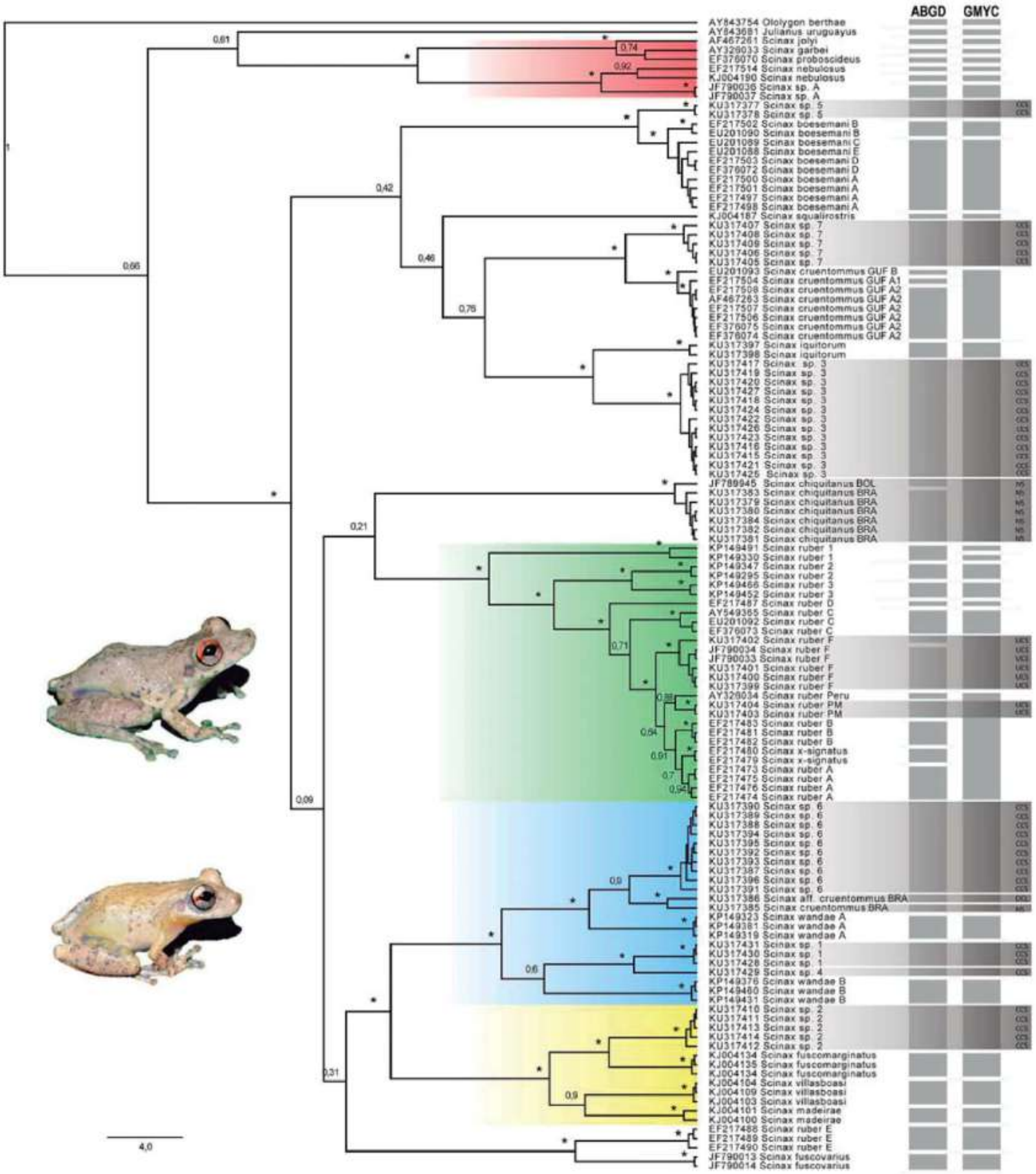

Fig 2. Maximum clade-credibility tree of *Scinax* from the Purus-Madeira interfluve and the east bank of the upper Madeira (Brazilian Amazonia) and correlated species. The 16S gene tree was recovered by Bayesian analyses in BEAST. Posterior probabilities are given near the nodes. Asterisks indicate PP > 0.95. Vertical gray bars indicate species delimitation with the molecular approach. Horizontal gray bars indicate species delimitation with the integrative approach. Colored areas in topology represent, from top to bottom, the *S. rostratus* species Group (red), *S. ruber* Clade (green), *S. wandae* Clade (blue), and *S. fuscomarginatus* Clade (yellow). Outgroup: members of *Scinax rostratus* species Group, plus *Julianus uruguayus* and *Ololygon berthae*. Abbreviations: ABGD, Automatic Barcoding Gap Discovery; GMYC, Generalized Mixed Yule Coalescent; CCS, Confirmed Candidate Species; UCS, Unconfirmed Candidate Species; DCL, Deep Conspecific Lineage; NS, Nominal Species.

doi:10.1371/journal.pone.0165679.g002

markers. There was concordance between GMYC and ABGD for the other putative units occurring in the study area.

Morphology and/or advertisement calls were able to differentiate most of the OTUs in PMIR and EBMR. *Scinax* sp. 1 differs morphologically from *Scinax* sp. 4 (SVL, supernumerary tubercles and dorsal coloration), *Scinax* sp. 6 (SVL, relative head length, TD/ED, relative length of Toe I, shape of dentigerous processes of vomers, dorsal coloration), *S. wandae* A (snout shape, dorsal skin texture, dorsal coloration), *S. wandae* B (dorsal coloration, dorsal skin texture) and morphologically and bioacoustically from *S. cruentommus* (SVL, relative length of Toe I, shape of dentigerous processes of vomers, dorsal coloration; call duration, number of pulses/note, pulse repetition rate, and dominant call frequency [64–65]). *Scinax* sp. 2 can be distinguished morphologically and bioacoustically from *S. fuscomarginatus* (snout shape, dorsal coloration pattern of tibia; note duration and dominant call frequency; [10]) and *S. madeirae* (dorsal coloration pattern of tibia and infraocular; note duration and dominant call frequency); and morphologically from *S. villasboasi* (snout shape, relative toe length II-III, toe webbing, color pattern of dorsum and of tibia). *Scinax* sp. 3 can be distinguished from *S. iquitorum* by the proportion of head and foot in adult specimens, and dorsal and ventral color pattern. *Scinax* sp. 4 differs morphologically from *Scinax* sp. 6 (SVL, supernumerary tubercles, and toe webbing), *S. wandae* A (snout shape, dorsal skin texture, dorsal coloration), *S. wandae* B (dorsal coloration, dorsal skin texture) and *S. cruentommus* (head shape, relative length of toe III and IV, skin texture of perianal area). *Scinax* sp. 5 differs from Guiana and French Guiana specimens of *S. boesemani* in color pattern of dorsum and venter. *Scinax* sp. 6 differs from *S. wandae* A (snout shape, dorsal skin texture, dorsal coloration), *S. wandae B* (dorsal coloration, dorsal skin texture) and *S. cruentommus* (supernumerary tubercles on the finger I, outer metatarsal tubercle shape, *canthus rostralis* shape and relative length of finger discs). *Scinax* aff. *cruentommus* BRA cannot be distinguished from *S. cruentommus* by morphology. *Scinax ruber* F and *S. ruber* PM are distinguished from each other by snout shape. The morphology and advertisement call of *S. chiquitanus* BRA are very similar to those of *S. chiquitanus* BOL.

The integration of molecular, morphological and bioacoustic evidence allowed the delineation of more species of *Scinax* than there are available epithets from the PMIR and EBMR. Our integrative analysis revealed seven CCS lineages (*Scinax* sp. 1–7), two UCS (*Scinax ruber* F and *S. ruber* PM), one DCL (*Scinax* aff. *cruentommus* BRA) and only two nominal species (*S. chiquitanus* BRA and *S. cruentommus* BRA) (Fig 3). *Scinax ruber* PM (UCS), *S.* aff. *cruentommus* BRA (DCL) and the seven CCS lineages delimited in this study were unknown until the current study. *Scinax chiquitanus* and *S. ruber* F are recorded for the first time in Brazil. If CCS and UCS are considered as lineages that represent undescribed species, 82% of the *Scinax* species richness in the PMIR and EBMR is not described, an increase of 450% in the currently-known regional species richness. More broadly, taking into account the lineages that are not associated with any species group occurring in the Brazilian Amazonia, 30% of the overall *Scinax* species richness revealed in this study is not formally described, representing an increase of 43% in the number of *Scinax* species currently-known.

Our 16S gene tree strongly supports three major clades where most of the OTUs from PMIR and EBMR were included. The *Scinax wandae* Clade comprises *S. cruentommus* BRA, *S.* aff. *cruentommus* BRA, *S. wandae* A, *S. wandae* B, *Scinax* sp. 1, *Scinax* sp. 4 and *Scinax* sp. 6. Pairwise genetic distances within the *S. wandae* Clade range from 2 to 14%, with the shortest distance recorded between *S.* aff. *cruentommus* BRA and. *S. cruentommus* BRA (2%). The *Scinax fuscomarginatus* Clade contains *S. fuscomarginatus*, *S. madeirae*, *S. villasboasi* and *Scinax* sp. 2. The pairwise genetic distances between *Scinax* sp. 2 and other members of this clade range from 8 to 12%. The *Scinax wandae* Clade and *S. fuscomarginatus* Clade are reciprocally monophyletic. *Scinax ruber* F and *S. ruber* PM were included within the highly supported clade

Fig 3. Specimens of *Scinax* from the Purus-Madeira interfluve and east bank of the upper Madeira River, Brazilian Amazonia. (A) *Scinax* sp. 1, male, SVL 20.2 mm, INPA-H 34688, from M-9. (B) *Scinax* sp. 2, male, SVL 18.1 mm, INPA-H 34667, from M-11. (C) *Scinax* sp. 3, male, SVL 31.3 mm, INPA-H 34584, from M-7. (D) *Scinax* sp. 5, male, not collected, from M-8. (E) *Scinax* sp. 6, male, SVL 25.2 mm, INPA-H 35562, from M-17. (F) *Scinax* sp. 7, male, SVL 23.9 mm, INPA-H 34623, from M-8. (G) *Scinax* aff. *cruentommus* BRA, male, SVL 25.4 mm, INPA-H 34596, from M-6. (H) *Scinax ruber* PM, couple, not collected. (I) *Scinax chiquitanus* BRA, female, SVL 33.7 mm, INPA-H 35554; male, 31.1 mm, INPA-H 35555, from M-14. Photographs by R. Fraga.

doi:10.1371/journal.pone.0165679.g003

containing *S. ruber* A–D, *S. ruber* Peru, and *S. x-signatus*. In turn, this clade is the sister of *S. ruber* 2 + *S. ruber* 3 and forms a major clade with *S. ruber* 1, the latter in basal position. Pairwise genetic distances among *S. ruber* F and *S. ruber* PM from other *S. ruber* OTUs (except *S. ruber* E) range from 2 to 11%. *Scinax ruber* E is placed as the sister of *S. fuscovarius* and so questions the monophyly of the currently recognized *S. ruber* OTUs. The distances between *S. ruber* E and other *S. ruber* OTUs range from 18 to 29%.

Discussion

Barcoding methods

We used the algorithms ABGD and GMYC to define *Scinax* candidate species in this study. Despite differences, in most cases, there was a convergence of both algorithms in delimitating *Scinax* candidate species from the study area. For the data set involving all putative units in the MCC tree, and using the candidate species proposed by [7, 66] as a reference (delimitated by using more than one molecular marker), ABGD showed greater accuracy in defining the candidate species when compared to GMYC, as this letter method tended to group two or more candidate species.

The incongruity between the results from ABGD and GMYC obtained in this study may be explained by the quality characteristics of the dataset quality. Although GMYC is a robust algorithm such conditions as the presence of gaps, large number of singletons and low species richness [67], the algorithm is sensitive to small genetic differences between species [68], which have been found between most of the species in the *S. ruber* Clade [7] [this study]. In turn, the main factor influencing the ABGD delimitation is the value of interspecific genetic divergence defined *a priori* [37], which requires existing knowledge of the target group. Despite the differences in the GMYC and ABGD delimitations, results highlight the importance of the use of both these barcoding algorithms as molecular evidence in integrative analyses. The use of just one algorithm in our data set would have given less accurate lineage delimitation.

Species richness and conservation

We used for the first time integrated molecular, morphological and bioacoustic data to evaluate species richness of *Scinax* treefrogs at a regional scale in Amazonia. Like other studies that have used an integrative approach to address frog richness in this biome (*e.g.* [2, 5, 36, 69]), our results show that the knowledge of the species diversity of Amazonian frogs is highly inadequate. The underestimation of Amazonian species of *Scinax* (30%) is similar to the percentage of unnamed amphibian species proposed by [70] for the whole Neotropics (39%). However, at a regional scale (PMIR and EBMR), the proportion of unidentified *Scinax* species is more than twice as high (82%) as the estimates for the Neotropics. The increase in the known *Scinax* species richness from the PMIR and EBMR (450%) is the highest increase in Amazonian frog diversity ever reported, being greater than estimates proposed in studies involving the genera *Engystomops* (150–250% [5]), *Hypsiboas* (200–350% [5]), *Osteocephalus* (37.5%–300% [3, 69]), and *Pristimantis* (200% [71]). Despite the cryptic diversity [7, 21] and the complex taxonomic history of several *Scinax* species, the high proportion of undescribed species found in the region of PMIR and EBMR is mainly due to (1) integration of different lines of evidence in the species identification process, and (2) the fact that the region represents one of the most poorly-studied areas in Brazilian Amazonia [72]. Our results suggest that further integrative studies of anurans from poorly investigated parts of the biome may significantly contribute to an improved knowledge of the real anuran diversity of the region and improve our understanding of the overall biodiversity of the Neotropics.

Unfortunately, most of the study area is threatened by infrastructure development associated with human settlements. The PMIR is intersected by the BR-319 federal highway. Although it was partially abandoned a few years after its construction in 1973 [22], the presence of the highway facilitated the process of deforestation in the region, coming especially from the state of Rondônia [22]. Currently, the BR-319 is being repaired and resurfaced, and modeling studies have predicted the resulting deforestation of up to 5.4 million hectares by 2050, which represents approximately one-third of the total area of the interfluve [23–24]. In addition to the imminent threat of reconstruction of the BR-319, the construction of two large hydroelectric projects on the southern PMIR and EBMR (Porto Velho, Rondônia) also threatens the high biodiversity of the area [22]. This is an alarming scenario for the conservation of local *Scinax* populations, considering that only two CCS lineages (*Scinax* sp. 2 and *S.* sp. 5) and two UCS lineages (*Scinax ruber* F and *S. ruber* PM) are known to be tolerant of habitat disturbance. Species with small geographic ranges are usually more susceptible to anthropogenic threats than widely distributed species [73–74]. Despite the high sampling effort, two CCS lineages (*Scinax* sp. 1, *S.* sp. 4) that inhabit the forested habitats were found in only one locality in the PMIR. The only sampling module in which *Scinax* sp. 4 was registered is currently under heavy pressure from illegal logging (M. Ferrão, personal communication). In addition, a rapid increase of deforestation of the northern region of the BR-319 is predicted by [24]. Considering a combination of current anthropic disturbance and limited range, *Scinax* sp. 4 may be classified as an endangered species.

Description of new species may contribute to identification of priority areas for biodiversity conservation [75], which potentially results in protection and management of natural resources [76]. Contrarily, lack of formal description of new species has led to neglect hundreds of species when mapping priority areas for conservation (e.g. [77]). Since formally named species are important for habitat and biodiversity assessment, especially in such threatened landscapes as the study area, descriptions of the seven CCS disclosed here will be the subject of our future papers.

Systematic remarks

Contrary to [17], this study did not place *Julianus* Duellman, Marion and Hedges, 2016 in a sister position to the genus *Scinax*. In our 16S gene tree, *Julianus uruguayus* (Schmidt, 1944) represents a sister lineage to the *Scinax rostratus* species Group (with low support), and together with it forms a sister clade to all remaining species of *Scinax* (with low support). This arrangement may be an artifact of our use of only one locus in our analyses. On the other hand, our 16S gene tree strongly supports the *S. rostratus* species Group as a monophyletic unit, as previously recognized by [18, 78–79]. Additionally, most of our OTUs were placed in three major clades (*S. fuscomarginatus*, *S. ruber*, *S. wandae*) by our phylogenetic analyses. Strong Bayesian support for both clades may be interpreted as evidence of species grouping. Nevertheless, a more extensive sampling and an appropriate morphological and phylogenetic approach will be required to better delimitate individual species groups.

Scinax cruentommus has been widely reported from Peru, Brazil, Ecuador and Colombia [65], and from French Guiana [7, 42, 80–82]. In our barcoding analyses, a *Scinax* specimen from PMIR identified as *S. cruentommus* (*S. cruentommus* BRA) differs from *S. cruentommus* GUF (*sensu* [7, 42, 80–81]) with genetic distances of 31 to 32%. Unlike *S. cruentommus* BRA, specimens of *S. cruentommus* GUF do not possess a horizontal red bar in the iris (see Figure 5 in [81]), which [64] proposed as an important diagnostic character of *S. cruentommus*. Moreover, notable differences between advertisement call of *S. cruentommus* from the upper Negro river (Amazonas, Brazil) and *S. cruentommus* from French Guiana (*sensu* [82]) were reported by [65]. Based on this evidence, and in the proposition that widely-distributed small-sized frogs may potentially represent species complexes [2, 5, 7, 21, 43, 71, 83], we argue that there is likely to be more than one species associated with the name *S. cruentommus*, and that specimens from French Guiana called *S. cruentommus* represent a different, and undescribed, taxon.

Scinax ruber F and *S. ruber* PM from PMIR and EBMR placed in the *Scinax ruber* Clade, as did *S. ruber* 1–3 from Colombia (in basal position). Although there is no doubt about the validity of the name *S. ruber* [19], the strong variance in pairwise genetic distance between all OTUs in this clade plus *S. ruber* E (1% to 29%) suggests cryptic diversity [7, 66] [this study], as well as misidentification (perhaps for *S. ruber* E and *S. x-signatus* from French Guiana). The different *Scinax* forms which this name has been applied are distributed over a wide geographic area (Brazil, French Guiana, Surinam, Colombia, Ecuador, Peru, Bolivia) indicating the need for a thorough revision. Investigation of morphological, bioacoustic and genetic characteristics of *S. ruber* from its neotype locality (Paramaribo, Surinam) might be the first step in resolving this taxonomic problem. This should then be followed by a collaborative international effort to clarify the taxonomic status and the evolutionary relationships of different OTUs related to *S. ruber*.

Supporting Information

S1 Appendix. Formulae for cryptic diversity estimates.
(PDF)

S2 Appendix. List of specimens examined for the morphological comparisons.
(PDF)

S1 Table. Specimens examined, voucher numbers, localities, and GenBank accession numbers.
(PDF)

S2 Table. Genetic divergence between *Scinax* species from the Purus-Madeira interfluve and east bank of the Upper Madeira river and related species.
(PDF)

S3 Table. Morphometric data of *Scinax* species from the Purus-Madeira interfluve and east bank of the upper Madeira river, Brazilian Amazonia.
(PDF)

S4 Table. Temporal and spectral parameters of the advertisement call of *Scinax* species from the Purus-Madeira interfluve and east bank of the upper Madeira river, Brazilian Amazonia.
(PDF)

Acknowledgments

We thank William Etges, Edgar Lehr and an anonymous reviewer for their suggestions on this manuscript; Santo Antônio Energia S.A. for support with the fieldwork on the upper Madeira river; Centro de Estudos Integrados da Biodiversidade Amazônica (CENBAM) for assistance with fieldwork at the northern interfluve between the Purus and Madeira rivers; Fernanda Werneck and Ariane Silva for access to the INPA-H zoological collection; Alexandre Pinheiro de Almeida for the advertisement call of *Scinax* sp. 3. Adrian Barnett helped with the English. While conducting this study Miquéias Ferrão had a fellowship from the Conselho Nacional de Desenvolvimento Científico e Tecnológico (CNPq) under grant CNPq—proc. 573721/2008-4, via Centro de Estudos Integrados da Biodiversidade Amazônica (CENBAM), while conducting this study. Currently, Miquéias Ferrão receives a PhD scholarship from the Fundação de Amparo à Pesquisa do Estado do Amazonas (FAPEAM). Rafael de Fraga had a PhD scholarship from the Coordenação de Aperfeiçoamento de Pessoal de Nível Superior (CAPES). Work of Jiří Moravec was financially supported by Ministry of Culture of the Czech Republic (DKRVO 2016/15, National Museum, 00023272).

Author Contributions

Conceptualization: MF.

Formal analysis: MF.

Funding acquisition: APL JM.

Methodology: MF RF OC.

Project administration: APL ILK.

Visualization: MF.

Writing – original draft: MF.

Writing – review & editing: MF RF JM ILK APL.

References

1. Stuart SN, Chanson JS, Cox NA, Young BE, Rodrigues ASL, Fischman DL, et al. Status and trends of amphibian declines and extinctions worldwide. Science. 2004; 306: 1783–1786. doi: 10.1126/science.1103538 PMID: 15486254
2. Fouquet A, Cassini CS, Haddad CFB, Pech N, Rodrigues MT. Species delimitation, patterns of diversification and historical biogeography of theNeotropical frog genus *Adenomera* (Anura, Leptodactylidae). J Biogeogr. 2013; 41(5): 855–870. doi: 10.1111/jbi.12250
3. Jungfer KH, Faivovich J, Padial JM, Castroviejo-Fisher S, Lyra MM, Berneck B, et al. Systematics of spiny-backed treefrogs (Hylidae: *Osteocephalus*): An Amazonian puzzle. Zool Scr. 2013; 42: 351–380. doi: 10.1111/zsc.12015
4. Fouquet A, Loebmann D, Castroviejo-Fisher S, Padial JM, Orrico VGD, Lyra ML, et al. From Amazonia to the Atlantic forest: Molecular phylogeny of Phyzelaphryninae frogs reveals unexpected diversity and a striking biogeographic pattern emphasizing conservation challenges. Mol Phylogenet Evol. 2012; 65 (2): 547–561. doi: 10.1016/j.ympev.2012.07.012 PMID: 22842094
5. Funk WC, Caminer M, Ron SR. High levels of cryptic species diversity uncovered in Amazonian frogs. Proc R Soc Lond B Biol Sci. 2012; 279: 1806–1814. doi: 10.1098/rspb.2011.1653 PMID: 22130600
6. Caminer MA, Ron SR. Systematics of treefrogs of the *Hypsiboas calcaratus* and *Hypsiboas fasciatus* species complex (Anura, Hylidae) with the description of four new species. Zookeys. 2014; 370: 1–68. doi: 10.3897/zookeys.370.6291 PMID: 24478591
7. Fouquet A, Vences M, Salducci MD, Meyer A, Marty C, Gilles A. Revealing cryptic diversity using molecular phylogenetics and phylogeography in frogs of the *Scinax ruber* and *Rhinella margaritifera* species groups. Mol Phylogenet Evol. 2007a; 43: 567–582. doi: 10.1016/j.ympev.2006.12.006 PMID: 17303441
8. Pombal JPJ, Bastos RP, Haddad CFB. Vocalizações de algumas espécies do gênero *Scinax* (Anura, Hylidae) do Sudeste do Brasil e comentários taxonômicos. Naturalia. 1995; 20: 213–225.
9. Nunes I, Kwet A, Pombal JPJ. Taxonomic revision of the *Scinax alter* species complex (Anura: Hylidae). Copeia. 2012; 2012(3): 554–569. doi: 10.1643/CH-11-088
10. Brusquetti F, Jansen M, Barrio-Amarós C, Segalla M, Haddad CFB. Taxonomic review of *Scinax fuscomarginatus* (Lutz, 1925) and related species (Anura; Hylidae). Zool J Linn Soc. 2014; 171: 783–821. doi: 10.1111/zoj.12148
11. Padial JM, De la Riva I. Integrative taxonomy reveals cryptic Amazonian species of *Pristimantis* (Anura). Zool J Linn Soc. 2009; 155: 97–122. doi: 10.1111/j.1096-3642.2008.00424.x
12. Simões PI, Lima AP, Farias I. The description of a cryptic species related to the pan-Amazonian frog *Allobates femoralis*. Zootaxa. 2010; 2406: 1–28.
13. Simões PI, Kaefer IL, Farias IP, Lima AP. An integrative appraisal of the diagnosis and distribution of *Allobates sumtuosus* (Morales, 2002) (Anura, Aromobatidae). Zootaxa. 2013; 3746: 401–421. doi: 10.11646/zootaxa.3746.3.1 PMID: 25113485
14. Lima AP, Simões PI, Kaefer IL. A new species of *Allobates* (Anura: Aromobatidae) from the Tapajós River basin, Pará State, Brazil. Zootaxa. 2014; 3889(3): 355–387. doi: 10.11646/zootaxa.3980.4.3 PMID: 26249969
15. Lima AP, Simões PI, Kaefer IL. A new species of *Allobates* (Anura: Aromobatidae) from Parque Nacional da Amazônia, Pará State, Brazil. Zootaxa. 2015; 3980(4): 501–525. doi: 10.11646/zootaxa.3980.4.3 PMID: 26249969
16. Kaefer IL, Tsuji-Nishikido BM, Mota EP, Farias IP, Lima AP. The early stages of speciation in Amazonian forest frogs: phenotypic conservatism despite strong genetic structure. Evol Biol. 2013; 40: 228–245. doi: 10.1007/s11692-012-9205-4
17. Duellman WE, Marion AB, Hedges SB. Phylogenetics, Classification, and Biogeography of the Treefrogs (Amphibia: Anura: Arboranae). Zootaxa. 2016; 4104(1): 1–109. doi: 10.11646/zootaxa.4104.1.1 PMID: 27394762
18. Faivovich J, Haddad CFB, Garcia PCA, Frost DR, Campbell JA, Weeler WC. Systematic review of the frog family Hylidae, with special reference to Hylinae: phylogenetic analysis and taxonomic revision. Bulletin of the American Museum of Natural History. 2005; 294; 1–240. doi: 10.1206/0003-0090(2005)294[0001:SROTFF]2.0.CO;2

19. Sturaro MJ, Peloso PLV. A new species of *Scinax* Wagler, 1830 (Anura: Hylidae) from the middle Amazon River Basin, Brazil. Pap Avulsos Zool. 2014; 54(2): 9–23. doi: 10.1590/0031-1049.2014.54.02

20. Nogueira L, Solé M, Siqueira S, Affonso PRAM, Strüssmann C, Sampaio I. Genetic analysis reveals candidate species in the *Scinax catharinae* Clade (Amphibia: Anura) from Central Brazil. Genet Mol Biol. 2016; 39(1): 49–53. doi: 10.1590/1678-4685-GMB-2015-0037 PMID: 27007898

21. Menezes L, Canedo C, Batalha-Filho H, Garda AA, Gehara M, et al. Multilocus Phylogeography of the Treefrog *Scinax eurydice* (Anura, Hylidae) Reveals a Plio-Pleistocene Diversification in the Atlantic Forest. PLoS One. 2016; 11(6): e0154626. doi: 10.1371/journal.pone.0154626 PMID: 27248688

22. Fearnside PM, Graça PMLA. BR-319: Brazil's Manaus-Porto Velho Highway and the potential impact of linking the arc of deforestation to central Amazonia. Environ Manage. 2006; 38(5): 705–716. doi: 10.1007/s00267-005-0295-y PMID: 16990982

23. Soares-Filho BS, Nepstad DC, Curran LM, Cerqueira GC, Garcia RA, Azevedo-Ramos C, et al. Modelling conservation in the Amazon basin. Nature. 2006; 440:520–523. doi: 10.1038/nature04389 PMID: 16554817

24. Maldonado FD, Keizer EWH, Graça PMLA, Fearnside PM, Vitel CS. (2012). Previsão temporal da distribuição espacial do desmatamento no interflúvio Purus-Madeira até o ano 2050. In Sousa-Junior WC, Waichman AV, Sinisgalli PAA, Angelis CF, Romeiro AR, editors. Rio Purus: Água, Território e Sociedade na Amazônia Sul-Ocidental. Ecuador: LibriMundi Press; 2012. pp. 183–196.

25. Sombroek W. Amazon landforms and soils relation to biological diversity. Acta Amazon. 2000; 30: 81–100.

26. Cintra BBL, Schietti J, Emilio T, Martins D, Moulatlet G, Souza P, et al. Soil physical restrictions and hydrology regulate stand age and wood biomass turnover rates of Purus—Madeira interfluvial wetlands in Amazonia. Biogeosciences. 2013; 10: 7759–7774. doi: 10.5194/bg-10-7759-2013

27. Rosetti DF, Toledo PM, Góes AM. New geological framework for Western Amazonia (Brazil) and implications for biogeography and evolution. Quat Res. 2015; 63: 78–89. doi: 10.1016/j.yqres.2004.10.001

28. IBGE Instituto Brasileiro de Geografia e Estatística. Recursos naturais e meio ambiente: uma visão do Brasil. Rio de Janeiro: IBGE; 1997.

29. Magnusson WE, Braga-Neto R, Pezzini F, Baccaro F, Bergallo H, Penha J, et al. Biodiversidade e monitoramento ambiental integrado: o sistema rapeld na Amazônia. Santo André: Publisher Attema; 2013.

30. Campbell HW, Christman SP. Field techniques for herpetofaunal community analysis. In Scott NJ Jr, editor. Herpetological Communities: a Symposium of the Society for the Study of Amphibians and Reptiles and the Herpetologists'League. Washington: U.S. Fish Wild. Serv; 1982. pp. 193–200.

31. Palumbi SR, Martin AP, Romano SL, McMillan WO, Stice L, Grabowski G. The sample tool's guide to PCR. Honolulu: University of Hawaii; 1991.

32. Kearse M, Moir R, Wilson A, Stones-Havas S, Cheung M, Sturrock S, et al. Geneious Basic: An integrated and extendable desktop software platform for the organization and analysis of sequence data. Bioinformatics. 2012; 28(12): 1647–1649. doi: 10.1093/bioinformatics/bts199 PMID: 22543367

33. Thompson JD, Higgins DG, Gibson TJ. Clustal W: improving the sensitivity of progressive multiple sequence alignment through sequence weighting, position-specific gap penalties and weight matrix choice. Nucleic Acids Res. 1994; 22(22): 4673–4680. doi: 10.1093/nar/22.22.4673 PMID: 7984417

34. Hall TA. BioEdit: a user-friendly biological sequence alignment editor and analysis program for Windows 95/98/NT. Nucleic Acids Symp Ser. 1999; 41: 95–98.

35. Vieites DR, Wollenberg KC, Andreone F, Köhler J, Glaw F, Vences M. Vast underestimation of Madagascar's biodiversity evidenced by an integrative amphibian inventory. Proc Natl Acad Sci U S A. 2009; 106(20): 8267–72. doi: 10.1073/pnas.0810821106 PMID: 19416818

36. Jansen M, Bloch R, Schulze A, Pfenninger M. Integrative inventory of Bolivia's lowland anurans reveals hidden diversity. Zool Scr. 2011; 40: 567–583. doi: 10.1111/j.1463-6409.2011.00498.x

37. Puillandre N, Lambert A, Brouillet S, Achaz G. ABGD, Automatic Barcode Gap Discovery for primary species delimitation. Mol Ecol. 2012; 21: 1864–1877. doi: 10.1111/j.1365-294X.2011.05239.x PMID: 21883587

38. Kimura M. A simple method for estimating evolutionary rate of base substitutions through comparative studies of nucleotide sequences. J Mol Evol. 1980; 16: 111–120. PMID: 7463489

39. Ward RD. DNA barcode divergence among species and genera of birds and fishes. Mol Ecol Resour. 2009; 9: 1077–1085. doi: 10.1111/j.1755-0998.2009.02541.x PMID: 21564845

40. Collins RA, Boykin LM, Cruickshank RH, Armstrong KF. Barcoding's next top model: an evaluation of nucleotide substitution models for specimen identification. Methods Ecol Evol. 2012; 3: 457–465. doi: 10.1111/j.2041-210X.2011.00176.x

41. Vences M, Thomas M, van der Meijden A, Chiari Y, Vieites D. Comparative performance of the 16S rRNA gene in DNA barcoding of amphibians. Front Zool. 2005; 2: 5. doi: 10.1186/1742-9994-2-5 PMID: 15771783
42. Fouquet A, Gilles A, Vences M, Marty C, Blanc M, Gemmell NJ. Underestimation of species richness in neotropical frogs revealed by mtDNA analyses. PloS One. 2007b; 10: e1109. doi: 10.1371/journal.pone.0001109 PMID: 17971872
43. Gehara M, Crawford AJ, Orrico VGD, Rodríguez A, Lötters S, Fouquet A, et al. High levels of diversity uncovered in a widespread nominal taxon: continental phylogeography of the Neotropical treefrog *Dendropsophus minutus*. PloS One. 2014; 9(9): e103958. doi: 10.1371/journal.pone.0103958 PMID: 25208078
44. Pons J, Barraclough TG, Gomez—Zurita J. Sequence based species delimitation for the DNA taxonomy of undescribed insects. Syst Biol. 2006; 55: 595–609. doi: 10.1080/10635150600852011 PMID: 16967577
45. Kingman JFC. The coalescent. Stoch Process Their Appl. 1982; 13: 235–248. doi: 10.1016/0304-4149(82)90011-4
46. Yule GU. A mathematical theory of evolution based on the conclusions of Dr. J. C. Willis, F.R.S. Philos Trans R Soc Lond B Biol Sci. 1924; 213: 21–87. doi: 10.1098/rstb.1925.0002
47. Fujisawa T, Barraclough TG. Delimiting species using single-locus data and the Generalized Mixed Yule Coalescent approach: a revised method and evaluation on simulated data sets. Syst Biol. 2013; 65: 707–724. doi: 10.1093/sysbio/syt033 PMID: 23681854
48. R Core Team. R: A language and environment for statistical computing. Vienna, Austria: R Foundation for Statistical Computing. 2016. Available: https://cran.r-project.org/doc/manuals/r-release/fullrefman.pdf
49. Drummond AJ, Suchard MA, Xie D, Rambaut A. Bayesian phylogenetics with BEAUti and the BEAST 1.7. Mol Biol Evol. 2012; 29: 1969–1973. doi: 10.1093/molbev/mss075 PMID: 22367748
50. Akaike H. A new look at the statistical model identification. IEEE Trans Automat Contr. 1974; 19(6): 716–723.
51. Darriba D, Taboada GL, Doallo R, Posada D. jModelTest 2: more models, new heuristics and parallel computing. Nat Methods. 2012; 9(8): 772. doi: 10.1038/nmeth.2109 PMID: 22847109
52. Rambaut A, Suchard MA, Drummond AJ. Tracer v1.6. 2014. Available: http://beast.bio.ed.ac.uk/Tracer.
53. Tamura K, Stecher G, Peterson D, Filipski A, Kumar S. MEGA6: Molecular Evolutionary Genetics Analysis version 6.0. Mol Biol Evol. 2013; 30: 2725–2729. doi: 10.1093/molbev/mst197 PMID: 24132122
54. Duellman WE. The hylid frogs of Middle America 1. 1st ed. Lawrence: University of Kansas. 1970
55. Napoli MF. A new species of allied to *Hyla circumdata* (Anura: Hylidae) from Serra da Mantiqueira, southeastern Brazil. Herpetologica. 2005; 61: 63–69. doi: 10.1655/03-41
56. Heyer WR, Rand AS, Cruz CAG, Peixoto OL, Nelson CE. Frogs of Boracéia. Arquivos de Zoologia. 1990; 31: 231–410.
57. Savage JM, Heyer WR. Variation and distribution in the tree-frog genus *Phyllomedusa* in Costa Rica, Central America. Stud Neotrop Fauna Environ. 1967; 5: 111–131.
58. Myers CW, Duellman WE. A new species of *Hyla* from Cerro Colorado, and other tree frog records and geographical notes from Western Panama. Am Mus Novit. 1982; 2752: 1–32.
59. Bioacoustics Research Program. Raven Pro: Interactive Sound Analysis Software. Ver. 1.5. Ithaca: The Cornell Lab of Ornithology: 2015.
60. Duellman WE, Wiens JJ. Hylid frogs of the genus *Scinax* Wagler, 1830, in Amazonian Ecuador and Peru. Occas. pap. Mus. Nat. Hist. (Lawrence). 1993; 153: 1–57.
61. Nunes I, Carvalho RRJ, Pereira EG. A new species of *Scinax* Wagler (Anura: Hylidae) from Cerrado of Brazil. Zootaxa. 2010; 2514: 24–34.
62. Nunes I, Pombal JPJ. A new snouted treefrog of the speciose genus *Scinax* Wagler (Anura, Hylidae) from northeastern Brazil. Herpetologica. 2011; 67(1): 80–88. doi: 10.1655/HERPETOLOGICA-D-10-00026.1
63. Juncá FA, Napoli MF, Nunes I, Mercês EA, Abreu RO. A New Species of the *Scinax ruber* Clade (Anura, Hylidae) from the Espinhaço Range, Northeastern Brazil. Herpetologica. 2015; 71(4): 299–309. doi: 10.1655/HERPETOLOGICA-D-14-00032
64. Duellman WE. A new species of *Hyla* from Amazonian Ecuador. Copeia. 1972; 1972: 265–271.

65. Carvalho TR, Teixeira BFV, Duellman WE, Giaretta A. *Scinax cruentommus* (Anura: Hylidae) in the upper Rio Negro drainage, Amazonas state, Brazil, with the redescription of its advertisement call. Phyllomedusa. 2015; 14(2): 139–146. doi: 10.11606/issn.2316-9079.v14i2p139-146

66. Guarnizo CE, Paz A, Muñoz-Ortiz A, Flechas SV, Méndez-Narvaéz J, Crawford AJ. DNA barcoding survey of anurans across the Eastern Cordillera of Colombia and the impact of the Andes on cryptic diversity. PloS One. 2015; 10(5): e0127312. doi: 10.1371/journal.pone.0127312 PMID: 26000447

67. Talavera G, Dinca V, Vila R. Factors affecting species delimitations with the GMYC model: insights from a butterfly survey. Methods Ecol Evol. 2013; 4: 1101–1110. doi: 10.1111/2041-210X.12107

68. Zhang J, Kapli P, Pavlidis P, Stamatakis A. A general species delimitation method with applications to phylogenetic placements. Bioinformatics. 2013; 29: 2869–2876. doi: 10.1093/bioinformatics/btt499 PMID: 23990417

69. Ron SR, Venegas PJ, Toral E, Read M, Ortiz DA, Manzano AL. Systematics of the *Osteocephalus buckleyi* species complex (Anura: Hylidae) from Ecuador and Peru. ZooKeys. 2012; 229: 1–52. doi: 10.3897/zookeys.229.3580 PMID: 23166473

70. Giam X, Scheffers BR, Sodhi NS, Wilcove DS, Ceballos G, Ehrlich PR. Reservoirs of richness: least disturbed tropical forest are centers of undescribed species diversity. Proc R Soc Lond B Biol Sci. 2011; 279: 67–76. doi: 10.1098/rspb.2011.0433 PMID: 21593037

71. Elmer KR, Dávila JA, Lougheed SC. Cryptic diversity and deep divergence in an upper Amazonian leaflitter frog, *Eleutherodactylus ockendeni*. BMC Evol Biol. 2007; 7: 247. doi: 10.1186/1471-2148-7-247 PMID: 18154647

72. Peloso P.L.V. A safe place for amphibians? A cautionary tale on the taxonomy and conservation of frogs, caecilians, and salamanders in the Brazilian Amazonia. Zoologia (Curitiba). 2010; 27(5): 667–673. doi: 10.1590/S1984-46702010000500001

73. Stuart BL, Inger RF, Voris HK. High level of cryptic species diversity revealed by sympatric lineages of Southeast Asian forest frogs. Biol Lett. 2006; 2: 470–475. doi: 10.1098/rsbl.2006.0505 PMID: 17148433

74. Toledo LF, Batista RF. Integrative Study of Brazilian Anurans: geographic Distribution, Size, Environment, Taxonomy, and Conservation. Biotropica. 2012; 44(6): 785–792. doi: 10.1111/j.1744-7429.2012.00866.x

75. Köhler J, Vieites DR, Bonett RM, Garcia FH, Glaw F, Steinke D, et al. New amphibians and global conservation: A boost in species discoveries in a highly endangered vertebrate group. Bioscience. 2005; 55: 693–696.

76. Bickford D, Lohman DJ, Sodhi NS, Ng PKL, Meier R, Winker K, et al. Cryptic species as a window on diversity and conservation. Trends Ecol Evol. 2007; 22(3): 148–155. doi: 10.1016/j.tree.2006.11.004 PMID: 17129636

77. Jenkins CN, Pimm SL, Joppa LN. Global patterns of terrestrial vertebrate diversity and conservation. Proc Natl Acad Sci U S A. 2013; 110(28): E2602–10. doi: 10.1073/pnas.1302251110 PMID: 23803854

78. Faivovich J. A cladistic analysis of *Scinax* (Anura: Hylidae). Cladistics. 2002; 18(4): 367–393.

79. Wiens JJ, Kuczynski CA, Hua X, Moen DS. An expanded phylogeny of treefrogs (Hylidae) based on nuclear and mitochondrial sequence data. Mol Phylogenet Evol. 2010; 55: 871–882. doi: 10.1016/j.ympev.2010.03.013 PMID: 20304077

80. Salducci MD, Marty C, Chappaz R, Gilles A. Molecular phylogeny of French Guiana Hylinae: implications for the systematic and biodiversity of the neotropical frogs. C R Biol. 2002; 325: 141–153. doi: 10.1016/S1631-0691(02)01423-3 PMID: 11980175

81. Salducci MD, Marty C, Fouquet A, Gilles A. Phylogenetic relationships and biodiversity in Hylids (Anura: Hylidae) from French Guiana. C R Biol. 2005; 328: 1009–1024. doi: 10.1016/j.crvi.2005.07.005 PMID: 16286090

82. Lescure J, Marty C. Atlas des amphibiens de Guyane. Patrimoines Naturales. 2000; 45: 1–388.

83. Ortega-Andrade HM, Rojas-Soto OR, Valencia JH, Espinosa de los Monteros A, Morrone JJ, Ron SR, et al. Insights from integrative systematics reveal cryptic diversity in *Pristimantis* frogs (Anura: Craugastoridae) from the Upper Amazon Basin. Plos One. 2015; 10(11): e0143392. doi: 10.1371/journal.pone.0143392 PMID: 26600198

CAPÍTULO 2

A new species of Amazonian snouted treefrog (Hylidae: *Scinax*) with description of a novel species-habitat association for an aquatic breeding frog. PeerJ 6: e4321. doi: 10.7717/peerj.4321

A new species of Amazonian snouted treefrog (Hylidae: *Scinax*) with description of a novel species-habitat association for an aquatic breeding frog

Miquéias Ferrão[1,2], Rafael de Fraga[1], Jiří Moravec[3], Igor L. Kaefer[1,4] and
Albertina P. Lima[1,5]

[1] Programa de Pós-Graduação em Ecologia, Instituto Nacional de Pesquisas da Amazônia, Manaus, Amazonas, Brazil
[2] Department of Biological Sciences, Macquarie University, Sydney, Australia
[3] Department of Zoology, National Museum, Prague, Czech Republic
[4] Instituto de Ciências Biológicas, Universidade Federal do Amazonas, Manaus, Amazonas, Brazil
[5] Coordenação de Biodiversidade, Instituto Nacional de Pesquisas da Amazônia, Manaus, Amazonas, Brazil

ABSTRACT

The genus *Scinax* is one of the most specious genera of treefrogs of the family Hylidae. Despite the high number of potential new species of *Scinax* revealed in recent studies, the rate of species descriptions for Amazonia has been low in the last decade. A potential cause of this low rate may be the existence of morphologically cryptic species. Describing new species may not only impact the taxonomy and systematics of a group of organisms but also benefit other fields of biology. Ecological studies conducted in megadiverse regions, such as Amazonia, often meet challenging questions concerning insufficient knowledge of organismal alpha taxonomy. Due to that, detecting species-habitat associations is dependent on our ability to properly identify species. In this study, we first provide a description of a new species (including its tadpoles) of the genus *Scinax* distributed along heterogeneous landscapes in southern Amazonia; and secondly assess the influence of environmental heterogeneity on the new species' abundance and distribution. *Scinax ruberoculatus* sp. nov. differs from all nominal congeners by its small size (SVL 22.6–25.9 mm in males and 25.4–27.5 mm in females), by having a dark brown spot on the head and scapular region shaped mainly like the moth *Copiopteryx semiramis* (or a human molar in lateral view, or a triangle), bicolored reddish and grey iris, snout truncate in dorsal view, bilobate vocal sac in males, by its advertisement call consisting of a single pulsed note with duration of 0.134–0.331 s, 10–23 pulses per note, and dominant frequency 1,809–1,895 Hz. Both occurrence and abundance of the new species are significantly influenced by silt content in the soil. This finding brings the first evidence that edaphic factors influence species-habitat association in Amazonian aquatic breeding frogs.

Subjects Ecology, Taxonomy, Zoology
Keywords Amazonia, Anura, Taxonomy, Ecology, Environmental heterogeneity, Edaphic factors

Submitted 13 July 2017
Accepted 13 January 2018
Published 9 February 2018

Corresponding author
Miquéias Ferrão,
miqueias.ferrao@inpa.gov.br,
uranoscodon@email.com

Academic editor
Ann Hedrick

Additional Information and Declarations can be found on page 24

DOI **10.7717/peerj.4321**

How to cite this article Ferrão et al. (2018), A new species of Amazonian snouted treefrog (Hylidae: *Scinax*) with description of a novel species-habitat association for an aquatic breeding frog. **PeerJ 6:e4321; DOI 10.7717/peerj.4321**

INTRODUCTION

Scinax Wagler, 1830 is the second most speciose genus of the family Hylidae Rafinesque, 1815 composed of small to medium sized treefrogs, distributed from Mexico to southern Argentina and Uruguay, including the Caribbean islands Trinidad and Tobago, and Santa Lucia (*Frost, 2017*). Despite the problematic taxonomic history (see *Faivovich, 2002*), the genus *Scinax* experienced a nomenclatural stability for almost ten years since *Faivovich et al. (2005)*. Recently, *Duellman, Marion & Hedges (2016)* revised Hylidae, making considerable changes in *Scinax* (*sensu Faivovich et al., 2005*): the genus *Ololygon* Fitzinger, 1843 was resurrected to harbour the former *Scinax catherinae* Clade (*sensu Faivovich, 2002*), the genus *Julianus Duellman, Marion & Hedges, 2016* was described to house the former *Scinax uruguayus* species group (*sensu Faivovich et al., 2005*), and the genus *Scinax* is now composed of species of the *Scinax ruber* Clade (*sensu Faivovich, 2002*). Currently, *Scinax* is composed of approximately 71 valid species, while *Ololygon* and *Julianus* are composed by 47 and two species, respectively (*Frost, 2017*). Furthermore, a new subfamily, Scinaxinae, was described by *Duellman, Marion & Hedges (2016)* to accommodate the high-supported clade *Scinax* + *Ololygon* + *Julianus* and its sister genus *Sphaenorhynchus* Tschudi, 1838.

Presently, twenty-nine valid species of *Scinax* occur in Amazonia *sensu lato* (*Eva & Huber, 2005*). However, the number of species occurring in this region (see Table S1) is currently underestimated (*Fouquet et al., 2007*; *Ferrão et al., 2016*). An integrative approach combining morphological, bioacoustics and DNA barcoding data revealed existence of seven confirmed candidate *Scinax* species distributed in different parts of the Purus-Madeira Rivers Interfluve (hereafter PMRI) (see *Ferrão et al., 2016*). Here we describe the confirmed candidate species *Scinax* sp. 7 from *Ferrão et al. (2016)*.

Species are widely recognized as fundamental units in ecology (*Gotelli, 2004*). Therefore, quantifying species-habitat associations, both at population and assemblage level, is dependent on accurate taxonomic classifications (*Isaac, Mallet & Mace, 2004*; *Bortolus, 2008*). Taxonomic inaccuracy may not affect the conclusions of ecological communities studies when a single target taxon is misidentified (e.g., *Bortolus, Schwindt & Iribarne, 2002*; *Bortolus, 2006*). However, misidentifying two or more morphologically similar species as a single species may considerably affect the degree of reliance indicated by patterns of species-habitat association (*Dexter, Pennington & Cunningham, 2010*) because frogs are globally threatened by habitat loss, habitat disconnection, disease and alien species (*Kats & Ferrer, 2003*; *Stuart et al., 2004*; *Lips et al., 2006*; *Becker et al., 2007*), and some attention have been focused on generating scientific knowledge to support its conservation and management. Species misidentifications should be more common in ecological studies from tropical regions because of the high levels of morphologically cryptic species that co-occur (*Kreft & Jetz, 2007*; *Jenkins, Pimm & Joppa, 2013*; *Pimm et al., 2014*). Therefore, only limited taxonomic data are available for many groups of organisms from tropical rainforests (*Giam et al., 2012*).

The Amazonia is the largest and most species-diverse tropical rainforest worldwide (*Corlett & Primack, 2011*). Nonetheless, molecular approaches applied in systematics have revealed that biodiversity in the Amazonia is greatly underestimated by cryptic biodiversity in many groups of organisms, such as frogs (*Ron et al., 2012*; *Jungfer et al., 2013*; *Caminer et al., 2017*). Different species of frogs react differently to the same anthropogenic effect, therefore the taxonomic knowledge is an important key to the conservation of frogs, especially in the Neotropics where the biodiversity is megadiverse. However, the taxonomy and systematics of many frog groups from the Amazonia and the role of environmental variables in shaping the distribution of species remain poorly understood. Furthermore, most taxonomic and ecological studies have been conducted on a local scale; thus, regional approaches are lacking (*Allmon, 1991*; *Tsuji-Nishikido & Menin, 2011*; *Rojas-Ahumada, Landeiro & Menin, 2012*; *Dias-Terceiro et al., 2015*; *Jorge et al., 2016*).

Studies that have used frogs to demonstrate patterns of species-habitat association in Amazonia were conducted mostly in the Manaus region (Brazil), on the north bank of the Amazon River (*Allmon, 1991*; *Menin et al., 2007*; *Menin, Waldez & Lima, 2011*; *Tsuji-Nishikido & Menin, 2011*; *Rojas-Ahumada, Landeiro & Menin, 2012*; *Jorge et al., 2016*). In this region, many terrestrial-breeding anurans are influenced by edaphic variables like slope, clay content and pH, while aquatic-breeding anurans are influenced by distance of streams and number of trees (*Menin et al., 2007*; *Menin, Waldez & Lima, 2011*; *Landeiro, Waldez & Menin, 2014*). However, anurans from other parts of Amazonia may present distinct patterns of species-habitat association, once the environmental factors that filter species occurrence and abundance may be expected as a response to regional sets of environmental conditions. As example, the Manaus region exhibits environmental elements that are not observed in the central and northern PMRI, which is the area sampled for this study. This portion of PMRI exhibits forests 17–27 m high, topography relatively flat with local variation from 1 to 3 m, silty soil and shallow water-table (*Cintra et al., 2013*; *Martins et al., 2014*; *Schietti et al., 2016*), whereas the Manaus region is characterized by forests with 30–37 m high closed canopy, undulating topography formed by valleys and plateaux ranging from 40 to 100 m a.s.l., low proportion of silt in the soil, and deep water-table (*Ribeiro et al., 1999*; *Castilho et al., 2006*; *Schietti et al., 2014*).

Reports have indicated that the treefrog genus *Scinax* is adequate for quantifying species-habitat associations because it is an extraordinarily species-rich genus that is widely distributed across different habitats in the Amazonia (*Duellman & Wiens, 1993*; *Fouquet et al., 2007*; *Ferrão et al., 2016*). However, the influence of environmental factors on the species distribution and abundance of *Scinax* is poorly understood, which is likely because of the lack of standardized sampling and the difficulty in identifying the species. Here, we also investigate the influence of environmental variables on the new species' spatial distribution based on sampling from standardized plots distributed along an approximately 600 km long transect in the PMRI.

MATERIAL AND METHODS

Study area

The interfluve between the Purus and Madeira rivers covers approximately 15.4 million hectares of the southern Brazilian Amazonia in an area that is drained by a large and complex stream network (*Maldonado et al., 2012*). At a broad scale, the northern portion

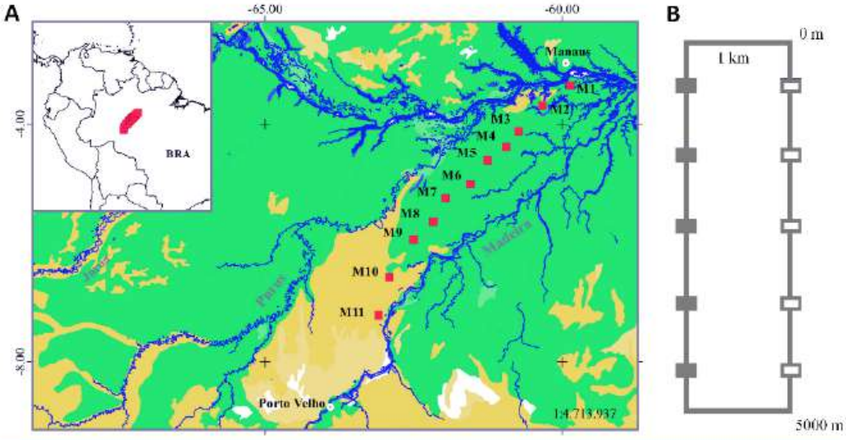

Figure 1 Sampling area in the Purus-Madeira Rivers Interfluve and schematic representation of RAPELD sampling modules and plots. (A) Distribution of RAPELD sampling modules along a 600 km transect. Legend: green colour (M1–M9) = tropical lowland rainforest with emergent canopy; gold colour (M10–M11) = open rainforest lowlands with palm trees. (B) General configuration of each module with ten sampling plots. Open squares represent plots where environmental variables used in this study were measured. BRA, Brazil.

Full-size DOI: 10.7717/peerj.4321/fig-1

of the PMRI is covered by a tropical lowland rainforest with emergent canopy and the south is covered by open rainforest lowlands with palm trees (*IBGE, 1997*) (Fig. 1A). At a finer scale, the number of trees and palms in the plots range from approximately 2,000 to 11,500 individuals per hectare (diameter at breast height > 1 cm) and the biomass of plants is lower in plots located in the northern and southern extremes (*Schietti et al., 2016*). The soil is generally shallow (*Martins et al., 2014*), with a predominance of silt, followed by sand and clay (*Cintra et al., 2013*). At a regional scale, the topography of PMRI is relatively flat and the altitude is between 27 and 80 m. Temporary ponds occur in lower areas during the rainy season (*Rossetti, Toledo & Góes, 2005*) and are formed by local ranges in elevation from 1–3 m.

Sampling design and collection effort

We collected data from 110 sampling plots (size 250 × 10 m) distributed along a 600 km transect in the PMRI, between the municipalities of Careiro da Várzea (03°11′32″S, 59°52′09″W) and Humaitá (07°13′06″S, 63°05′31″W) (Fig. 1B). The plots were distributed in 11 long-term ecological research sites (hereafter RAPELD) (*Magnusson et al., 2013*), with approximately 50 km of space between neighbouring modules. Each RAPELD module consists of two parallel 5 km trails and 10 sampling plots, with five plots per trail. The plots were spaced 1 km apart (Fig. 1). The sampling plots followed altitudinal contours to reduce the environmental heterogeneity within each sampling unit (*Magnusson et al., 2013*).

We sampled *Scinax* specimens using time- and space-constrained visual searches (modified from *Campbell & Christman, 1982*) and acoustic searches for males in breeding activity. All sampling plots were surveyed by two observers over 90 min. The plots were surveyed three times during the rainy season: in January/February 2013, November 2013, and January/February 2014 (990 sampling hours in total). Although the breeding seasons of most species of *Scinax* are seasonal, and some of them are explosive breeders, the new species was observed breeding along the entire rainy season. Due to that, we do not expect changes in abundance along RAPELD sampling modules caused by our sampling protocol or by sampling sessions. Adults were collected via occasional encounters on access trails and in areas surrounding sampling sites. Tadpoles were encountered in ponds unconnected to streams in the RAPELD module 9, where active breeding adults were encountered.

Adult specimens were killed with a 2% benzocaine solution, fixed in 10% formalin and conserved with 70% ethanol. Tadpoles were killed with a 5% lidocaine solution and conserved in 5% formalin. We used 5% formalin in tadpoles because the labial papillae and jaws are malleable after fixation at that concentration and it facilitates posterior description. Muscular tissue samples of all adults and one tadpole were collected before fixation in formalin, and preserved in absolute ethanol. Adults and tadpoles were deposited in the herpetological section of the Zoological Collections of the Instituto Nacional de Pesquisas da Amazônia (INPA-H), Manaus, Brazil. Tissue samples were deposited in the Albertina Pimentel Lima's Laboratory at Instituto Nacional de Pesquisas da Amazônia (INPA). See Appendix S1 for the specimens used in the comparisons.

Specimens were collected from RAPELD sampling modules under permit of Instituto Chico Mendes de Conservação da Biodiversidade (ICMBio) and Centro Nacional de Pesquisa e Conservação de Répteis e Anfíbios (RAN) Number 13777. ICMBio and RAN are institutes of Ministry of Environment, Government of Brazil. These permits were subject to approval of all procedures for collecting and euthanizing frogs.

Morphometric and acoustic data

Morphometric data were collected for adults using a digital calliper, and measurements were performed to the nearest 0.1 mm. Small measurements were taken with a digital calliper under a stereomicroscope. Specimens were sexed through the presence or absence of vocal sac, nuptial pads, vocal slits, and/or eggs. Males were defined as sexually active adults by the observation of expanded vocal sacs. Females were classified as adults when eggs were observed inside the body cavity, or when they were collected in amplexus with or near active males in temporary ponds. All males and females analysed in this study were classified as adults. Sixteen taxonomically important traits for identifying *Scinax* were measured as explained bellow (see Appendix S3 for measurement data). Ten morphometric characteristics were measured according to *Duellman (1970)*: snout-vent length (SVL), head length (HL), head width (HW), horizontal eye diameter (ED), upper eyelid width (UEW), internarial distance (IND), interorbital distance (IOD), horizontal tympanum diameter (TD), tibia length (TL) and foot length (FL). Three characteristics were measured according to *Napoli (2005)*: eye-nostril distance (END), fourth finger disk diameter (4FD), and fourth toe disk diameter (4TD). The length of the tarsus (TAL), hand

(HAL) and thigh (THL) followed *Heyer et al. (1990)*. The webbing formulae follow *Savage & Heyer (1967)* as modified by *Myers & Duellman (1982)*. The enumeration of fingers followed *Fabrezi & Alberch (1996)* that demonstrated the loss of finger I in the anuran evolution. Description of the colour in preservative is based on all paratypes and given in percentage (between parentheses). Colour in life is described based on photographs of five specimens (except the colour of iris, which was denoted in all paratypes).

The identity of the tadpoles was confirmed by *Ferrão et al. (2016)* through two distinct molecular barcoding approaches: Automatic Barcoding Gap Discovery—ABGD (*Puillandre et al., 2012*) and Generalized Mixed Yule Coalescent—GMYC (*Pons, Barraclough & Gomez-Zurita, 2006*). The 16S rRNA sequence under GenBank accession number KU317405 included in the analyses of *Ferrão et al. (2016)* was obtained from tissue sample of one tadpole of the lot INPA-H 35410. The developmental stages of the tadpoles were classified according *Limbaugh & Volpe (1957)*, as modified by *Gosner (1960)*. Fourteen morphometric characteristics of 13 tadpoles (stages 34–39) were measured under a stereo-microscope. The terminology and methods of seven measurements followed *Altig & McDiarmid (1999)*: total length (TL), body length (BL), interorbital distance (IOD), tail length (TAL), maximum width of the tail muscle (TMW), maximum height of the tail (MTH), and maximal tail muscle height (TMH). Seven measurements followed *Randrianiaina et al. (2011)*: body width (BW), body height (BH), eye diameter in dorsal view (ED), length of the spiracle (SL), vent tube length (VL), rostro-narial distance (RN), naris-pupil distance (NP).

We used a Principal Components Analysis (PCA) to detect sexual dimorphism in the morphometric data by visually checking for overlapping individuals in the morphometric multivariate space. The PCA was performed using the SVL and 15 morphometric ratios (measurement/SVL) from 28 males and 6 females. Because the SVL and ratios have different scales, we used the command line "*scale = TRUE*" in the *prcomp* function of the R platform (*R Core Team, 2016*). We also used a Multivariate Analysis of Variance (MANOVA) to test for significant differences between the PCA scores by sex. The first two Principal Components (PCs) of the PCA were used as dependent variables, and sex was used as a factor in the MANOVA model implemented in the R platform (*R Core Team, 2016*).

Because of the wide distribution of the new species along the PMRI, we verified whether morphological variation occurred in males and females across the RAPELD modules. Given that no significant morphological dimorphism was found between males and females (see results), we performed a MANOVA where the first two components of the PCA quoted above were used as dependent variables and RAPELD sampling modules were used as a factor.

The advertisement call of one male was recorded using a PMD 660 digital recorder (Marantz, Kanagawa, Japan) and a ME 66 directional microphone (Sennheiser, Wedemark, Germany). The calls were analysed using oscillogram and spectrogram (Blackman window, 80 Hz of frequency resolution and 1,024-point Fast Fourier Transform) generated using Raven 1.5 software (*Bioacoustics Research Program, 2014*). Terminology of acoustic parameters following *Köhler et al. (2017)*. As the advertisement call of the new species consists of a single note, we considered this unit a call (see *Köhler et al., 2017*). The following spectral and temporal parameters were obtained from 20 calls of the recorded male: call duration (s), number of pulses per call, pulse duration, inter-pulse interval, pulse repetition rate (pulse/s), and minimum, maximum and dominant frequency (Hz) of the call.

Species-habitat association

Given that the term "habitat" has different concepts and confusion over its use can be result of ambiguity, we follow the definition by *Block & Brennan (1993)*: "the subset of physical environmental factors that a species requires for its survival and reproduction".

We selected three predictor variables to investigate the influence of the environment on the distribution and abundance of the new *Scinax* species from the PMRI: (1) Forest structure, which was represented by the number of trees (diameter at breast height > 1 cm). We selected tree density to represent forest structure because this variable has been identified as an important factor affecting the distribution and abundance of frogs with aquatic reproduction in Amazonia (*Menin, Waldez & Lima, 2011*; *Landeiro, Waldez & Menin, 2014*). (2) Soil structure, which was represented by the percentage of silt because the soil texture in the study area consists primarily of silt (*Cintra et al., 2013*). Additionally, silty soils are structurally unstable, which increases water retention (*Juo & Franzluebbers, 2003*). (3) Depth of underground water, which was selected because shallow underground water can overflow lower areas of the study transect. Both soil structure and depth of underground water are variables directly related to the water availability in the pond, and indirectly related to the breeding preferences of the new species, which deposits its eggs only in ponds not connected to streams. Although the distance of stream is a variable commonly used to explain the distribution of aquatic breeding frogs in Amazonia, we do not evaluate it because the reproduction of the new species occurs only in ponds not connected to lotic water bodies. See Appendix S2 for sampling methods related to predictor variables.

Our standardized sampling procedures registered a higher number of *Scinax* individuals compared with previous studies conducted in the Brazilian Amazonia (e.g., *Ribeiro, Lima & Magnusson, 2012*). However, the number of recorded specimens was low. Hence, we used the sum of recorded individuals (instead of the mean) for the three sampled periods to represent the abundance of *Scinax* in each plot (*Bueno et al., 2012*). Occasional encounters were not included in the ecological analyses described below.

The normality of the data was assessed using the Shapiro–Wilk test ($P < 0.05$ in all cases). The soil and forest structure data were normalized using $\log(x)$, and the underground water and frog abundance data were normalized with $\log(x+1)$. We tested for correlations among the environmental variables using Spearman's coefficient. The environmental variables were not correlated to each other. We investigated the effects of the predictor variables on the distribution (presence/absence) of the new species of *Scinax* using the inflated zero regression model (*Zeileis, Kleiber & Jackman, 2008*), which was run using the R-package pscl (*Jackman, 2015*). The effect of each predictor variable on the abundance of the new species was tested using simple linear regression. The significance level in regression models and zero-inflated model was $\alpha = 0.05$

Taxonomic statement

The electronic version of this article in Portable Document Format (PDF) will represent a published work according to the International Commission on Zoological Nomenclature (ICZN), and hence the new names contained in the electronic version are effectively published under that Code from the electronic edition alone. This published work and the nomenclatural acts it contains have been registered in ZooBank, the online registration system for the ICZN. The ZooBank LSIDs (Life Science Identifiers) can be resolved and the associated information viewed through any standard web browser by appending the LSID to the prefix http://zoobank.org/. The LSID for this publication is: urn:lsid:zoobank.org:pub:D50A0044-0EA6-4619-B0FF-42A7443C4EAB. The online version of this work is archived and available from the following digital repositories: PeerJ, PubMed Central and CLOCKSS.

RESULTS

Taxonomic account

Scinax ruberoculatus sp. nov.
Scinax sp. 7 Ferrão et al. (2016), p. 7, 9, Figs. 2–3.

Holotype. INPA-H 34665 (Figs. 2 and 3), adult male collected by Miquéias Ferrão on 18 November 2013, from RAPELD sampling module 9 at kilometre 450 of the BR-319 federal highway (5°56′40″S, 62°30′04″W; 68 m a.s.l.; WGS84), Nascentes do Lago Jari National Park, municipality of Tapauá, Amazonas State, Brazil.

Paratopotypes. Three specimens: two adult males (INPA-H 34613, 34619) and one adult female (INPA-H 34605) collected by Miquéias Ferrão and Rafael de Fraga in January and November 2013.

Paratypes. Thirty specimens, all collected in Amazonas State, Brazil. Ten: one adult female (INPA-H 34600) and nine adult males (INPA-H 34601, 34604, 34614, 34615, 34622, 34598, 34624, 34627, 34629) collected by Miquéias Ferrão and Rafael de Fraga in February 2011, March 2013, and February 2014 from the RAPELD sampling module 2 at km 100 of the BR-319 federal highway (3°40′40″S, 60°18′56″W; 43 m a.s.l.; WGS84), municipality of Careiro da Várzea. One: an adult male (INPA-H 34602) collected by Pedro Leitão on 18 January 2011 from RAPELD sampling module 3 at km 168 of the BR-319 federal highway (4°8′40″S, 60°43′20″W; 39 m a.s.l.; WGS84), municipality of Careiro da Várzea. Two: one adult male (INPA-H 34610) and one adult female (INPA-H 34620) collected by Miquéias Ferrão in February 2014 from RAPELD sampling module 4 at km 220 of the BR-319 federal highway (4°23′26″S, 60°56′11″W; 47 m a.s.l.; WGS84), municipality of Borba. One: an adult male (INPA-H 34608) collected by Rafael de Fraga on 29 January 2013 from RAPELD sampling module 5 at km 260 of the BR-319 federal highway (4°36′34″S, 61°15′00″W; 50 m a.s.l.; WGS84), municipality of Beruri. Twelve: two adult females (INPA-H 34607, 34630) and ten adult males (INPA-H 34599, 34609, 34611, 34612, 34617, 34618, 34621, 34625, 34626, 34628) collected by Miquéias Ferrão and Rafael de Fraga in

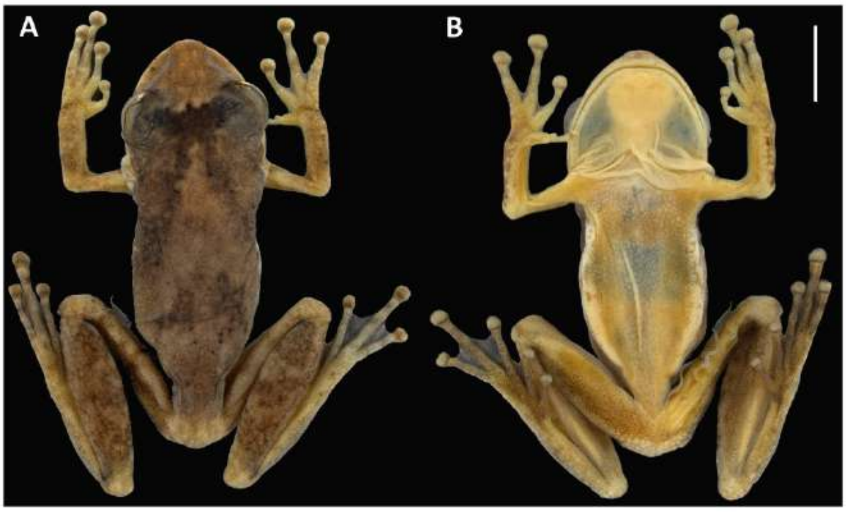

Figure 2 **Holotype of *Scinax ruberoculatus.* sp. nov. INPA-H 34665.** (A) Dorsal view. (B) Ventral view. Scale = 5 mm. Photos by M Ferrão.

Full-size DOI: 10.7717/peerj.4321/fig-2

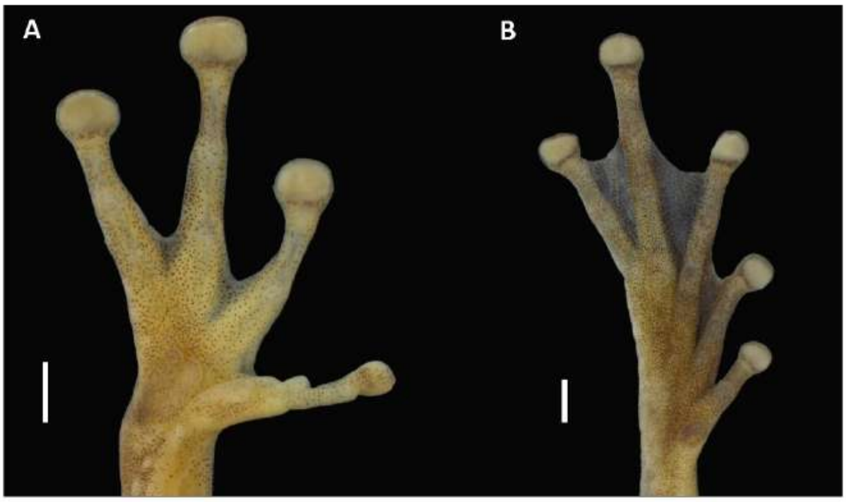

Figure 3 **Hand and foot of the holotype of *Scinax ruberoculatus* sp. nov. INPA-H 34665.** Scale = 1 mm. Photos by M Ferrão.

Full-size DOI: 10.7717/peerj.4321/fig-3

January 2013, November 2013, and January 2014 from RAPELD sampling module 7 at km 350 of the BR-319 federal highway (5° 15′57″S, 61°55′58″W, 59 m a.s.l.; WGS84), Igapó-Açú Sustainable Development Reserve, municipality of Beruri. Four: three adult males (INPA-H 34603, 34616, 34623) and one adult female (INPA-H 34606), collected by Miquéias Ferrão and Rafael de Fraga in January 2013, November 2013, and January 2014 from RAPELD sampling module 8 at km 400 of the BR-319 federal highway (5°37′31″S, 62°10′56″W, 67 m a.s.l.; WGS84), Lago do Capanã Grande Extractive Reserve, municipality of Manicoré.

Etymology. The specific epithet *ruberoculatus* is composed of two words in Latin, "ruber" (red) and "oculatus" (having eyes). The name is an adjective in concordance with the masculine gender of the genus *Scinax* and refers to the reddish colour of the upper part of the iris. Suggested English common name: 'Red-eyed snouted treefrog'.

Generic placement. We assign the new species to *Scinax* (*sensu* Duellman, Marion & Hedges, 2016) based on general morphological similarity to other members of the genus, cloacal tube of tadpoles positioned above the margin of the lower fin (a putative synapomorphy of the former *S. ruber* Clade according Faivovich et al., 2005), and our previous molecular data (Ferrão et al., 2016).

Diagnosis. A small species of the genus *Scinax* characterized by the following combination of characteristics: SVL 22.6–25.9 mm in males and 25.4–27.5 mm in females; snout truncate in dorsal view and rounded in lateral view; tarsal tubercles indistinct; tubercles on the lower jaw, knee, and heel absent; diameter of disc on fourth finger represents 60% of tympanum diameter; skin on dorsum smooth; dentigerous processes of vomers triangular; bilobate vocal sac and nuptial pads in males; Finger III<V; in life, ground colour of dorsum light grey or light brown; a large brown or grey spot on the head and scapular region shaped like the moth of the species *Copiopteryx semiramis* (Cramer, 1775), or a human molar in lateral view, or a triangle; dorsal or dorsolateral stripes absent; whitish cream stripe in the lower portion of the flanks; anterior and posterior surfaces of thighs brown; webbing between toes light to dark grey; belly white to greyish-white with light brown to brown blotches laterally; males with vocal sac semi-translucent white; iris bicolored, upper half reddish, lower half grey; advertisement call consisting of a single pulsed note, with note duration of 0.134–0.331 s, 10–23 pulses/note, dominant frequency 1809–1895 Hz; tadpoles with labial teeth formula 2 (2)/3, absence of labial arm, and presence of dark brown blotch on the distal part of the tail.

Comparison. Currently, the genus *Scinax sensu* Duellman, Marion & Hedges (2016) includes 71 species (Frost, 2017). Morphologically, *Scinax ruberoculatus* sp. nov. can be distinguished from all these species and from six confirmed candidate species identified by Ferrão et al. (2016) by following combination of characters (characters of other species in parentheses or brackets unless otherwise stated).

The new species differs from *S. boulengeri* (Cope, 1887), *S. constrictus* Lima, Bastos & Giaretta, 2005, *S. garbei* (Miranda-Ribeiro, 1926), *S. jolyi* Lescure & Marty, 2000, *S. kennedyi* (Pyburn, 1973), *S. nebulosus* (Spix, 1824), *S. pedromedinae* (Henle, 1991), *S. proboscideus* (Brongersma, 1933), *S. rostratus* (Peters, 1863), and *S. sugillatus* (Duellman, 1973) by the absence of tubercles on the lower jaw and on knee, and by the absence of an elongated or pointed snout (tubercles on the lower jaw and on knee present, snout elongated or pointed; Duellman, 1972a; Duellman, 1973; Duellman & Wiens, 1992; Lescure & Marty, 2000; Lima, Bastos & Giaretta, 2005). Furthermore, tadpoles of *S. ruberoculatus* sp. nov. differ from tadpoles of *S. boulengeri*, *S. garbei*, *S. nebulosus*, *S. pedromedinae*, *S. rostratus*, *S. sugillatus* by the absence of labial arm and by presence of dark brown blotch on the distal portion of the tail (labial arm present, blotch on the distal portion of the tail absent; Duellman, 1978; McDiarmid & Altig, 1990; Hero & Mijares-Urrutia, 1995; Duellman, 2005; Gomes, Alves & Peixoto, 2014).

The small body size of the males (SVL 22.6–25.9 mm) distinguishes *S. ruberoculatus* sp. nov from the following species: *S. acuminatus* (Cope, 1862) (SVL 39.0–45.0 mm; Lutz, 1973); *S. baumgardneri* (Rivero, 1961) (SVL 29.0–32.0 mm; Rivero, 1961); *S. blairi* (Fouquette & Pyburn, 1972) (SVL 27.8–30.1 mm; Fouquette & Pyburn, 1972); *S. boesemani* (Goin, 1966) (SVL 28.4–31.8 mm; Duellman, 1986); *S. camposseabrai* (Bokermann, 1968) (SVL 28.9–33.5 mm; Caramaschi & Cardoso, 2006); *S. castroviejoi* De la Riva, 1993 (SVL 45.0 mm; De la Riva, 1993); *S. chiquitanus* (De la Riva, 1990) (SVL 27.9–33.3 mm; Duellman & Wiens, 1993); *S. dolloi* (Werner, 1903) (male syntype SVL 34.9 mm; according Araujo-Vieira, Brandão & Faria, 2015); *S. elaeochrous* (Cope, 1875) (SVL 26–32 mm; Savage, 2002); *S. eurydice* (Bokermann, 1968) (SVL 44.0–52.0 mm; Bokermann, 1968); *S. funereus* (Cope, 1874) (SVL 29.8–36.9 mm; Duellman, 1971; Duellman & Wiens, 1993); *S. fuscovarius* (Lutz, 1925) (SVL 41–44 mm; Cei, 1980); *S. granulatus* (Peters, 1871) (SVL 32.0–38.0 mm; Cei, 1980); *S. haddadorum* Araujo-Vieira, Valdujo & Faivovich, 2016 (SVL 29.4–35.4 mm; Araujo-Vieira, Valdujo & Faivovich, 2016); *S. hayii* (Barbour, 1909) (SVL 39.0–42.0 mm; Lutz, 1973); *S. ictericus* Duellman & Wiens, 1993 (SVL 26.3–31.8 mm; Duellman, 2005); *S. iquitorum* (Moravec et al., 2009) (SVL 35.0–38.5 mm; Moravec et al., 2009); *S. manriquei* Barrio-Amorós, Orellana & Chacón-Ortiz, 2004 (SVL 27.7 mm; Barrio-Amorós, Orellana & Chacón-Ortiz, 2004); *S. maracaya* (Cardoso & Sazima, 1980) (SVL 26.7–28.0 mm; Cardoso & Sazima, 1980); *S. nasicus* (Cope, 1862) (SVL 27–35 mm; Cei, 1980); *S. oreites* Duellman & Wiens, 1993 (SVL 28.4–33.5 mm; Duellman & Wiens, 1993); *S. perereca* Pombal Jr, Haddad & Kasahara, 1995 (SVL 34.0–38.5 mm; Pombal Jr, Haddad & Kasahara, 1995); *S. quinquefasciatus* (Fowler, 1913) (SVL 29.6–34.0 m; Duellman, 1971); *S. rossaferesae* Conte et al., 2016 (SVL 27.8–31.6 mm; Conte et al., 2016); *S. ruber* (Laurenti, 1768) (SVL 29.4–41.2 mm; Duellman & Wiens, 1993), *S. sateremawe* Sturaro & Peloso, 2014 (SVL 35.2–38.1 mm; Sturaro & Peloso, 2014); *S. similis* (Cochran 1952) (SVL 30.4–36.8 mm; Juncá et al., 2015); *S. tigrinus* Nunes, Carvalho Jr & Pereira, 2010 (SVL 28.4–30.8 mm; Nunes, Carvalho Jr & Pereira, 2010), and *S. x-signatus* (Spix, 1824) (SVL 32.4–38.7 mm; Juncá et al., 2015). In the PMRI, males of the new species are smaller than males of *Scinax onca* Ferrão et al., 2017 (SVL 31.3–34.3 mm; Ferrão et al., 2017), *Scinax* sp. 5 (SVL 29.6–33.9 mm; Ferrão et al., 2016).

Males of *S. ruberoculatus* sp. nov. are larger than those of *S. exiguus* (Duellman, 1986) (SVL 18.0–20.8 mm; Duellman, 1986).

The body size of females (SVL 25.4–27.5 mm) of *S. ruberoculatus* sp. nov. differs from those of *S. cabralensis* Drummond, Baêta & Pires, 2007 (SVL 24.2–25.1 mm; Drummond, Baêta & Pires, 2007), *S. cretatus* Nunes & Pombal Jr, 2011 (SVL 29.2–32.5 mm; Nunes & Pombal Jr, 2011), *S. curicica* Pugliese, Pombal Jr & Sazima, 2004 (SVL 28.5–31.5 mm; Pugliese, Pombal Jr & Sazima, 2004), *S. danae* Duellman, 1986 (SVL 27.8–29.5 mm; Duellman, 1986), *S. imbegue* Nunes, Kwet & Pombal Jr, 2012 (SVL 28.8–38.0 mm; Nunes, Kwet & Pombal Jr, 2012), *S. montivagus* Juncá et al., 2015 (SVL 28.9–32.2 mm; Juncá et al., 2015), *S. rogerioi* Pugliese, Baêta & Pombal Jr, 2009 (SVL 28.0–34.5 mm; Pugliese, Baêta & Pombal Jr, 2009).

The absence of distinct dorsolateral stripe and the presence of a dark brown spot on the head/scapular region shaped like the moth species *C. semiramis* (or like a human molar in lateral view, or a triangle in living specimens) differ the new species from *S. altae* (Dunn, 1933) (longitudinal dorsolateral stripes present; Savage, 2002), *S. auratus* (Wied-Neuwied, 1821) (light dorsolateral stripes present; Santana et al., 2009), *S. caldarum* (Lutz, 1968) (longitudinal stripes on the back present; Lutz, 1973), *S. cardosoi* (Carvalho-e Silva & Peixoto, 1991) (dorsolateral stripes present; Carvalho-e Silva & Peixoto, 1991), *S. fuscomarginatus* (Lutz, 1925) (divergent or parallel dorsolateral stripes present; Brusquetti et al., 2014), *S. madeirae* (Bokermann, 1968) (convergent dorsolateral stripes present; Brusquetti et al., 2014), *S. pachycrus* (Miranda-Ribeiro, 1937) (dorsolateral stripes present; Lutz, 1973), *S. villasboasi* Brusquetti et al., 2014 (divergent dorsolateral stripes present; Brusquetti et al., 2014), *S. rupestris* (scattered small round and irregular dark blotches on dorsum: Araujo-Vieira, Brandão & Faria, 2015), *S. squalirostris* (Lutz, 1925) (double black lateral bands divided by a white interspace; Lutz, 1973), *S. tymbamirim* Nunes, Kwet & Pombal Jr, 2012 (internal and external dark brown stripes border dorsolateral white stripes; Nunes, Kwet & Pombal Jr, 2012), and *Scinax* sp. 2 *sensu* Ferrão et al. (2016) (dark brown dorsolateral stripes present; Ferrão et al., 2016).

The number of pulses (10–23) in the advertisement call differs *Scinax ruberoculatus* sp. nov. from *S. alter* (Lutz, 1973) (29–152 pulses; Pombal Jr, Bastos & Haddad, 1995; Nunes, Kwet & Pombal Jr, 2012), *S. crospedospilus* (Lutz, 1925) (5–7 pulses; Magrini et al., 2011), *S. cuspidatus* (Lutz, 1925) (5–6 pulses; Pombal Jr, Bastos & Haddad, 1995, *S. duartei* (Lutz, 1951) (4–8 pulses; Pugliese, Pombal Jr & Sazima, 2004), and *S. juncae* Nunes & Pombal Jr, 2010 (4–5 pulses; Nunes & Pombal Jr, 2010).

The smooth dorsal skin differs *Scinax ruberoculatus* sp. nov. differs of from *S. staufferi* (Cope, 1865) (tuberculate: Savage, 2002).

The new species differs from *S. cruentomma* (Duellman 1972) by having 10–23 pulses in the advertisement call (39–54 pulses; Carvalho et al., 2015), upper iris red and lower iris grey (horizontal red bar in the iris; Duellman, 1972b), diameter of disc on fourth finger represents 60% of tympanum diameter (diameter of disc equal to tympanum diameter; Duellman, 1972b), presence of nuptial pad and bilobate vocal sac in males (absence of nuptial pad, and simple vocal sac; Duellman, 1972b), labial teeth formula 2 (2)/3 in tadpoles (2 (2)/3 (1); Duellman, 1972b) and presence of dark brown blotch on the distal part of the tail (absence; Duellman, 1972b).

Scinax ruberoculatus sp. nov. can be distinguished from *S. lindsayi* Pyburn, 1992 by the snout truncate in dorsal view (rounded; Pyburn, 1992), presence of nuptial pad in males (absence; Pyburn, 1992), Finger III<V (Finger III = V; Pyburn, 1992), diameter of disc on

fourth finger 60% of tympanum diameter (diameter of disc equal to tympanum diameter; *Pyburn, 1992*), call duration 0.134–0.331 s (0.08–0.10 s; *Pyburn, 1992*), upper iris reddish and lower iris grey (iris pinkish bronze; *Pyburn, 1992*).

The new species can be differentiated from *S. wandae* (Pyburn & Fouquette, 1971) by 10–23 pulses in the advertisement call (70–108 pulses; *Pombal Jr et al., 2011*), absence of dorsolateral dark brown stripes (presence; *Pyburn & Fouquette, 1971*), diameter of disc on fourth finger represents 60% of tympanum diameter (diameter of disc equal to tympanum diameter; *Pyburn & Fouquette, 1971*), tongue lanceolate (rounded; *Pyburn & Fouquette, 1971*), vocal sac smooth (finely granular; *Pyburn & Fouquette, 1971*).

Scinax ruberoculatus sp. nov. can be distinguished from *S. karenanneae* (Pyburn, 1973) by having snout truncate in dorsal view (rounded; *Pyburn, 1993*), SVL 22.6–25.9 mm in males (SVL 26.6–28.9 mm; *Pyburn, 1993*); presence of nuptial pad in males (absence; *Pyburn, 1993*), Finger III<V (Finger III = V; *Pyburn, 1993*), diameter of disc on fourth finger 60% of tympanum diameter (diameter of disc about equal to tympanum diameter; *Pyburn, 1992*), males with vocal sac semi-translucent white (yellow; *Pyburn, 1993*), upper iris red and lower iris grey (bright golden bronze; *Pyburn, 1993*).

The bicolored iris (reddish upper and grey lower) distinguishes *Scinax ruberoculatus* sp. nov. from *Scinax* sp. 1 (red horizontal band in the central portion of the iris; *Ferrão et al., 2016*), *Scinax* sp. 4 (red horizontal band in the central portion of the iris; *Ferrão et al., 2016*), and *Scinax* sp. 6 (red horizontal band in the central portion of the iris; *Ferrão et al., 2016*).

Holotype description. Adult male (Figs. 2 and 3). Body moderately slender; head wider than body; HL 37% of the SVL; HW 34% of the SVL; head slightly longer than wide (HL/HW = 1.09); snout truncate in dorsal view and rounded in lateral view; END 95% of ED; nostrils slightly protuberant in dorsolateral position; internarial region slightly concave; canthus rostralis rounded; loreal area slightly concave; ED 32% of HL; supratympanic fold weakly marked; TD 48% of ED; vocal sac subgular, bilobate, moderately sized, reaching the pectoral region; vocal slits present, and positioned parallel to edge of the lower lips, between the lateral base of tongue and the angle of jaws; tongue lanceolate; dentigerous processes of vomers triangular, slightly separated, with 4/2 teeth (left/right); choanae oval; pectoral fold present but weakly marked; axillar membrane absent; arm slender; forearm moderately robust; ulnar tubercles indistinct; fingers moderately long and slender, basally webbed, bearing medium-sized elliptical discs (4FD/TD = 0.59); relative length of fingers II<III<V<IV (Fig. 3A); palmar tubercle flat and bifid; thenar tubercle elliptical and moderately protuberant; subarticular tubercle on Finger II subconical; subarticular tubercles on Finger III, IV and V rounded and protuberant; supernumerary tubercles indistinct; nuptial pad white, barely evident covering the preaxial surface of Metacarpal II, not obscuring the thenar tubercle (Fig. 3A); TL 50% of the SVL, THL 47% of the SVL; tarsal fold absent; tarsal tubercles indistinct; FL 37% of the SVL; TAL 75% of FL; internal metatarsal tubercle low and elliptical; external metatarsal tubercle small, rounded, slightly pronounced; subarticular tubercles rounded and pronounced; supernumerary tubercles indistinct; toe discs elliptical (4TD/TD = 0.59); relative toe length I<II<III<V<IV; toe webbing formula I vestigial II 1^{+}–2^{+}III 1–2^{+} IV 2^{+}–1 V (Fig. 3B); cloacal opening directed

posteroventrally at the thigh midlevel; skin on dorsum smooth with small tubercles in postocular and scapular regions; vocal sac smooth; chest, belly and ventral surface of the thigh areolate; perianal region with small round warts.

Holotype measurements (mm). SVL 25.9; HL 9.6; HW 8.8; ED 3.2; TD 1.5; UEW 2.4; IND 2.0; TAL 7.2; FL 9.7; HAL 7.6; 3FD 0.9; 4TD 0.9; END 2.9; TL 13.0; THL 12.1; NSD 0.8.

Holotype colouration. In preservative, dorsum light grey dorsum (Fig. 2A); anterior portion of the head amber-yellow; a dark brown blotch similar in shape to the moth *Copiopteryx semiramis* extending from the interocular region to middle flanks; infraocular and infratympanic regions white; grey chevron-shaped blotch and dark grey dots on the sacral region; background of hand beige-coloured , arm and forearm with diffuse amber-yellow pigmentation; a narrow horizontal amber-yellow stripe between the hand and forearm and on the anterior portion of the arm; anterior and posterior area of thigh light brown, dorsal surface of thigh beige; beige blotch on the knee; tibia light grey with three diffuse brown stripes; beige-coloured blotch on the tibia-tarsus articulation; tarsus, feet and toes light cream; throat cream with inconspicuous light grey blotches (Fig. 2B); vocal sac and chest cream; belly yellowish cream; white band between the flanks and belly with few light grey blotches; perianal region white. Except by the colour of the bicolored iris (reddish upper and grey lower), the colour in life was not recorded.

Variation. The adult paratopotypes and paratypes are similar to the holotype. Variation occurs in the presence and number of small dorsal tubercles (completely absent in some individuals). Variation in foot webbing is as follows: I vestigial II $(1–1^{1/2})–(2–2^{1/2})$ III $(1–1^{1/3})–(2–2^{1/2})$ IV $(2–2^{1/3})–(1–1^{+})$ V. Measurements are provided in Appendix S3 and summarized in Table 1.

The first axis (PC) of the PCA summarized 23% of the variation in the morphometric data, whereas PC2 summarized 16.3%. See Appendix S4 for values of other axes. Sexual dimorphism was not observed in the body shape (morphometric ratios) of *S. ruberoculatus* sp. nov. (Pillai trace = 0.100, $df = 31$, $P = 0.19$), and the body shape of both sexes overlapped in the morphometric multivariate space (Fig. 4A). Males and females of *S. ruberoculatus* sp. nov. did not show distinct morphological variations along the RAPELD sampling modules (Pillai trace = 0.38, $df = 54$, $P = 0.41$). The body shape of specimens from all modules overlapped in the morphometric multivariate space (Fig. 4B).

In preservative (Figs. 5A–5I), the colour pattern of the paratypes shows the following variations (frequency in % of paratype specimens): Dorsal ground colour varies from light grey (Fig. 5B) to brown (Fig. 5E). A grey to dark brown blotche on the head and scapular region is shaped like the Neotropical moth *Copiopteryx semiramis* (60%), a human molar in lateral view (26%), or a triangle (14%). A grey to dark brown chevron in the sacral region is present in 42% of paratypes (Figs. 5C–5H). Some individuals have tiny black spots (Figs. 5A–5C) on the dorsal surface of the body and limbs (42%). Light brown or dark grey spots on the upper lip are more concentrated and conspicuous in some individuals (60%). Grey to brown stripe between the eye and the tympanum is present in some individuals (31%); a grey or dark brown supratympanic stripe (95%); a cream to yellowish cream stripe in the lower portion of the flanks bordered by brown spots dorsally (100%). One to three light

Table 1 Measurements (in mm) of type series of *Scinax ruberoculatus* sp. nov. Values are presented as the mean ± standard deviation, with the range in parentheses.

Measurements	Males ($n = 28$)	Females ($n = 6$)
SVL	24.4 ± 0.87 (22.6–25.9)	26.3 ± 0.73 (25.4–27.5)
HL	9 ± 0.41 (8.3–9.8)	9.6 ± 0.16 (9.4–9.8)
HW	8.4 ± 0.28 (7.9–8.9)	9.1 ± 0.40 (8.6–9.6)
ED	3 ± 0.20 (2.7–3.4)	3 ± 0.15 (2.9–3.2)
TD	1.4 ± 0.12 (1.1–1.6)	1.5 ± 0.07 (1.4–1.6)
UEW	2.3 ± 0.20 (1.8–2.6)	2.4 ± 0.22 (2.1–2.7)
IOD	2.4 ± 0.12 (2.2–2.7)	2.5 ± 0.15 (2.4–2.8)
IND	1.8 ± 0.10 (1.5–2)	1.9 ± 0.12 (1.8–2.1)
TAL	6.6 ± 0.23 (6–7.2)	7.2 ± 0.34 (6.8–7.9)
FL	9.6 ± 0.44 (8.6–10.3)	10.3 ± 0.45 (9.5–10.8)
HAL	6.5 ± 0.35 (5.9–7.6)	7.2 ± 0.53 (6.2–7.8)
3FD	0.9 ± 0.13 (0.7–1.2)	1 ± 0.14 (0.9–1.2)
4TD	1 ± 0.14 (0.7–1.3)	1 ± 0.10 (0.8–1.1)
END	2.8 ± 0.17 (2.4–3.1)	3.1 ± 0.15 (2.9–3.3)
TL	12.3 ± 0.49 (11.2–13.1)	13.4 ± 0.49 (12.9–14.2)
THL	11.5 ± 0.48 (10.2–12.1)	12.2 ± 1.01 (10.2–13.4)

Notes.

n, number of measured specimens.

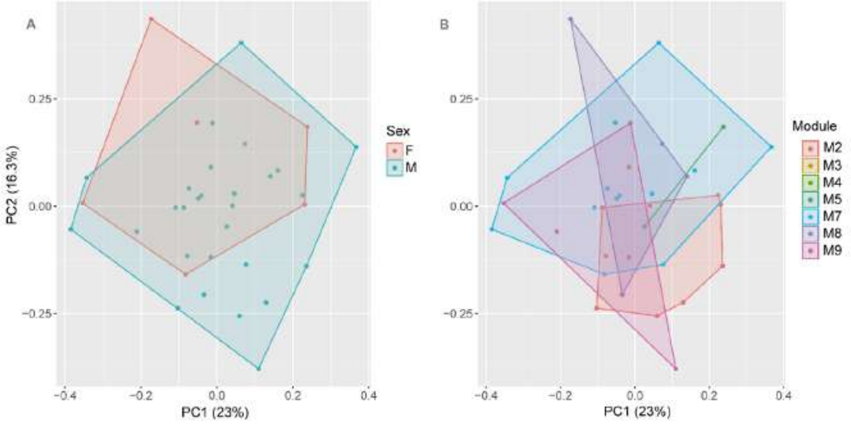

Figure 4 Multivariate morphometric space of *Scinax ruberoculatus* sp. nov. Principal Components Analysis of the SVL and 15 body ratios of males ($N = 28$) and females ($N = 6$). (A) Sampled by sex and (B) sampled by RAPELD sampling modules. Abbreviations: M2–5 and M7–9, RAPELD sampling modules where specimens were collected; F, females; M, males.

Full-size DOI: 10.7717/peerj.4321/fig-4

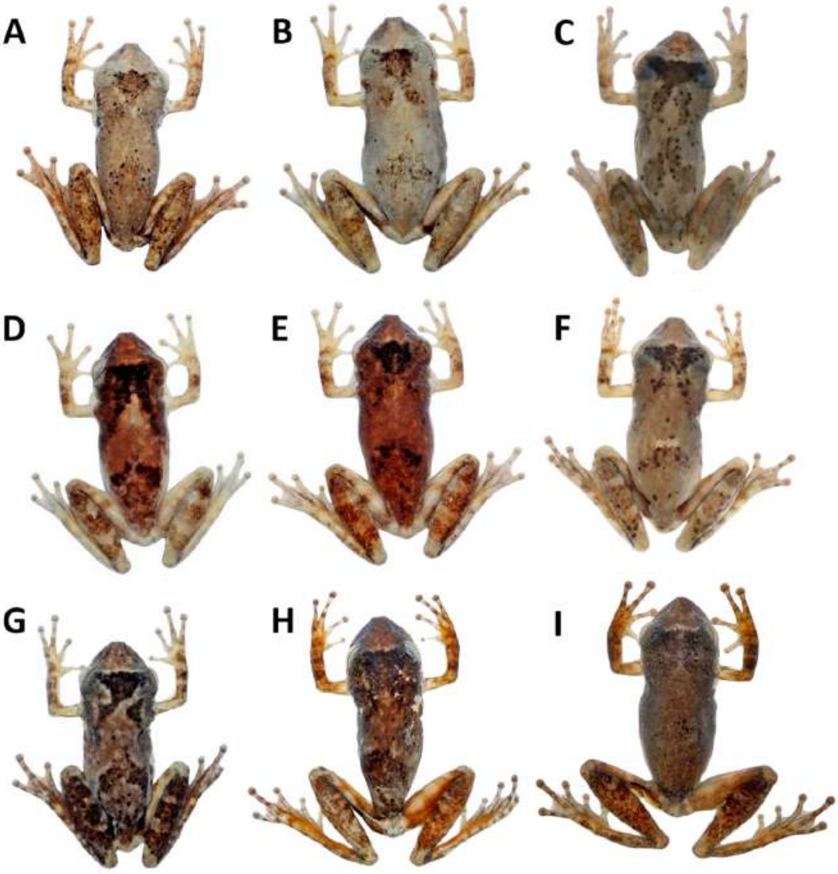

Figure 5 Variation in the dorsal colouration from preserved specimens of *Scinax ruberoculatus* sp. nov. (A) INPA-H 34601, male, SVL 24.1 mm. (B) INPA-H 34600, female, SVL 27.5 mm. (C) INPA-H 34609, male, SVL 24.5 mm. (D) INPA-H 34598, male, SVL 25.5 mm. (E) INPA-H 34614, male, SVL 25.5. (F) INPA-H 34611, male, SVL 23.8 mm. (G) INPA-H 34612, male, SVL 24.4 mm. (H) INPA-H 34618, male, SVL 25.2 mm. (I) INPA-H 34605, female, SVL 26.2 mm. Photos: M Ferrão.

Full-size DOI: 10.7717/peerj.4321/fig-5

brown stripes on the dorsal side of the thigh (48%); three grey or brown stripes on the upper tibia (92%); light cream blotch on the heel (100%).Throat, vocal sac, chest and belly vary from cream to yellowish cream; light to dark brown or light to dark grey blotches on the lateral portion of the belly in all paratypes.

In life (Figs. 6A–6F), dorsal ground colour varies from light grey (Fig. 6D) to brown (Fig. 6E). Blotches, chevrons, or stripes on the dorsal surfaces are more conspicuous than in preservative. Iris bicolored, upper half reddish, lower half grey; both parts separated by a narrow central red streak (Fig. 6). Dorsal surface of the arm cream (Fig. 6A) to yellowish

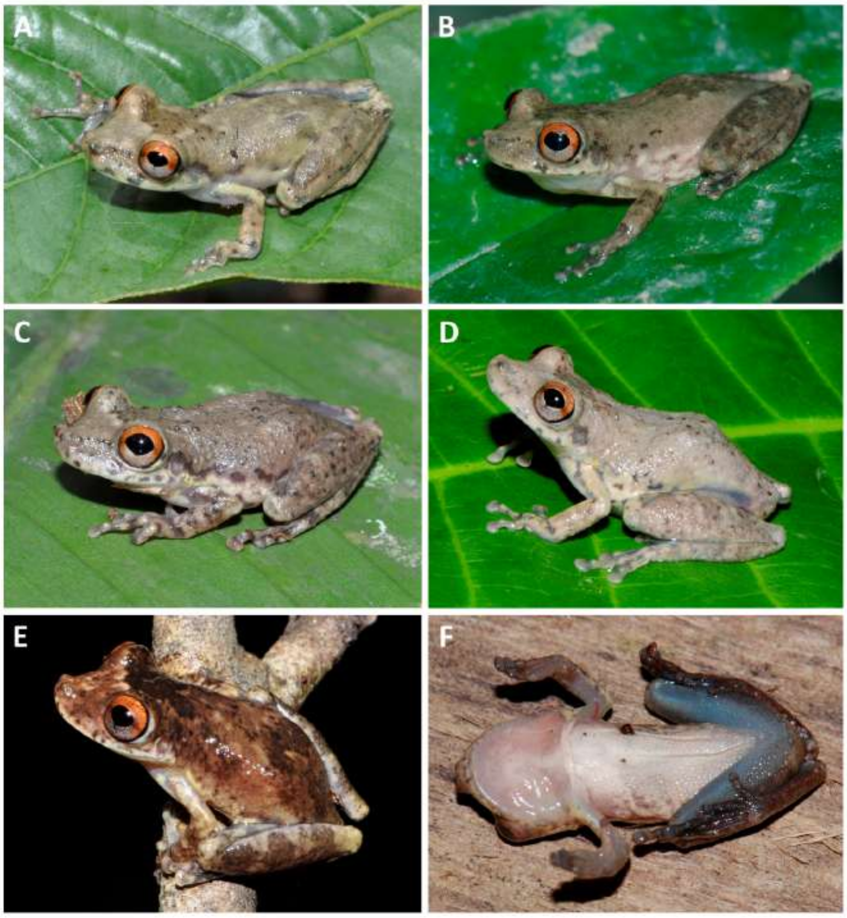

Figure 6 Variation in the colouration of living specimens of the paratypes of *Scinax ruberoculatus* sp. nov. (A) INPA-H 34607, female, SVL 25.4 mm. (B) INPA-H 34602, male, SVL 22.6 mm. (C) INPA-H 34603, male, SVL 23.3 mm. (D) INPA-H 34604, male, SVL 25.8 mm. (E) INPA-H 34623, male, SVL 23.9 mm. (F) INPA-H 34602, male, SVL 22.6 mm. Photos: AP Lima (B, F) and R Fraga (A, C, D, E).

Full-size DOI: 10.7717/peerj.4321/fig-6

cream (Fig. 6E). Anterior and posterior surfaces of thighs uniformly brown, dorsal surface of thigh yellowish cream to light brown. A whitish cream stripe in the lower portion of the flanks. Throat, vocal sac, and chest grey to semi-translucent white; belly white to greyish-white with light brown to brown blotches laterally (Fig. 6F). Ventral surface of the hand light grey, ventral surface of foot light grey to brown. Webbing light to dark grey.

Vocalization. The advertisement call of *Scinax ruberoculatus* sp. nov. consists of a single moderately long pulsed note (Fig. 7). The quantitative call parameters are as follows (range followed by mean ± standard deviation in parentheses): call duration, 0.134–0.331 s (0.20

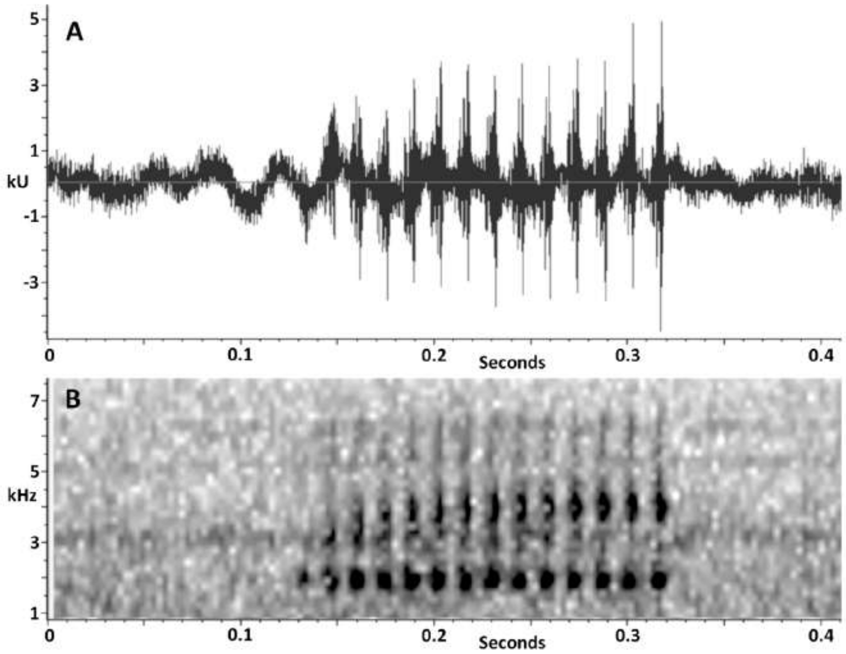

Figure 7 **Advertisement call of *Scinax. ruberoculatus* sp. nov.** (A) Waveform. (B) Audiospectrogram. Call recorded at RAPELD sampling module 9, Nascentes do Lago Jari National Park, Beruri Municipality, Amazonas, Brazil. Male recorded: INPA-H 34665 (SVL 25.9 mm). Temperature: 25 °C.

Full-size DOI: 10.7717/peerj.4321/fig-7

± 0.05, $n = 20$); pulses per call, 10–23 (14.5 ± 3.4, $n = 20$); pulse duration, 0.007–0.009 s (0.008 ± 0.001, $n = 20$); inter-pulse interval, 0.007–0.009 s (0.007 ± 0.001, $n = 20$); pulse repetition rate, 59–71 pulses per sec (66.6 ± 3.6, $n = 20$); dominant frequency, 1,809–1,895 Hz (1,852 ± 19.7, $n = 20$); minimum frequency, 1,170–1,681 Hz (1,452 ± 185, $n = 20$); maximum frequency, 2,378–2,579 Hz (2,420 ± 49, $n = 20$).

Tadpoles. The following description is based on one tadpole of the lot INPA-H 35410 in Gosner stage 34 (Fig. 8; Table 2). Body ovoid in dorsal view and almost triangular in lateral view; total length 22.2 mm; body wider than high at the spiracle level (BW/BH = 1.13); snout rounded in dorsal and lateral views; eyes moderately large (ED = 1.0 mm), oriented dorsolaterally and separated by approximately twice the eye diameter (IOD/ED = 1.8); sinistral spiracle; spiracle opening oriented postero-laterally below the midline of the body on the third portion of the body; dextral vent tube, positioned above the margin of the lower fin; vent tube opening on the right side of the ventral fin; slender caudal musculature with greater height than width (TMH/TMW = 1.2) that gradually tapers towards the tail tip; caudal musculature approximately 1.2 higher than the ventral fin and represents 75% of the dorsal fin at the central portion of the tail; dorsal fin originating at the level of the

Figure 8 Tadpole of *Scinax. ruberoculatus* sp. nov. (INPA-H 35410) in developmental stage 34. (A) Lateral view. (B) Dorsal view. (C) Ventral views. (D) Details of the opened oral disc. (E) closed oral disc. Tadpoles were collected at RAPELD sampling module 9, Nascentes do Lago Jari National Park, Amazonas, Brazil. Scales for A–C = 5 mm. Scales for D–E = 0.5 mm. Photos: M Ferrão.

Full-size DOI: 10.7717/peerj.4321/fig-8

Table 2 Morphometric data (in mm) from tadpoles of *Scinax ruberoculatus* sp. nov. Values are presented as the mean ± standard deviation, with the range in parentheses.

Measurements (mm)	**Stage 34 (*n* = 3)**	**Stages 35–38 (*n* = 7)**	**Stage 39 (*n* = 3)**
TL	20.9 ± 1.4 (19.4–22.2)	24.7 ± 1.9 (22.9–27.0)	26.6 ± 1.0 (25.4–27.2)
BL	7.1 ± 0.1 (7.0–7.2)	8.1 ± 0.4 (7.2–8.5)	8.5 ± 0.2 (8.3–8.6)
TAL	13.8 ± 1.3 (12.4–15.0)	16.5 ± 1.3 (14.9–18.5)	18.1 ± 1.1 (16.9–18.9)
BW	4.2 ± 0.3 (3.8–4.4)	5.0 ± 0.3 (4.6–5.4)	5.5 ± 0.1 (5.4–5.5)
BH	3.9 ± 0.4 (3.5–4.3)	4.3 ± 0.2 (4.0–4.7)	4.6 ± 0.1 (4.5–4.6)
TMW	1.5 ± 0.1 (1.4–1.6)	1.9 ± 0.2 (1.6–2.2)	2.2 ± 0.1 (2.1–2.2)
MTH	4.8 ± 0.5 (4.3–5.3)	5.8 ± 0.6 (5.0–6.7)	6.2 ± 0.3 (6.0–6.5)
TMH	1.7 ± 0.1 (1.7–1.8)	2.0 ± 0.1 (1.8–2.1)	2.2 ± 0.1 (2.1–2.2)
IOD	1.8 ± 0.1 (1.8–1.9)	2.1 ± 0.1 (2.0–2.2)	2.3 ± 0.1 (2.3–2.4)
NP	0.6 ± 0.1 (0.6–0.7)	0.8 ± 0.1 (0.6–0.9)	0.9 ± 0.1 (0.8–1.0)
RN	1.4 ± 0.1 (1.3–1.4)	1.5 ± 0.0 (1.5–1.6)	1.6 ± 0.1 (1.5–1.7)
ED	1.1 ± 0.1 (1.0–1.1)	1.1 ± 0.3 (0.7–1.4)	1.3 ± 0.1 (1.2–1.4)
VL	0.7 ± 0.1 (0.6–0.7)	1.0 ± 0.1 (0.7–1.4)	1.1 ± 0.1 (1.0–1.2)
SL	0.7 ± 0.1 (0.6–0.8)	0.9 ± 0.1 (0.7–1.1)	0.8 ± 0.2 (0.6–0.9)

Notes.

n, number of measured tadpoles.

spiracle opening; maximum height of the tail higher than body height (MTH/BH = 1.2). The intestinal mass is visible and positioned subparallel to the longitudinal body axis.

Oral disc is in anteroventral position (Fig. 8). Marginal lip papillae bordering the entire posterior region of the lip up to second third of the anterior lip; one row of papillae on the

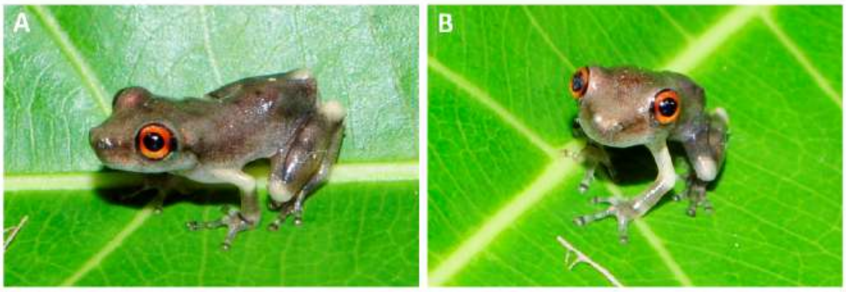

Figure 9 Newly metamorphosed *Scinax. ruberoculatus* sp. nov. (INPA-H 35412). (A) Dorso-lateral view. (B) Fronto-dorsal views. This specimen developed under our care from a typical tadpole of the new species. Photos: R de Fraga.

Full-size DOI: 10.7717/peerj.4321/fig-9

anterior lip and three rows of papillae on the posterior lip. Labial teeth formula 2 (2)/3; A-2 hiatus 0.1 mm; teeth more developed in rows A-1, A-2 and P-1 than in P-2 and P-3. Posterior border of the upper jaw bow with serrated cutting edge; and V-shaped lower jaw with serrated cutting edge.

Colouration of tadpoles (stages 34–39, $n = 13$). In live and preserved specimens, bronze body and tail muscle; tiny dark brown spots on body and tail that are denser posteriorly and may resemble small bars in the lower portion of the tail; dark brown stripe from snout to eye; dark brown postocular stripe; translucent tail; dark brown blotches conglomerated in the last third of the tail; and dark brown tip of tail (Fig. 8).

Colouration of newly metamorphosed specimens (INPA-H 35412, $n = 1$). Living specimens, greyish-brown dorsally with small dark grey spots in the sacral region; loreal region brown; iris red with black border; postocular region and anterior portion of flanks brown; inguinal region light grey; dorsal surfaces of arm and elbow, knee and heel cream; three dark grey stripes on dorsal surface of tibia; dorsal surface of discs dark grey; belly light grey, semi-translucent (Fig. 9).

Notes on the natural history. Individuals of *Scinax ruberoculatus* sp. nov. were observed mainly in primary and old-growth secondary lowland rainforests (39–68 m a.s.l.) where they occupied edge situations. Its breeding season was correlated with the rainy season in the northern PMRI (November–March). Active males vocalized while sitting on the vegetation in horizontal position 1–2 m above the ground around temporary ponds. The number of calling males was higher on rainy nights. In two large temporary ponds (>25 m^2) males of *S. ruberoculatus* sp. nov. shared calling sites with *Dendropsophus minutus* (Peters, 1872), *D. rhodopeplus* (Günther, 1858), *D. sarayacuensis* (Shreve, 1935), and *Scinax* sp. 1 (*sensu* Ferrão et al., 2016). Only males of *S. ruberoculatus* sp. nov. were found in small temporary ponds (<4 m^2). During the day, inactive individuals were observed between leaves of palm trees.

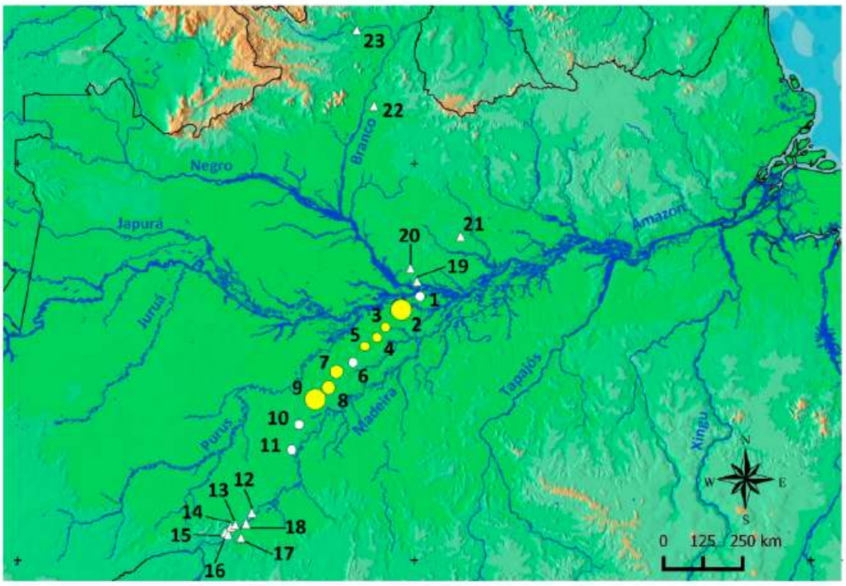

Figure 10 **Geographic range of *Scinax. ruberoculatus* sp. nov.** Numbers indicate the RAPELD sampling module. Yellow circles: RAPELD sampling modules where the new species was observed. White circles: RAPELD sampling modules where the new species was not observed. Triangles: RAPELD sampling modules outside the study area where the new species was not observed. The diameter of the yellow circles indicates the percentage of plots occupied by the new species within each sampling module (10% in 3–5; 20% in 7–8; 40% in 9; 50% in 2).

Full-size DOI: 10.7717/peerj.4321/fig-10

Species-habitat association

Scinax ruberoculatus sp. nov. is distributed in forested habitat of PMRI along the BR-319 federal highway from RAPELD sampling modules 2 (km 100) to 9 (km 450) (Fig. 10). The zero-inflated model revealed a significative and positive effect of soil silt content on the occurrence of this species across the whole study area (occurrence = −5.836 intercept −4.978 number of trees + 3.402 silt content + 0.242 underground water; $\Theta = 3.299$ silt $P = 0.012$). The soil silt content also explained 41% of the abundance of *S. ruberoculatus* sp. nov. (Fig. 11) in the plots where the species was found (abundance = −2.261 + 1.214 silt content; $r^2 = 0.41$, $F1,9 = 6.48$, $P = 0.031$). Forest structure ($P = 0.567$) and underground water ($P = 0.260$) did not have a significant effect on the abundance of the new species.

DISCUSSION

Scinax ruberoculatus sp. nov. is the 72nd described species of the genus *Scinax* (*sensu Duellman, Marion & Hedges, 2016*) and the 30th *Scinax* species known to occur in the Amazonia *sensu lato* (see Table S1). Recent studies have demonstrated that the species richness of the genus *Scinax* is greatly underestimated (*Fouquet et al., 2007*; *Ferrão et al., 2016*; *Menezes et al., 2016*). Despite that, the rate of species descriptions for Amazonian

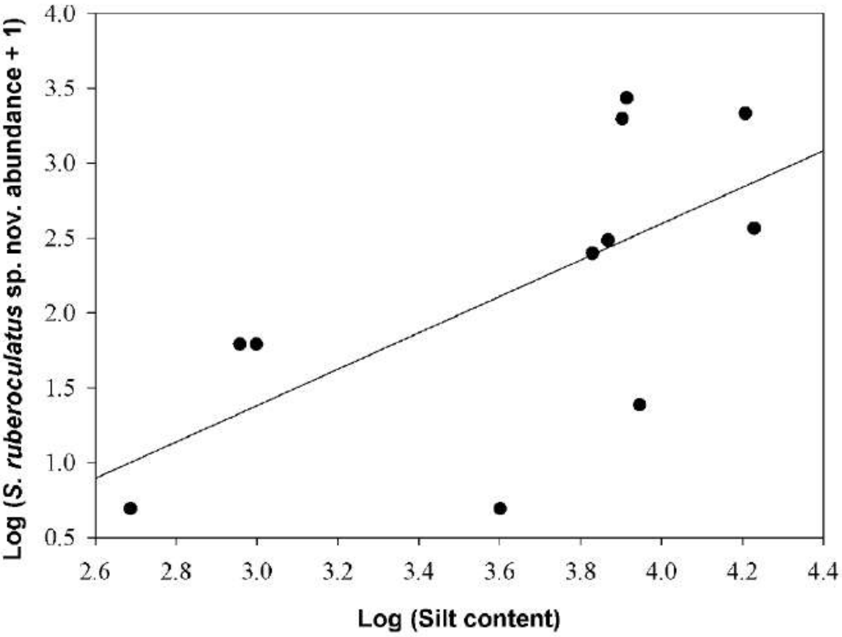

Figure 11 Relationship between the abundance of *Scinax ruberoculatus* sp. nov. and silt content in the Purus-Madeira Rivers Interfluve, Amazonas, Brazil. Model: Log (abundance + 1) = constant + log (silt content). $r^2 = 0.41$, F1,9 = 6.48, $P = 0.031$.

Full-size DOI: 10.7717/peerj.4321/fig-11

Scinax has been low in the last decade (2006–2016; 0.3 species per year) compared with that of other frog genera, e.g., *Allobates* Zimmermann and Zimmermann, 1988 (0.8 species per year) and *Boana* Gray, 1825 (0.7 species per year). However, the description rate of Amazonian *Scinax* may increase in the next years. At least other six potential unnamed species of *Scinax* pending formal description have recently been reported in the PMRI (*Ferrão et al., 2016*). Additionally, the geographic distribution of some species (e.g., *S. blairi*, *S. cruentomma*, *S. iquitorum*, and *S. wandae*) needs to be reviewed.

Over the past decade, our research group has conducted standardized frog sampling along 23 permanent RAPELD sampling modules and/or grids (~450 plots) distributed across a longitudinal gradient of approximately 1,500 km in the Brazilian Amazonia (Fig. 10). Despite this high level of sampling effort, *S. ruberoculatus* sp. nov. has only been observed in seven sampling modules in northern PMRI. However, sampling gaps occur in areas closer to the banks of the PMRI and the neighbouring interfluves in the southern Amazon; therefore, the range of *S. ruberoculatus* sp. nov. may be broader than shown here.

In this study, we addressed the influence of environmental heterogeneity on the distribution of a species of the genus *Scinax* in Amazonia for the first time. Our results indicated that the occurrence and abundance of *S. ruberoculatus* sp. nov. is positively affected by the silt content in the soil. An explanation for this phenomenon can be seen in the fact that increased silt content directly reduces the soil drainage capacity (*Juo & Franzluebbers, 2003*). In areas with slight altitude variations (1–3 m in the northern PMRI; *Rossetti, Toledo & Góes, 2005*), temporary water bodies in silty soils persist for longer periods of time compared with temporary ponds in well-drained, sandier substrates. Because temporary water bodies play a crucial role in the reproduction of *S. ruberoculatus* sp. nov., the soil structure represents an important ecological factor that affects the spatial distribution of the species in the study area. Alternatively, the soil texture may also affect the species composition of invertebrates in Amazonia, such as ants (*Vasconcelos, Macedo & Vilhena, 2003*; *Oliveira et al., 2009*; *Souza et al., 2016*), mites (*Moraes et al., 2011*) and termites (*Dambros et al., 2013*). Therefore, the distribution of *S. ruberoculatus* sp. nov. could be indirectly affected by the soil texture, which promotes the availability of certain invertebrate groups that represent prey species. However, the relationships between invertebrates and soil texture have not been investigated in the PMRI, and additional data are necessary to test this hypothesis.

Environmental heterogeneity may have different effects on frog distribution and abundance in the northern Amazon River depending on the reproductive mode (*Menin et al., 2007*; *Menin, Waldez & Lima, 2011*). Species that exhibit terrestrial reproduction are primarily affected by soil characteristics, such as the clay content and pH, whereas species that exhibit an aquatic reproductive mode are influenced by the tree density and distance from streams (*Landeiro, Waldez & Menin, 2014*). Since *S. ruberoculatus* sp. nov. uses temporary ponds to reproduction, our results are inconsistent with the above generalization made for aquatic breeding frogs but similar with generalization for terrestrial breeding frogs. Nevertheless, we conclude that environmental variables with the ability to filter the occurrence and abundance of species can also cause regional variations in species-habitat associations, independent of the species' reproductive modes. Future investigations should include additional frog species and a wider spatial scale to further elucidate this relationship.

By investigating a species of snouted treefrog, our study showed that alpha-taxonomy and ecology can be integrated into a single framework via the sampling of standardized units along a heterogeneous Amazonian landscape. Such an approach has the potential to reveal additional species and their ecological relationships not only in the study area but also in other megadiverse regions for which insufficient data on both the biota and environmental predictors are still available.

ACKNOWLEDGEMENTS

Many people helped us with our fieldwork, and we are thankful to all of them; however, we would like to especially thank Philip Gleeson (Phill), João Souza (Joãozinho), Moises Mello (Neneco), Pinduca, Eveline Salvático, Guilherme Rezende, and Rubico for their assistance and friendship during the extensive fieldwork. We are in debt to Juliana Schietti, Thaise Emilio, and all people who collected the environmental-data. We thank Ann Hedrick and four anonymous reviewers for comments and suggestions. We also thank Fernanda

Werneck and Ariane Silva for access to the INPA-H zoological collection, and José Albertino Rafael and Dayse Willkenia for taken holotype and tadpole photographs.

ADDITIONAL INFORMATION AND DECLARATIONS

Funding

This study was funded and supported by PRONEX-FAPEAM/CNPq (proj. 003/2009, proc. 653/2009), Ministry of Culture of the Czech Republic (DKRVO 2017/15, National Museum, 00023272), and Centro de Estudos Integrados da Biodiversidade Amazônica (CENBAM). The collection of soil, water table and forest structure data used in this study was funded by FAPESP/FAPEAM (465/2010) and CNPq (473308/2009-6) by the HIDROVEG project, and additional funding was provided by PRONEX-FAPEAM (1600/2006), PPBio Manaus (CNPq 558318/2009-6). The holotype and tadpole photographs were taken with equipment acquired under a grant from PRONEX-FAPEAM (ed. 016/2006, proc. 1437/2007) provided to José Albertino Rafael. Miquéias Ferrão was granted a fellowship from CNPq (proc. 573721/2008-4), FAPEAM and CAPES. Rafael de Fraga was granted a PhD scholarship from CAPES. Jiří Moravec was financially supported by the Ministry of Culture of the Czech Republic (DKRVO 2016/15, 2017/15, and 2018/15). The funders had no role in study design, data collection and analysis, decision to publish, or preparation of the manuscript.

Grant Disclosures

The following grant information was disclosed by the authors:
PRONEX-FAPEAM/CNPq: proj. 003/2009, proc. 653/2009.
Ministry of Culture of the Czech Republic: DKRVO 2016/15, 2017/15, 2018/15.
National Museum: 00023272.
Centro de Estudos Integrados da Biodiversidade Amazônica (CENBAM).
FAPESP/FAPEAM: 465/2010.
CNPq: 473308/2009-6.
HIDROVEG project.
PRONEX-FAPEAM: 1600/2006.
PPBio Manaus: CNPq 558318/2009-6.
PRONEX-FAPEAM: ed. 016/2006, proc. 1437/2007.
CNPq: proc. 573721/2008-4.
FAPEAM.
CAPES.

Competing Interests

The authors declare there are no competing interests.

Author Contributions

- Miquéias Ferrão conceived and designed the experiments, performed the experiments, analyzed the data, wrote the paper, prepared figures and/or tables, reviewed drafts of the paper.

- Rafael de Fraga performed the experiments, analyzed the data, wrote the paper, reviewed drafts of the paper.
- Jiří Moravec analyzed the data, contributed reagents/materials/analysis tools, wrote the paper, reviewed drafts of the paper.
- Igor L. Kaefer conceived and designed the experiments, analyzed the data, wrote the paper, reviewed drafts of the paper.
- Albertina P. Lima conceived and designed the experiments, performed the experiments, analyzed the data, contributed reagents/materials/analysis tools, wrote the paper, reviewed drafts of the paper.

Animal Ethics

The following information was supplied relating to ethical approvals (i.e., approving body and any reference numbers):

Specimens were collected under ICMBio/RAN permit number Number 13777. ICMBio and RAN are institutes of Ministry of Environment, Government of Brazil. These permits were subject to approval of all procedures for collecting and euthanizing frogs.

Data Availability

The following information was supplied regarding data availability:

The raw data is included in Appendix S3.

New Species Registration

The following information was supplied regarding the registration of a newly described species:

Genus name:
urn:lsid:zoobank.org:act:6C6C5E27-39C7-49F4-AE2D-B41DCE6C17C2
New species name: *Scinax ruberoculatus*
urn:lsid:zoobank.org:act:2B83C876-453B-4199-A872-5CED04DB25A5
Publication LSID:
urn:lsid:zoobank.org:pub:D50A0044-0EA6-4619-B0FF-42A7443C4EAB.

Supplemental Information

Supplemental information for this article can be found online at http://dx.doi.org/10.7717/peerj.4321#supplemental-information.

REFERENCES

Allmon WD. 1991. A plot study of forest floor litter frogs, Central Amazon, Brazil. *Journal of Tropical Ecology* **7**:503–522 DOI 10.1017/S0266467400005885.

Altig R, McDiarmid RW. 1999. Body plan: development and morphology. In: McDiarmid RW, Altig R, eds. *Tadpoles: the biology of anuran larvae.* Chicago: University of Chicago Press, 24–51.

Araujo-Vieira K, Brandão RA, Faria DCC. 2015. A new species of rock-dwelling *Scinax* Wagler (Anura: Hylidae) from Chapada dos Veadeiros, central Brazil. *Zootaxa* **3915**:52–66 DOI 10.11646/zootaxa.3915.1.2.

Araujo-Vieira K, Valdujo PH, Faivovich J. 2016. A new species of *Scinax* Wagler (Anura: Hylidae) from Mato Grosso, Brazil. *Zootaxa* **4061**:261–273 DOI 10.11646/zootaxa.4061.3.4.

Barrio-Amorós CL, Orellana A, Chacón-Ortiz A. 2004. A new species of *Scinax* (Anura: Hylidae) from the Andes of Venezuela. *Journal of Herpetology* **38**:105–112 DOI 10.1670/82-01N.

Becker CG, Fonseca CR, Haddad CFB, Batista RF, Prado PI. 2007. Habitat split and the global decline of amphibians. *Science* **318(5857)**:1775–1777 DOI 10.1126/science.1149374.

Bioacoustics Research Program. 2014. Raven Pro: interactive sound analysis software. Version 1.5. Ithaca: The Cornell Lab of Ornithology. *Available at http:// www.birds.cornell.edu/ brp/ raven/ RavenOverview.html*.

Block WM, Brennan LA. 1993. The habitat concept in ornithology. *Currently Ornithology* **11**:35–91.

Bokermann WCA. 1968. Three new *Hyla* from the Plateau of Maracás, central Bahia, Brazil. *Journal of Herpetology* **1**:25–31 DOI 10.2307/1563259.

Bortolus A. 2006. The austral cordgrass *Spartina densiflora* Brong: its taxonomy, biogeography and natural history. *Journal of Biogeogrphy* **33**:158–168 DOI 10.1111/j.1365-2699.2005.01380.x.

Bortolus A. 2008. Error cascades in the biological sciences: the unwanted consequences of using bad taxonomy in ecology. *AMBIO* **37(2)**:114–118 DOI 10.1579/0044-7447(2008)37[114:ECITBS]2.0.CO;2.

Bortolus A, Schwindt E, Iribarne O. 2002. Positive plant–animal interactions in the high marsh of an Argentinean coastal lagoon. *Ecology* **83**:733–742 DOI 10.1890/0012-9658(2002)083[0733:PPAIIT]2.0.CO;2.

Brusquetti F, Jansen M, Barrio-Amarós C, Segalla M, Haddad CFB. 2014. Taxonomic review of *Scinax fuscomarginatus* (Lutz, 1925) and related species (Anura; Hylidae). *Zoological Journal of the Linnean Society* **171**:783–821 DOI 10.1111/zoj.12148.

Bueno AS, Bruno RS, Pimentel TP, Sanaiotti TM, Magnusson WE. 2012. The width of riparian habitats for understory birds in an Amazonian forest. *Ecological Applications* **22**:722–734 DOI 10.1890/11-0789.1.

Caminer MA, Milá B, Jansen M, Fouquet A, Venegas PJ, Chávez G, Lougheed SC, Ron SR. 2017. Systematics of the *Dendropsophus leucophyllatus* species complex (Anura: Hylidae): cryptic diversity and the description of two new species. *PLOS ONE* **12(3)**:e0171785 DOI 10.1371/journal.pone.0171785.

Campbell HW, Christman SP. 1982. Field techniques for herpetofaunal community analysis. In: Scott NJ, ed. *Herpetological communities: a symposium of the society for the study of amphibians and reptiles and the herpetologists' league.* Washington, D.C.: United State Fish Wild Service, 193–200.

Caramaschi U, Cardoso MCS. 2006. Taxonomic status of Hyla camposseabrai Bokermann, 1968 (Anura: Hylidae). *Journal of Herpetology* **40**:549–552.

Cardoso AJ, Sazima I. 1980. Nova espécie de *Hyla* do sudeste brasileiro (Amphibia, Anura, Hylidae). *Revista Brasileira de Biologia* **40**:75–79.

Carvalho TR, Teixeira BFV, Duellman WE, Giaretta AA. 2015. *Scinax cruentommus* (Anura: Hylidae) in the upper Rio Negro drainage, Amazonas state, Brazil, with the redescription of its advertisement call. *Phyllomedusa* **14(142)**:139–146 DOI 10.11606/issn.2316-9079.v14i2p139-146.

Carvalho-e Silva SP, Peixoto OL. 1991. Duas novas espécies de *Ololygon* para os Estados do Rio de Janeiro e Espírito Santo (Amphibia, Anura, Hylidae). *Revista Brasileira de Biologia* **51**:263–270.

Castilho CV, Magnusson WE, Araújo RNO, Luizão RCC, Luizão FJ, Lima AP, Higuchi N. 2006. Variation in aboveground tree life biomass in a central Amazonian forest: effects of soil and topography. *Forest Ecology and Management* **234**:85–96 DOI 10.1016/j.foreco.2006.06.024.

Cei JM. 1980. Amphibians of Argentina. *Monitore Zoologico Italiano, Monografia* **2**:1–609.

Cintra BBL, Schietti J, Emillio T, Martins D, Moulatlet G, Souza P, Levis C, Quesada CA, Schöngart J. 2013. Soil physical restrictions and hydrology regulate stand age and wood biomass turnover rates of Purus–Madeira interfluvial wetlands in Amazonia. *Biogeosciences* **10**:7759–7774 DOI 10.5194/bg-10-7759-2013.

Conte CE, Araujo-Vieira K, Crivellari LB, Berneck BVM. 2016. A new species of *Scinax* Wagler (Anura: Hylidae) from Paraná, southern Brazil. *Zootaxa* **4193**:245–265 DOI 10.11646/zootaxa.4193.2.3.

Corlett RT, Primack RB. 2011. *Tropical rain forests: an ecological and biogeographical comparison*. Hoboken: Blackwell.

Dambros CS, Silva VNV, Azevedo R, Morais JW. 2013. Road-associated edge effects in Amazonia change termite community composition by modifying environmental conditions. *Journal for Nature Conservation* **21(5)**:279–285 DOI 10.1016/j.jnc.2013.02.003.

De la Riva I. 1993. A new species of *Scinax* (Anura, Hylidae) from Argentina and Bolivia. *Journal of Herpetology* **27**:41–46 DOI 10.2307/1564903.

Dexter KG, Pennington TD, Cunningham CW. 2010. Using DNA to assess errors in tropical tree identifications: how often are ecologists wrong and when does it matter? *Ecological Monographs* **80(2)**:267–286 DOI 10.1890/09-0267.1.

Dias-Terceiro RG, Kaefer IL, Fraga R, Araújo MC, Simões PI, Lima AP. 2015. A matter of scale: historical and environmental factors structure anuran assemblages from the Upper Madeira River, Amazonia. *Biotropica* **47(2)**:259–266 DOI 10.1111/btp.12197.

Drummond LO, Baêta D, Pires MRS. 2007. A new species of *Scinax* (Anura, Hylidae) of the S. ruber clade from Minas Gerais, Brazil. *Zootaxa* **1612**:45–63.

Duellman WE. 1970. The hylid frogs of Middle America 1. *Monograph of the Museum of Natural History, the University of Kansas* **1**:1–428.

Duellman WE. 1971. The identities of some Ecuadorian hylid frogs. *Herpetologica* **27**:212–227.

Duellman WE. 1972a. South American frogs of the *Hyla rostrata* group (Amphibia, Anura, Hylidae). *Zoologische Mededelingen. Leiden* **47**:177–192.

Duellman WE. 1972b. A new species of *Hyla* from Amazonian Ecuador. *Copeia* **1972**:265–271 DOI 10.2307/1442487.

Duellman WE. 1973. Descriptions of new hylid frogs from Colombia and Ecuador. *Herpetologica* **29**:219–227.

Duellman WE. 1978. The biology of an equatorial herpetofauna in Amazonian Ecuador. *Miscellaneous Publications of the University of Kansas Museum of Natural History* **65**:1–352.

Duellman WE. 1986. Two new species of *Ololygon* (Anura: Hylidae) from the Venezuelan Guyana. *Copeia* **1986**:864–870 DOI 10.2307/1445281.

Duellman WE. 2005. *Cusco Amazónico: the lives of amphibians and reptiles in an Amazonian rainforest.* Ithaca: Cornell University Press.

Duellman WE, Marion AB, Hedges SB. 2016. Phylogenetics, classification, and biogeography of the treefrogs (Amphibia: Anura: Arboranae). *Zootaxa* **4104(1)**:1–109 DOI 10.11646/zootaxa.4104.1.1.

Duellman WE, Wiens JJ. 1992. The status of the hylid frog genus *Ololygon* and the recognition of *Scinax* Wagler, 1830. *Occasional Papers of the Museum of Natural History, University of Kansas* **151**:1–23.

Duellman WE, Wiens JJ. 1993. Hylid frogs of the genus *Scinax* Wagler, 1830, in Amazonian Ecuador and Peru. *Occasional Paper of the Museum of Natural History, University of Kansas* **153**:1–57.

Eva HD, Huber O. 2005. A proposal for defining the geographical boundaries of Amazonia. Rep. EUR 21808-EN. Luxembourg, European Commission. *Available at http://publications.jrc.ec.europa.eu/repository/bitstream/JRC68635/eur%2021808%20en.pdf*.

Fabrezi M, Alberch P. 1996. The carpal elements of anurans. *Herpetologica* **52(2)**:188–204.

Faivovich J. 2002. A cladistic analysis of *Scinax* (Anura: Hylidae). *Cladistics* **18**:367–393 DOI 10.1016/S0748-3007(02)00001-4.

Faivovich J, Haddad CFB, Garcia PCA, Frost DR, Campbell JA, Weeler WC. 2005. Systematic review of the frog family Hylidae, with special reference to Hylinae: phylogenetic analysis and taxonomic revision. *Bulletin of the American Museum of Natural History* **294**:1–240 DOI 10.1206/0003-0090(2005)294[0001:SROTFF]2.0.CO;2.

Ferrão M, Colatreli O, Fraga R, Kaefer IL, Moravec J, Lima AP. 2016. High species richness of *Scinax* treefrogs (Hylidae) in a threatened Amazonian Landscape revealed by an integrative approach. *PLOS ONE* **11(11)**:e0165679 DOI 10.1371/journal.pone.0165679.

Ferrão M, Moravec J, Fraga R, Almeida AP, Kaefer IL, Lima AP. 2017. A new species of *Scinax* from the Purus-Madeira interfluve, Brazilian Amazonia (Anura, Hylidae). *ZooKeys* **706**:137–162 DOI 10.3897/zookeys.706.14691.

Fouquet A, Vences M, Salducci MD, Meyer A, Marty C, Gilles A. 2007. Revealing cryptic diversity using molecular phylogenetics and phylogeography in frogs of the *Scinax ruber* and *Rhinella margaritifera* species groups. *Molecular Phylogenetics and Evolution* **43**:567–582 DOI 10.1016/j.ympev.2006.12.006.

Fouquette MJ, Pyburn WF. 1972. A new Colombian treefrog of the *Hyla rubra* complex. *Herpetologica* **28**:176–181.

Frost DR. 2017. Amphibian species of the world: an online reference. Version 6.0. *Available at http://research.amnh.org/herpetology/amphibia/index.html*.

Giam X, Scheffers BR, Sodhi NS, Wilcove DS, Ceballos G, Ehrlich PR. 2012. Reservoirs of richness: least disturbed tropical forest are centres of undescribed species diversity. *Proceedings of the Royal Society* **279**:67–76 DOI 10.1098/rspb.2013.0879.

Gomes MR, Alves ACR, Peixoto O. 2014. O girino de *Scinax nebulosus* (Amphibia, Anura, Hylidae). *Iheringia: Série Zoologia* **104(2)**:184–188 DOI 10.1590/1678-476620141042184188.

Gosner KL. 1960. A simplified table for staging anuran embryos and larvae with notes on identification. *Herpetologica* **16**:183–190.

Gotelli NJ. 2004. A taxonomic wish-list for community ecology. *Philosophical Transactions of the Royal Society B: Biological Science* **359**:585–597 DOI 10.1098/rstb.2003.1443.

Hero JM, Mijares-Urrutia A. 1995. The tadpole of Scinax rostrata. *Journal of Herpetology* **29(2)**:307–311 DOI 10.2307/1564575.

Heyer WR, Rand AS, Cruz CAG, Peixoto OL, Nelson CE. 1990. Frogs of Boracéia. *Arquivos de Zoologia* **31**:231–410 DOI 10.11606/issn.2176-7793.v31i4p231-410.

IBGE–Instituto Brasileiro de Geografia e Estatística. 1997. *Recursos naturais e meio ambiente: uma visão do Brasil.* Rio de Janeiro: IBGE Press.

Isaac NJB, Mallet J, Mace GM. 2004. Taxonomic inflation: its influence on macroecology and conservation. *Trends in Ecology & Evolution* **19(9)**:464–469 DOI 10.1016/j.tree.2004.06.004.

Jackman S. 2015. pscl: classes and methods for R developed in the Political Science Computational Laboratory, Stanford University. R package version 1.4.9. Stanford: Department of Political Science, Stanford University. *Available at http://pscl.stanford.edu/* (accessed on 15 July 2016).

Jenkins CN, Pimm SL, Joppa LN. 2013. Global patterns of terrestrial vertebrate diversity and conservation. *Proceedings of the National Academy of Sciences of the United States of America* **110(28)**:2602–2610 DOI 10.1073/pnas.1302251110.

Jorge RF, Simões PI, Magnusson WE, Lima AP. 2016. Fine-scale habitat heterogeneity explains the local distribution of two Amazonian frog species of concern for conservation. *Biotropica* **48(5)**:694–703 DOI 10.1111/btp.12333.

Juncá FA, Napoli MF, Nunes I, Mercês EA, Abreu RO. 2015. A new species of the *Scinax ruber* clade (Anura, Hylidae) from the Espinhaço Range, northeastern Brazil. *Herpetologica* **71**:299–309 DOI 10.1655/HERPETOLOGICA-D-14-00032.

Jungfer K-H, Faivovich J, Padial JM, Castroviejo-Fisher S, Lyra MM, Berneck B, Iglesias PP, Kok PJR, MacCulloch RD, Rodrigues MT, Verdade VK, Torres Gastello CP, Chaparro JC, Valdujo PH, Reichle S, Moravec J, Gvoždík V, Gagliardi-Urrutia G, Ernst R, De la Riva I, Means DB, Lima AP, Señaris JC, Wheeler WC, Haddad CFB. 2013. Systematics of spiny-backed treefrogs (Hylidae: *Osteocephalus*): an Amazonian puzzle. *Zoologica Scripta* **42**:351–380 DOI 10.1111/zsc.12015.

Juo ASR, Franzluebbers K. 2003. *Tropical soils: properties and management for sustainable agriculture.* New York: Oxford University Press.

Kats LB, Ferrer RP. 2003. Alien predators and amphibian declines: review of two decades of science and the transition to conservation. *Diversity and Distributions* **9(2)**:99–110 DOI 10.1046/j.1472-4642.2003.00013.x.

Köhler J, Jansen M, Rodriguez A, Kok PJR, Toledo LP, Emmrich M, Glaw F, Haddad CFB, Rödel MO, Vences M. 2017. The use of bioacoustics in anuran taxonomy: theory, terminology, methods and recommendations for best practice. *Zootaxa* **4251(1)**:1–124 DOI 10.11646/zootaxa.4251.1.1.

Kreft H, Jetz W. 2007. Global patterns and determinants of vascular plant diversity. *Proceedings of the National Academy of Sciences of the United States of America* **104**:5925–5930 DOI 10.1073/pnas.0608361104.

Landeiro VL, Waldez F, Menin M. 2014. Spatial and environmental patterns of Amazonian anurans: differences between assemblages with aquatic and terrestrial reproduction, and implications for conservation management. *Natureza & Conservação* **12(1)**:42–46 DOI 10.4322/natcon.2014.008.

Lescure J, Marty C. 2000. Atlas des Amphibiens de Guyane. *Collections Patrimoines Naturels* **45**:1–388.

Lima LP, Bastos RP, Giaretta AA. 2005. A new *Scinax* Wagler, 1830 of the *S. rostratus* group from central Brazil (Amphibia, Anura, Hylidae). *Arquivos do Museu Nacional. Rio de Janeiro* **62**:505–512.

Limbaugh BA, Volpe EP. 1957. Early development of the Gulf Coast toad, *Bufo valliceps* Weigmann. *American Museum Novitates* **1842**:1–32.

Lips KR, Brem F, Brenes R, Reeve JD, Alford RA, Voyles J, Carey C, Livo L, Pessier AP, Collins JP. 2006. Emerging infectious disease and the loss of biodiversity in a Neotropical amphibian community. *Proceedings of the National Academy of Sciences of the United States of America* **103(9)**:3165–3170 DOI 10.1073/pnas.0506889103.

Lutz B. 1973. *Brazilian species of Hyla.* Austin: University of Texas Press.

Magnusson WE, Braga-Neto R, Pezzini F, Baccaro F, Bergallo H, Penha J, Rodrigues D, Lima AP, Albernaz A, Hero JM, Lawson B, Castilho C, Drucker C, Franklin E, Mendonça F, Costa F, Galdino G, Castley G, Zuanon J, Vale J, Santos JLC, Luizão R, Cintra R, Barcosa RI, Lisboa A, Koblitz RV, Cunha CN, Pontes ARM. 2013. *Biodiversidade e monitoramento ambiental integrado: o sistema RAPELD na Amazônia.* Santo André: Attema.

Magrini L, Carvalho-e Silva SP, Béda AF, Giaretta AA. 2011. Calls of five species of the *Scinax ruber* (Anura: Hylidae) clade from Brazil with comments on their taxonomy. *Zootaxa* **3066**:37–51.

Maldonado FD, Keizer EWH, Graça PMLA, Fearnside PM, Vitel CS. 2012. Previsão temporal da distribuição espacial do desmatamento no interflúvio Purus-Madeira até o ano 2050. In: Sousa-Junior WC, Waichman AV, Sinisgalli PAA, Angelis CF, Romeiro AR, eds. *Rio Purus: Água, Território e Sociedade na Amazônia Sul-Ocidental.* Quito: LibriMundi Press, 183–196.

Martins DL, Schietti J, Feldpausch TR, Luizão FJ, Oliver L, Andrade A, Castilho CV, Laurance SG, Oliveira Á, Ieda L, Quesada CA. 2014. Soil-induced impacts on forest structure drive coarse woody debris stocks across central Amazonia. *Plant Ecology & Diversity* **8**:1–13 DOI 10.1080/17550874.2013.879942.

McDiarmid RW, Altig R. 1990. Description of a bufonid and two hylid tadpoles from western Ecuador. *Alytes* **8(2)**:51–60.

Menezes L, Canedo C, Batalha-Filho H, Garda AA, Gehara M, Napoli MF. 2016. Multilocus Phylogeography of the Treefrog *Scinax eurydice* (Anura, Hylidae) reveals a plio-pleistocene diversification in the Atlantic Forest. *PLOS ONE* **11(6)**:e0154626 DOI 10.1371/journal.pone.0154626.

Menin M, Lima AP, Magnusson WE, Waldez F. 2007. Topographic and edaphic effects on the distribution of terrestrially reproducing anurans in Central Amazonia: mesoscale spatial patterns. *Journal of Tropical Ecology* **17(2)**:86–91 DOI 10.1017/S0266467407004269.

Menin M, Waldez F, Lima AP. 2011. Effects of environmental and spatial factors on the distribution of anuran species with aquatic reproduction in Central Amazonia. *Herpetological Journal* **21**:255–261 DOI 10.4322/natcon.2014.008.

Moraes J, Franklin E, Morais JW, Souza JLP. 2011. Species diversity of edaphic mites (Acari: Oribatida) and effects of topography, soil properties and litter gradients on their qualitative and quantitative composition in 64 km2 of forest in Amazonia. *Experimental and Applied Acarology* **55**:39–63 DOI 10.1007/s10493-011-9451-7.

Moravec J, Tuanama IA, Pérez-Peña PE, Lehr E. 2009. A new species of *Scinax* (Anura: Hylidae) from the area of Iquitos, Amazonian Peru. *South American Journal of Herpetology* **4**:9–16 DOI 10.2994/057.004.0102.

Myers CW, Duellman WE. 1982. A new species of *Hyla* from Cerro Colorado, and other tree frog records and geographical notes from Western Panama. *American Museum Novitates* **2752**:1–32.

Napoli MF. 2005. A new species of allied to *Hyla circumdata* (Anura: Hylidae) from Serra da Mantiqueira, southeastern Brazil. *Herpetologica* **61**:63–69 DOI 10.1655/03-41.

Nunes I, Carvalho Jr RR, Pereira EG. 2010. A new species of *Scinax* Wagler (Anura: Hylidae) from Cerrado of Brazil. *Zootaxa* **2514**:24–34.

Nunes I, Kwet A, Pombal Jr JP. 2012. Taxonomic revision of the *Scinax alter* species complex (Anura: Hylidae). *Copeia* **2012**:554–569 DOI 10.1643/CH-11-088.

Nunes I, Pombal Jr JP. 2010. A new *Scinax* Wagler (Amphibia, Anura, Hylidae) from the Atlantic rain forest remains of southern State of Bahia, north-eastern Brazil. *Amphibia-Reptilia* **31**:347–353 DOI 10.1163/156853810791769482.

Nunes I, Pombal Jr JP. 2011. A new snouted treefrog of the speciose genus *Scinax* Wagler (Anura, Hylidae) from northeastern Brazil. *Herpetologica* **67**:80–88 DOI 10.1655/HERPETOLOGICA-D-10-00026.1.

Oliveira PY, Souza JLP, Baccaro FB, Franklin E. 2009. Ant species distribution along a topographic gradient in a "terra-firme" forest reserve in Central Amazonia. *Pesquisa Agropecuária Brasileira* **44(8)**:852–860 DOI 10.1590/S0100-204X2009000800008.

Pimm SL, Jenkins CN, Abell R, Brooks TM, Gittleman JL, Joppa LN, Raven PH, Roberts CM, Sexton JO. 2014. The biodiversity of species and their rates of extinction, distribution, and protection. *Science* **344(6187)**:1246752 DOI 10.1126/science.1246752.

Pombal Jr JP, Bastos RP, Haddad CFB. 1995. Vocalizações de algumas espécies do gênero *Scinax* (Anura, Hylidae) do sudeste do Brasil e comentários taxonômicos. *Naturalia* **20**:213–225.

Pombal Jr JP, Bilate M, Gambale PG, Signorelli L, Bastos RP. 2011. A new miniature treefrog of the *Scinax ruber* clade from the Cerrado of Central Brazil (Anura: Hylidae). *Herpetologica* **67(3)**:288–299 DOI 10.1655/HERPETOLOGICA-D-10-00067.1.

Pombal Jr JP, Haddad CFB, Kasahara S. 1995. A new species of *Scinax* (Anura: Hylidae) from southeastern Brazil, with comments on the genus. *Journal of Herpetology* **29**:1–6 DOI 10.2307/1565078.

Pons J, Barraclough TG, Gomez-Zurita J. 2006. Sequence based species delimitation for the DNA taxonomy of undescribed insects. *Systematic Biology* **55**:595–609 DOI 10.1080/10635150600852011.

Pugliese A, Baêta D, Pombal Jr JP. 2009. A new species of *Scinax* (Anura: Hylidae) from rocky montane fields in southeastern and central Brazil. *Zootaxa* **2269**:53–64 DOI 10.5281/ZENODO.190903.

Pugliese A, Pombal Jr JP, Sazima I. 2004. A new species of *Scinax* (Anura: Hylidae) from rocky montane fields of the Serra do Cipo, southeastern Brazil. *Zootaxa* **688**:1–5 DOI 10.11646/zootaxa.688.1.1.

Puillandre N, Lambert A, Brouillet S, Achaz G. 2012. ABGD, Automatic Barcode Gap Discovery for primary species delimitation. *Molecular Ecology* **21**:1864–1877 DOI 10.1111/j.1365-294X.2011.05239.x.

Pyburn WF. 1992. A new tree frog of the genus *Scinax* from the Vaupes River of northwestern Brazil. *Texas Journal of Science* **44**:405–411.

Pyburn WF. 1993. A new species of dimorphic tree frog, genus *Hyla* (Amphibia: Anura: Hyldiae), from the Vaupés River of Colombia. *Proceedings of the Biological Society of Washington* **106**:46–50.

Pyburn WF, Fouquette MJ. 1971. A new striped treefrog from central Colombia. *Journal of Herpetology* **5**:97–101 DOI 10.2307/1562731.

R Core Team. 2016. A laneuaee and environment for statistical computing. Vienna: R Foundation for Statistical Computing. *Available at http://www.r-project.org/* (accessed on 1 July 2016).

Randrianiaina RD, Strauß A, Glos J, Glaw F, Vences M. 2011. Diversity, external morphology and 'reverse taxonomy' in the specialized tadpoles of Malagasy river bank frogs of the subgenus *Ochthomantis* (genus *Mantidactylus*). *Contributions to Zoology* **80**:17–65.

Ribeiro JELS, Hopkins MJG, Vicentini A, Sothers CA, Costa MAS, Brito JM, Souza MAD, Martins LH, Lohmann LG, Assunção PA, Pereira EC, Silva CF, Mesquita MR, Procópio LC. 1999. Flora da Reserva Ducke. In: *Guia de identificação das plantas vasculares de uma floresta de terra firme na Amazônia Central.* Manaus: INPA –DFID.

Ribeiro JW, Lima AP, Magnusson WE. 2012. The effect of riparian zones on species diversity of frogs in Amazonian forests. *Copeia* **2012**:375–381 DOI 10.1643/CE-11-117.

Rivero JA. 1961. Salientia of Venezuela. *Bulletin of the Museum of Comparative Zoology* **126**:1–207.

Rojas-Ahumada DP, Landeiro VL, Menin M. 2012. Role of environmental and spatial processes in structuring anuran communities across a tropical rain forest. *Austral Ecology* **37**:865–873 DOI 10.1111/j.1442-9993.2011.02330.x.

Ron SR, Venegas PJ, Toral E, Read M, Ortiz DA, Manzano AL. 2012. Systematics of the *Osteocephalus buckleyi* species complex (Anura: Hylidae) from Ecuador and Peru. *ZooKeys* **229**:1–52 DOI 10.3897/zookeys.229.3580.

Rossetti DF, Toledo PM, Góes AM. 2005. New geological framework for Western Amazonia (Brazil) and implications for biogeography and evolution. *Quaternary Research* **63**:78–89 DOI 10.1016/j.yqres.2004.10.001.

Santana DJ, Costa HC, Drummond LO, Ferreira PL, Feio RN. 2009. Amphibia, Anura, Hylidae, *Scinax auratus*: distribution extension, new state records, and distribution map. Check List. *Journal of Species Lists and Distribution* **5**:246–248 DOI 10.15560/5.2.246.

Savage JM. 2002. *The amphibians and reptiles of Costa Rica*. Chicago: University of Chicago Press.

Savage JM, Heyer WR. 1967. Variation and distribution in the tree-frog genus *Phyllomedusa* in Costa Rica, Central America. *Beiträge zur Neotropischen Fauna* **5**:111–131 DOI 10.1080/01650526709360400.

Schietti J, Emilio T, Rennó CD, Drucker DP, Costa FRC, Nogueira A, Baccaro FB, Figueiredo F, Castilho CV, Kinupp V, Guillaumet JL, Garcia ARM, Lima AP, Magnusson WE. 2014. Vertical distance from drainage drives floristic composition changes in an Amazonian rainforest. *Plant Ecology & Diversity* **7**:241–253 DOI 10.1080/17550874.2013.783642.

Schietti J, Martins D, Emilio T, Souza PF, Levis C, Baccaro FB, Pinto JLPV, Moulatlet GM, Stark SC, Sarmento K, Araújo RNO, Costa FRC, Schöngart J, Quesada CA, Saleska SR, Tomasella J, Magnusson WE. 2016. Forest structure along a 600 km transect of natural disturbances and seasonality gradients in central-southern Amazonia. *Journal of Ecology* **104**:1335–1346 DOI 10.1111/1365-2745.12596.

Souza JP, Baccaro FB, Landeiro VL, Franklin E, Magnusson WE, Pequeno PACL, Fernandes IO. 2016. Taxonomic sufficiency and indicator taxa reduce sampling costs and increase monitoring effectiveness for ants. *Diversity and Distribution* **22**:111–122 DOI 10.1111/ddi.12371.

Stuart SN, Chanson JS, Cox NA, Young BE, Rodrigues ASL, Fischman DL, Waller RW. 2004. Status and trends of amphibian declines and extinctions worldwide. *Science* **306**:1783–1786 DOI 10.1126/science.1103538.

Sturaro MJ, Peloso PLV. 2014. A new species of *Scinax* Wagler, 1830 (Anura: Hylidae) from the middle Amazon River Basin, Brazil. *Papéis Avulsos de Zoologia* **54(2)**:9–23 DOI 10.1590/0031-1049.2014.54.02.

Tsuji-Nishikido BM, Menin M. 2011. Distribution of frogs in riparian areas of an urban forest fragment in Central Amazonia. *Biota Neotropica* **11(2)**:63–70 DOI 10.1590/S1676-06032011000200007.

Vasconcelos HL, Macedo ACC, Vilhena JMS. 2003. Influence of topography on the distribution of ground-dwelling ants in an Amazonian forest. *Studies on Neotropical Fauna and Environment* **38**:115–124 DOI 10.1076/snfe.38.2.115.15923.

Zeileis A, Kleiber C, Jackman S. 2008. Regression models for count data in R. *Journal of Statistical Software* **27**:1–25 DOI 10.18637/jss.v027.i08.

CAPÍTULO 3

A New Species of *Scinax* (Anura: Hylidae) with Red-Striped Eyes from Brazilian Amazonia. *Manuscrito aceito para publicação no* ***Journal of Herpetology***

JOURNAL OF HERPETOLOGY

A New Species of *Scinax* (Anura: Hylidae) with Red-Stripped Eyes from Brazilian Amazonia

Miquéias Ferrão[1,2,5], Jiří Moravec[3], Igor Luis Kaefer[4], Rafael de Fraga[1], and Albertina Pimentel Lima[2]

[1]*Programa de Pós-Graduação em Ecologia, Instituto Nacional de Pesquisas da Amazônia (INPA), Manaus, Brazil; Email: MF, uranoscodon@gmail.com. RF, r.defraga@gmail.com*
[2]*Coordenação de Biodiversidade (CBIO), Instituto Nacional de Pesquisas da Amazônia, Manaus, AM, Brazil; Email: lima@inpa.gov.br*
[3]*Department of Zoology, National Museum, Prague, Czech Republic, Email:* jiri.moravec@nm.cz
[4]*Instituto de Ciências Biológicas, Universidade Federal do Amazonas, Manaus, Amazonas, Brazil; Email: kaefer@ufam.edu.br*
[5]Corresponding author: *uranoscodon@gmail.com*

LRH: M. Ferrão et al.

RRH: New *Scinax* from Purus-Madeira Interfluve

Abstract.– We describe a new small species of *Scinax* from the rainforests on the interfluve between Purus and Madeira rivers, Brazilian Amazonia. The new species is diagnosed by snout-vent length 20.2–22.5 mm in males; yellowish-bronze dorsum, showing small spots along the body and limbs; a red stripe horizontally extended on the medial portion of the iris; posterior surface of thigh brown, both in live and preserved specimens. The advertisement call consists of two types of calls. The call type A represents a series of multi-pulsed notes (note duration 0.097–0.115 s, dominant frequency 2,541–3,015 Hz). The call type B consists of a single tonal note (note duration 0.015–0.019 s, dominant frequency 2,584–2,950 Hz).

Key words: Bioacoustics; Brazil; Purus-Madeira Interfluve; Scinaxinae; Snouted Treefrog; Taxonomy

The genus *Scinax* Wagler, 1830 consists of 71 species of small to medium sized treefrogs distributed from Mexico to southern South America (Frost, 2018). Currently, 30 *Scinax* species are known to occupy different habitats in the Amazonian lowlands (Sturaro and Peloso, 2014; Ferrão et al., 2016). Nevertheless, it turns out that diversity of Amazonian *Scinax* species is considerably underestimated due to insufficient sampling and misidentification of morphologically similar species (Ferrão et al., 2016). In fact, classifying *Scinax* species in the megadiverse Amazonian rainforests is a complex task, which cannot be solved without an integrative approach to the taxonomy of this genus (e.g. Ferrão et al., 2016).

An example of commonly misidentified Amazonian *Scinax* species is *Scinax cruentommus* (Duellman, 1972a), a small sized treefrog with a red horizontal stripe on the iris, which was described from Santa Cecilia, Ecuador. During subsequent decades the name *S. cruentommus* has been attributed to several populations from different parts of South America, such as French Guiana (Lescure and Marty, 2000; Salducci et al., 2002; Salducci et al., 2005; Fouquet et al., 2007a,b), Colombia (Malambo-L and Madrid-Ordóñez, 2008), Peru

(Duellman and Wiens, 1993) and Brazil (Souza, 2009; França and Venâncio, 2010; Bernarde et al., 2011; Bernarde et al., 2013; Zimmerman and Rodrigues, 1990; Carvalho et al., 2015; Ferrão et al., 2016). However, comparison of morphological and genetic characteristics of the above populations revealed that the name *S. cruentommus* is actually applied to several closely related but different species (Carvalho et al., 2015; Ferrão et al., 2016). This finding calls for a thorough taxonomic review of these cryptic species.

In recent study Ferrão et al. (2016) revealed the occurrence of three candidate-species of *Scinax* (*Scinax* sp. 1, *S.* sp. 4, and *S.* sp. 6) in the interfluve between the Purus and Madeira rivers (PMI), in Brazilian Amazonia, that are genetically and morphologically close to *S. cruentommus*. The territory of the PMI is crossed by an abandoned Trans-Amazonian highway (BR-319) and current proposals to reconstruct this highway bring a very serious threat for regional forest habitats and their fauna (see Maldonado et al., 2012). Therefore, studies addressing species richness, species-habitat relations and describing new taxa from the territory of the PMI are of great importance for future actions addressing protection the biological diversity of this area. Herein, we formally describe the first of the above-mentioned candidate species (*Scinax* sp. 1), which may be easily diagnosed by genetic, morphological and bioacoustic characters.

MATERIAL AND METHODS

Sampling and storage.—We collected specimens during the rainy season in November 2013, at the Nascentes do Lago Jari National Park (5°56'40" S, 62°30'04" W, 71 m a.s.l., datum WGS 84), near the kilometer 450 of the highway BR-319, in the municipality of Tapauá (Amazonas, Brazil), PMI. We euthanized the specimens with a 2% benzocaine solution, preserved in 10% formaldehyde and stored in 70% ethanol. We deposited the specimens in the Herpetological section of the zoological collection of the Instituto Nacional de Pesquisas da Amazônia, Manaus, Brazil (INPA-H).

Morphology.—We sexed specimens by observing the presence or absence of vocal sac and vocal slits. We obtained morphometric data using a digital caliper 0.1 mm accurate. We measured nine morphometric characters, following Duellman (1970): SVL (snout-vent length), HL (head length), HW (head width), ED (horizontal eye diameter), IND (internarial distance), IOD (interorbital distance), TD (horizontal tympanum diameter), TL (tibia length) and FL (foot length). Four additional measures followed Napoli (2005): END (eye-nostril distance), NSD (nostril to snout tip distance), 3FD (third finger disk diameter) and 4TD (fourth toe disk diameter). We followed Heyer et al. (1990) to measure length of tarsus (TAL), hand (HAL) and thigh (THL), and to describe the snout shape in dorsal and lateral view. Toe webbing formula follows Savage and Heyer (1967) and Myers and Duellman (1982). We described color in life based on field observations and digital photos.

Call recording. —We recorded advertisement and territorial calls of one male in November 2013, at Tapauá (5°56’40” S, 62°30’04” W, 71 m a.s.l., datum WGS 84), Amazonas State, Brazil. We used a Sennheiser ME 66 directional microphone (Wedemark, Hanover, Germany) connected to a Marantz PMD 660 digital recorder (Kawasaki, Kanagawa Prefecture, Japan), at sample rate of 44.1 kHz. We positioned the microphone approximately 1 m from the acoustically active male. We recorded calls at 2200 h at air temperature of 25 °C.

Call description.—Oscillograms and spectrograms (Blackman window, 80 Hz of frequency resolution and 1024 of Discrete Fourier Transform-DFT) were generated in Raven 1.5 (Bioacoustics Research Program, 2014). We measured the following spectral and temporal parameters of the advertisement call type A: duration, number of pulses per note, pulse rate per second, upper, lower and dominant frequencies, silent interval between calls and call repetition rate per minute. We measured the following spectral and temporal parameters of the advertisement call type B: duration, silent interval between the call type B and the previous call type A, and upper, lower and dominant frequencies. The acoustic terminology followed Köhler et al. (2017) and the advertisement call figures were generated through seewave package (Sueur et al., 2008) using FFT=256 points and 85% overlap.

Generic placement.—Based on molecular data, the subfamily Scinaxinae was proposed by Duellman et al. (2016) to harbour the genera *Sphaenorhynchus*, *Scinax*, *Julianus*, and *Ololygon*. The last three genera are diagnosed by reduced or absent webbing between toes I and II, a feature shared with the new species (Duellman et al., 2016). However, there is no known adult morphological characteristic allowing to distinguish *Scinax*, *Julianus*, and *Ololygon* from each other. Until now, the genus *Scinax* is the only among poorly-webbed Scinaxinae genera occurring in the Amazonia (Sturaro and Peloso, 2014; Ferrão et al., 2017).

We performed a molecular phylogenetic analysis to confirm the generic placement of the new species in the genus *Scinax*. We used 16S rRNA sequences of three individuals of the new species obtained by Ferrão et al. (2016); GenBank accession numbers KU317428 [INPA-H 34688], KU317430 [INPA-H 34700], and KU317431 [INPA-H 34690]. We included additional 16S sequences from other poorly-webbed species of Scinaxinae (*Scinax*, *Ololygon*, and *Julianus*) and from *Sphaenorhynchus* obtained from the Genbank, as well as the sequences of *Osteocephalus taurinus* and *Trachycephalus resinifictrix* used as root (Appendix I).

We preliminarily aligned the sequence dataset through ClustalW algorithm (Thompson et al., 1994) as implemented in BioEdit 7.0 (Hall, 1999) and we checked the resultant alignment by eye. After that we pruned the entire dataset to 517 bp due to avoiding the influence of large amount of missing data in the phylogenetic reconstruction. The most probable evolutionary model to explain sequence diversity in the final alignment was selected by Akaike Information Criteria (AIC: Akaike, 1974) and Bayesian Information Criteria (BIC: Schwarz, 1978) in jModelTest 2.1.7 (Darriba et al., 2012). Both AIC and BIC recovered GTR+G+I as the most probable evolutionary model. We used Bayesian Inference to infer the phylogenetic tree in MrBayes 3.2 (Ronquist et al., 2011). We executed four runs of 10 million generations with a Metropolis-coupled Markov chain Monte Carlo algorithm (MCMC). Each run had four Markov chains with probabilities sampled every 1000 generations. We examined stationarity of the posterior distributions (Effective Sample Sizes > 200) in Tracer v1.7 (Rambaut et al., 2018). MrBayes calculated the 50% majority rule consensus tree after discarding the first 25% of trees as burn-in. Interspecific pairwise Kimura-2-parameter (Kimura, 1980) and uncorrected-pairwise distances were generated in MEGA 6.06 (Tamura et al., 2013).

RESULTS

Scinax sp. nov.

(Figures 1–5)

Scinax sp. 1 Ferrão et al. (2016); Ferrão et al. (2017); Ferrão et al. (2018)

ZooBank ID. — urn:lsid:zoobank.org:act:E1FF0AF1-7E1D-4CFE-B75D-18202CF8A8C2

Holotype.—INPA-H 34688 (field number APL 20286; GenBank accession number KU317428). An adult male (Fig. 1–3, 4C) from Nascentes do Lago Jari National Park, kilometer 450 of BR-319 Highway, Purus-Madeira Interfluve (5°56'40" S, 62°30'04" W, 71 m a.s.l., datum WGS 84), municipality of Tapauá, State of Amazonas, Brazil, collected on 18th November 2013 by M. Ferrão.

Paratypes. —Five specimens: four adult males INPA-H 34689, INPA-H 34690 (GenBank accession number KU317431), INPA-H 34691, INPA-H 34692 (field numbers APL 20288, APL 20293, APL 20287, APL 20292, respectively), and one adult female INPA-H 34700 (field number APL 20295; GenBank accession number KU317430) collected together with the holotype.

Diagnosis. —A small species assigned to the genus *Scinax* based on molecular data, which can be distinguished from other *Scinax* by the combination of the following characters: (1) SVL 21.8 ± 1.1mm (20.2–22.5 mm) in males; (2) truncate snout in dorsal view; (3) HL/SVL ratio = 0.36–0.40; (4) absence of tubercles on the lower jaw; (5) absence of tubercles on knee; (6) absence of dark brown bars on limbs; (7) posterior portion of the thigh uniformly brown; (8) absence of dorsal and dorsolateral dark stripes; (9) red horizontal stripe in the iris; (10) advertisement call consists of two call types: the call type A representing a series of multi-pulsed notes (note duration 0.097–0.115 s, dominant frequency 2,541–3,015 Hz) and the call type B consisting of a single tonal note (note duration 0.015–0.019 s, dominant frequency 2,584–2,950 Hz).

Comparisons.— We compared the new species with the 30 valid species of *Scinax* occurring in Amazonia *sensu lato* (Eva and Huber, 2005): *S. baumgardneri* (Rivero, 1961); *S. blairi* (Fouquette & Pyburn, 1972); *S. boesemani* (Goin, 1966); *S. chiquitanus* (De la Riva, 1990); *S. cruentommus* (Duellman, 1972); *S. danae* (Duellman, 1986); *S. exiguus* (Duellman, 1986); *S. funereus* (Cope, 1874); *S. fuscomarginatus* (Lutz, 1925); *S. fuscovarius* (A. Lutz, 1925); *S. garbei* (Miranda-Ribeiro, 1926); *S. ictericus* Duellman & Wiens, 1993; *S. iquitorum* Moravec, Tuanama, Pérez & Lehr, 2009; *S. jolyi* Lescure & Marty, 2000; *S. karenanneae* (Pyburn, 1992); *S. kennedyi* (Pyburn, 1973); *S. lindsayi* Pyburn, 1992; *S. madeirae* (Bokermann, 1964); *S. nebulosus* (Spix, 1824); *S. onca* Ferrão, Moravec, Fraga, Almeida, Kaefer & Lima, 2017; *S. oreites* Duellman & Wiens, 1993; *S. pedromedinae* (Henle, 1991); *S. proboscideus* (Brongersma, 1933); *S. rostratus* (Peters, 1863); *S. ruber* (Laurenti, 1768); *S. ruberoculatus* Ferrão, Fraga, Moravec, Kaefer & Lima, 2018; *S. sateremawe* Sturaro & Peloso, 2014; *S. villasboasi* Brusquetti, Jansen, Barrio-Amorós, Segalla & Haddad, 2014; *S. wandae* (Pyburn & Fouquette, 1971); *S. x-signatus* (Spix, 1824).

Scinax sp. nov. differs from *S. garbei*, *S. jolyi*, *S. kennedyi*, *S. nebulosus*, *S. pedromedinae*, *S. proboscideus* and *S. rostratus* (all in *S. rostratus* species group) by having truncated snout in dorsal view, absence of tubercles on the lower jaw, absence of tubercles on the knee, and by having posterior portion of the thigh uniformly brown (elongated or pointed snout; tubercles on the lower jaw and/or on the heel present; posterior portion of thigh spotted, marbled or brindle: Duellman, 1972a; Duellman, 1973; Duellman & Wiens, 1992; Duellman and Wiens, 1993; Lescure and Marty, 2000).

The adult male body length is smaller in *S.* sp. nov. (20.2–22.5 mm) than in males of: *S. baumgardneri* (SVL 29.0–32.0 mm; Rivero, 1961); *S. blairi* (SVL 27.8–30.1 mm; Fouquette and Pyburn, 1972); *S. boesemani* (SVL 28.4–31.8 mm; Duellman, 1986); *S. chiquitanus* (SVL 27.9–33.3 mm; Duellman and Wiens, 1993); *S. funereus* (SVL 29.8–36.9 mm; Duellman, 1971; Duellman and Wiens, 1993); *S. fuscovarius* (SVL 36–54 mm; Goldberg et al., 2018); *S. ictericus* (SVL 26.3–31.8 mm; Duellman, 2005); *S. iquitorum* (SVL 35.0–38.5 mm; Moravec et al., 2009); *S. karenanneae* (SVL 26.6–28.9 mm; Pyburn, 1993); *S. onca* (SVL 31.3–34.5 mm; Ferrão et al., 2017); *S. oreites* (SVL 28.4–33.5 mm; Duellman and Wiens, 1993); *S. ruber* (SVL 29.4–41.2 mm; Duellman and Wiens, 1993); *S. sateremawe* (SVL 35.2–38.1 mm; Sturaro and Peloso, 2014); *S. x-signatus* (SVL 32.4–38.7 mm; Juncá et al., 2015).

The absence of dorsal and dorsolateral dark stripes differs *S.* sp. nov. from *S. fuscomarginatus*, *S. madeirae*, and *S. villasboasi* (dark dorsal and/or dorsolateral stripes present; Brusquetti et al., 2014). The dominant frequency (2,541–3,015 Hz) of the advertisement call of *S.* sp. nov. differs from those of *S. exiguus* (3,811–4,802 Hz; Duellman, 1986; Carvalho et al., 2017) and *S. ruberoculatus* (1,809–1,895 Hz; Ferrão et al., 2018).

Superficially, the new species is most similar to *S. cruentommus*, *S. wandae* and *S. lindsayi*. However, males of the new species are distinguishable from those of *S. cruentommus* by smaller SVL (20.2–22.5 mm *vs.* 24.8–27.7 mm; Duellman 1972b; Duellman and Wiens, 1993), and by higher ratio HL/SVL (0.36–0.40 *vs.* 0.31–0.35; Duellman, 1972b). In addition, *S.* sp. nov. differs from *S. cruentommus* by advertisement call parameters, such as shorter call duration (0.097–0.115 s *vs.* 0.215–0.370 s; Duellman, 1972b; Carvalho et al., 2015), lower number of pulses per call (23–27 *vs.* 39–54; Carvalho et al., 2015). The stained pattern of the dorsal color in *S.* sp. nov. is easily distinguished from the striped pattern of *S. wandae* (Pyburn and Fouquette, 1971). Additionally, the new species differs from *S. wandae* by the smaller body size in males (20.2–22.5 mm *vs.* 23.4–26.9 mm; Pyburn and Fouquette, 1971), and by shorter call (0.097–0.115 s *vs.* 0.442–0.710 s; Pombal et al., 2011) and lower dominant frequency (2,541–3,015 Hz in *vs.* 3,359–5,167 Hz; Pombal et al., 2011). *Scinax* sp. nov. differs from *S. lindsayi* by having snout truncated in dorsal view (rounded; Pyburn, 1992), red horizontal stripe on the iris (absence of red horizontal stripe on the iris; Pyburn, 1992), absence of dark brown bars on limb (present; Pyburn, 1992), and by having pulsed call (not pulsed; Pyburn, 1992).

There is an available name (*Hyla affinis* Spix, 1824) in the synonymy of *Scinax x-signatus*. The Spix's description is based on a specimen (ZSM 2495/0) from Brazilian Amazonia and depicts the species with red color of iris. However, *Scinax* sp. nov. differs *H. afiinis* by having snout truncate in dorsal view (rounded in the holotype of *H. affinis*), canthus rostralis curved (straight in the holotype of *H. affinis*), absence of bars on the thigh, tibia, forearms, and flanks (present in *H. affinis*: Spix, 1824), and dorsum yellowish (greenish in *H. affinis*: Spix, 1824).

Description of holotype.—Adult male (Fig. 1), 20.2 mm SVL; head longer than wide, HW 90% of HL; HL 38% of SVL; HW 34% of SVL; snout truncated in dorsal view and rounded in lateral view; END equal to 91% of ED; nostrils protruding dorsolaterally; region between nostrils slightly concave; *canthus rostralis* well defined, curved medially; ED 33% of HL; interocular portion flattened; supratympanic fold distinct; tympanum round and small, TD 35% of the ED; medium-sized vocal sac, subgular, externally expanded; vocal slits present, extending from lateral base of tongue to the mouth angles; tongue lanceolate; triangular dentigerous processes of vomers, separated from each other by half their length, each of them with six (right) and five (left) teeth; oval choanae; axillary membrane absent.

Arm slender, forearm moderately robust; ulnar tubercle absent; fingers long, relative length of fingers I < II < IV < III (Fig. 2A); finger webbing formula, I vestigial II 2–3$^{1/3}$ III 3–3 IV; finger discs large and elliptical (3FD/TD = 1.11); palmar tubercle flattened and bifid; tenar tubercle flattened and elliptical; subarticular tubercle of Finger I slightly conical, subarticular tubercles protruding on fingers II–IV; supernumerary tubercles distinct; nuptial pad present on the thumbs, extending from proximal margin of thenar tubercle to proximal margin of the subarticular tubercle.

Posterior limbs long, TL 52% of SVL, THL 50% of SVL; tarsal fold and tubercles absent; tubercles on knee and heel absent; foot length equals 42% of SVL; TAL 65% of FL; inner metatarsal tubercle elliptical and protuberant; outer metatarsal tubercle small, rounded, slightly protuberant, three times smaller than the inner metatarsal tubercle; subarticular tubercle on Toe I subconical and protuberant, subarticular tubercles rounded and slightly protruding on the toes II–V; supernumerary tubercles not evident; toe discs elliptical; 4TD the same size of ED (4TD/TD = 1.00); vestigial membrane between toes I and II, webbing formula II $1^{1/3}$–$2^{1/2}$ III $1^{1/3}$–$2^{1/2}$ IV $2^{1/2}$–1^{+} V (Fig. 2B). Anal opening at the middle level of the thighs.

Skin on the dorsal surface smooth, except in the upper and anterior regions of the tympanum, where it is shagreen; skin on flanks slightly areolate; vocal sac smooth; chest, belly and ventral surface of the thigh areolate.

Color in life of the holotype.—Dorsum yellowish-bronze with light-brown spots, darker over the snout and eyelids (Fig. 3). An irregularly shaped light-brown spot on the interorbital region. Brown canthal stripe. Upper lip light-cream, yellowish-cream below the eye and tympanum. Iris golden, with a broad medial horizontal red stripe. Brown supratympanic band extending from the corner of the eye to the medial portion of the flank. Yellowish-cream inconspicuous stripe on ventrolateral portion of the flanks. Inguinal region greenish-bronze. Dorsal surface of hand yellowish-cream. Dorsal surface of the forearm yellowish-bronze, with a dark-gray spot on distal portion, a small dark-gray spot on the medial portion, and an inconspicuous brown spot in the proximal portion. Dorsal surface of arm yellowish-cream. Anterior and dorsal surfaces of thigh greenish-bronze. Posterior portion of thigh brown. Dorsal surface of the tibia and tarsus yellowish-bronze, with small marbled light-brown spots. Cream spots on the ankles. Dorsal surface of the feet greenish-bronze. Vocal sac bright-yellow. Chest cream and belly gray. Ventral surface of thigh grayish. Ventral surface of tarsus grayish-green. Palmar and plantar surfaces gray.

Variation within the type series.—In preservative, dorsal color light brown, brownish-gray to brown. Small to large dark-brown spots present on the snout in 83% of the type-series (Fig. 4B–F) and absent on the others (Fig. 4A). Dorsal dark-brown spots denser in specimens brown (Fig. 4D–F), except in the female specimen (Fig. 4A). Brown spots on the eyelids varying in size and number. Light brown band in the interorbital region present on 67% of individuals, absent on remaining specimens. Gray to dark-brown band between nostril and eye present in all specimens. Upper lip cream with light or dark brown spots in all specimens, varying in number and size. Light to dark brown supratympanic band evident in all specimens, extending to above of axillar region in 50% of individuals, to the inguinal region in 33% and on 17% it extends to 1/3 of the flanks. Light dorsolateral stripe extending from the postocular portion to the inguinal region in 17% of specimens, absent on the remaining. Light stripe on the lower portion of the flanks, ventrally bordered by a light brown or light gray stripe or spots in 83% of the individuals, absent on the others. Inguinal region grayish-cream in 50% of the series, light brown in the other half.

Upper distal portion of the finger digits cream to light-brown, brown in the proximal portion. Dorsal surface of hand and fingers light-brown. Light to dark brown stripe on the proximal surface of the hand. Dorsal surface of the forearm cream to light-brown, with dark-brown spots or bars. Arm cream on 67% of specimens, light brown on 33%; dark brown spots just on 50% of the series. Anterior surface of the thigh light brown on 67% of the specimens, light gray on 17% and brown on 17%. Upper surface of the thigh cream on 50% of the series, light brown on 33% and brown on the remaining. Posterior surface of the thigh brown on 67% of the specimens, and light brown on 33%. Dorsal surface of the tibia cream to brown, with dark brown spots on 67% of the series, light brown on 17% and gray on the remaining. The number of spots on the dorsal surface of the tibia varies in number, 67% of the specimens have conspicuous dark spots, inconspicuous on 33% of them. Dorsal surface of the tarsus cream on 67% and light brown on 33% of the specimens, with brown spots or blotches. Dorsal surface of foot and toes cream on 67% of specimens and light brown on the remaining. Proximal portion of toe and finger digits dark brown in all specimens, distal portion of digits cream on 83% and light brown on 17% of the series. Toe webbing translucent cream on 67% of specimens and light brown on 33%. Vocal sac, chest and belly cream. Ventral surface of the hand cream on 67% of specimens and light brown on the others. Ventral surface of the tarsus light cream on 50%, brown on 33% and light brown on 17% of the specimens. Ventral surface of foot light brown on 67% of specimens and brown on the remaining.

Toe webbing of *S.* sp. nov. varies subtly within the series type, and it follows the formula: I vestigial II $(1^{1/2}–1^{1/3})–(2^{1/2}–2^{2/3})$ III $(1^{+1/3}–1^{1/2})–(2^{1/3}–2^{2/3})$ IV $(2^{1/2}–2^{2/3})$ $–1^{+}$ V. Dentigerous processes of vomers are absent on the left side in 42% of the specimens. Number of teeth 2–7 on the right side and 3–5 on the left side. The proportional ratios between morphometric characters of the single female in our sample follow the same range as in the males. Measures and morphometric ratios of the type series are presented in Table 1.

Vocalization.—The advertisement call of *S.* sp. nov. is composed of two types of calls: call type A and call type B (Fig. 5). The call type A (Fig. 5C) consists of a series of single short multipulsed notes and can be characterized by the following numerical call parameters (range followed by mean ± standard deviation in parentheses): notes/call 17–30 (24 ± 6.6, n = 3); note duration 0.097–0.115 s (0.106 ± 0.005, n = 21); note repetition rate 85–175 notes/min (139 ± 24); pulse/note 23–27 (25.1 ± 1.1, n = 21); pulse duration 0.002–0.003 s (0.002 ± 0.0005, n = 63); interval between pulses 0.001–0.003 s (0.002 ± 0.0004, n = 63); pulse repetition rate 200–250 pulses/s (225 ± 25, n = 42); silent interval between calls 0.221–0.601 s (0.338 ± 0.093, n = 21); lower frequency 2,213–2,441 Hz (2,255 ± 49, n = 21); upper frequency 3,595–3,803 Hz (3,696 ± 80, n = 21); dominant frequency 2,541–3,015 Hz (2,816 ± 93, n = 21).

The call type B (Fig. 5D) consists of a single tonal note and may intercalate the call A. Its characteristics are as follows: note duration 0.015–0.019 s (0.017 ± 0.001, n = 6); lower frequency 2,200–2,354 Hz (2,280 ± 55, n = 6); upper frequency 3,125–3,621 Hz (3,380 ± 210, n = 6); dominant frequency is 2,584–2,950 Hz (2,774 ± 147, n = 6). The silent interval between call B and previous call A is 0.250–0.883 s (0.388 ± 0.246, n = 6).

Phylogenetic relationships and genetic distances.—The Bayesian phylogenetic tree based on a fragment of 517 bp of the 16S rRNA indicated that *S.* sp. nov. is closely related to other nominal and candidate species characterized by having red-striped iris (*S. cruentommus* and *S.* sp. 1, *S.* sp. 4, and *S.* sp. 6 sensu Ferrão et al., 2016) and to *S. wandae* (Fig. 6). Excepted by *S. wandae* that occur in Colombia and Venezuela, all the other taxa in this clade occur in the PMI. The uncorrected pairwise and K2P distance between sequences of the new species and *S. cruentommus* is 9% and 10%, respectively. The genetic distances between *S.* sp. nov. and *S. wandae* are larger, ranging from 10% (p-distance) to 11% (K2P). The clade composed by *S.* sp. nov., *S. cruentommus*, *S. wandae* and other Amazonian taxa with red-striped iris was grouped with the clade comprising the small species of *Scinax* characterized mainly by having dorsolateral marks or stripes (*S. fuscomarginatus*, *S. madeirae*, *S. villasboasi*) and with *S. staufferi*. The smallest and largest genetic distances between sequences of *S.* sp. nov. and those from the above-mentioned species was recovered with *S. staufferi* (11% p-distance; 12% K2P) and *S. villasboasi* (16% p-distance: 18% K2P), respectively.

Distribution and natural history.—*Scinax* sp. nov. has been found only in the Nacentes do Lago Jari National Park, Purus-Madeira rivers interfluve, Amazonas, Brazil (Fig. 7). All the specimens in our sample were collected in primary rainforest, which is classified as dense ombrophylous lowland forest with emergent canopy (IBGE, 1997). The males call from low vegetation and dry branches around small temporary pools. The specimen which we recorded in this study was calling on a dry palm leaf, approximately 80 cm above a small isolated (not connected to a stream) pool. The reproduction of the new species has an explosive character. Although we have spent approximately 1,000 hours sampling frogs along the study area during rainy season, just a single explosive reproductive event was observed.

Etymology.—The specific epithet honors Christine Strüssmann for her friendship and outstanding contribution to Brazilian herpetology.

Suggested common English name. — Strüssmann's Snouted Treefrogs.

DISCUSSION

Scinax sp. nov. groups with other diminutive species of *Scinax* with a red and brown horizontal stripe in the middle portion of the iris (*S. cruentommus*, *S. wandae*). However, the new species is not cryptic in relation to any of these correlated species. The new species can be easily distinguished based on external morphology and bioacoustical characters. Additionally, 16S rRNA sequences of *Scinax* sp. nov. showed high uncorrected pairwise genetic distances in relation to close related nominal species, as *S. wandae* (10%) and *S. cruentommus* (9%). These levels of genetic divergence among species are greater than those suggested by Vences et al. (2005) and Fouquet et al. (2007b) as evidence for interspecific difference among tropical frogs.

Our research group has applied a massive frog sampling along 450 RAPELD plots (see Magnusson et al., 2013) longitudinally distributed over more than 1,500 km in the Brazilian Amazonia. Despite that, *S.* sp. nov. was found in less than 1% of the plots, and during a single event of explosive reproduction. These findings suggest that the new species is narrowly distributed in the Amazonian rainforests, probably because it is an habitat-specialist, however, detectability seems to be strongly affected by sparse calling events. Although the new species occurs in the Nascentes do Lago Jari National Park, the specimens reported here inhabit forests in the border between the park and the BR-319 federal highway, where native habitats are strongly threatened by illegal logging (M. Ferrão and R. Fraga pers. com.). In fact, a third of the primary and old secondary forests in the PMI should be deforested until 2050 due to the human occupation expanding by the road reconstruction (Fearnside et al., 2009; Maldonado et al., 2012; Graça et al., 2014).

In addition to *S.* sp. nov., the PMI is the type locality of nine recently described frogs (Lima and Caldwell, 2001; Caldwell and Lima, 2003; Lima et al., 2010; Simões et al., 2010; Brown et al., 2011; Sturaro and Peloso, 2014; Ferrão et al. 2017; Ferrão et al. 2018; Melo-Sampaio et al., 2018) and one salamander (Brcko et al., 2013). Furthermore, *Hydrolaetare dantasi* (Bokermann, 1959) and *Osteocephalus castaneicola* Moravec, Aparicio, Guerrero-Reinhard, Calderón, Jungfer and Gvoždík, 2009 were recently found in the PMI, which represented the species' first records in the Amazonas state (Ferrão et al., 2014) and Brazil (Meneghelli and Entiauspe, 2014), respectively. Finally, two discontinuously distributed frog species that are usually rare in collections [*Hyalinobatrachium cappellei* Van Lidth de Jeude, 1904 and *Callimedusa* (*=Phyllomedusa*) *atelopoides* (Duellman, Cadle and Cannatella, 1988)] have been recently reported from the PMI (Simões et al., 2012; Fraga et al., 2014.). These studies highlight the remarkable amphibian diversity in the PMI, which should not be overlooked in environmental impact assessments. The PMI is under rapidly increasing anthropogenic pressure, which has caused habitat loss by road paving (Soares-Filho et al., 2006; Fearnside et al., 2009) and artificial flooding by hydroelectric power plants (Fearnside, 2014).

ACKNOWLEDGMENTS

This study was supported by PRONEX - FAPEAM / CNPq (proj 003/2009, proc. 653/2009). We thank Paul E. Bartelt and anonymous reviewers for valuable comments and suggestions. We thank Centro de Estudos Integrados da Biodiversidade Amazônica (CENBAM) for field assistance. To Fernanda Werneck and Michael Franzen for access to the INPA-H and ZSM collection. Photos of holotype and paratypes were taken with equipment acquired under grant from PRONEX-FAPEAM Ed. 016/2006, proc. 1437/2007 to José

Albertino Rafael. Miquéias Ferrão had fellowship from the Conselho Nacional de Desenvolvimento Científico e Tecnológico (CNPq – proc. 573721/2008-4). Miquéias Ferrão received PhD fellowship from Fundação de Amparo à Pesquisa do Estado do Amazonas (FAPEAM) and Coordenação de Aperfeiçoamento de Pessoal de Nível Superior (CAPES). Rafael Fraga had PhD fellowship from CAPES. Work of Jiří Moravec was financially supported by Ministry of Culture of the Czech Republic (DKRVO 2016/15, 2017/15 National Museum, 00023272). Collecting permits were provided by RAN/ICMBio (Reg. 659755 process Nº 13777).

LITERATURE CITED

AKAIKE, H. 1974. A new look at the statistical model identification. IEEE Trans Automat Control 19:716–723.

ARAUJO-VIEIRA, K., A. TACIOLI, J. FAIVOVICH, V. G. ORRICO, AND T. GRANT. 2015. The tadpole of *Sphaenorhynchus caramaschii*, with comments on larval morphology of *Sphaenorhynchus* (Anura: Hylidae). Zootaxa 3904:270–282.

BELL, R. C., C. A. BRASILEIRO, C. F. B. HADDAD, AND K. R. ZAMUDIO. 2012. Evolutionary history of *Scinax* treefrogs on land-bridge islands in south-eastern Brazil. Journal of Biogeography 39:1733–1742.

BERNARDE, P. S., R. A. MACHADO, AND L. C. B. TURCI. 2011. Herpetofauna da área do Igarapé Esperança na Reserva Extrativista Riozinho da Liberdade, Acre – Brasil. Biota Neotropica 11:117−144.

BERNARDE, P. S., S. ALBUQUERQUE, D. B. MIRANDA, AND L. C. B. TURCI. 2013. Herpetofauna da floresta do baixo rio Moa em Cruzeiro do Sul, Acre – Brasil. Biota Neotropica 13:220−244.

BIOACOUSTICS RESEARCH PROGRAM. 2014. Raven Pro: Interactive Sound Analysis Software. Ver. 1.5. [Computer software]. Ithaca, NY: The Cornell Lab of Ornithology.

BOKERMANN, W. C. A. 1959. Una nueva especies de *Leptodactylus* de la region Amazonica (Amphibia, Salientia, Leptodactylidae). Neotropica. La Plata 5:5–8.

BRCKO, I., M. S. HOOGMOED, AND S. NECKEL-OLIVEIRA. 2013. Taxonomy and distribution of the salamander genus *Bolitoglossa* Duméril, Bibron & Duméril, 1854 (Amphibia, Caudata, Plethodontidae) in Brazilian Amazonia. Zootaxa 3686:401–431.

BROWN, J. L., E. TWOMEY, A. AMÉZQUITA, M. B. DE SOUZA, J. P. CALDWELL, S. LÖTTERS, R. VON MAY, P. R. MELO-SAMPAIO, D. MEJÍA-VARGAS, P. E. PÉREZ-PEÑA, M. PEPPER, E. H. POELMAN, M. SANCHEZ-RODRIGUEZ, AND K. SUMMERS. 2011. A taxonomic revision of the Neotropical poison frog genus *Ranitomeya* (Amphibia: Dendrobatidae). Zootaxa 3083:1–120.

BRONGERSMA, L. D. 1933. Ein neuer Laubfrosch aus Surinam. Zoologischer Anzeiger 103:267–270.

BRUSQUETTI, F., M. JANSEN, C. BARRIO-AMARÓS, M. SEGALLA, AND C. F. B. HADDAD. 2014. Taxonomic review of *Scinax fuscomarginatus* (Lutz, 1925) and related species (Anura; Hylidae). Zoological Journal of the Linnean Society 171:783–821.

CALDWELL, J. P., AND A. P. LIMA. 2003. A new Amazonian species of *Colostethus* (Anura: Dendrobatidae) with a nidicolous tadpole. Herpetologica 59:219–234.

CARVALHO, T. R., B. F. V. TEIXEIRA, W. E. DUELLMAN, AND A. GIARETTA. 2015. *Scinax cruentommus* (Anura: Hylidae) in the upper Rio Negro drainage, Amazonas state, Brazil, with the redescription of its advertisement call. Phyllomedusa: Journal of Herpetology 14:139-146.

CARVALHO, T. R., P. AZARAK, D. BANG, W. E. DUELLMAN, AND A. GIARETTA. 2017. A reassessment of the vocalization and distribution of *Scinax exiguus* (Duellman, 1986)

(Anura: Hylidae) in the Amazonian savanna of Roraima, northern Brazil, with the description of its aggressive call. Neotropical Biodiversity 3:196–202.

Cope, E. D. 1874. On some Batrachia and Nematognathi brought from the upper Amazon by Prof. Orton. Proceedings of the Academy of Natural Sciences of Philadelphia 26:120–137.

Darriba, D., G. L. Taboada, R. Doallo, and D. Posada. 2012. jModelTest 2: more models, new heuristics and parallel computing. Nature Methods 9:772.

Darst, C. R., and D. C. Cannatella. 2004. Novel relationships among hyloid frogs inferred from 12S and 16S mitochondrial DNA sequences. Molecular Phylogenetics and Evolution 31:462–475.

De la Riva, I. 1990. Una especie nueva de *Ololygon* (Anura: Hylidae) procedente de Bolivia. Revista Española de Herpetología 4:81–86.

Duellman, W. E. 1970. The hylid frogs of Middle America 1. Monograph of the Museum of Natural History, The University of Kansas 1:1−428.

Duellman, W. E. 1971. The identities of some Ecuadorian hylid frogs. Herpetologica 27:212–227.

Duellman, W. E. 1972a. South American frogs of the *Hyla rostrata* group (Amphibia, Anura, Hylidae). Zoologische Mededelingen 47:177−192.

Duellman, W. E. 1972b. A new species of *Hyla* from Amazonian Ecuador. Copeia 1972:265−271.

Duellman, W. E. 1973. Descriptions of new hylid frogs from Colombia and Ecuador. Herpetologica 29:219–227.

Duellman, W. E. 1986. Two new species of *Ololygon* (Anura: Hylidae) from the Venezuelan Guyana. Copeia 1986:864−870.

Duellman, W. E., J. E. Cadle, and D. C. Cannatella. 1988. A new species of terrestrial *Phyllomedusa* (Anura: Hylidae) from southern Peru. Herpetologica 44:91–95.

Duellman, W. E, and J. J. Wiens. 1992. The status of the hylid frog genus *Ololygon* and the recognition of *Scinax* Wagler, 1830. Occasional Papers of the Museum of Natural History, University of Kansas 151:1–23.

Duellman, W. E., and J. J. Wiens. 1993. Hylid frogs of the genus *Scinax* Wagler, 1830, in Amazonian Ecuador and Peru. Occasional Paper of the Museum of Natural History, University of Kansas 153:1−57.

Duellman, W. E. 2005. Cusco Amazónico: the lives of amphibians and reptiles in an Amazonian rainforest. Cornell University Press, USA.

Duellman, W. E., A. B. Marion, and S. B. Hedges. 2016. Phylogenetics, Classification, and Biogeography of the Treefrogs (Amphibia: Anura: Arboranae). Zootaxa 4104:1–109.

Eva, H. D. and O. Huber. 2005. A proposal for defining the geographical boundaries of Amazonia. Rep. EUR 21808-EN. Luxembourg, European Commission. Available at http://publications.jrc.ec.europa.eu/repository/bitstream/JRC68635/eur%2021808%20en.pdf .

Faivovich, J., P. C. García, F. Ananias, L. Lanari, N. G. Basso, and W. C. Wheeler. 2004. A molecular perspective on the phylogeny of the *Hyla pulchella* species group (Anura, Hylidae). Molecular Phylogenetics Evolution 32:938–50.

Faivovich, J., C. F. B. Haddad, P. C. A. Garcia, D. R. Frost, J. A. Campbell, and W. C. Weeler. 2005. Systematic review of the frog family Hylidae, with special reference to Hylinae: phylogenetic analysis and taxonomic revision. Bulletin of the American Museum of Natural History 294:1–240.

Fearnside, P., P. M. L. A. Graça, E. W. H. Keizer, F. D. Maldonado, I. R. Barbosa, and E. M. Nogueira. 2009. Modelagem de desmatamento e emissões de gases de efeito estufa na região sob influência da Rodovia Manaus-Porto Velho (BR-319). Revista Brasileira de Meteorologia 24:208–233.

FEARNSIDE, P. 2014. Impacts of Brazil's Madeira River Dams: Unlearned lessons for hydroelectric development in Amazonia. Environmental Science and Policy 38:164–172.

FERRÃO, M., R. FRAGA, P. I. SIMÕES, AND A. P. LIMA. 2014. On the poorly sampled Amazonian frogs genus *Hydrolaetare* (Anura: Leptodactylidae): geographic ranges and species identification. Salamandra 50:77–84.

FERRÃO, M., O. COLATRELI, R. FRAGA, I. L. KAEFER, J. MORAVEC, AND A. P. LIMA. 2016. High species richness of *Scinax* (Anura, Hylidae) in a threatened Amazonian landscape revealed by integrative approach. PLoS ONE 11:e0165679. doi:10.1371/journal.pone.0165679

FERRÃO, M., J. MORAVEC, R. FRAGA, A. P. ALMEIDA, I. L. KAEFER, AND A. P. LIMA. 2017. A new species of *Scinax* from the Purus-Madeira interfluve, Brazilian Amazonia (Anura, Hylidae). ZooKeys 706:137–162.

FERRÃO, M., R. FRAGA, J. MORAVEC, I. L. KAEFER, AND A. P. LIMA. 2018. A new species of Amazonian snouted treefrog (Hylidae: *Scinax*) with description of a novel species-habitat association for an aquatic breeding frog. PeerJ 6:e4321. doi:10.7717/peerj.4321

FOUQUET, A., M. VENCES, M. D. SALDUCCI, A. MEYER, C. MARTY, AND A. GILLES. 2007a. Revealing cryptic diversity using molecular phylogenetics and phylogeography in frogs of the *Scinax ruber* and *Rhinella margaritifera* species groups. Molecular Phylogenetics and Evolution 43:567–582.

FOUQUET, A., A. GILLES, M. VENCES, C. MARTY, M. BLANC, AND N. J. GEMMELL. 2007b. Underestimation of species richness in neotropical frogs revealed by mtDNA analyses. PloS One 10:e1109. doi:10.1371/journal.pone.0001109

FOUQUETTE, M. J., AND W. F. PYBURN. 1972. A new Colombian treefrog of the *Hyla rubra* complex. Herpetologica 28:176−181.

FRAGA, R., M. FERRÃO, AND V. T. CARVALHO. 2014. Geographic range extension of the Toad Leaf Frog *Phyllomedusa atelopoides* Duellman, Cadle and Cannatella, 1988 (Anura, Hylidae). Herpetology Notes 7:203–205.

FRANÇA, F.G.R., AND N. M. VENÂNCIO. 2010. Reptiles and amphibians of a poorly known region in southwest Amazonia. Biotemas 23:71–84.

FROST, D. R. 2018. Amphibian Species of the World: an Online Reference. Version 6.0. Available at http://research.amnh.org/herpetology/amphibia/index.html. Archived by WebCite at http://www.webcitation.org/71dLHGYSy on 13 August 2018.

GOIN, C. J. 1966. Description of a new frog of the genus *Hyla* from Suriname. Zoologische Mededelingen. Leiden 4:229–232.

GOLDBERG, J., D. CARDOZO, F. BRUSQUETTI, D. BUENO VILLAFAÑE, A. CABALLERO GINI, AND C. BIANCHI. 2018. Body size variation and sexual size dimorphism across climatic gradients in the widespread treefrog *Scinax fuscovarius* (Anura, Hylidae). Austral Ecology 43:35–45.

GRAÇA, P. M. L. A., M. A. SANTOS, V. M. ROCHA, P. M. FEARNSIDE, T. EMILIO, J. MENGER, R. MARCIENTE, P. E. D. BOBROWIEC, E. M. VENTICINQUE, A. P. ANTUNES, A. N. BASTOS, AND F. ROHE. 2014. Cenários de desmatamento para região de influência da rodovia BR-319: perda potencial de habitats, status de proteção e ameaça para a biodiversidade, Pp. 91–101 in T. Emilio and F. Luizão. (Eds.), Cenários para a Amazônia: Clima, Biodiversidade e Uso da Terra. Editora-INPA, Brazil.

GUARNIZO, C. E., A. PAZ, A. MUÑOZ-ORTIZ, S.V. FLECHAS, J. MÉNDEZ-NARVAÉZ, AND A. J. CRAWFORD. 2015. DNA barcoding survey of anurans across the Eastern Cordillera of Colombia and the impact of the Andes on cryptic diversity. PloS One 10:e0127312. doi:10.1371/journal.pone.0127312

Hall, T. A. 1999. BioEdit: a user-friendly biological sequence alignment editor and analysis program for Windows 95/98/NT. Nucleic Acids Symposium Series 41:95–98.

Henle, K. 1991. *Ololygon pedromedinae* sp. nov., ein neuer Knickzehenlaubfrosch (Hylidae) aus Peru. Salamandra 27:76–82.

Heyer, W. R., A. S. Rand, C. A. G. Cruz, O. L. Peixoto, and C. E. Nelson. 1990. Frogs of Boracéia. Arquivos de Zoologia 31:231−410.

IBGE (Instituto Brasileiro de Geografia e Estatística). 1997. Recursos naturais e meio ambiente: uma visão do Brasil. IBGE press, Brazil.

Jansen, M., R. Bloch, A. Schulze, and M. Pfenninger. 2011. Integrative inventory of Bolivia's lowland anurans reveals hidden diversity. Zoologica Scripta 40: 567–583.

Juncá, F. A., M. F. Napoli, I. Nunes, E.A. Mercês, and R. O. Abreu. 2015. A new species of the *Scinax ruber* clade (Anura, Hylidae) from the Espinhaço Range, northeastern Brazil. Herpetologica 71:299–309.

Jungfer, K. H., J. Faivovich, J. M. Padial, S. Castroviejo-Fisher, M. M. Lyra, B. Berneck, P. P. Iglesias, P. J. R. Kok, R. D. MacCulloch, M. T. Rodrigues, V. K. Verdade, C. P. Torres Gastello, J. C. Chaparro, P. H. Valdujo, S. Reichle, J. Moravec, V. Gvoždík, G. Gagliardi-Urrutia, R. Ernst, I. De la Riva, D. B. Means, A. P. Lima, J. C. Señaris, W. C. Wheeler, and C. F. B. Haddad. 2013. Systematics of spiny-backed treefrogs (Hylidae: *Osteocephalus*): an Amazonian puzzle. Zoologica Scripta 42:351–380.

Kimura, M. 1980. A simple method for estimating evolutionary rate of base substitutions through comparative studies of nucleotide sequences. Journal of Molecular Evolution 16:111–120.

Köhler, J., M. Jansen, A. Rodriguez, P. J. R. Kok, L. F. Toledo, M. Emmrich, F. Glaw, C. F. B. Haddad, M. O. Rödel, and M. Vences. 2017. The use of bioacoustics in anuran taxonomy: theory, terminology, methods and recommendations for best practice. Zootaxa 4251:1–124.

Laurenti, J. N. 1768. Specimen Medicum, Exhibens Synopsin Reptilium Emendatum cum Experimentis Circa Venena et Antidota Reptilium Austriacorum. Wien, Austria: Joan. Thom. nob. de Trattnern.

Lescure, J., and C. Marty. 2000. Atlas des amphibiens de Guyane. Patrimoines Naturales 45:1−388.

Lima, A. P., and J. P. Caldwell. 2001. A new Amazonian species of *Colostethus* with sky blue digits. Herpetologica 57:133–138.

Lima, A. P., J. P. Caldwell, G. Biavati, and A. Montanarin. 2010. A new species of *Allobates* (Anura: Aromobatidae) from Paleovárzea Forest in Amazonas, Brazil. Zootaxa 2337:1–17.

Lutz, A. 1925. Batraciens du Brésil. Comptes Rendus des Seances de la Societe de Biologie, Paris 93:137–139.

Lutz, A. 1925. Batraciens du Brésil. Comptes Rendus et Mémoires Hebdomadaires des Séances de la Société de Biologie et des ses Filiales. Paris 93:211–214.

Lyra, M. L., C. F. B. Haddad, and A. M. L. Azeredo-Espin. 2017. Meeting the challenge of DNA barcoding Neotropical amphibians: polymerase chain reaction optimization and new COI primers. Molecular Ecology Resource 17:966–980.

Magnusson, W. E, R. Braga-Neto, F. Pezzini, F. Baccaro, H. Bergallo, J. Penha, D. Rodrigues, A.P. Lima, A. Albernaz, J. M. Hero, B. Lawson, C. Castilho, C. Drucker, E. Franklin, F. Mendonça, F. Costa, G. Galdino, G. Castley, J. Zuanon, J. Vale, J. L. C. Santos, R. Luizão, R. Cintra, R. I. Barcosa, A. Lisboa, R.

V. Koblitz, C. N. Cunha, and A. R. M. Pontes. 2013. Biodiversidade e monitoramento ambiental integrado: o sistema RAPELD na Amazônia. Publisher Attema, Brazil.

Malambo-L., C., and M. A. Madrid-Ordóñez. 2008. Geographic distribution of *Limnophys sulcatus*, *Rhinella castaneotica* and *Scinax cruentommus* (Amphibia: Anura) for Colombia. Revista de Academia Colombiana de Ciencias 32:285–289.

Maldonado, F. D., E. W. H. Keizer, P. M. L. A. Graça, P. M. Fearnside, and C. S. Vitel. 2012. Previsão temporal da distribuição espacial do desmatamento no interflúvio Purus-Madeira até o ano 2050. Pp. 183–196 in W. C. Sousa-Junior, A. V. Waichman, P. A. A. Sinisgalli, C.F. de Angelis, and A. R. Romeiro (Eds.), Rio Purus: Água, Território e Sociedade na Amazônia Sul-Ocidental. LibriMundi Press, Ecuador.

Melo-Sampaio, P. R., R. M. de Oliveira, and I. Prates. 2018. A new Nurse Frog from Brazil (Aromobatidae: *Allobates*), with data on the distribution and phenotypic variation of western Amazonian species. South American Journal of Herpetology 13:131–149.

Meneghelli, D., and O. M. Entiauspe, Neto. 2014. New records from Brazil and first record from the state of Rondônia of *Osteocephalus castaneicola* Moravec, Aparicio, Guerrero-Reinhard, Calderón, Jungfer & Gvoždík, 2009 (Anura: Hylidae) with an update on its geographical distribution. Check List 10:957–959.

Miranda-Ribeiro, A. de. 1926. Notas para servirem ao estudo dos Gymnobatrachios (Anura) Brasileiros. Arquivos do Museu Nacional. Rio de Janeiro 27:1–227.

Moravec, J., I. A. Tuanama, P. E. Pérez-Peña, and E. Lehr. 2009. A new species of *Scinax* (Anura: Hylidae) from the area of Iquitos, Amazonian Peru. South American Journal of Herpetology 4:9–16.

Moravec, J., J. Aparicio, M. Guerrero-Reinhard, G. Calderón, K.-H. Jungfer, and V. Gvoždík. 2009. A new species of *Osteocephalus* (Anura: Hylidae) from Amazonian Bolivia: first evidence of tree frog breeding in fruit capsules of the Brazil nut tree. Zootaxa 2215:37–54.

Myers, C. W., and W. E. Duellman. 1982. A new species of *Hyla* from Cerro Colorado, and other tree frog records and geographical notes from Western Panama. American Museum Novitates 2752:1–32.

Napoli, M. F. 2005. A new species allied to *Hyla circumdata* (Anura: Hylidae) from Serra da Mantiqueira, southeastern Brazil. Herpetologica 61:63–69.

Nogueira, L., M. Solé, S. Siqueira, P. R. A. M. Affonso, C. Strüssmann, and I. Sampaio. 2016. Genetic analysis reveals candidate species in the *Scinax catharinae* clade (Amphibia: Anura) from Central Brazil. Genetics and Molecular Biology 39:49–53.

Peters, W. C. H. 1863. Fernere Mittheilungen über neue Batrachier. Monatsberichte der Königlichen Preussische Akademie des Wissenschaften zu Berlin 1863:445–470.

Pombal, J. P., M. Bilate, P. G. Gambale, L. Signorelli, and R. P. Bastos. 2011. A new miniature treefrog of the *Scinax ruber* clade from the Cerrado of central Brazil (Anura: Hylidae). Herpetologica 67:288–299.

Pyburn, W. F., and M. J. Fouquette. 1971. A new striped Treefrog from Central Colombia. Journal of Herpetology 5:97–101.

Pyburn, W. F. 1973. A new hylid from the Llanos of Colombia. Journal of Herpetology 7:297–301.

Pyburn, W. F. 1992. A new tree frog of the genus *Scinax* from the Vaupes River of northwestern Brazil. Texas Journal of Science 44:405–411.

Pyburn, W. F. 1993. A new species of dimorphic tree frog, genus *Hyla* (Amphibia: Anura: Hyldiae), from the Vaupés River of Colombia. Proceedings of the Biological Society of Washington 106:46–50.

RAMBAUT, A., A. J. DRUMMOND, D. XIE, G. BAELE AND M. A. SUCHARD. 2018 Posterior summarisation in Bayesian phylogenetics using Tracer 1.7. Systematic Biology: Syy032. doi:10.1093/sysbio/syy032

RIVERO, J. A. 1961. Salientia of Venezuela. Bulletin of the Museum of Comparative Zoology 126:1−207.

RONQUIST, F., M. TESLENKO, P. VAN DER MARK, D. AYRES, A. DARLING, S. HÖHNA, B. LARGET, L. LIU, M. A. SUCHARD, AND J. P. HUELSENBECK. 2011. MrBayes 3.2: efficient Bayesian phylogenetic inference and model choice across a large model space. Systematic Biology 61:539–542.

SALDUCCI, M. D., C. MARTY, R. CHAPPAZ, AND A. GILLES. 2002. Molecular phylogeny of French Guiana Hylinae: implications for the systematic and biodiversity of the neotropical frogs. Comptes Rendus Biologies 325:141–153.

SALDUCCI, M. D., C. MARTY, A. FOUQUET, AND A. GILLES. 2005. Phylogenetic relationships and biodiversity in Hylids (Anura: Hylidae) from French Guiana. Comptes Rendus Biologies 328:1009–1024.

SAVAGE, J. M., AND W. R. HEYER. 1967. Variation and distribution in the tree-frog genus *Phyllomedusa* in Costa Rica, Central America. Beiträge zur Neotropischen Fauna 5:111−131.

SCHULZE, A., M. JANSEN, AND G. KÖHLER. 2015. Tadpole diversity of Bolivia's lowland anuran communities: molecular identification, morphological characterisation, and ecological assignment. Zootaxa 4016:1–111.

SCHWARZ, G. E. 1978. Estimating the dimension of a model. Annals of Statistics 6:461–464.

SIMÕES, P. I., A. P. LIMA, AND I. P. FARIAS. 2010. The description of a cryptic species related to the pan-Amazonian frog *Allobates femoralis* (Boulenger 1883) (Anura: Aromobatidae). Zootaxa 2406:1–28.

SIMÕES, P. I., I. L. KAEFER, F. B. R. GOMES, AND A. P. LIMA. 2012. Distribution extension of *Hyalinobatrachium cappellei* (van Lidth de Jeude, 1904) (Anura: Centrolenidae) across Central Amazonia. Check List 8:636–637.

SOARES-FILHO, B. S., D. C. NEPSTAD, L. M. CURRAN, G. C. CERQUEIRA, R. A. GARCIA, C. AZEVEDO-RAMOS, E. VOLL, A. MCDONALD, P. LEFEBVRE, AND P. SCHESINGER. 2006. Modelling conservation in the Amazon basin. Nature 440:520–523.

SOUZA, M. B. 2009. Anfíbios: Reserva Extrativista do Alto Juruá e Parque Nacional da Serra do Divisor, Acre. IFCH press, Brazil.

SPIX, J. B. 1824. Animalia nova sive species novae Testudinarum Ranarum, quas in itinere per Brasiliam annis MDCCCXVII-MDCCCXX jussu et auspiciis Maximiliani Josephi I. Bavariae regis. Munich, Typis Franc. Seraph. Hübschmanni.

STURARO, M. J., AND P. L. V. PELOSO. 2014. A new species of *Scinax* Wagler, 1830 (Anura: Hylidae) from the middle Amazon River Basin, Brazil. Papéis Avulsos de Zoologia 54:9–23.

SUEUR, J., T. AUBIN, AND C. SIMONIS. 2008. Seewave, a free modular tool for sound analysis and synthesis. Bioacoustics 18:213–226.

TAMURA, K., G. STECHER, D. PETERSON, A. FILIPSKI, AND S. KUMAR. 2013. MEGA6: Molecular Evolutionary Genetics Analysis version 6.0. Molecular Biology and Evolution 30:2725–2729.

THOMPSON, J. D., D. G. HIGGINS, AND T. J. GIBSON. 1994. Clustal W: improving the sensitivity of progressive multiple sequence alignment through sequence weighting, position-specific gap penalties and weight matrix choice. Nucleic Acids Research 22:4673–4680.

VAN LIDTH DE JEUDE, T. W. 1904. Reptiles and batrachians from Surinam. Notes from the Leyden Museum 25:83–94.

VENCES, M., M. THOMAS, A. VAN DER MEIJDEN, Y. CHIARI, AND D. VIEITES. 2005. Comparative performance of the 16S rRNA gene in DNA barcoding of amphibians. Frontiers in Zoology 2:5. doi:10.1186/1742-9994-2-5

WAGLER, J. 1830. Natürliches System der Amphibien, mit vorangehender Classification der Säugthiere und Vogel. Ein Beitrag zur vergleichenden Zoologie. München, Stuttgart and Tübingen: J. G. Cotta.

ZIMMERMAN, B. L., AND RODRIGUES, M. T. 1990. Frogs, Snakes, and Lizards of the INPA/WWF Reserves near Manaus, Brazil. Pp. 426–454 in A. H. Gentry (Ed.), Four Neotropical Rainforests. Yale University Press, USA.

Appendix I. Voucher numbers, localities, and GenBank accession numbers of samples used for phylogenetic analyses.

Species	**Voucher**	**Location**	**GenBank**	**Authors**
Julianus uruguayus	CFBH 5788	Brazil, Rio Grande do Sul, Cambará do Sul	AY843681	Brusquetti et al., 2014
Ololygon agilis	CFBHT 09033	Brazil, Espirito Santo, Paraju	KU495534	Lyra et al., 2017
O. albicans		Brazil	KM390788	Chaves et al. Unpublished
O. argyreornata	CFBHT 02212	Brazil, Espirito Santo, Vitoria	KU495540	Lyra et al. 2017
O. berthae	MLPA 2137	Argentina, Buenos Aires, Atalaya	AY843754	Faivovich et al. 2005
O. faivovichi	MNRJ40902	Brazil, São Paulo, Porcos Pequena	JN100002	Bell et al. 2012
O. flavoguttatus		Brazil	KM390789	Chaves et al. Unpublished
O. humilis		Brazil	KM390790	Chaves et al. Unpublished
O. peixotoi	CFBH 9437	Brazil, São Paulo, Ilha da Queimada Grande	JN100005	Bell et al. 2012
O. perpusilla	CFBH12869	Brazil, São Paulo, Ubatuba	JN100014	Bell et al. 2012
O. strigilata	MZUESC 11080	Brazil, Camacan, Bahia	KT438896	Nogueira et al. 2016
S. acuminatus	IIBPH 277	Paraguay, Estancia San Jose, Neembucu	KJ004189	Brusquetti et al. 2014
S. alter	CFBHT 03712	Brazil, Espirito Santo, Mimoso do Sul	KU495537	Lyra et al. 2017
S. boesemani A		French Guiana, Savane roche virginie	EF217500	Fouquet et al. 2007a
S. boesemani B		French Guiana, Grand santi	EF217502	Fouquet et al. 2007a
S. chiquitanus	INPAH 35560	Brazil, Rondônia, Porto Velho, module 14	KU317384	Ferrão et al. 2016
S. crospedospilus	CFBHT 16741	Brazil, Sao Paulo, Sao Luis do Paraitinga	KU495541	Lyra et al. 2017
S. cruentommus	INPAH 34697	Brazil, Amazonas, BR-319, module 1	KU317385	Ferrão et al. 2016
S. aff. *cruentommus*	INPAH 34596	Brazil, Amazonas, BR-319, módulo 6	KU317386	Ferrão et al. 2016
S. elaeochroa	MVZFC 14457	Costa Rica, Heredia, Starkey's Woods	AY843757	Faivovich et al. 2005
S. eurydice	CFBHT 04365	Brazil, Rio de Janeiro, Petropolis	KU495545	Lyra et al. 2017
S. fuscomarginatus	CFBH24362	Brazil, Minas Gerais, Lagoa Santa	KJ004136	Brusquetti et al. 2014
S. fuscovarius	AS 502	Bolivia, Los Lagos	JF790013	Schulze et al. 2015

S. fuscovarius	MNKA 9772	Bolivia, Santa Cruz, Ñuflo de Chavez, San Sebastián	JF790014	Jansen et al. 2011
S. garbei	KU 202764	Ecuador, Chimborazo	AY326033	Darst & Cannatella 2004
S. iquitorum	NMP6V 71267-1	Peru, Puerto Almendras	KU317397	Ferrão et al. 2016
S. jolyi		French Guiana	AF467261	Salducci et al. 2002
Scinax cf. *kennedyi*	AJC 4074	Colombia, Casanare, Sabanalarga, Sabanalarga	KP149463	Guarnizo et al. 2015
S. madeirae	CFBH25469	Brazil, Rondônia, Porto Velho	KJ004101	Brusquetti et al. 2014
S. nebulosus	CFBHT10951	Brazil, Piauí, Baixa Grande	KJ004190	Brusquetti et al. 2014
S. nebulosus		French Guiana, Road 8/pk6	EF217514	Fouquet et al. 2007a
S. proboscideus		French Guiana, Kaw	EF376070	Salducci et al. unpublished
S. perereca	CFBHT 1470	Brazil, Paraná, Ararapira	KU306387	Souza et al. Unpublished
Scinax onca	INPAH34586	Brazil, Amazonas, BR-319, module 7	KU317425	Ferrão et al. 2016
Scinax onca	INPAH34595	Brazil, Rondônia, Porto Velho	KU317419	Ferrão et al. 2016
S. rostratus	AJC 3422	Colombia, Santander, San Vicente de Chucuri	KP149284	Guarnizo et al. 2015
S. ruber A	137bm	French Guiana, Cacao	EF217476	Fouquet et al. 2007a
S. ruber B		French Guiana	EF217481	Fouquet et al. 2007a
S. ruber C	IWK 109	Guyana, Iwokrama, Muri Scrub camp	AY549365	Faivovich et al. 2004
S. ruber D	QCAZ25275	Ecuador, parroquia Dayuma, canton coca,Orellana	EF217487	Fouquet et al. 2007a
S. ruber F	MNKA 9539	Bolivia, Santa Cruz, Velasco, Caparu	JF790034	Jansen et al. 2011
S. ruber PM	INPAH34645	Brazil, Amazonas, BR-319, módulo 2	KU317404	Ferrão et al. 2016
S. ruber 1	AJC 2324	Colombia, Orocué, Casanare	KP149491	Guarnizo et al. 2015
S. ruber 2	AJC 3532	Colombia, San Vicente, Santander	KP149347	Guarnizo et al. 2015
S. ruber 3	AJC 3378	Colombia, Sabanalarga, Casanare	KP149452	Guarnizo et al. 2015
S. ruber Peru	KU 207622	Peru, Madre de Dios, Cusco Amazonico	AY326034	Darst & cannatella 2004
Scinax ruberoculatus	INPAH34623	Brazil, Amazonas, BR-319, module 8	KU317409	Ferrão et al. 2016

S. squalirostris	CFBH21975	Brazil, São Paulo, Serra da Bocaina	KJ004187	Brusquetti et al. 2014
S. staufferi	UTA A-50749	Guatemala, Zacapa, 2.9 km S Teculutan	AY843761	Faivovich et al. 2005
S. villasboasi	CHUNB40161	Brazil, Pará, Serra do Cachimbo	KJ004109	Brusquetti et al. 2014
S. wandae	AJC 4105	Colombia, Sabanalarga, Casanare	KP149381	Guarnizo et al. 2015
S. aff. *wandae*	AJC 3464	Colombia, San Juan de Arama, Meta	KP149460	Guarnizo et al. 2015
S. x-signatus	260mc	French Guiana, Arataï	EF217480	Fouquet et al. 2007a
Scinax sp. nov.	INPAH34688	Brazil, Amazonas, BR-319, module 9	KU317428	Ferrão et al. 2016
Scinax sp. nov.	INPAH34690	Brazil, Amazonas, BR-319, module 9	KU317431	Ferrão et al. 2016
Scinax sp. nov.	INPAH34700	Brazil, Amazonas, BR-319, module 9	KU317430	Ferrão et al. 2016
Scinax sp. 2	INPAH34670	Brazil, Amazonas, BR-319, module 11	KU317412	Ferrão et al. 2016
Scinax sp. 2 FG		French Guiana, Kaw	EF217507	Fouquet et al. 2007a
Scinax sp. 4	INPAH34693	Brazil, Amazonas, BR-319, module 11	KU317429	Ferrão et al. 2016
Scinax sp. 5	INPAH34703	Brazil, Amazonas, BR-319, module 5	KU317377	Ferrão et al. 2016
Scinax sp. 6	INPAH35562	Brazil, Rondônia, Porto Velho, module 17	KU317387	Ferrão et al. 2016
Scinax sp. A	MNKA 9134	Bolivia, Santa Cruz, Ñuflo de Chavez, San Sebastián	JF790036	Jansen et al. 2011
Sphaenorhynchus caramaschii	CFBHT 12419	Brazil, Sao Paulo, Ribeirao Grande	KP096220	Araujo-Vieira et al. 2015
Sphaenorhynchus dorisae	MJH 46	Brazil, Amazonas, Manaus, Lago Janauri	AY843766	Faivovich et al. 2005
Sphaenorhynchus lacteus	MNK:A 9387	Bolivia	JF790144	Jansen et al. 2011
Sphaenorhynchus surdus	CFBHT05536	Brazil, Santa Catarina, Lebon Regis	KU495592	Lyra et al. 2017
Trachycephalus resinifictrix	MTR_UFCX22P46	Brazil, Mato Grosso, Vila Rica	KU495603	Lyra et al. 2017
Osteocephalus taurinus	PHV 2692	Brazil, Mato Grosso, Barra do Garcas	KF002153	Jungfer et al. 2013

Appendix II. List of specimens examined for morphological comparisons.

Abbreviations: (AM) Highway at State of Amazonas, Brazil; (PDBFF) Projeto Dinâmica Biológica de Fragmentos Florestais (a project in Brazil focused on dynamics of forest fragments), (km) kilometre; (INPA-H) Herpetological Section of the Zoological Collection of the Instituto Nacional de Pesquisas da Amazônia, Manaus, Brazil; (RMNH) Nationaal Natuurhistorisch Museum, Leiden, The Netherlands; (QCAZ) Museo de Zoología, Pontificia Universidad Católica del Ecuador, Quito, Ecuador; (KU) University of Kansas, Museum of Natural History, Division of Herpetology, Lawrence, Kansas, USA; (ANDES-A) Museo de Historia Natural ANDES, Universidad de los Andes, Bogotá, Colombia; (ZSM) Zoologische Staatssammlung München, München, Germany.

Hyla affinis: BRAZIL: "fluminis Amazonum" = Rio Amazonas (ZSM 2495/0, holotype, photo).

Scinax boesemani: SURINAME: Paramaribo: near Zanderij (RMNH12601, holotype, photo). BRAZIL: Roraima: Caracaraí, Viruá National Park (INPA-H 25972, INPA-H 25974).

Scinax chiquitanus: BRAZIL: Rondônia: Porto Velho (INPA-H 35554, INPA-H 35555, INPA-H 35556, INPA-H 35557, INPA-H 35558, INPA-H 35560).

Scinax cruentommus: ECUADOR: Napo: Santa Cecilia (KU 126587, holótipo, photo); Orellana: Parque Nacional Yasuní (QCAZ 8184), Río Napo (QCAZ 43772, QCAZ 44754). BRAZIL: Amazonas: Careiro da Várzea, Ramal do Purupuru (INPA-H 34697).

Scinax funereus: ECUADOR: Orellana: Río Napo, Primavera (QCAZ 43799, photo), Tambococha (QCAZ 55280, QCAZ 55283; photo).

Scinax fuscomarginatus: BRAZIL: Roraima: Boa Vista, Maracá Ecological Station (INPA-H 34662, INPA-H 34634, INPA-H 34646, INPA-H 34661); Caracaraí, Viruá National Park (INPA-H 19371, INPA-H 19372, INPA-H 19376, INPA-H 19378, INPA-H 19383, INPA-H 19384).

Scinax garbei: BRAZIL: Roraima: Caracaraí, Viruá National Park (INPA-H 25964, INPA-H 27496).

Scinax madeirae: BRAZIL: Rondônia: Alta Floresta, Corumbiaria Park (INPA-H 7050, INPA-H 7051).

Scinax nebulosus: BRAZIL: Pará: Alter do Chão (INPA-H 34647, INPA-H 34653); Rondônia: Costa Marques, Real Forte Príncipe da Beira (INPA-H 34641); Roraima: Caracaraí, Parque Nacional do Viruá (INPA-H 27535, INPA-H 27536, INPA-H 27537).

Scinax onca: BRAZIL: Amazonas: Berurí (INPA-H 20582, INPA-H 20586, INPA-H 34585, INPA-H 34584, INPA-H 34581, INPA-H 34583, INPA-H 34587); Rondônia: Porto Velho (INPA-H 34591, INPA-H 34590, INPA-H 34589, INPA-H 34592, INPA-H 34595, INPA-H 34588, INPA-H 34594, INPA-H 34593).

Scinax proboscideus: BRAZIL: Amazonas: Manaus, Colosso Reserve at PDBFF (INPA-H 10304); Presidente Figueiredo, Vila Pitinga (INPA-H 1870); Pará: Oriximiná (INPA-H 304).

Scinax ruberoculatus: BRAZIL: Amazonas: Careiro da Várzea, BR-319, km 100 (INPAH 34600, INPA-H 34601, INPA-H 34604, INPA-H 34614, INPA-H 34615, INPA-H 34622, INPA-H 34598, INPA-H 34624, INPA-H 34627, INPA-H 34629), km 168 (INPA-H 34602); Borba, BR-319, km 220 (INPA-H 34610, INPA-H 34620); Beruri, BR-319, km 220 (INPA-H 34608), km 360 (INPAH 34599, INPA-H 34607, INPA-H 34609, INPA-H 34611, INPA-H 34612, INPA-H 34617, INPA-H 34618,

INPA-H 34621, INPA-H 34625, INPA-H 34626, INPA-H 34628, INPA-H 34630); Manicoré, BR-319, km 400 (INPA-H 34603, INPA-H 34606, INPA-H 34616, INPA-H 34623); Tapauá, BR-319, km 450 (INPA-H 34613, INPA-H 34619, INPA-H 34605, INPA-H 34665).

Scinax sateremawe: BRAZIL: Amazonas: Borba, Ramal Novo Horizonte (INPA-H 34695, INPA-H 34708).

Scinax wandae: COLOMBIA: Casanare, Sabanalarga (ANDES-A 1234, ANDES-A 1071, ANDES-A 1072, ANDES-A 1234: photo).

Table 1. Measurements (mm) and morphometric ratios of the type-series of *Scinax* sp. nov. Abbreviations are defined in the Material and Methods section (holotype in bold). Morphometric ratios are presented with two decimals.

INPA-H	34691	**34688**	34689	34692	34690	34700
Sex	M	**M**	M	M	M	F
SVL	22.5	**20.2**	20.7	22.5	21.6	26.5
HL	8.3	**7.6**	7.6	9.0	8.3	9.7
HW	7.3	**6.8**	7.0	7.6	7.1	9.0
ED	2.8	**2.5**	2.5	2.9	2.8	3.0
TD	1.0	**0.9**	0.7	1.4	1.1	1.5
IOD	2.3	**2.0**	2.3	2.5	2.2	2.9
IND	1.9	**1.7**	1.6	1.9	1.7	1.9
TAL	5.9	**5.5**	5.6	6.0	5.8	6.8
FL	8.5	**8.5**	8.7	9.5	9.1	10.6
HAL	5.9	**5.7**	5.8	6.1	6.0	7.3
3FD	0.9	**1.0**	1.0	1.1	1.0	1.0
4TD	0.9	**0.9**	0.9	1.1	1.1	0.9
END	2.5	**2.2**	2.6	2.5	2.3	3.0
TL	11.1	**10.6**	10.7	11.2	11.2	13.0
THL	10.4	**10.0**	10.1	9.8	10.4	11.9
NSD	0.6	**0.7**	0.7	0.7	0.6	0.9
HL/HW	1.14	**1.12**	1.09	1.18	1.17	1.08
HL/SVL	0.37	**0.38**	0.37	0.40	0.38	0.37
HW/SVL	0.32	**0.34**	0.34	0.34	0.33	0.34
IOD/HW	0.32	**0.29**	0.33	0.33	0.31	0.32
END/ED	0.89	**0.88**	1.04	0.86	0.82	1.00
TD/ED	0.36	**0.36**	0.28	0.48	0.39	0.50
TL/SVL	0.49	**0.52**	0.52	0.50	0.52	0.49
THL/SVL	0.46	**0.50**	0.49	0.44	0.48	0.45
TAL/FL	0.69	**0.65**	0.64	0.63	0.64	0.64

FIGURE LEGENDS

Figure 1. Holotype of *Scinax* sp. nov. (INPA-H 34688), from Nascentes do Lago Jari National Park, Tapauá, Amazonas, Brazil. Scale bar = 5 mm.

Figure 2. Ventral view of **hand** (A) and foot (B) of the holotype of *Scinax* sp. nov. (INPA-H 34688), from Nascentes do Lago Jari National Park, Tapauá, Amazonas, Brazil. Scale: 2 mm.

Figure 3. Holotype of *Scinax* sp. nov. (INPA-H 34688, SVL = 20.2 mm), Nascentes do Lago Jari National Park, Tapauá, Amazonas, Brazil. Photo: Rafael de Fraga.

Figure 4. Color in preservative of the type series of *Scinax* sp. nov. from Nascentes do Lago Jari National Park, Tapauá, Amazonas, Brazil. A: INPA-H 34700, female, SVL 26.5 mm. B: INPA-H 34689, male, SVL 20.7 mm. C: INPA-H 34688, male, 20.2 mm. D: INPA-H 34692, male, SVL 22.5 mm. E: INPA-H 34691, male, SVL 22.5 mm. F: INPA-H 34690, male, SVL 21.6 mm.

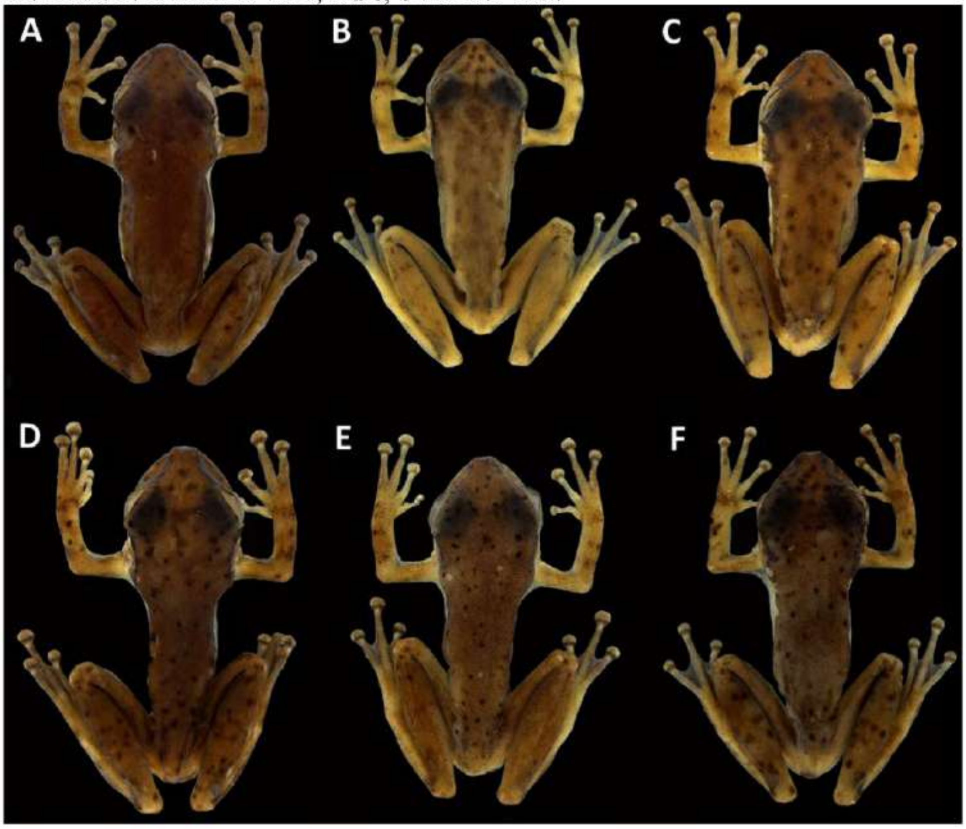

Figure 5. Wave form and audiospectrogram of the advertisement call type A interspersed with advertisement call type B of *Scinax* sp. nov. (INPA-H 34691, SVL 22.5 mm) from the Nascentes do Lago Jari National Park, Tapauá, Amazonas, Brazil (A). Wave form and detailed audiospectrogram (B) of the advertisement call type A (C) and type B (D).

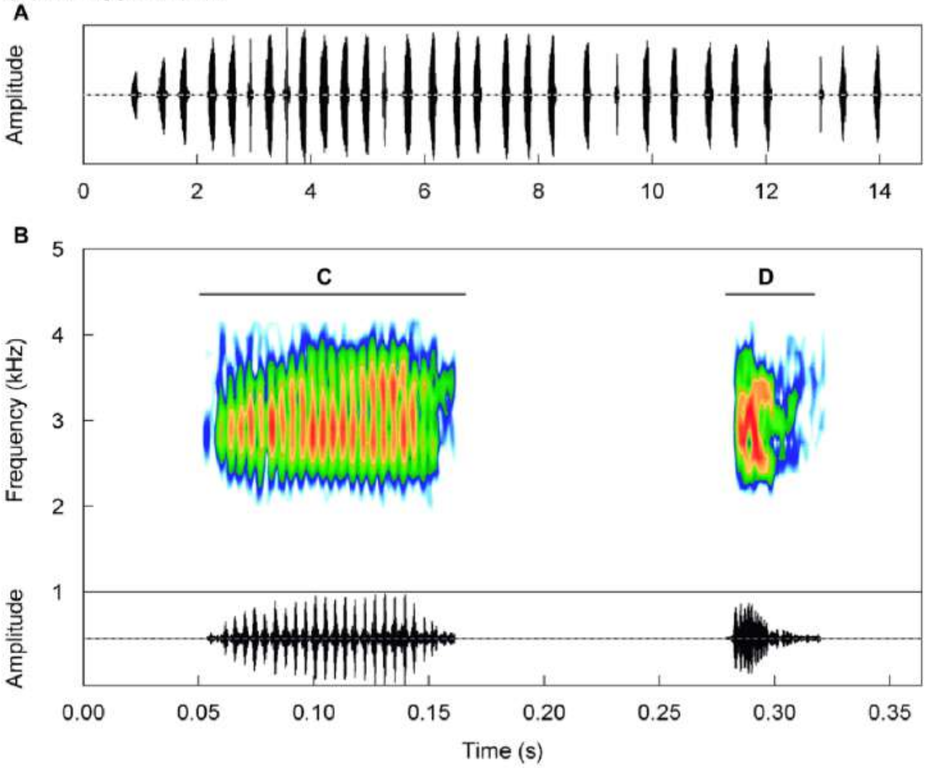

Figure 6. Bayesian 50% consensus tree inferred from mitochondrial 16S rRNA. Posterior probabilities are given above the node when ≥ than 0.95. Blue area highlights the new species.

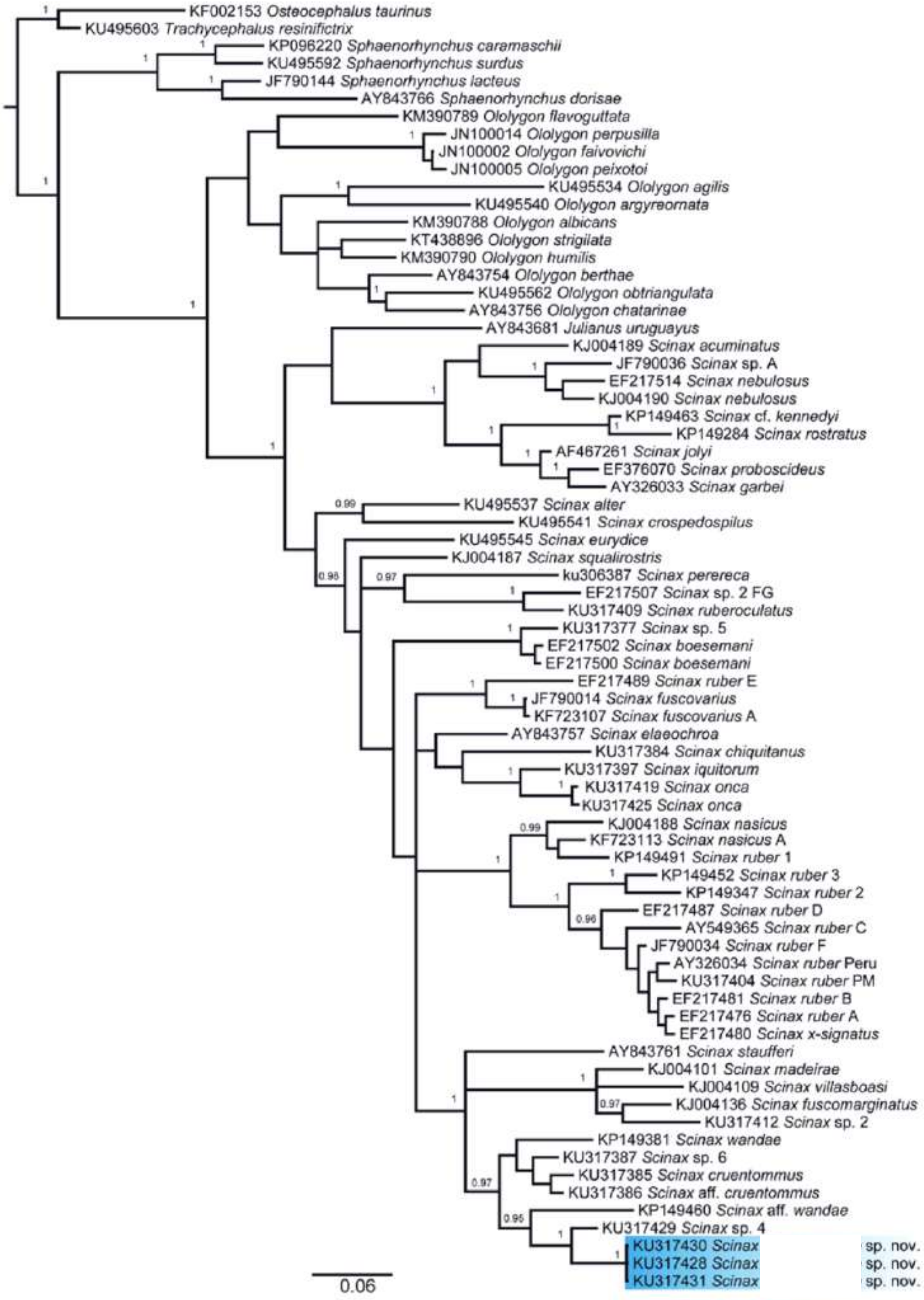

Figure 7. Geographic range of *Scinax* sp. nov. in the interfluve between the Purus and Madeira rivers, Brazilian Amazonia. Black star: type locality, border of the Nascentes do Lago Jari National Park (green polygon) in contact with the federal highway BR-319, Municipality of Tapauá, Amazonas, Brazil.

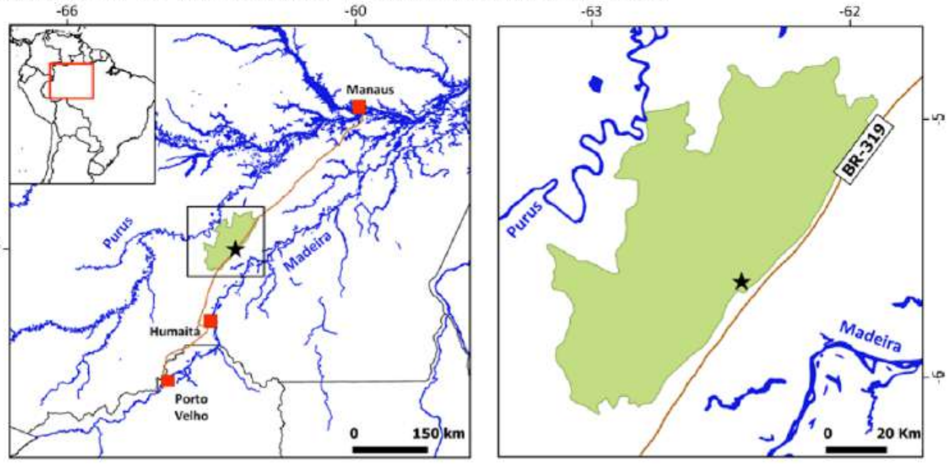

CAPÍTULO 4

A new species of *Scinax* from the Purus-Madeira interfluve, Brazilian Amazonia (Anura, Hylidae). Zookeys, 706: 137–162. doi:10.3897/zookeys.706.14691

ZooKeys 706: 137–162 (2017)
doi: 10.3897/zookeys.706.14691
http://zookeys.pensoft.net

RESEARCH ARTICLE

A peer-reviewed open-access journal
ZooKeys
Launched to accelerate biodiversity research

A new species of *Scinax* from the Purus-Madeira interfluve, Brazilian Amazonia (Anura, Hylidae)

Miquéias Ferrão[1], Jiří Moravec[2], Rafael de Fraga[1], Alexandre Pinheiro de Almeida[3], Igor Luis Kaefer[4], Albertina Pimentel Lima[5]

1 *Programa de Pós-Graduação em Ecologia, Instituto Nacional de Pesquisas da Amazônia, Av. André Araújo, 2936, 69060-001, Manaus, Amazonas, Brazil* **2** *Department of Zoology, National Museum, Cirkusová 1740, 19300, Prague 9, Czech Republic* **3** *Programa de Pós-Graduação em Zoologia, Universidade Federal do Amazonas, Av. Rodrigo Octávio 6200, 69080-900, Manaus, Amazonas, Brazil* **4** *Instituto de Ciências Biológicas, Universidade Federal do Amazonas, Av. Rodrigo Octávio 6200, 69080-900, Manaus, Amazonas, Brazil* **5** *Coordenação de Biodiversidade - CBIO, Instituto Nacional de Pesquisas da Amazônia, Av. André Araújo, 2936, 69060-001, Manaus, Amazonas, Brazil*

Corresponding author: *Miquéias Ferrão* (uranoscodon@gmail.com)

Academic editor: *A. Crottini* | Received 25 June 2017 | Accepted 14 September 2017 | Published 4 Octomber 2017

http://zoobank.org/5AF4775E-803F-4B1D-AAF6-6FFB94BDCD82

Citation: Ferrão M, Moravec J, Fraga R, Almeida AP, Kaefer IL, Lima AP (2017) A new species of *Scinax* from the Purus-Madeira interfluve, Brazilian Amazonia (Anura, Hylidae). ZooKeys 706: 137–162. https://doi.org/10.3897/zookeys.706.14691

Abstract

A new tree frog species of the genus *Scinax* from the interfluve between the Purus and Madeira rivers, Brazilian Amazonia, is described and illustrated. The new species is diagnosed by medium body size, snout truncate in dorsal view, ulnar and tarsal tubercles absent, nuptial pads poorly developed, skin on dorsum shagreen, dorsum light brown with dark brown spots and markings, white groin with black spots, anterior and posterior surfaces of thighs black, and iris bright orange. The advertisement call consists of a single short note, with 16–18 pulses and dominant frequency at 1572–1594 Hz. Tadpoles are characterized by body ovoid in dorsal view and triangular in lateral view, tail higher than body, oral disc located anteroventrally and laterally emarginated, dorsum of body uniformly grey-brown with dark brown eye-snout stripe in preservative, fins translucent with small to large irregular diffuse dark brown spots.

Keywords

Amazonian rainforest, Amazonas, anuran diversity, Brazil, Rondônia, *Scinax onca* sp. n.

Introduction

With nearly 70 currently recognized species, the genus *Scinax* Wagler, 1830 represents one of the most species-rich hylid genera in the Neotropics. Nevertheless, an increasing rate of new *Scinax* species recognition in the few last years (e.g., Fouquet et al. 2007, Brusquetti et al. 2014; Sturaro and Peloso 2014; Araujo-Vieira et al. 2015; Araujo-Vieira et al. 2016; Juncá et al. 2015; Ferrão et al. 2016) indicates that our knowledge of the actual species diversity in this genus is still very incomplete. Similarly, despite an intensive research in the last decades (e.g. Faivovich 2002, Faivovich et al. 2005, Duellman et al. 2016) many questions concerning our knowledge of phylogenetic relationships of this and correlated genus remain still an object of discussion.

The *Hyla rubra* species group was first recognized by Leon (1969). Several years later, Fouquette and Delahoussaye (1977) resurrected the generic name *Ololygon* Fitzinger, 1843 (type species *Hyla strigilata* Spix, 1824) to harbour the members of the *H. rubra* group and delimited five other species groups. However, the correct generic name to these tree frogs is *Scinax* Wagler, 1830 (type species *Hyla aurata* Wied, 1821) as noted by Pombal and Gordo (1991). Consequently, Duellman and Wiens (1992) defined the genus *Scinax* based on external morphology of adults and tadpoles, osteology, and reproductive behaviour.

Faivovich (2002) tested monophyly of species groups traditionally recognized in *Scinax* and defined two main monophyla: the *S. ruber* Clade (comprising members of the *S. rostratus* and *S. ruber* species groups) and the *S. catharinae* Clade (involving members of the *S. catharinae* and *S. perpusillus* species groups). In following comprehensive review of the systematics of Hylidae, Faivovich et al. (2005) confirmed the monophyly of *S. ruber* and *S. catharinae* Clades and recovered *Hyla uruguaya* (Schmidt, 1944) in sister position to the *S. ruber* Clade (*H. uruguaya* was transferred to *Scinax* to avoid paraphyly of the genus). In the phylogeny proposed by Faivovich et al. (2005) the *S. ruber* Clade is composed by *S. rostratus* and *S. uruguayus* species groups plus species unassigned to any group and the *S. catharinae* Clade consists of *S. catharinae* and *S. perpusillus* species groups.

Recently, Duellman et al. (2016) revised the phylogeny of the family Hylidae and proposed three major changes in *Scinax* taxonomy: (i) resurrection of the genus *Ololygon* to harbour species of the former *Scinax catherinae* Clade, (ii) introduction of a new genus *Julianus* for members of the former *Scinax uruguayus* species group (sensu Faivovich et al. 2005), and (iii) restriction of the genus *Scinax* to the members of the former *S. ruber* Clade. As noted by Duellman et al. (2016), the separation of *Ololygon* and *Scinax* was evident in the cladistic analyses published by Faivovich (2002) and Faivovich et al. (2005). Moreover, Faivovich (2002) already stated that "*Scinax* could be partitioned at the level of the *catharinae* and *rubra* clades, and certainly there are names available for them. If desired, *Scinax* is available for the *rubra* clade, and the name *Ololygon* could be applied to the *catharinae* clade". In this paper, we follow Duellman et al. (2016) whose analysis is based on presently widest dataset.

The genus *Scinax* has a wide distribution area ranging from Mexico to central Argentina and Uruguay (Frost 2017). At present, 28 *Scinax* species are known to occur in Amazonia (see Sturaro and Peloso 2014, Brusquetti et al. 2014). However, a surprisingly high *Scinax* species diversity was recently revealed in the rainforests covering the area of the Purus-Madeira Interfluve (PMI; Fig. 1), where at least seven confirmed candidate species remain unnamed (Ferrão et al. 2016).

The PMI is crossed by an abandoned Trans-Amazonian highway (BR-319). Current proposals to reconstruct this highway bring a very serious threat for regional forest habitats and their fauna. Recent studies warn that one third of the PMI rainforest will be lost as a consequence of massive logging if this road improvement scheme goes ahead (Maldonado et al. 2012). Habitat loss has been widely reported as the major cause for populations decline and local extinctions for many groups of organisms, including frogs (e.g Soto-Azat et al. 2013). Therefore, current need of conservation of PMI is more urgent than ever before. In this respect, studies of species diversity resulting in descriptions of new species are of particular importance as they bring needed supporting data for wildlife conservation.

Here, we describe a new species of *Scinax* (*Scinax* sp. 3 *sensu* Ferrão et al. 2016) from the middle to southern PMI. The new species is described through external morphology of adults and tadpoles, and advertisement call.

Materials and methods

Adult specimens of the new species were collected in four sampling areas in the PMI (Fig. 1). Two sampling areas are located in the middle portion of the study area, one at the kilometre 350 of the BR-319 highway (5°15'57"S, 61°55'58"W, ca. 59 m a.s.l.: Fig. 1A) and the other at the Floresta Estadual Tapauá Reserve (06°22'37"S, 63°17'19"W, ca. 69 m a.s.l.: Fig. 1B). The remaining two sampling areas are located in the southern region of the PMI, near the left margin of upper Madeira river, about 100 kilometres from the municipality of Porto Velho (9°9'32"S, 64°37'60"W, ca. 105 m a.s.l., Fig. 1C; 9°17'52"S, 64°46'10"W, *ca.* 101 m a.s.l., Fig. 1D).

All adult specimens were collected at night, anesthetised, and killed with topic solution of 10% benzocaine, fixed in 10% formaldehyde solution and stored in 70% ethanol. Tissue samples were obtained from all adult specimens and stored in 96% ethanol at Albertina Lima´s laboratory at INPA (Instituto Nacional de Pesquisas da Amazônia), Manaus, Brazil. Measurements were taken to the nearest 0.1 mm with digital calliper under a dissecting microscope. Sex and maturity of specimens were identified by observing secondary sexual characters (vocal sac, vocal slits), and gonads through dissection. The format for the description and diagnostic characters follows Duellman and Wiens (1993) and Duellman et al. (2006). Webbing formulae follow the standards of Savage and Heyer (1967) and Myers and Duellman (1982), while all other terminology is that of Duellman (1970), Heyer et al. (1990) and Napoli (2005). Measurement abbreviations used throughout the text are: SVL (snout–vent length), HL (head length, the straight line distance from the posterior edge of the jaw articulation to the tip of the snout), HW (head width at angle of jaw), IND (internarial dis-

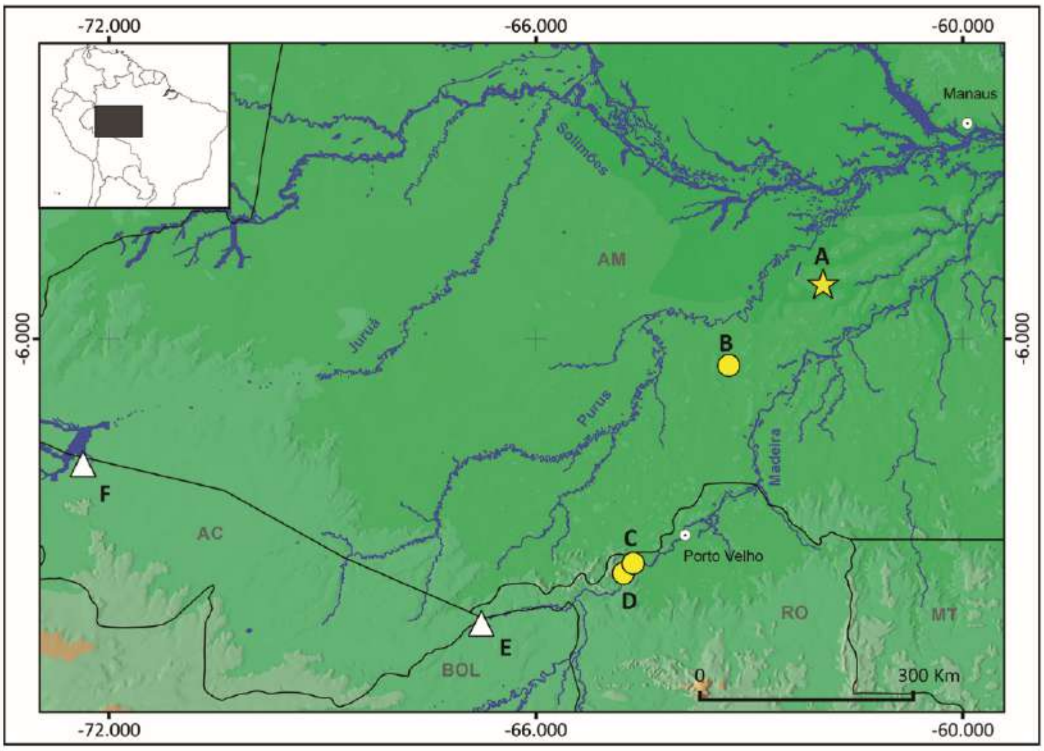

Figure 1. Distribution of *Scinax onca* sp. n. and *Scinax iquitorum* in Brazilian Amazonia. Yellow star: **A** type locality of *S. onca* sp. n., kilometre 350 of the BR-319 Highway, municipality of Beruri, State of Amazonas. Yellow circles: **B** paratype locality of *S. onca* sp. n., Floresta Estadual Tapauá Reserve, municipality of Tapauá, State of Amazonas **C–D** paratype localities of *S. onca* sp. n., municipality of Porto Velho, State of Rondônia. White triangles: **E** record of *S. iquitorum* near southern distribution of *S. onca* sp. n. according Melo-Sampaio and Souza (2015), municipality of Plácido de Castro, State of Acre, Brazil **F** record of *S. iquitorum* according Machado et al. (2015), municipality of Cruzeiro do Sul, State of Acre, Brazil.

tance), EN (eye to nostril distance), ED (horizontal eye diameter), ELW (upper eyelid width), IOD (minimal interorbital distance), TD (horizontal tympanum diameter), HAL (hand length), THL (thigh length) TL (tibia length), TAL (tarsus length), FL (foot length as the distance from the heel to the tip of the fourth toe), Fin3DW (Finger III disk width), Toe4DW (Toe IV disk width). Field notes and colour images were used for descriptions of coloration in life. Collected specimens were deposited in the herpetological section of the Zoological Collections of INPA (INPA-H). Specimens examined for comparative diagnoses are listed in the Appendix 1.

Tadpoles of the new species were collected in a $25 m^2$ pond not connected to stream, in the sampling area near the kilometre 350 of the BR-319 highway (5°15'57"S, 61°55'58"W, ca. 59 m a.s.l.: Fig. 1A). Tadpoles were killed with a 5% lidocaine solution diluted in water, and preserved in 5% formalin (tail of one tadpole was stored in 100% ethanol). All tadpoles were deposited in one lot (INPA-H 35411) in the INPA-H collection. The determination of the tadpoles was verified using molecular barcoding (GenBank accession number KU317421; see Ferrão et al. [2016]). Tadpoles were staged according to Gosner (1960). The format for the tadpole description follows Schulze et al. (2015). The description was based on six tadpoles in the Gosner Stage 37. Following morphometric characters were measured according to Lavilla and Scrocchi (1986) and Altig and McDiarmid (1999): total length (TL), body length (BL), tail length (TAL), maximum width of the tail muscle (TMW), maximum height of the tail (MTH), maximum tail muscle height (TMH), interorbital distance (IOD), internarial distance (IND); eye diameter (ED) and eye-nostril distance (END).

The interspecific pairwise genetic distances in the 16S rRNA between the new species and other available *Scinax* species were presented by Ferrão et al. (2016). However, the intraspecific pairwise genetic distances between specimens of the new species remain unknown. Due to that, we calculated uncorrected p and Kimura-2-parameter distances (Kimura 1980) between 16S rRNA sequences from specimens of the two clades of the new species (see Ferrão et al. 2016, Fig. 2) with MEGA 6.06 (Tamura et al. 2013). Sequences of adults and one tadpole from middle PMI clade (KU317415, KU317416, KU317421, KU317422, KU317423, KU317425, KU317426) and of adults from southern PMI clade (KU317417, KU317418, KU317419, KU317420, KU317424, KU317427) were obtained from GenBank. Preliminarily to distance calculations, the sequence set was aligned using the Clustal W algorithm (Thompson et al. 1994) implemented in BioEdit (Hall 1999). Genetic distance is presented in the subsection "Variation".

Advertisement calls of one male (INPA-H 26624) from the Floresta Estadual Tapauá Reverve (middle PMI: Fig. 1B) were recorded in 12 October 2013 using a Sony PCM - D50 digital recorder. Air temperature at the time of recording was not measured. We analysed fifteen calls with the sound analysis software Raven 1.5 (Bioacoustics Research Program 2014). Obtained oscillograms and spectrograms were analysed through Blackman window, 80 Hz of frequency resolution and Fast Fourier Transformation (FFT) of 1024 points. The following call parameters were measured: call duration, inter-call interval, number of pulses per call, dominant frequency, and call repetition rate (number of calls emitted within one minute of vocalization). Terminology of call descriptions follows Köhler et al. (2017).

Institutional abbreviations are as follows:

INPA-H	Collection of amphibians and reptiles of Instituto Nacional de Pesquisas da Amazônia, in Manaus, Brazil
KU	University of Kansas, Museum of Natural History, Division of Herpetology, Lawrence, Kansas, USA
QCAZ	Museo de Zoología, Pontifica Universidad Católica del Ecuador, Quito, Ecuador
RMNH	Rijksmuseum van Natuurlijke Historie, Leiden, The Netherlands
NHMG	Naturhistoriska Museet, Göteborg, Sweden
NMP6V	National Museum, Prague, Czech Republic
ZFMK	Zoologisches Forschungsinstitut und Museum Alexander Koenig, Bonn, Germany

Taxonomy

Scinax onca sp. n.

http://zoobank.org/91C1811A-D2FC-4699-8E2D-76D203D0BCC7
Figs 2–3, 5–7, 9–10
Suggested English name: Jaguar Snouted Treefrog.

Scinax iquitorum: Almeida et al. 2015: 142, Appendix II.
Scinax sp. 3: Ferrão et al. 2016: 7–9, figs 1 & 2B, Supporting table S2–S4.

Holotype (Figs 2–3, 4A–B). INPA-H 34584, an adult male from kilometre 350 of the BR-319 Highway (5°15'57"S, 61°55'58"W, ca. 59 m a.s.l., Fig. 1A), municipality of Beruri, State of Amazonas, Brazil, collected on 15 November 2013 by Miquéias Ferrão and Rafael de Fraga.

Paratypes (Figs 5C–F, 6–7). Sixteen specimens: five adult males (INPA-H 34581, INPA-H 34582, INPA-H 34585, INPA-H 34586, INPA-H 34587) and one adult female (INPA-H 34583), same locality and collecting data as the holotype; one adult male (INPA-H 26624) and one adult female (INPA-H 26625) from the Floresta Estadual Tapauá Reserve (06°22'37"S, 63°17'19"W, ca. 69 m a.s.l., Fig. 1B), municipality of Tapauá, State of Amazonas, Brazil, collected on 12 October 2013 by Alexandre P. Almeida; five adult males (INPA-H 34588, INPA-H 34592, INPA-H 34593, INPA-H 34594, INPA-H 34595) and one adult female (INPA-H 34589) from municipality of Porto Velho (9°9'32"S, 64°37'60"W, ca. 105 m a.s.l., Fig. 1C), State of Rondônia, Brazil, collected on 2 November and 7 February 2014 by Albertina P. Lima; one adult male (INPA-H 34590) and one adult female (INPA-H 34591) from municipality of Porto Velho (9°17'52"S, 64°46'10"W, ca. 101 m a.s.l., Fig. 1D), State of Rondônia, Brazil, collected on 25 February 2010 by Albertina P. Lima.

Referred material. Two: INPA-H 35413 and INPA-H 35414, newly metamorphosed specimens from the kilometre 350 of the BR-319 Highway (5°15'57"S, 61°55'58"W, ca. 59 m a.s.l., Fig. 1A), municipality of Beruri, State of Amazonas, Brazil, collected on 17 January 2014 by Miquéias Ferrão.

Generic placement. We assign the new species to *Scinax* based on general morphological similarity to other members of the genus, cloacal tube of tadpoles positioned above the margin of the lower fin (a synapomorphy of the former *S. ruber* Clade sensu Faivovich [2002], currently *Scinax* sensu Duellman et al. [2016]).

Diagnosis. A medium-sized species of *Scinax* characterized by the following combination of characters: (1) SVL 31.3–34.5 mm (n = 13) in males and 35.5–40.4 mm (n = 4) in females; (2) snout truncate in dorsal view, bluntly rounded in lateral view; (3) tarsal tubercles absent; (4) tubercles on lower jaw and knee absent; (5) skin on dorsum shagreen; (6) dentigerous processes of vomers triangular; (7) in life, ground colour of dorsum light brown with dark brown spots and markings; dorsolateral stripes or X-shaped blotch on dorsum absent; flanks light brown with or without dark brown spots; axillar region and groin white with black irregular spots; anterior and posterior surfaces

Taxonomy

***Scinax onca* sp. n.**
http://zoobank.org/91C1811A-D2FC-4699-8E2D-76D203D0BCC7
Figs 2–3, 5–7, 9–10
Suggested English name: Jaguar Snouted Treefrog.

Scinax iquitorum: Almeida et al. 2015: 142, Appendix II.
Scinax sp. 3: Ferrão et al. 2016: 7–9, figs 1 & 2B, Supporting table S2–S4.

Holotype (Figs 2–3, 4A–B). INPA-H 34584, an adult male from kilometre 350 of the BR-319 Highway (5°15'57"S, 61°55'58"W, ca. 59 m a.s.l., Fig. 1A), municipality of Beruri, State of Amazonas, Brazil, collected on 15 November 2013 by Miquéias Ferrão and Rafael de Fraga.

Paratypes (Figs 5C–F, 6–7). Sixteen specimens: five adult males (INPA-H 34581, INPA-H 34582, INPA-H 34585, INPA-H 34586, INPA-H 34587) and one adult female (INPA-H 34583), same locality and collecting data as the holotype; one adult male (INPA-H 26624) and one adult female (INPA-H 26625) from the Floresta Estadual Tapauá Reserve (06°22'37"S, 63°17'19"W, ca. 69 m a.s.l., Fig. 1B), municipality of Tapauá, State of Amazonas, Brazil, collected on 12 October 2013 by Alexandre P. Almeida; five adult males (INPA-H 34588, INPA-H 34592, INPA-H 34593, INPA-H 34594, INPA-H 34595) and one adult female (INPA-H 34589) from municipality of Porto Velho (9°9'32"S, 64°37'60"W, ca. 105 m a.s.l., Fig. 1C), State of Rondônia, Brazil, collected on 2 November and 7 February 2014 by Albertina P. Lima; one adult male (INPA-H 34590) and one adult female (INPA-H 34591) from municipality of Porto Velho (9°17'52"S, 64°46'10"W, ca. 101 m a.s.l., Fig. 1D), State of Rondônia, Brazil, collected on 25 February 2010 by Albertina P. Lima.

Referred material. Two: INPA-H 35413 and INPA-H 35414, newly metamorphosed specimens from the kilometre 350 of the BR-319 Highway (5°15'57"S, 61°55'58"W, ca. 59 m a.s.l., Fig. 1A), municipality of Beruri, State of Amazonas, Brazil, collected on 17 January 2014 by Miquéias Ferrão.

Generic placement. We assign the new species to *Scinax* based on general morphological similarity to other members of the genus, cloacal tube of tadpoles positioned above the margin of the lower fin (a synapomorphy of the former *S. ruber* Clade sensu Faivovich [2002], currently *Scinax* sensu Duellman et al. [2016]).

Diagnosis. A medium-sized species of *Scinax* characterized by the following combination of characters: (1) SVL 31.3–34.5 mm (n = 13) in males and 35.5–40.4 mm (n = 4) in females; (2) snout truncate in dorsal view, bluntly rounded in lateral view; (3) tarsal tubercles absent; (4) tubercles on lower jaw and knee absent; (5) skin on dorsum shagreen; (6) dentigerous processes of vomers triangular; (7) in life, ground colour of dorsum light brown with dark brown spots and markings; dorsolateral stripes or X-shaped blotch on dorsum absent; flanks light brown with or without dark brown spots; axillar region and groin white with black irregular spots; anterior and posterior surfaces

Comparisons. Until now, the following 28 valid species of *Scinax* occur in Amazonia (Sturaro and Peloso 2014, Brusquetti et al. 2014, Frost 2017): *S. baumgardneri* (Rivero, 1961), *S. blairi* (Fouquette & Pyburn, 1972), *S. boesemani* (Goin, 1966), *S. chiquitanus* (De la Riva, 1990), *S. cruentommus* (Duellman, 1972), *S. danae* (Duellman, 1986), *S. exiguus* (Duellman, 1986), *S. funereus* (Cope, 1874), *S. fuscomarginatus* (Lutz, 1925), *S. fuscovarius* (A. Lutz, 1925), *S. garbei* (Miranda-Ribeiro, 1926), *S. ictericus* Duellman & Wiens, 1993, *S. iquitorum* Moravec, Tuanama, Pérez & Lehr, 2009, *S. jolyi* Lescure & Marty, 2000, *S. karenanneae* (Pyburn, 1992), *S. kennedyi* (Pyburn, 1973), *S. lindsayi* Pyburn, 1992, *S. madeirae* (Bokermann, 1964), *S. nebulosus* (Spix, 1824), *S. oreites* Duellman & Wiens, 1993, *S. pedromedinae* (Henle, 1991), *S. proboscideus* (Brongersma, 1933), *S. rostratus* (Peters, 1863), *S. ruber* (Laurenti, 1768), *S. sateremawe* Sturaro & Peloso, 2014, *S. villasboasi* Brusquetti, Jansen, Barrio-Amorós, Segalla & Haddad, 2014, *S. wandae* (Pyburn & Fouquette, 1971), and *S. x-signatus* (Spix, 1824). Members of the genus *Julianus* occur in Uruguay, extreme southern Brazil, and in northern Corrientes, Argentina (*J. uruguayus* [Schmidt, 1944]) and in Serra do Cipó, Minas Gerais, Brazil (*J. pinimus* [Bokermann & Sazima, 1973]). Species of the genus *Ololygon* are distributed in Atlantic Coastal Forest of eastern Brazil, gallery forests of the Brazilian Cerrado and in Argentina (see Duellman et al. 2016). Among species of *Scinax* distributed in Amazonia, except by the species that occur in open habitats, all other species are endemic to the biome. Regarding the fact that *Scinax onca* sp. n. is an exclusive forest dweller known from the lowland rainforest of southern part of Central Amazonia we focus the comparison on Amazonian *Scinax* species, including six confirmed candidate species discovered recently in PMI (*Scinax* sp. 1–2 and *Scinax* sp. 4–7 of Ferrão et al. 2016).

Morphologically, *Scinax onca* sp. n. can be distinguished from all other Amazonian *Scinax* species by having bright orange iris and white groin with black spots in life and by the following combinations of characters (characters of other species in parentheses or brackets unless otherwise stated):

The new species differs from *S. baumgardneri*, *S. garbei*, *S. jolyi*, *S. kennedyi*, *S. nebulosus*, *S. pedromedinae*, *S. proboscideus*, and *S. rostratus* by snout truncate in dorsal view and bluntly rounded in lateral view, and by the absence of tubercles on the lower jaw and knee (elongated or pointed snout, and tubercles present on the lower jaw and knee; Duellman 1972, Pyburn 1973, Duellman and Wiens 1992, Lescure and Marty 2000, Lima et al. 2004). In addition, tadpoles of *S. onca* sp. n. differ from those of *S. garbei*, *S. nebulosus*, *S. pedromedinae*, and *S. rostratus* by the absence of labial arm (labial arm present; Duellman 1978, Hero and Mijares-Urrutia 1995, Duellman 2005, Gomes et al. 2014).

The male SVL 31.3–34.5 mm of *S. onca* sp. n. is larger than male SVL of *S. blairi* (27.8–30.1 mm; Fouquette and Pyburn 1972), *S. cruentommus* (24.8–27.7 mm; Duellman 1972), *S. danae* (24.5–27.4 mm; Duellman 1986), *S. exiguus* (18.0–20.8 mm; Duellman 1986), *S. fuscomarginatus* (15.7–26.7 mm; Brusquetti et al. 2014), *S. karenanneae* (SVL 26.6–28.9 mm; Pyburn 1993), *S. lindsayi* (about 24 mm; Pyburn 1992), *S. madeirae* (18.0–23.1 mm; Brusquetti et al. 2014), *S. villasboasi* (16.7–20.0 mm; Brusquetti et al. 2014), *S. wandae* (23.4–26.9 mm; Pyburn and Fouquette 1971), *Scinax* sp. 1 (20.2–22.5 mm, n = 5), *Scinax* sp. 2 (*sensu* Ferrão et al. 2016) (18.1–20.4 mm, n = 15), *Scinax* sp. 4 (*sensu* Ferrão et al. 2016) (23.2 mm), *Scinax* sp. 6 (*sensu* Ferrão et al. 2016) (25.1–26.7 mm, n = 6), and *Scinax* sp. 7 (*sensu* Ferrão et al. 2016) (22.6–25.9 mm, n = 28). The males of *S. onca* sp. n. are smaller than those of *S. fuscovarius* (SVL 41.0–44.0 mm; Cei 1980) and *S. sateremawe* (35.2–38.1 mm; Sturaro and Peloso 2014).

Scinax onca sp. n. can be distinguished from *S. boesemani* by conspicuous dark brown spots on the dorsum (light spots on dorsum) and belly (no spots), black posterior surfaces of thighs (light brown), and black webbing between toes (light brown; Goin 1966). The call of *S. onca* sp. n. differs from that of *S. boesemani* in duration (102–121 ms vs.160–290 ms in *S. boesemani*; Duellman and Pyles 1983).

The new species differs from *S. chiquitanus* in having snout truncate in dorsal view (rounded), head wider than body (narrower), black posterior surfaces of thighs (brown), and in having dark brown spots on the belly (light brown when present; De la Riva 1990). The call of *Scinax onca* sp. n. differs from the call of *S. chiquitanus* in duration (102–121 ms vs.185.3–338.8 ms in *S. chiquitanus*), number of pulses (16–18 vs. 23–42 in *S. chiquitanus*) and dominant frequency (1572–1594 Hz vs. 2100–2261.5 Hz in *S. chiquitanus*; De la Riva et al. 1994, Ferrão et al. 2016).

Scinax onca sp. n. differs from *S. ruber* by the snout truncate in dorsal view (rounded), black posterior surfaces of thighs (brown with yellow or orange mottling), and absence of dorsolateral stripes (tan to yellow dorsolateral stripes present; Duellman and Wiens 1993). There are seven available names in the synonymy of *S. ruber*: *Hyla conirostris* Peters, 1863 (type locality "Surinam"), *Hyla lateristriga* Spix, 1824 (type locality: Brazil, by implication), *Hyla lineomaculata* Werner, 1899 (type locality "Arima, Trinidad"), *Hyla robersimoni* Donoso-Barros, 1965 "1964" (type locality "Pajonales al sur de Macuro, Penisula de Paria, Venezuela"), *Hyla rubra hübneri* Melin, 1941 (type locality "Taracuá, Rio Uaupes", "São Gabriel, Rio Negro", and "Vicinity of Manaus", all localities in the State of Amazonas, Brazil), *Scytopis alleni* Cope, 1870 (type locality State of Pará, Brazil, by lectotype designation of Duellman and Wiens 1993), and *Scytopis cryptanthus* Cope, 1874 (type locality "Nauta", Region Loreto, Peru). According to their original descriptions, all these names are associated with specimens that have yellow blotches on the anterior and posterior surfaces of the thighs, and in some cases undersurfaces of tibiae (Moravec et al. 2009).

From *Scinax x-signatus* (Spix, 1824) the new species can be distinguished by absence of the X-shaped mark (present) and presence of dark brown spots on the dorsum (absent; Lutz 1973).

Scinax onca sp. n. differs from *S. ictericus* by snout truncate in dorsal view (bluntly round), absence of ulnar and tarsal tubercles (tubercles present), and by black posterior surfaces of thighs (light to dark brown; Duellman and Wiens 1993). The call of *Scinax onca* sp. n. differs from the call of *S. ictericus* in duration (102–121 ms vs. 70–90 ms in *S. ictericus*). The tadpoles of the new species differ in having triangular body in lateral view (ovoid; Duellman and Wiens 1993).

The new species can be distinguished from *S. funereus* (Fig. 4A) by its truncate snout in dorsal view (acutely rounded; Duellman 1978), absence of tarsal tubercles (a

Figure 4. Adult specimens of *Scinax funereus* and *S. iquitorum*. **A** Female specimen of *Scinax funereus* (KU221960b) from San Jacinto, Region Loreto, Peru, and **B** male paratype of *Scinax iquitorum* (NMP6V 71267/1) from Puerto Almendras, Region Loreto, Peru. Photograph by W.E. Duellman (**A**) and Jiří Moravec (**B**).

row of low tubercles on outer edge of tarsus; Duellman 1971), shagreen skin (strongly tuberculate; Duellman and Wiens 1993), flanks light brown (yellow; Duellman and Wiens 1993), orange iris (bicolored iris; see Fig. 4A), and black posterior surfaces of thighs (yellow with dark brown spots or pale with discrete dark brown blotches; Duellman and Wiens 1993). Labial tooth row formula 2(2)/3(1) of the tadpoles of *S. onca* sp. n. differs from that of *S. funereus* (2(2)/3; Duellman 1978). There are two available names in the synonymy of *S. funereus*: *Hyla depressiceps* Boulenger, 1882 (type locality "Ecuador") and *Hyla rubra inconspicua* Melin, 1941 (type locality "Roque, Region San Martín, Peru"). According to the original description, *H. depressiceps* differs from the new taxon in having black and whitish marbled limbs. An examination of the holotype of *Hyla rubra inconspicua* shows that it differs by the presence of small tubercles on the head, dorsum and limbs including the tarsal area (see Moravec et al. 2009).

The new species differs from *S. iquitorum* (Fig. 4B) by snout truncate in dorsal view (bluntly rounded), dentigerous processes of vomers triangular (transverse), presence of conspicuous dark brown spots on dorsum (small dark brown dots concentrated only on head and in areas of scapular and sacral blotches), light brown flanks with or without dark brown spots (bright yellow flanks with numerous distinct round black spots), and by white long bones of hindlimbs (green; Moravec et al. 2009).

Scinax onca sp. n. differs from *Scinax* sp. 5 (*sensu* Ferrão et al. 2016) by light brown dorsum with dark brown spots (yellowish green with diminutive black spots), dark spots on belly (absent), and anterior and posterior surfaces of thighs black (uniformly yellowish green).

Description of the holotype. Adult male 31.3 mm SVL. Body moderately slender; head wider than body, slightly longer than wide (HL/HW = 1.2, HL = 38.0% of SVL, HW = 32.3% of SVL); snout truncate in dorsal view, bluntly rounded in lateral view; nostrils markedly protuberant, elliptic, directed dorsolaterally; eye-nostril distance 76% of ED; internarial region moderately depressed; canthus rostralis rounded in both dorsal and lateral views; loreal region concave, more concave near to nostril;

interorbital distance longer than upper eye width (IOD/ELW = 1.1), IOD 31% of HW; eye diameter 34% of HW; tympanic annulus distinct, tympanic membrane evident, rounded, 51% of ED; supratympanic fold present, slightly distinct; vocal sack subgular, bilobate; vocal slits extend from lateral base of tongue (slightly behind the half distance from the anterior edge) to the mouth angles; dentigerous processes of vomers triangular, bearing 7/6 (left/right) teeth; choanes rounded; tongue lanceolate.

Arm and forearm slender; axillary membrane absent; pectoral fold present; hand length 29% of SVL; fingers long bearing horizontally expanded discs; diameter of disc on finger III 49% of ED; relative length of fingers I<II<IV<III; palmar tubercle bifid, flat, longer than wide; thenar tubercle elongated; distal subarticular tubercle conical on Finger I, subconical on Finger II, rounded on fingers III–IV; supernumerary tubercles small, slightly distinct; nuptial pad poorly developed, slender, extending from proximal base of thenar tubercle to distal base of distal subarticular tubercle on Finger I; fingers II–IV basally webbed; fingers with narrow lateral fringes, external fringe on Finger IV extends to distal portion of thenar tubercle.

Hind limb long; tibia longer than femur, tibia length 52% of SVL, femur length 47% of SVL; tarsus length 27% of SVL; foot length 44% of SVL; toe discs more rounded than finger discs; diameter of disc on Finger IV 44% of eye ED; relative length of toes I<II<III<V<IV; inner metatarsal tubercle oval and flat; outer metatarsal tubercle rounded, flat, three times smaller than inner metatarsal tubercle; subarticular tubercles subconical on toes I–II, rounded on toes III–V; supernumerary tubercles small, rounded, and flat; webbing on toes I 2–2^{+} II 1^{+}–2 III 1^{+}–2 IV 2–1^{+} V; distinct external lateral fringe on Toe V extending to outer metatarsal tubercle; fringe on external margin of Toe I extends to inner metatarsal tubercle; tarsal folds and tarsal tubercles absent; tubercles on heels absent.

Skin on dorsum shagreen, almost granular in supratympanic and anterotympanic region; skin smooth on forelimbs, hind limbs, throat, chest, and vocal sac; skin areolate on belly and ventral surface of thighs.

Measurements of the holotype (in mm). SVL 31.3; HL 11.9; HW 10.9; ED 3.7; EN 3.6; ELW 3.1; IND 2.8; IOD 3.4; TD 1.9; HAL 9.1; Fin3DW 1.8; TL 16.3; THL 14.8; TSL 8.6; FL 13.7; Toe4DW 1.6.

Colouration of the holotype in life (Fig. 5A–B). Ground colour of dorsal surfaces of head, body, and limbs light brown; dorsal pattern consisting of W-shaped interorbital mark on the head, an irregular dark brown spot in scapular region, a Λ-shaped mark in sacral region, and numerous round dark brown spots distributed randomly on the head (including lips) and body; a conspicuous dark brown canthal stripe extends to tip of snout; a dark brown supratympanic stripe extends from corner of eye to anterior region of flanks; three dark brown transverse bars on the forearm, the proximal one extends to arm; three brown transverse bars on the tibia; fingers and toes light brown, distal surfaces of disc cream to tan, proximal surfaces grey; toe webbing black; axillar region white with small dark brown spots; flanks light brown with dark brown spots; groin white with dark brown spots; anterior surfaces of thighs black; posterior surfaces of thighs black, bordered with an irregular white streak; throat and vocal sac yellow-

Figure 5. Colour in life of *Scinax onca* sp. n. Colour variation in life of *Scinax onca* sp. n. from the Purus-Madeira Interfluve, Brazilian Amazonia. **A–B** INPA-H 34584 (holotype), adult male from the kilometre 350 of the BR-319 highway, State of Amazonas **C–D** INPA-H 34591, adult female from municipality of Porto Velho, State of Rondônia **E–F** INPA-H 26625, adult female from the Floresta Estadual Tapauá Reserve, municipality of Tapauá, State of Amazonas. Photographs A–D and F were taken after transport of the specimens to the camp, while the image of E was taken immediately in the field.

ish; chest translucent; belly yellowish laterally, white medially, covered with randomly distributed round dark brown spots; anterior ventral surfaces of thighs greyish with black spots; posterior ventral surfaces of thighs dark grey to black; ventral surfaces of hand and foot black; nuptial pad cream; iris bright orange, without black reticulation, bordered by black externally.

Colouration of the holotype in alcohol (Figs 2–3). Dorsal surfaces of head, body, and limbs brown; throat, belly, and axillar area yellowish; groin white; dark brown dorsal and ventral pattern as in life with exception of inconspicuous transverse bars on thighs.

Variations. Both uncorrected p and K2P distances between specimens from southern and specimens from middle PMI groups range between 0.4 and 1.1%. Both the p and K2P distances between individuals from middle PMI varied from 0% to 0.2% and between individuals from southern PMI varied from 0% to 0.6% (Table 1). Despite the high genetic similarity, it appears that some variation in measurements and coloration is evident between specimens from middle PMI and specimens from southern PMI (the straight distance between the closest localities is ca. 500 km).

The specimens from southern PMI exhibit slightly larger average size ($t = -3.1$, $df = 10.4$, $p = 0.009$) and significantly lower values of nine following male body proportions: HL/SVL ($t = 2.3$, $df = 10.9$, $p = 0.01$), IND/SVL ($t = 3.4$, $df = 10.8$, $p = 0.005$), IOD/SVL ($t = 3.2$, $df = 9.6$, $p = 0.009$), HAL/SVL ($t = 6.9$, $df = 8.5$, $p < 0.001$), THL/SVL ($t = 2.8$, $df = 11$, $p = 0.01$), TL/SVL ($t = 3.9$, $df = 8.8$, $p = 0.003$), TAL/SVL ($t = 2.6$, $df = 10.2$, $p = 0.02$), FL/SVL ($t = 5.1$, $df = 10.3$, $p = 0.0003$), and X3FD/SVL ($t = 2.9$, $df = 6.7$, $p = 0.02$). Variation of measurements and body proportions of the type specimens is given in Table 2.

Colour change was observed after (Fig. 5A–D, F) and before (Fig. 5E) human manipulation of the specimens. After manipulation, general colouration of individuals became darker and spots and blotches became more conspicuous. In preservative, individuals from the middle PMI (Fig. 6A–C) had a larger number of dorsal spots and blotches in comparison to specimens from southern PMI (Fig. 6D–F). Regarding ventral coloration in preservative, individuals from the middle PMI (Fig. 7A–C) had a larger number of spots, which were concentrated on the belly. In the south, individuals had smaller ventral spots, and these were concentrated on the throat (Fig. 7D–F).

Vocalization. The advertisement call of *Scinax onca* sp. n. consists of a single short multipulsed note (Fig. 8). Quantitative call parameters are as follows (range followed by mean ± standard deviation in parentheses): call duration, 102–121 ms (110 ± 5, n = 15); silent interval between calls 526–1844 ms (1089 ± 438, n = 15), pulses/call 16–18 (16.8 ± 0.8, n = 15); dominant frequency 1572–1594 Hz (1573 ± 6, n = 15). Calls were repeated at an approximate rate of 16 notes per minute.

Tadpole description. The following description is based on six tadpoles (Stage 37) of the lot INPA-H 35411. Total length 34.6–38.3 mm (37 ± 1.5, n = 6), body length 9.1–10.5 mm (9.8 ± 0.5, n = 6), and tail length 24.6–28.7 mm (27 ± 1.5, n = 5). Body ovoid in dorsal view, triangular in lateral view (Fig. 9). Snout rounded in

Table 1. Intraspecific and interspecific genetic divergence. Uncorrected p-distance (upper-right) and K2P distance (lower-left) between 16S rRNA sequences of the paratype of *Scinax iquitorum* (1) and specimens of *S. onca* sp. n. from the southern (2–7) and middle (8–14) Purus-Madeira Interfluve. * = denote the sequence obtained from one tadpole of the lot INPA-H 35411.

	Specimens	1	2	3	4	5	6	7	8	9	10	11	12*	13	14
1	NMP6V 71267/3		0.059	0.063	0.059	0.059	0.057	0.059	0.059	0.059	0.059	0.061	0.059	0.059	0.059
2	INPA-H 34592	0.065		0.004	0.000	0.000	0.002	0.000	0.004	0.004	0.004	0.006	0.004	0.004	0.004
3	INPA-H 34588	0.070	0.004		0.004	0.004	0.006	0.004	0.008	0.008	0.008	0.011	0.008	0.008	0.008
4	INPA-H 34594	0.065	0.000	0.004		0.000	0.002	0.000	0.004	0.004	0.004	0.006	0.004	0.004	0.004
5	INPA-H 34593	0.065	0.000	0.004	0.000		0.002	0.000	0.004	0.004	0.004	0.006	0.004	0.004	0.004
6	INPA-H 34595	0.062	0.002	0.006	0.002	0.002		0.002	0.006	0.006	0.006	0.008	0.006	0.006	0.006
7	INPA-H 34589	0.065	0.000	0.004	0.000	0.000	0.002		0.004	0.004	0.004	0.006	0.004	0.004	0.004
8	INPA-H 20586	0.065	0.004	0.009	0.004	0.004	0.006	0.004		0.000	0.000	0.002	0.000	0.000	0.000
9	INPA-H 34585	0.065	0.004	0.009	0.004	0.004	0.006	0.004	0.000		0.000	0.002	0.000	0.000	0.000
10	INPA-H 34581	0.065	0.004	0.009	0.004	0.004	0.006	0.004	0.000	0.000		0.002	0.000	0.000	0.000
11	INPA-H 34583	0.068	0.006	0.011	0.006	0.006	0.009	0.006	0.002	0.002	0.002		0.002	0.002	0.002
12	INPA-H 35411*	0.065	0.004	0.009	0.004	0.004	0.006	0.004	0.000	0.000	0.000	0.002		0.000	0.000
13	INPA-H 35413	0.065	0.004	0.009	0.004	0.004	0.006	0.004	0.000	0.000	0.000	0.002	0.000		0.000
14	INPA-H 35414	0.065	0.004	0.009	0.004	0.004	0.006	0.004	0.000	0.000	0.000	0.002	0.000	0.000	

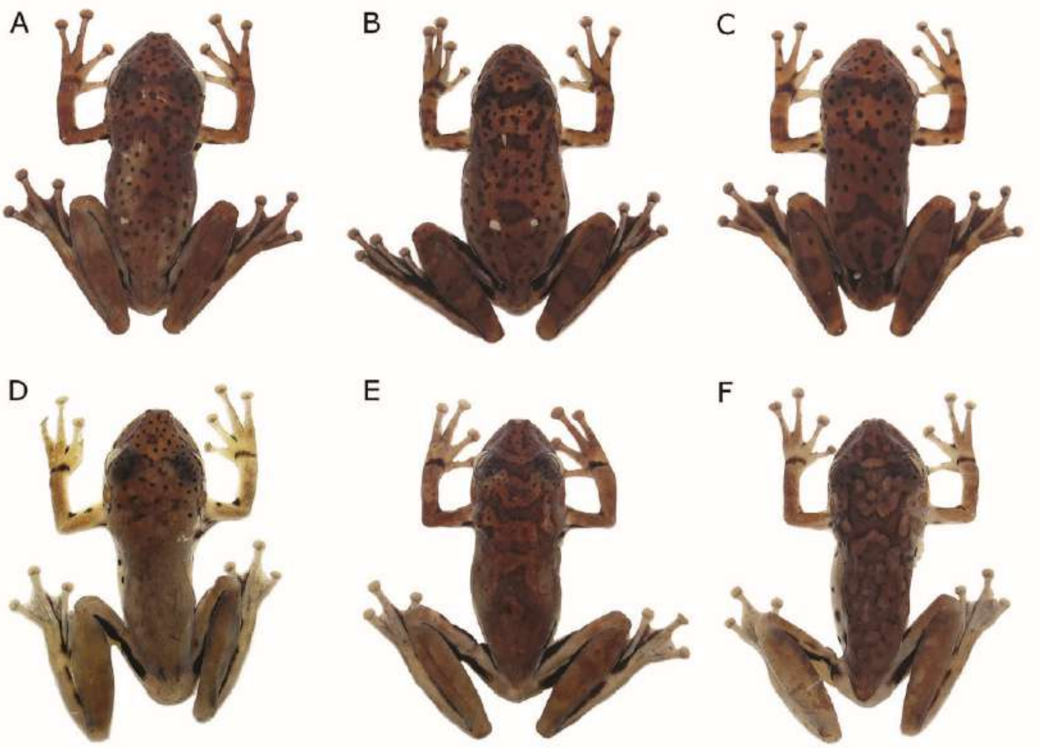

Figure 6. Colour in preservative of dorsum of *Scinax onca* sp. n. Dorsal colour variation of preserved specimens of *Scinax onca* sp. n. Specimens from middle (**A–C**) and southern (**D–F**) Purus-Madeira Interfluve, Brazilian Amazonia. **A** INPA-H 34581, male, SVL 34.3 mm **B** INPA-H 34583, female, SVL 35.5 mm **C** INPA-H 34582 male, SVL 31.5 mm **D** INPA-H 34594, male, SVL 32.6 mm **E** INPA-H 34589, female, SVL 38.9 mm **F** INPA-H 34593, male, SVL 34.5 mm.

dorsal and lateral view, distinct from body. Nostrils large, rounded, positioned and directed dorsally, eye-nostril distance represents 63–88% (74 ± 9, n = 6) of eye diameter. Inter nostril distance represents 62–70% (65 ± 3, n = 6) of inter orbital distance. Eyes large, positioned and directed laterally, with diameter 15–19 % (17 ± 1, n = 6) of body length. Spiracle tube single, sinistral, visible from dorsal view, inner wall and ventral right wall of the tube free from the body. Tail higher than body, point of maximum height of tail about half tail length. Tail musculature visible. Dorsal fin emerging nearly in the middle of the body, rising moderately, descending gradually to flagellum. Ventral fin approximately of the same height and shape as the dorsal fin. Cloacal tube positioned above the margin of the lower fin. Oral disc located anteroventrally, emarginated laterally, protuberant when closed (Fig. 10). Upper labium with uniseriate marginal papillae on distal portion and two rows of papillae (with small median gap) close to mouth angle. Lower labium with triseriate marginal papillae close to mouth angle and biseriate papillae on medial portion. Papillae are long, rounded on tip, distributed irregularly. Jaw sheaths moderately robust and serrated, upper jaw M-shaped and lower jaw V-shaped. Labial tooth row formula 2(2)/3(1). The row A-1 nearly the

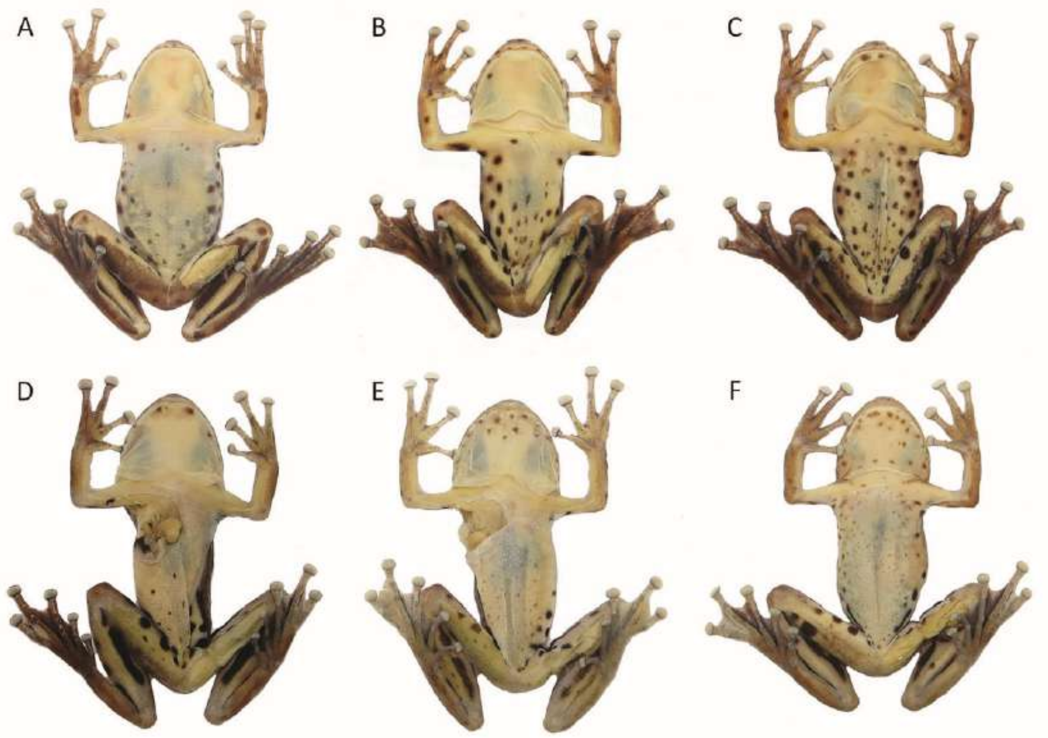

Figure 7. Colour in preservative of venter of *Scinax onca* sp. n. Ventral colour variation of preserved specimens of *Scinax onca* sp. n. Specimens from middle (**A–C**) and southern (**D–F**) Purus-Madeira Interfluve, Brazilian Amazonia. **A** INPA-H 34583, female, SVL 35.5 mm **B** INPA-H 34582, male, SVL 31.5 mm **C** INPA-H 34581 male, SVL 34.3 mm **D** INPA-H 34588, male, SVL 34.1 mm **E** INPA-H 34593, male, SVL 34.5 mm **F** INPA-H 34589, female, SVL 38.9 mm.

same length of A-2, P-2 slightly longer than P-1, P-3 shorter than P-1 and P-2. The gap in P-1 approximately the same length of the gap in A-2.

In life, dorsal and lateral surfaces of body silvery-green. Fins silvery-green, translucent, having dark grey spots. In preservative, dorsum of body uniformly grey-brown. A dark brown eye-snout stripe and dark brown interorbital blotch present. Fins translucent with small to large irregular diffuse dark brown spots. Tail musculature light brown. Ventral surfaces of the body white, slightly transparent.

Etymology. The specific name *onca* refers to the Brazilian common name for the jaguar *Pantera onca* (Linnaeus, 1758) due the blotchy colour pattern of the new species. Furthermore, the specific name is a reference to frequent encounters of *P. onca* during the fieldwork in the PMI. The name is used as a noun in apposition.

Distribution, ecology, and threat status. *Scinax onca* sp. n. is an exclusive forest dweller, known from two small areas located in the middle section of the PMI (State of Amazonas, Brazil), and two small areas lying in southern part of PMI, close to municipality of Porto Velho (Rondônia, Brazil). The maximum straight distance between the localities is around 500 km (Fig. 1). The middle PMI is covered by tropical lowland

Table 2. Morphometric data (in mm) of *Scinax onca* sp. n. from the Purus-Madeira interfluve, Brazilian Amazonia. Means followed by standard deviation, and ranges in parentheses. For abbreviations, see Materials and methods.

	Middle Purus-Madeira interfluve		Southern Purus-Madeira interfluve	
	Males (n = 7)	**Females (n = 2)**	**Males (n = 6)**	**Females (n = 2)**
SVL	32 ± 1.1 (31.3–34.3)	36.5 ± 1.0 (35.5–37)	33.6 ± 0.7 (32.6–34.5)	39.6 ± 1 (38.9–40.4)
HL	12.1 ± 0.3 (11.8–12.6)	13.1 ± 0 (13.1–13.1)	12.3 ± 0.3 (12–12.7)	13.6 ± 0.1 (13.6–13.7)
HW	11.3 ± 0.4 (10.9–11.9)	12.3 ± 0.3 (12.1–12.6)	11.8 ± 0.3 (11.4–12.1)	13.2 ± 0.1 (13.1–13.3)
ED	3.7 ± 0.3 (3.5–4.2)	3.7 ± 0.3 (3.5–3.9)	3.6 ± 0.2 (3.3–3.9)	3.9 ± 0.1 (3.8–4)
TD	2.1 ± 0.2 (1.9–2.4)	2.3 ± 0.3 (2.1–2.4)	2.2 ± 0.1 (2–2.4)	2.3 ± 0.1 (2.3–2.4)
UEW	3.1 ± 0.2 (2.7–3.2)	3.1 ± 0.1 (3–3.2)	3.2 ± 0.2 (2.9–3.4)	3 ± 0.1 (2.9–3.1)
IOD	3.3 ± 0.2 (3.1–3.7)	3.7 ± 0.3 (3.5–3.9)	3.2 ± 0.2 (3–3.4)	3.8 ± 0.2 (3.7–4)
IND	2.7 ± 0.1 (2.6–2.8)	3.2 ± 0.1 (3.1–3.3)	2.7 ± 0.1 (2.7–2.8)	3 ± 0.1 (2.9–3.1)
TAL	9 ± 0.3 (8.6–9.6)	10 ± 0.3 (9.8–10.2)	9 ± 0.3 (8.7–9.3)	10.5 ± 0 (10.5–10.5)
FL	13.7 ± 0.4 (13.4–14.4)	15.7 ± 0.4 (15.4–16)	13.4 ± 0.4 (12.9–14.1)	16.5 ± 0.4 (16.2–16.7)
HAL	9.5 ± 0.5 (9.1–10.4)	10.9 ± 0 (10.9–10.9)	9.2 ± 0.2 (8.9–9.5)	11.4 ± 0.7 (11–11.9)
3FD	1.8 ± 0.1 (1.7–1.9)	2.2 ± 0 (2.2–2.2)	1.7 ± 0.2 (1.5–1.9)	2 ± 0.2 (1.8–2.2)
4TD	1.7 ± 0.1 (1.6–1.8)	2 ± 0.1 (1.9–2.1)	1.6 ± 0.2 (1.4–1.8)	1.9 ± 0.2 (1.8–2.1)
END	3.9 ± 0.2 (3.6–4.2)	3.9 ± 0.2 (3.6–4.2)	4 ± 0.2 (3.7–4.2)	4.4 ± 0.1 (4.4–4.5)
TL	17 ± 0.5 (16.3–17.6)	19.2 ± 0.6 (18.7–19.6)	17 ± 0.4 (16.5–17.7)	19.8 ± 0.5 (18.5–19.2)
THL	15.9 ± 0.6 (14.8–16.5)	18.2 ± 0.7 (17.8–18.7)	15.8 ± 0.7 (14.7–16.9)	18.2 ± 0.7 (17.8–18.7)
HL/SVL	0.38 ± 0.01 (0.37–0.39)	0.36 ± 0.01 (0.35–0.37)	0.37 ± 0.01 (0.36–0.38)	0.34 ± 0.01 (0.34–0.35)
HW/SVL	0.35 ± 0.01 (0.35–0.37)	0.35 ± 0.01 (0.35–0.37)	0.35 ± 0.01 (0.34–0.37)	0.33 ± 0.01 (0.33–0.34)
ED/SVL	0.12 ± 0.01 (0.11–0.13)	0.10 ± 0.01 (0.10–0.11)	0.11 ± 0.01 (0.10–0.12)	0.10 ± 0.01 (0.09–0.10)
TD/SVL	0.06 ± 0.01 (0.06–0.07)	0.06 ± 0.01 (0.06–0.07)	0.06 ± 0.01 (0.06–0.07)	0.06 ± 0 (0.06–0.06)
UEW/SVL	0.10 ± 0.01 (0.09–0.10)	0.09 ± 0.01 (0.08–0.09)	0.10 ± 0.01 (0.09–0.10)	0.08 ± 0.01 (0.07–0.08)
IOD/SVL	0.10 ± 0.01 (0.10–0.11)	0.10 ± 0.01 (0.09–0.11)	0.09 ± 0.01 (0.09–0.10)	0.10 ± 0.01 (0.09–0.10)
IND/SVL	0.09 ± 0.01 (0.08–0.09)	0.09 ± 0 (0.09–0.09)	0.08 ± 0 (0.08–0.08)	0.08 ± 0.01 (0.07–0.08)
TAL/SVL	0.28 ± 0.01 (0.27–0.30)	0.28 ± 0.01 (0.27–0.28)	0.27 ± 0.01 (0.26–0.28)	0.27 ± 0.01 (0.26–0.27)
FL/SVL	0.43 ± 0.01 (0.42–0.45)	0.43 ± 0 (0.43–0.43)	0.40 ± 0.01 (0.38–0.41)	0.42 ± 0.02 (0.40–0.43)
HAL/SVL	0.30 ± 0.01 (0.29–0.31)	0.30 ± 0.01 (0.29–0.31)	0.27 ± 0.01 (0.27–0.28)	0.29 ± 0.02 (0.27–0.31)
3FD/SVL	0.06 ± 0.01 (0.05–0.06)	0.06 ± 0 (0.06–0.06)	0.05 ± 0.01 (0.05–0.06)	0.05 ± 0.01 (0.05–0.06)
4TD/SVL	0.05 ± 0 (0.05–0.05)	0.06 ± 0.01 (0.05–0.06)	0.05 ± 0.01 (0.04–0.05)	0.05 ± 0.01 (0.04–0.05)
END/SVL	0.12 ± 0.01 (0.12–0.13)	0.12 ± 0 (0.12–0.12)	0.12 ± 0.01 (0.11–0.13)	0.11 ± 0 (0.11–0.11)
TL/SVL	0.53 ± 0.01 (0.51–0.55)	0.53 ± 0 (0.53–0.53)	0.51 ± 0.01 (0.49–0.51)	0.50 ± 0.03 (0.48–0.52)
THL/SVL	0.50 ± 0.02 (0.47–0.52)	0.50 ± 0.01 (0.50–0.51)	0.47 ± 0.01 (0.45–0.49)	0.47 ± 0.02 (0.46–0.49)

rainforest characterized by closed canopy with emergent trees whereas the southern part has a more open lowland rainforest formation with frequent palm trees.

The new species is an explosive breeder. All specimens were encountered after (or during) heavy rains when aggregated at middle-sized or large temporary forest ponds. The ponds were not connected to streams. The males were calling from shrubs growing in or next to the water. Calling males adopted both horizontal and vertical positions on leaves and shrub trunks ca. 50–200 cm above the ground. Other tree frogs found in sympatry with *S. onca* sp. n. included *Dendropsophus leucophyllatus* (Beireis, 1783), *D. marmoratus* (Laurenti, 1768), *D. minutus* (Peters, 1872), *D. parviceps* (Boulenger,

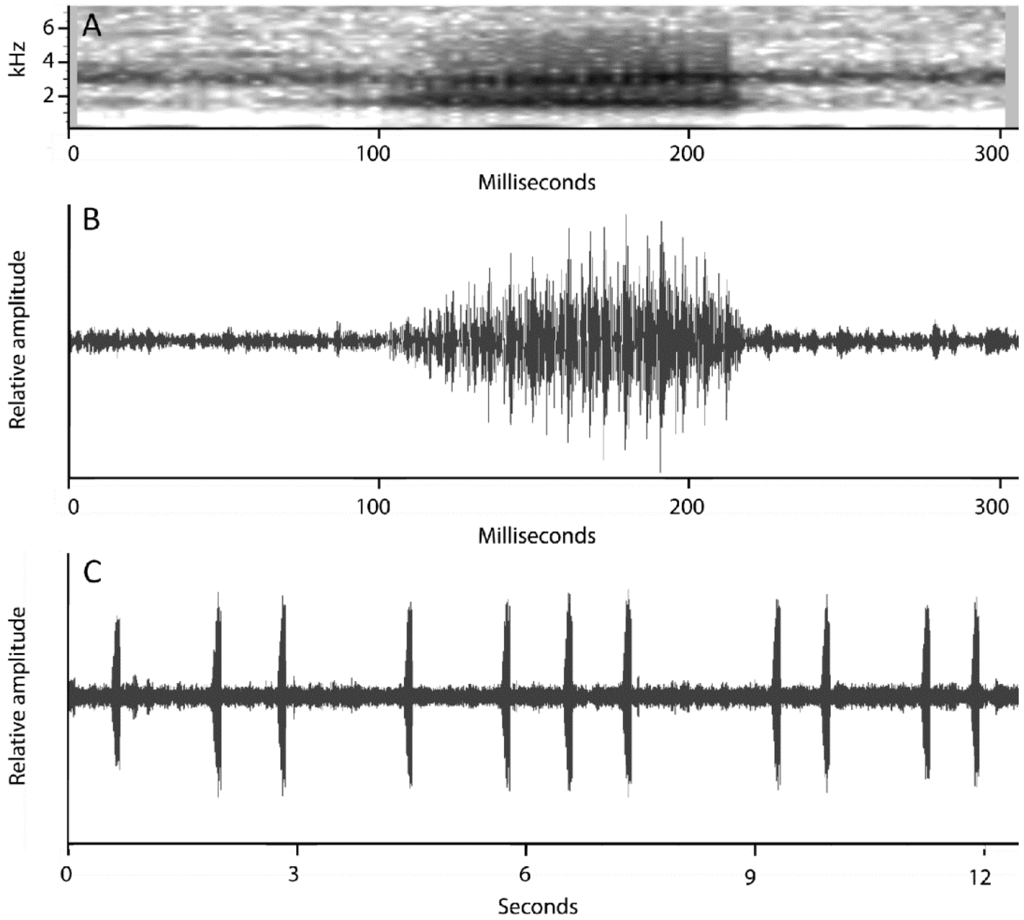

Figure 8. Advertisement call of *Scinax onca* sp. n. Spectrogram (**A**) and oscillogram (**B**) of an advertisement call of *Scinax onca* sp. n. The specimen (INPA-H 26624, SVL 32.1 mm) was recorded in Floresta Estadual Tapauá Reserve, middle Purus-Madeira Interfluve, Amazonas, Brazil **C** A series with eleven calls. Air temperature not measured.

1882), *D. rhodopeplus* (Boulenger, 1882), *D. sarayacuensis* (Shreve, 1935), *Phyllomedusa vaillantii* Boulenger, 1882, and *Scinax* sp. 7 (*sensu* Ferrão et al. 2016).

Based on the sparse data available and due to threats, it is suggested that *S. onca* sp. n. be classified as "Data Deficient" according to the IUCN red list criteria (IUCN 2016). It is necessary to stress out, however, that the known range of the new species is seriously threatened by the planned reconstruction of the Trans-Amazonian highway BR-319 connecting Manaus and Porto Velho. This initiative will facilitate human migration from the "Arc of Deforestation" in southern Rondônia to the PMI (Fearnside and Graça 2006). According to recent predictions, this immigration could result in the deforestation of up 5.4 million hectares of mostly undisturbed rainforests between 2012 and 2050 (Maldonado et al. 2012). Three of four known *S. onca* sp. n. localities occur in the area of predicted deforestation. Only the fourth locality lies within the Floresta Tapauá Reserve, which can serve as refuge for this and other species.

Figure 9. Tadpole of *Scinax onca* sp. n. from the middle Purus-Madeira Interfluve (lot INPA-H 35411). Specimen collected at kilometre 350 of the BR-319 highway, municipality of Beruri, State of Amazonas, Brazil. From top to bottom: dorsal, ventral, and lateral views of preserved tadpole in developmental Stage 37. Scale bar 5 mm.

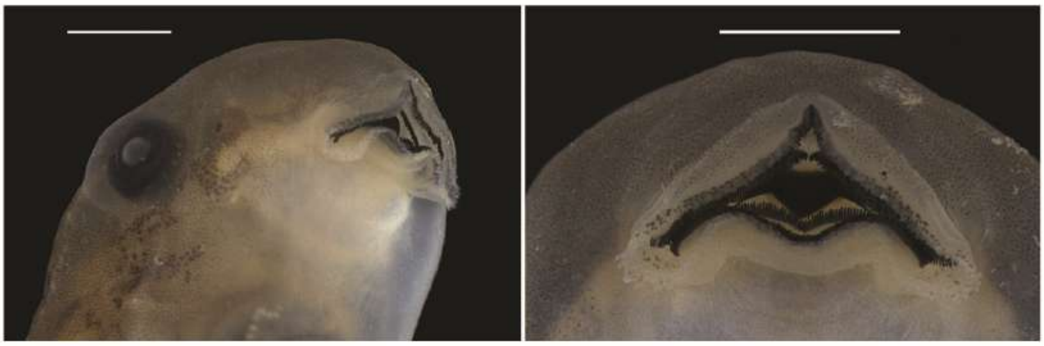

Figure 10. Oral disc of the tadpole of *Scinax onca* sp. n. (lot INPA-H 35411; developmental Stage 37). Left: ventrolateral and right: ventral view. The tadpole was collected in the middle Purus-Madeira Interfluve, at the kilometre 350 of the BR-319 highway, municipality of Beruri, State of Amazonas, Brazil. Scale bar 2 mm.

Discussion

The morphological data presented here show slight differences between members of the middle and southern PMI populations of *Scinax onca* sp. n. These differences are consistent with previously obtained molecular phylogeny (Ferrão et al. 2016), where the new taxon is structured into two slightly differentiated lineages corresponding to the middle and southern PMI populations. Nevertheless, until more robust evidence of specific distinction between the two populations is available, we decided to use the same specific epithet for the representatives of the both PMI populations. The observed differences may be a result of local adaptation to different environmental conditions, since the populations live under different climate conditions (drier in south) and inhabit different types of lowland forest. Other possibility is that the differences in measurements and coloration represent two examples of peripheral intraspecific variation, as the known populations are separated by ca. 500 km from each other. Till now we were not able to find individuals corresponding to *S. onca* sp. n. in the central region of the study area. Therefore, more complete sampling within this distributional gap is necessary to obtain a more exact picture of the morphological variation and genetic structure of *S. onca* sp. n.

Three records of *Scinax iquitorum*, species most closely related to *S. onca* sp. n., were recently reported from Brazilian western Amazonia (State of Acre; Machado et al. 2015, Melo-Sampaio and Souza 2015) and from Floresta Estadual Tapauá Reserve (State of Amazonas; Almeida et al. 2015). Two individuals reported by Almeida et al. (2015) were examined in this study. Since their morphology did not agree with the diagnosis of *S. iquitorum*, but corresponded fairly well with that of *Scinax onca* sp. n. (sensu Ferrão et al. 2016) from kilometre 350 of the BR-319 highway (type locality of *S. onca* sp. n., ca. 190 km from Floresta Estadual Tapauá Reserve) we included them into the type series of the new species described here. Individuals of *S. iquitorum* reported by Melo-Sampaio and Souza (2015) from the eastern corner of the Acre have very similar colour pattern to *S. onca* sp. n. from southern PMI, and we tentatively associate them with *S. onca* sp. n. Nevertheless, DNA barcoding as well as thorough morphological and bioacoustic data are necessary for a definitive determination of the specimens reported from eastern Acre. The same applies also for the proper determination of the individuals of *S. iquitorum* reported by Machado et al. (2015) from the municipality of Cruzeiro do Sul. In the light of contemporary knowledge of the extensive diversity of *Scinax* species in the State of Amazonas, we stress out that occurrence of *S. iquitorum* in the State of Acre should be verified by non-morphological traits.

It is evident that Brazilian States of Acre, Amazonas, and Rondônia house much more diverse fauna of *Scinax* tree frogs than previously thought. Similarly, this region is probably also home of many other, still unnamed, anuran species. Although a number of new species will be described in the near future, a more complete evaluation of the unique anuran diversity of the PMI is a long-term process, which is unlikely to be successfully completed without an effective wide-scale protection of the lowland Amazonian rainforest.

Acknowledgements

We thank Edgar Lehr and an anonymous reviewer for the careful revision of the manuscript and William E. Duellman for providing comparative photographs of *Scinax funereus*. This work was supported by PRONEX – FAPEAM/CNPq (proj. 003/2009, proc. 653/2009) and by Ministry of Culture of the Czech Republic (DKRVO 2016/15, National Museum, 00023272). We thank Centro de Estudos Integrados da Biodiversidade Amazônica (CENBAM) by assistance in fieldwork at the interfluve between the Purus and Madeira Rivers. Miquéias Ferrão received research fellowships from Conselho Nacional de Desenvolvimento Científico e Tecnológico (CNPq) under Grant CNPq – proc. 573721/2008-4, via CENBAM while conducting this study. Currently, Miquéias Ferrão receives a PhD fellowship from Fundação de Amparo à Pesquisa do Estado do Amazonas (FAPEAM), and Rafael de Fraga a PhD fellowship from Coordenação de Aperfeiçoamento de Pessoal de Nível Superior (CAPES). We are indebted to Fernanda Werneck and Ariane Silva for access to INPA-H collection. Holotype and tadpole photographs were taken with equipment acquired under Grant PRONEX-FAPEAM Ed. 016/2006, proc. 1437/2007. Collecting permits were provided by RAN/ICMBio (Reg. 659755 No. 13777). Adrian Barnett helped with the English.

References

Almeida AP, Carvalho VT, Gordo M (2015) Levantamento da herpetofauna em cinco Unidades de conservação na região do Interflúvio Madeira-Purus, estado do Amazonas. In: Gordo M, Pereira HS (Eds) Unidades de Conservação do Amazonas no interflúvio Purus-Madeira: Diagnóstico Biológico. EDUA Press, Manaus, 117–148.

Altig R, McDiarmid RW (1999) Body plan: development and morphology. In: McDiarmid RW, Altig R (Eds) Tadpoles: The Biology of Anuran Larvae. University of Chicago Press, Chicago, 24–51.

Araujo-Vieira K, Brandão RA, Faria DCC (2015) A new species of rock-dwelling *Scinax* Wagler (Anura: Hylidae) from Chapada dos Veadeiros, central Brazil. Zootaxa 3915: 52–66. https://doi.org/10.11646/zootaxa.3915.1.2

Araujo-Vieira K, Valdujo PH, Faivovich J (2016) A new species of *Scinax* Wagler (Anura: Hylidae) from Mato Grosso, Brazil. Zootaxa 4061: 261–273. https://doi.org/10.11646/zootaxa.4061.3.4

Bioacoustics Research Program (2015) Raven Pro: Interactive Sound Analysis Software. Ver. 1.5. The Cornell Lab of Ornithology, Ithaca.

Cei JM (1980) Amphibians of Argentina. Monitore Zoologico Italiano, Monografia 2: 1–609.

Brusquetti F, Jansen M, Barrio-Amorós CL, Segalla MV, Haddad CFB (2014) Taxonomic review of *Scinax fuscomarginatus* (Lutz, 1925) and related species (Anura; Hylidae). Zoological Journal of the Linnean Society 171: 783–821. https://doi.org/10.1111/zoj.12148

De la Riva I (1990) Una especie nueva de *Ololygon* (Anura: Hylidae) procedente de Bolivia. Revista Española de Herpetología 4: 81–86.

De la Riva I, Márquez R, Bosch J (1994) Advertisement calls of Bolivian species of *Scinax* (Amphibia, Anura, Hylidae). Contributions to Zoology 64: 75–85.

Duellman WE (1970) The hylid frogs of Middle America 1. Monograph of the Museum of Natural History, The University of Kansas 1: 1–428. https://doi.org/10.5962/bhl.title.2835

Duellman WE (1971) The Identities of Some Ecuadorian Hylid Frogs. Herpetologica 27(2): 212–227.

Duellman WE (1972) A new species of *Hyla* from Amazonian Ecuador. Copeia 1972: 265–271. https://doi.org/10.2307/1442487

Duellman WE (1978) The biology of an equatorial herpetofauna in Amazonian Ecuador. Miscellaneous Publications of the University of Kansas Museum of Natural History 65:1–352.

Duellman WE, Pyles RA (1983) Acoustic resource partitioning in anuran communities. Copeia 1983: 639–49. https://doi.org/10.2307/1444328

Duellman WE (1986) Two new species of *Ololygon* (Anura: Hylidae) from the Venezuelan Guyana. Copeia 1986: 864–870. https://doi.org/10.2307/1445281

Duellman WE, Wiens JJ (1992) The status of the hylid frog genus *Ololygon* and the recognition of *Scinax* Wagler, 1830. Occasional Papers of the Museum of Natural History, University of Kansas 151: 1–23.

Duellman WE, Wiens JJ (1993) Hylid frogs of the genus *Scinax* Wagler, 1830, in Amazonian Ecuador and Peru. Occasional Paper of the Museum of Natural History, University of Kansas 153: 1–57.

Duellman WE (2005) Cusco Amazonico – the lives of amphibians and reptiles in an Amazonian rainforest. Cornell University Press, Ithaca, New York, 488 pp.

Duellman WE, Lehr E, Venegas PJ (2006) Two new species of *Eleutherodactylus* (Anura: Leptodactylidae) from northern Peru. Zootaxa 1285: 51–64. https://doi.org/10.11646/zootaxa.1285.1.4

Duellman WE, Marion AB, Hedges SB (2016) Phylogenetics, classification, and biogeography of the treefrogs (Amphibia: Anura: Arboranae). Zootaxa 4104(1): 1–681 109. https://doi.org/10.11646/zootaxa.4104.1.1

Faivovich J (2002) A cladistic analysis of *Scinax* (Anura: Hylidae). Cladistic 18(4): 367–393. https://doi.org/10.1111/j.1096-0031.2002.tb00157.x

Faivovich J, Haddad CFB, Garcia PCA, Frost DR, Campbell JA, Weeler WC (2005) Systematic review of the frog family Hylidae, with special reference to Hylinae: phylogenetic analysis and taxonomic revision. Bulletin of the American Museum of Natural History 294: 1–240. https://doi.org/10.1206/0003-0090(2005)294[0001:SROTFF]2.0.CO;2

Fearnside PM, Graça PMLA (2006) BR-319: Brazil's Manaus-Porto Velho Highway and the potential impact of linking the arc of deforestation to central Amazonia. Environmental Management 38: 705–716. https://doi.org/10.1007/s00267-005-0295-y

Ferrão M, Colatreli O, Fraga R, Kaefer IL, Moravec J, Lima AP (2016) High species richness of *Scinax* Treefrogs (Hylidae) in a threatened amazonian landscape revealed by an integrative approach. PLoS ONE 11(11): e0165679. https://doi.org/10.1371/journal.pone.0165679

Fouquet A, Vences M, Salducci MD, Meyer A, Marty C, Gilles A (2007) Revealing cryptic diversity using molecular phylogenetics and phylogeography in frogs of the *Scinax ruber* and

Rhinella margaritifera species groups. Molecular Phylogenetics and Evolution 43: 567–582. https://doi.org/10.1016/j.ympev.2006.12.006.pmid:17303441

Fouquette MJ, Pyburn WF (1972) A new Colombian treefrog of the *Hyla rubra* complex. Herpetologica 28: 176–181.

Fouquette MJ, Delahoussaye AJ (1977) Sperm morphology in the *Hyla rubra* group (Amphibia, Anura, Hylidae), and its bearing on generic status. Journal of Herpetology 11: 387–396. https://doi.org/10.2307/1562720

Frost DR (2017) Amphibian Species of the World: An Online Reference. Version 6.0 (20 June 2017). Electronic Database accessible at http://research.amnh.org/herpetology/amphibia/index.html. American Museum of Natural History, New York, USA.

Goin CJ (1966) Description of a new frog of the genus *Hyla* from Suriname. Zoologische Mededelingen, Leiden 41: 229–232.

Gomes MDR, Alves ACR, Peixoto OL (2014) The tadpole of *Scinax nebulosus* (Amphibia, Anura, Hylidae). Iheringia. Série Zoologia 104(2): 184–188. https://doi.org/10.1590/1678-476620141042184188

Gosner KL (1960) A simplified table for staging anuran embryos and larvae with notes on identification. Herpetologica 16: 183–190.

Hall TA (1999) BioEdit: a user-friendly biological sequence alignment editor and analysis program for Windows 95/98/NT. Nucleic Acids Symposium Series 41: 95–98.

Hero JM, Mijares-Urrutia A (1995) The tadpole of *Scinax rostrata*. Journal of Herpetology 29(2): 307–311. https://doi.org/10.2307/1564575

Heyer WR, Rand AS, Cruz CAG, Peixoto OL, Nelson CE (1990) Frogs of Boracéia. Arquivos de Zoologia 31: 231–410. https://doi.org/10.11606/issn.2176-7793.v31i4p231-410

IUCN (2016) The IUCN Red List of Threatened Species. Version 2016-3. http://www.iucnredlist.org [Downloaded on 13 May 2016]

Juncá FA, Napoli MF, Nunes I, Mercês EA, Abreu RO (2015) A new species of the *Scinax ruber* clade (Anura, Hylidae) from the Espinhaço Range, northeastern Brazil. Herpetologica 71: 299–309. https://doi.org/10.1655/HERPETOLOGICA-D-14-00032

Kimura M (1980) A simple method for estimating evolutionary rate of base substitutions through comparative studies of nucleotide sequences. Journal of Molecular Evolution 16: 111–120. https://doi.org/10.1007/BF01731581

Köhler J, Jansen M, Rodriguez A, Kok PJR, Toledo LP, Emmrich M, Glaw F, Haddad CFB, Rödel MO, Vences M (2017) The use of bioacoustics in anuran taxonomy: theory, terminology, methods and recommendations for best practice. Zootaxa 4251(1): 1–124. https://doi.org/10.11646/zootaxa.4251.1.1

Lavilla EO, Scrocchi GJ (1986) Morfometría larval de los géneros de Telmatobiinae (Anura, Leptodactylidae) de Argentina y Chile. Physis 44: 39–43.

Lescure J, Marty C (2000) Atlas des Amphibiens de Guyane. Collections Patrimoines Naturels. Paris 45: 1–388.

Lima LP, Bastos RP, Giaretta AA (2004) A new *Scinax* Wagler, 1830 of the *S. rostratus* group from Central Brazil (Amphibia, Anura, Hylidae). Arquivos do Museu Nacional 62: 505–512.

Lutz B (1973) Brazilian species of *Hyla*. University of Texas Press, Austin, 260 pp.

Machado DC, Machado RA, Paiva D, Moravec J (2015) First record of *Scinax iquitorum* Moravec, Tuanama, Pérez-Peña & Lehr, 2009, from Brazil. Herpetozoa 27: 189–190.

Maldonado FD, Keizer EWH, Graça PMLA, Fearnside PM, Vitel CS (2012) Previsão temporal da distribuição espacial do desmatamento no interflúvio Purus-Madeira até o ano 2050. In: Sousa-Junior WC, Waichman AV, Sinisgalli PAA, Angelis CF, Romeiro AR (Eds) Rio Purus: Água, Território e Sociedade na Amazônia Sul-Ocidental. LibriMundi Press, Quito, 183–196.

Melo-Sampaio PR, Souza M (2015) New and noteworthy distributional records of treefrogs (Anura) from southwestern Amazonia. Check List 11: 1–7. https://doi.org/10.15560/11.4.1681

Moravec J, Tuanama IA, Pérez-Peña PE, Lehr E (2009) A new species of *Scinax* (Anura: Hylidae) from the area of Iquitos, Amazonian Peru. South American Journal of Herpetology 4: 9–16. https://doi.org/10.2994/057.004.0102

Myers CW, Duellman WE (1982) A new species of *Hyla* from Cerro Colorado, and other tree frog records and geographical notes from Western Panama. American Museum Novitates 2752: 1–32.

Napoli MF (2005) A new species of allied to *Hyla circumdata* (Anura: Hylidae) from Serra da Mantiqueira, southeastern Brazil. Herpetologica 61: 63–69. https://doi.org/10.1655/03-41

Pombal JP, Gordo M (1991) Duas novas espécies de *Hyla* da floresta atlântica no estado de São Paulo (Amphibia, Anura). Memórias do Instituto Butantan 53(1): 135–144.

Pyburn WF, Fouquette MJ (1971) A new striped treefrog from Central Colombia. Journal of Herpetology 5: 97–101. https://doi.org/10.2307/1562731

Pyburn WF (1973) A new hylid frog from the Llanos of Colombia. Journal of Herpetology 7: 297–301. https://doi.org/10.2307/1563014

Pyburn WF (1992) A new tree frog of the genus *Scinax* from the Vaupes River of northwestern Brazil. The Texas Journal of Science 44: 405–411.

Pyburn WF (1993) A new species of dimorphic tree frog, genus *Hyla* (Amphibia: Anura: Hylidae), from the Vaupés River of Colombia. Proceedings of the Biological Society of Washington 106: 46–50.

Savage JM, Heyer WR (1967) Variation and distribution in the tree-frog genus *Phyllomedusa* in Costa Rica, Central America. Beiträge zur Neotropischen Fauna 5: 111–131. https://doi.org/10.1080/01650526709360400

Schulze A, Jansen M, Köhler G (2015) Tadpole diversity of Bolivia's lowland anuran communities: molecular identification, morphological characterization, and ecological assignment. Zootaxa 4016: 1–111. https://doi.org/10.11646/zootaxa.4016.1.1

Soto-Azat C, Valenzuela-Sánchez A, Collen B, Rowcliffe JM, Veloso A, Cunningham AA (2013) The population decline and extinction of Darwin's Frogs. PLoS ONE 8(6): e66957. https://doi.org/10.1371/journal.pone.0066957

Sturaro MJ, Peloso PLV (2014) A new species of *Scinax* Wagler, 1830 (Anura: Hylidae) from the Middle Amazon River Basin, Brazil. Papéis Avulsos de Zoologia 54: 9–23. https://doi.org/10.1590/0031-1049.2014.54.02

Tamura K, Stecher G, Peterson D, Filipski A, Kumar S (2013) MEGA6: Molecular Evolutionary Genetics Analysis version 6.0. Molecular Biology and Evolution 30: 2725–2729. https://doi.org/10.1093/molbev/mst197

Thompson JD, Higgins DG, Gibson TJ (1994) Clustal W: improving the sensitivity of progressive multiple sequence alignment through sequence weighting, position-specific gap penalties and weight matrix choice. Nucleic Acids Research 22: 4673–4680. https://doi.org/10.1093/nar/22.22.4673

Appendix I

List of specimens examined for morphological comparisons. Abbreviations: AM, state highway, State of Amazonas, Brazil; BR, Federal highway, Brazil; PDBFF, Biological Dynamics of Forest Fragments Project; UHE, Hydroelectric Power Plant.

Scinax sp. 1: BRAZIL: *AMAZONAS*: Tapauá, BR-319, km 450 (INPA-H 34688, INPA-H 34691, INPA-H 34689, INPA-H 34692, INPA-H 34690, INPA-H 34700).

Scinax sp. 2: BRAZIL: *AMAZONAS*: Humaitá, BR-319, km 620 (INPA-H 34651, INPA-H 34657, INPA-H 34664, INPA-H 34666, INPA-H 34667, INPA-H 34668, INPA-H 34669, INPA-H 34670, INPA-H 34671, INPA-H 34672, INPA-H 34673, INPA-H 34674, INPA-H 34675, INPA-H 34676, INPA-H 34677, INPA-H 34678).

Scinax sp. 4: BRAZIL: *AMAZONAS*: Humaitá, BR-319, km 620 (INPA-H 34693).

Scinax sp. 5: BRAZIL: *AMAZONAS*: Tapauá, BR-319, km 450 (INPA-H 34648, INPA-H 34656, INPA-H 34639, INPA-H 34640, INPA-H 34632); Berurí, BR-319, Km 260 (INPA-H 34703, INPA-H 34693, INPA-H 34696); Borba, BR-319, Km 220 (INPA-H 34710).

Scinax sp. 6: BRAZIL: *AMAZONAS*: Careiro da Várzea, BR-319, km 34, Ramal do Purupuru (INPA-H 34597); *RONDÔNIA*: Porto Velho, UHE Santo Antônio (INPA-H 35559, INPA-H 35561, INPA-H 35562, INPA-H 35563, INPA-H 35564, INPA-H 35565, INPA-H 35566, INPA-H 35567, INPA-H 35568).

Scinax sp. 7: BRAZIL: *AMAZONAS*: Careiro da Várzea, BR-319, km 100 (INPA-H 34600, INPA-H 34601, INPA-H 34604, INPA-H 34614, INPA-H 34615, INPA-H 34622, INPA-H 34598, INPA-H 34624, INPA-H 34627, INPA-H 34629), km 168 (INPA-H 34602); Borba, BR-319, km 220 (INPA-H 34610, INPA-H 34620); Beruri, BR-319, km 220 (INPA-H 34608), km 360 (INPA-H 34599, INPA-H 34607, INPA-H 34609, INPA-H 34611, INPA-H 34612, INPA-H 34617, INPA-H 34618, INPA-H 34621, INPA-H 34625, INPA-H 34626, INPA-H 34628, INPA-H 34630); Manicoré, BR-319, km 400 (INPA-H 34603, INPA-H 34606, INPA-H 34616, INPA-H 34623); Tapauá, BR-319, km 450 (INPA-H 34613, INPA-H 34619, INPA-H 34605, INPA-H 34665).

Scinax boesemani: SURINAME: *PARAMARIBO* (*SURINAME*): near Zanderij (RMNH12601, holotype). BRAZIL: *RORAIMA*: Caracaraí, Parque Nacional do Viruá (INPA-H 25972, INPA-H 25974).

Scinax chiquitanus: BRAZIL: *RONDÔNIA*: Porto Velho, UHE Santo Antônio, M-14 (INPA-H 35554, INPA-H 35555, INPA-H 35556, INPA-H 35557, INPA-H 35558, INPA-H 35560).

Scinax cruentommus: ECUADOR: *NAPO*: Santa Cecilia (KU 126587, holotype); *ORELLANA*: Parque Nacional Yasuní (QCAZ 8184), Río Napo (QCAZ 43772, QCAZ 44754). BRAZIL: *AMAZONAS*: Careiro da Várzea, BR-319, km 34, Ramal do Purupuru (INPA-H 34697).

Scinax funereus: ECUADOR: *ORELLANA*: Río Napo, Primavera (QCAZ 43799), Tambococha (QCAZ 55280, QCAZ 55283). PERU: *LORETO*: San Jacinto (KU221960b).

Scinax fuscomarginatus: BRAZIL: *RORAIMA*: Boa Vista, Estação Ecológica de Maracá (INPA-H 34662, INPA-H 34634, INPA-H 34646, INPA-H 34661); Caracaraí, Parque Nacional do Viruá (INPA-H 19371, INPA-H 19372, INPA-H 19376, INPA-H 19378, INPA-H 19383, INPA-H 19384).

Scinax garbei: BRAZIL: *RORAIMA*: Caracaraí, Parque Nacional do Viruá (INPA-H 25964, INPA-H 27496).

Scinax cf. *ictericus*: PERU: *MADRE DE DIOS*: Rio Tambopata (ZFMK 39353, ZFMK 39361, ZFMK 39363, ZFMK 39366).

Scinax iquitorum: PERU: *LORETO*: ca. 17 km straight SW of Iquitos, (NMP6V 71267/1-3; paratypes).

Scinax madeirae: BRAZIL: *RONDÔNIA*: Alta Floresta, Parque Estadual Corumbiaria (INPA-H 7050, INPA-H 7051).

Scinax nebulosus: BRAZIL: *PARÁ*: Alter do Chão (INPA-H 34647, INPA-H 34653); *RONDÔNIA*: Costa Marques, Real Forte Príncipe da Beira (INPA-H 34641); *RORAIMA*: Caracaraí, Parque Nacional do Viruá (INPA-H 27535, INPA-H 27536, INPA-H 27537).

Scinax onca sp. n. (tadpoles): BRAZIL: *AMAZONAS*: Beruri, BR-319, km 350 (lot INPA-H 35411).

Scinax pedromedinae: BOLIVIA: *BENI*: 5 km NE of Riberalta (NMP6V 70700); PERU: *UCAYALI*: Masisea (NMP6V 74902/1–3).

Scinax proboscideus: BRAZIL: *AMAZONAS*: Manaus, Reserva Colosso do PDBFF (INPA-H 10304); Presidente Figueiredo, Vila Pitinga (INPA-H 1870); *PARÁ*: Oriximiná, UHE Cachoeira Porteira, Rio Trombetas (INPA-H 304).

Scinax sateremawe: BRAZIL: *AMAZONAS*: Borba, Ramal Novo Horizonte (INPA-H 34695, INPA-H 34708).

Scinax ruber F: BRAZIL: *AMAZONAS*: Borba, BR-319, km 220 (INPA-H 34642, INPA-H 34652); *RONDÔNIA*: Porto Velho, UHE Santo Antônio, (INPA-H 34633, INPA-H 34635, INPA-H 34649, INPA-H 34655).

Scinax ruber PM: BRAZIL: *AMAZONAS*: Careiro da Várzea, AM-354, km 10 (INPA-H 34645, INPA-H 34654, INPA-H 34658, INPA-H 34659).

CAPÍTULO 5

Genomic landscape analysis reveals the role of ecological gradients on gene flow of an Amazonian frog. Manuscrito em preparação para ***Molecular Ecology***.

Article type: Original Article

Genomic landscape analysis reveals the role of ecological gradients on gene flow of an Amazonian frog

Running title: A genomic test of ecological gradients in Amazonia

Miquéias Ferrão[1,2], Albertina P. Lima[1,3] Anthony S. Ferreira[1,2], Rafael de Fraga[4], Igor L. Kaefer[1,5], Adam Stow[2]

1: Programa de Pós-Graduação em Ecologia, Instituto Nacional de Pesquisas da Amazônia, Manaus, Amazonas, Brazil.
2: Department of Biological Sciences, Macquarie University, Sydney, Australia.
3: Coordenação de Biodiversidade, Instituto Nacional de Pesquisas da Amazônia, Manaus, Amazonas, Brazil.
4: Instituto de Ciências e Tecnologia das Águas, Universidade Federal do Oeste do Pará, Santarém, Pará, Brazil.
5: Instituto de Ciências Biológicas, Universidade Federal do Amazonas, Manaus, Amazonas, Brazil.

82

Abstract

Amazonia has the most species-rich forest of the Neotropics and scientists have attempted to understand the mechanisms driving the diversification of its biota. Among the hypotheses evoked to explain processes promoting species diversification, the ecological gradient hypothesis predicts that divergences between populations reflect environmental changes across the species range, even in the presence of gene flow. Herein, we used a diminutive terrestrial anuran (*Phyzelaphryne miriamae*) widely distributed in the interfluve between the Purus and Madeira rivers as a model to test whether gene flow along the landscape can be explained by the ecological gradient hypothesis. For the first time in Amazonia, genomic landscape analyses and thousands of single nucleotide polymorphisms (SNPs) were used to test this hypothesis. Genetic structure analyses estimated five populations in *P. miriamae*. Results indicated that the effect of environmental gradients on gene flow of this species is pronounced. After accounting the effect of geographic distance, the explanation of environmental variables on gene flow ranged from 24.7 % (silt content) to 30.2% (temperature seasonality). On the other hand, geographic distance between demes also explained gene flow but its effect was less pronounced (2.3–3.7%) and restricted to short and long distances, being null in moderated distances. Overall, the genetic diversification of our model agrees with predictions of the ecological gradient hypothesis. The effects of environmental changes on gene flow were stronger in our species model than in other organisms distributed in the same region. Such pronounced effect is likely related to behavioural and physiological features of *P. miriamae* linked to its small body size, terrestrial reproductive mode and low dispersal ability.

Introduction

Amazonia has the major and most diverse forest of the Neotropical region, being considered a global biodiversity hotspot (Hansen et al., 2013; Antonelli et al., 2018). Evaluating the mechanisms that drive gene flow in organisms across the landscape, preventing or favoring genetic differentiation, is crucial to explain the extraordinarily high biodiversity of Amazonia and has been one of the major issues in evolutionary biology. Since the 19th century, speciation hypotheses have been argued to explain the diversification of Amazonian biota (e.g., Wallace, 1852; Haffer, 1969; Endler, 1977; Vanzolini & Williams, 1981; Endler, 1982; Räsänan, Salo, Jungnert, & Pittman, 1990; Bush, 1994).

Among these hypotheses, the riverine barrier (Wallace, 1852) has been extensively tested along more than two decades (e.g., Gascon, Lougheed, & Bogart, 1996; Lougheed, Gascon, Jones, Bogart, & Boag, 1999; Gascon et al., 2000; Funk et al., 2007; Fernandes, Wink, Sardelli, & Aleixo, 2012; Fouquet, Ledoux, Dubut, Noonan, & Scotti, 2012a; Ribas, Aleixo, Nogueira, Miyaki, & Cracraft, 2012; Kaefer, Tsuji-Nishikido, Mota, Farias, & Lima, 2013; Alfaro et al., 2015; Fouquet et al., 2015; Ferreira, Aleixo, Ribas, & Santos, 2017; Maia, Lima, & Kaefer, 2017; Nazareno, Dick, & Lohmann, 2017; Ortiz, Lima, & Werneck, 2018; Ribas et al., 2018). This hypothesis postulates that large Amazonian rivers promote allopatric isolation by suppressing gene flow between populations inhabiting different river margins (Wallace, 1852). Differently to the former, the ecological gradients hypothesis (Endler 1977, 1982) does not require allopatric isolation by physical barriers to generate genetic divergence. Instead, it predicts that populations differentiate, even in the presence of gene flow, as result of adaptive divergence induced by environmental gradients, such as changes in temperature, precipitation, soil moisture, and forest structure. Supporting or not this hypothesis depends on the significant correlation between gene flow among populations and ecological differences along the species range after accounting for the effects of geographic distance (Funk et al., 2007). Despite its plausibility to explain genetic divergence within species across heterogeneous landscapes, the ecological gradient hypothesis has been poorly explored in Amazonia (Moritz, Patton, Schneider, & Smith, 2000; Leite & Rogers, 2013).

Difficulties to test the ecological gradient hypothesis could arise because of different factors. The existence of present or past physical barriers (e.g. rivers, mountains, structural arches) within the range of the target species would generate dissimilarities that are larger than predicted and led to misinterpretations. Taking it into account, species distributed along intervening landscapes between large rivers in lowland forests may represent a formidable study system to evaluate the role of environment gradients on gene flow of Amazonian organisms. Another important concern in evaluating the ecological gradient hypothesis is the heterogeneity of a given landscape since genetic differentiation is not expected as result of homogeneous habitats but other mechanisms, such as isolation by distance (Wright, 1943).

Although its complex geological history (Hoorn et al., 2010; Hayakawa & Rossetti, 2015; Ruokolainen, Moulatlet, Zuquim, Hoorn , & Tuomisto, 2018), the Madeira River has been reported as a barrier to gene flow in many organisms (Ribas, Aleixo, Nogueira, Miyaki, & Cracraft, 2012; Kaefer, Tsuji-Nishikido, Mota, Farias, & Lima, 2013; Fernandes, Cohn-Haft, Hrbek, & Farias, 2014; Thom & Aleixo, 2015; Ribas et al., 2018), and restricting the sampling design of studies to just one shore would avoid biases related to river effect on genetic differentiation. In fine-scale, the landscape of northern Purus-Madeira Interfluve (PMI) is characterized by lowland dense forests, silty soils, shorter dry period and less seasonal temperature (Cintra et al., 2013; Martins et al., 2015; Schietti et al., 2016; Ferreira, Jehle, Stow, & Lima, 2018). Southward it changes to lowland open forests, clay soils, longer dry periods and more seasonal temperature (Cintra et al., 2013; Martins et al., 2015; Schietti et al., 2016; Ferreira, Jehle, Stow, & Lima, 2018). All these features turn the PMI a suitable landscape scenario to test the ecological gradient hypothesis.

Other important consideration when testing the ecological gradient hypothesis lies in the choice of the target organism. Anuran amphibians have permeable skin (Ludwig, 1945), eggs and tadpoles susceptible to dehydration (Rudin-Bitterli, Evans, & Mitchell, 2018; Rudin-Bitterli, Mitchell, & Evans, 2018), and usually low vagility (Blaustein, Wake, & Sousa, 1994). Changes on soil moisture and temperature can directly influence the anuran bacterial skin communities (Varela, Lesbarrères, Ibáñez, & Green, 2018), which are a crucial component of the immune system (Kueneman et al., 2016), affecting the susceptibility of species to disease and survival. Additionally, variation in dry periods may negatively affect anurans by maximizing the cutaneous evaporative water loss (Mitchell & Bergman, 2016). Physiological features make anurans advantageous subjects for investigating the role of environmental gradients on genetic differentiation across landscapes.

In this study, we use the miniaturized Amazonian frog *Phyzelaphryne miriamae* Heyer, 1977 to test the ecological gradient hypothesis. This species inhabits the litter of non-flooded lowland forest along the PMI and has direct development of terrestrial eggs. These traits may turn both adults and eggs susceptible to changes in environmental variables directly or indirectly related to temperature and humidity of their habitat. Herein, we sequenced thousands of single nucleotide polymorphisms (SNPs) and applied genomic landscape approaches to evaluate the effect of environmental variables on gene flow of *P. miriamae* along ~900 km of heterogeneous forests. The main prediction of our hypothesis is that the environmental variables should better explain gene flow than geographic distance.

MATERIAL AND METHODS

Study system and sampling

Phyzelaphryne miriamae is a small (~15 mm), leaf-litter, and crepuscular frog occurring south of the Amazon River. This is the sole species in the genus *Phyzelaphryne* and prior to this study was known only from few localities (Fouquet et al., 2012). Males are territorial and call on large decomposing trunks or inside of heaps of leaf-litter in twilight (MF and APL personal communication). Females oviposit between humid leaf-litter and eggs do not develop into aquatic free-living tadpoles but directly into froglets (MF and APL personal communication).

The PMI is located south of the Amazon River and covers approximately 15.4 million hectares. The hydrography is characterized by a network of small streams that drain mainly into Madeira River (Maldonado, Keizer, Graça, Fearnside, & Vitel, 2012). The PMI has a recent geological origin with unstable sediments from Late Pleistocene or Early Holocene, with flat topography in regional scale, ranging from 27 to 80 m above sea level (Sombroek, 2000). Soils are Plinthosols and Gleysols (Martins et al., 2013) with predominance of silt in the north and clay in the south (Ferreira, Jehle, Stow, & Lima, 2018). The mean annual precipitation varies from 1900 to 2700 mm with rainfall concentrated in the middle portion of the interfluve. The northern portion of the PMI is characterized by dense lowland rainforest with approximately 8000 stems by ha (Schietti et al., 2016; Ferreira, Jehle, Stow, & Lima, 2018), while open lowland rainforests (~ 4000 stems by ha; Ferreira, Jehle, Stow, & Lima, 2018) cover the southern portion. These forests are separated by patches of Savanna and ecotonal environments (Rosseti et al., 2018).

We sampled *P. miriamae* in 15 RAPELD modules (Magnusson et al., 2013) distributed across approximately 900 km in the PMI. RAPELD modules have two parallel trails (equidistant 1 km) and each trail has five plots distant 1 km from each other. RAPELD modules were sampled three times in the rainy season (October–March) from 2011 to 2014. Searching was carried out during twilight and used both acoustic and visual cues to locate individuals. In addition to specimens collected in RAPELD modules, *P. miriamae* were sampled at its type locality (Humaitá, Amazonas, Brazil) in November 2016. Tissue samples were collected, and specimens were deposited in the herpetological section of the zoological collection of the Instituto Nacional de Pesquisas da Amazonia (Manaus, Brazil). Fifty-nine specimens were collected in 14 RAPELD modules and four additional specimens were collected in the type locality. Specimens were not found in RAPELD module M4.

SNP discovery and filtering

Tissue samples from 63 *P. miriamae* were sent to Diversity Arrays Technology Pty. Ltd (Canberra, Australia) for DNA extraction, and SNP discovering and genotyping. SNP discovering and genotype followed the DArTSeq^{TM} protocol that combine Diversity Arrays markers (Jaccoud, Peng, Feinstein, & Kilian, 2001; Kilian et al., 2012) and next-generation sequencing on Illumina platforms (Sansaloni et al., 2011) to genotype thousands of SNPs across the genome of a target species. SNPs were discovered and genotyped using the reference genome from *Nanorana parkeri* (Sun et al., 2015). Diversity Arrays Technology genotyped 18,863 SNPs.

SNPs were filtered through the R package *radiator* 0.0.10 (Gosselin, 2017). We ran *radiator* in the interactive mode, which allows the user to inspect tables and graphs before selecting values for each parameter. We excluded monomorphic loci and retained only loci common in all samples. We also excluded loci with reproducibility < 90%, call rate < 60%, read depth < 8, and minor allele frequencies (MAF) < 2%. Only one SNP per locus was retained to avoid bias caused by physical linkage (Morin, Martien, & Taylor, 2009). The filtering process excluded two specimens and resulted in a dataset of 5462 SNPs. We used the packages *radiator*, *LEA* v.1.8.1 (Frichot & François, 2015) and *adegenet* (Jombart, 2008; Jombart & Ahmed, 2011) to convert the filtered data set into the genotype code required by downstream analyses.

Exploratory analysis of genetic differentiation retrieved extremely high values of F_{ST} between samples from M1–M3 and those from M5–M15 (e.g. $F_{ST} = 0.846$ between M3 and M5), while relatively low F_{ST} was recovered between samples within M1–M3, and within M5–M15 (see Supplemental Material S1). Additionally, a species tree using the entire SNP dataset retrieved the clade composed by samples from M1–M3 as deeply divergent in relation to those clades representing samples from M5–M15 (See Supplemental Material S1). To avoid biases associated to inclusion of historical effects in the ecological analyses and results, we excluded samples from M1–M3 in the original dataset (18863 SNPs) and refiltered it following the same methods as previously cited. The refiltered dataset consisted of 47 specimens and 4,459 SNPs that were considered in the following analyses.

SNPs potentially under selection

We used F_{ST} outlier analysis (OA) and environmental association analysis (EAA) to detect putatively adaptive SNPs. The OA method is based on Bayesian modeling implemented in *BaysScan* v.2.1 (Foll & Gaggiotti, 2008), does not assume equal differentiation between populations, and is powerful in detecting outliers in scenarios with low-admixtured samples (Luu, Bazin, & Blum, 2017). *BayeScan* was run using prior odds of 100, sample size of 200,000, thinning interval of 10, 20 pilot runs of length 10,000, and burn-in of 50,000. Outlier SNPs discovered by *BayeScan* were filtered by a *q-value* of 0.01. The EAA method uses latent factor mixed models (LFMM) to test correlations between genetic variation and environmental variables (Frichot, Schoville, Bouchard, & Francois, 2013) and was implemented in the package *LEA*. These correlations were tested by LFMM when estimating latent factors that correct the effect of population structure. SNPs are considered outliers after associations between environmental variables and allelic frequencies are corrected for confounding effects (Frichot & François, 2015). We selected four environmental variables (see above) that would potentially drive differentiation in allele frequencies in frogs. LFMM was run with 10,000 iterations with burn in of 5,000 and 5 repetitions. The K value used to run LFMM was selected through the function *find.clusters* (Jombart, Devillard & Balloux, 2010) as implemented in *adegenet* v.2.1.0 (Jombar & Ahmed, 2011). The α value of False Discovery Rate (FDR) of 0.01 was used in LFMM. We considered putatively adaptive the SNPs identified by *BayeScan* plus SNPs in common among all environmental variables used in LFMM. BayeScan and LFMM identified 14 and 3 putatively adaptive SNPs, respectively. The following analyses were performed only with neutral SNPs data set.

Summary statistics

We tested for significant deviation from Hardy-Weinberg equilibrium (HWE) at each sampling location using the exact test implemented by the package *diveRsity*

(Keenan, McGinnity, Cross, Crozier, & Prodöhl, 2013). The probability that loci deviate from HWE across all sampling locations was calculated by exact tests in the package *pegas* (Paradis, 2010) and *p*-values were corrected by FDR correction (Benjamini & Yekutieli, 2001) using $\alpha = 0.01$ in the package *stats* (R Core Team, 2018). Levels of expected (H_E) and observed (H_O) heterozygosity and their standard error were computed in GenAlEx 6.5 (Peakall & Smouse, 2012). Fixation index (F_{IS}) ($F = 1 - (H_O/H_E)$) and its 95% confidence interval was calculated for each population using 999 bootstraps in package *diveRsity*. We calculated pairwise genetic differentiation (F_{ST}) following Weir & Cockerham (1984) in Arlequin 3.5.2 (Excoffier & Lischer, 2010) and the significance level ($\alpha = 0.05$) was calculated using 1000 permutations. We performed an analysis of molecular variance (AMOVA) using 1000 permutations to calculate the level of genetic variation between populations, between samples within population and within samples as implemented in package *poppr* (Kamvar, Brooks, & Grünwald, 2014). The alpha values for the three levels of genetic variation was obtained via Monte Carlo permutations testing (1000 random permutations) implemented in package *ade4* (Dry & Dufour, 2007).

A single specimen was collected at M11 and M15, and we included these two samples in the nearby sampling module (M12 and M14, respectively) for population analyses. Sampling site M11 is far ~20 km from M12 and M15 is far ~15 km from M14. Clustering analyses showed that these two samples were grouped within these respective clusters, indicating that this act would not impact the results of population analyses.

Accessing genetic structure

DAPC (Jombart, Devillard, & Balloux, 2010) and sNMF (Frichot, Mathieu, Trouillon, Bouchard, & François, 2014) were used to infer the best-fit number of ancestral populations. DAPC is a multivariate method that performs discriminant analysis (DA) to group individuals based on largest between-group variance and smallest within-group variance. Given that DA requires number of alleles to be smaller than the number of individuals (Jombart, Pontier, & Dufour, 2009), DAPC firstly performs a principal component analysis to reduce the dataset into a small number of synthetic variables. DAPC was ran as implemented in the package *adegenet* using the first 5 principal components (PC) and k = 5. We set the number of PCs used in DAPC trough function *xvalDapc* and *K* was set by *find.clusters* function using 46 PCs.

sNMF implements sparse non-negative matrix factorization and least-square optimization algorithms to estimate ancestry coefficients of large genomic datasets (Frichot, Mathieu, Trouillon, Bouchard, & François, 2014). sNMF estimates both homozygote and heterozygote frequencies and avoids Hardy–Weinberg and linkage equilibrium assumptions (Frichot, Mathieu, Trouillon, Bouchard, & François, 2014). The k values (2–10) were tested with 10 replicates for each value of k and 10000 interactions. The best-supported k and the best run were selected by estimation of the lowest error value of ancestry through cross-entropy criterion. sNMF was performed in the R package LEA.

Isolation by distance

Isolation by distance (IBD) is commonly recovered to explain spatially limited gene flow in natural populations. Two complementary tests were carried out to evaluate the effect of geographic distance on genetic differentiation of *P. miriamae*. As recommended by Rousset (1997), pairwise Fst was linearized using the formula Fst/(1-

Fst) and geographic distances (km) were log-transformed using natural base (~2.718). Firstly, we performed a global simple Mantel test (Mantel, 1967) correlating the Fst/(1-Fst) matrix against the pairwise log-transformed geographic distance matrix. Mantel test was conducted using the function *mantel* as implemented by Legendre & Legendre (2012) in the package *vegan* 2.5.1 (Oksanen et al., 2018) and the statistical significance was obtained by 1000 permutations. To assess the correlation of Fst/(1-Fst) and log(geographic distance) along classes of distances, we carried out a Mantel correlogram (Sokal, 1986; Oden & Sokal, 1986). The Mantel correlogram was computed through 10000 permutations using the function *mantel.correlog* in *vegan*. Classes of geographic distances were selected by Sturges' equation (Sturges, 1926). Correlation used to perform *mantel* and *mantel.correlog* functions were Pearson, and significance levels for both tests were assumed when $\alpha < 0.05$. *P* values of Mantel correlogram were corrected through FDR.

The log(geographic distance) matrix was highly correlated with all environmental resistance matrices used in this study (Pearson correlation higher than 0.80 in all cases). As results from Mantel and Partial Mantel using log(geographic distance) alone may be biased by indirect effect from environmental variables, we alternatively ran distance-based Redundancy Analyses — dbRDA (Legendre & Anderson, 1999) to compute the effect of geographic distance conditioned by environmental variables. dbRDA analyses were computed separately for each environmental variable because all variables were highly correlated among them (Pearson correlation higher than 0.80 in all cases). The significance of geographical dbRDAs were assessed through an ANOVA-like permutation test using 1000 permutations as implemented in *vegan*.

Isolation by resistance

Isolation by resistance (IBR) was estimated using an approach similar to Dudaniec et al. (2013) and Dudaniec et al. (2016). Differently from these studies, models of resistance surface were constructed and evaluated separately for each environmental variable due to high values of correlation among them, rather than included in the same models. First, values in the original raster of each environmental variable were converted to range from 1 to 100 to facilitate posterior comparisons. A series of raster representing different models of resistance surfaces were developed separately for each of the four environmental variables (described below) as follows:

$$r_i = 1 + \alpha\left(\frac{F_i - 1}{99}\right)^{\gamma}$$

where r is the resistance of the raster cell i; α is the parameter that determines the maximum possible resistance value; F_i is the value of the cell i ($1 \leq F_i \geq 100$); the exponent γ determines the shape of the relation between the environmental variable and resistance being linear when $\gamma = 1$ and non-linear when $\gamma \neq 1$ (Fig. 1). This model assumes that resistance increases as environmental variable increases. Five different values of α (0,5,10,100,1000) and seven values of γ (0.01,0.1,0.5,1,5,10,100) were used. The combination of values of α and γ resulted in 35 raster files representing different models of resistance surfaces. Raster models were created in R using the packages *sp* 1.2.5 (Bivand, Pebesma, & Gomez-Rubio, 2013), *rgdal* 1.2.16 (Bivand, Keitt, & Rowlingson, 2017), *raster* 2.6.7 (Hijmans, 2017), *DT* 0.2 (Xie, 2016) and *dbplyr* 1.1.0 (Wickham, 2017). Resistance values between localities in each raster model were calculated using *circuitscape* 4.0.5 (McRae, Shah, & Mohapatra, 2013).

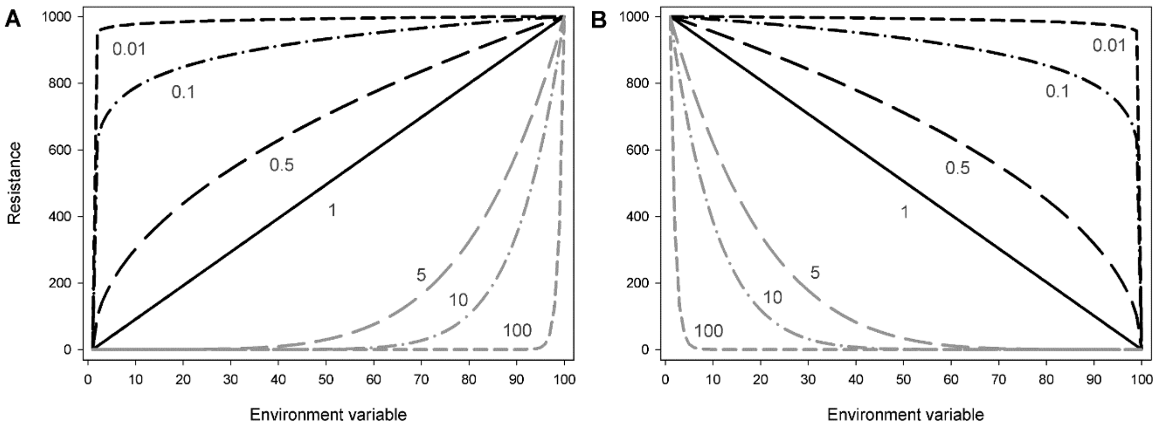

Figure 1. Hypothetical representation of slopes of isolation by resistance (IBR) hypotheses tested for the effect of environmental variables on Fst/(1-Fst) using seven values of γ (0.01, 0.1, 0.5, 1, 5, 10, 100) and α = 1000. Relationships between resistance and environmental variables for which high values were interpreted as restrictive (A) or permissive to gene flow (B). Numbers close to lines represent γ values. Remaining α values (0.5, 10, 100) were not shown to simplify visualization.

Many methods have been used to evaluate resistance distances against genetic distance: correlation between distances based on Mantel test (Mantel, 1967), regression on distance matrices (Legendre, Lapointe & Casgrain, 1994), linear mixed effects models, and Procrustes rotation test (Gower, 1975). In a recent comparison of methods for model selection, Shirk, Landguth, & Cushman (2017) showed that linear mixed effects model is the most accurate method among the seven methods evaluated by them, including those cited above. Herein, a maximum likelihood population effects (MLPE) mixed effects model (Clarke, Rothery, & Raybould, 2002) was fit for each combination of α and γ using pairwise resistance distance, Fst/(1-Fst) and population as independent, dependent and random variable, respectively. MLPE mixed effect models were performed through *ResistanceGA* 4.0.2 (Peterman, 2018) and *lme4* 1.1.16 (Bates, Mächler, Bolker, & Walker, 2015) using the function *mlpe_rga*. The robustness of MLPE mixed effect models for each environmental variable were accessed through 1000 pseudo bootstrap replications using the function *Resist_boot* of the *ResistanceGA* package. *Resist_boot* sampled 85% of the samples in each bootstrap iteration and used Akaike Information Criteria corrected for small sample size (AICc) to rank models. Despite AIC calculated from MLPE mixed effect models may represent unreliable scores (Clarke, Rothery, & Raybould, 2002), models were computed setting REML=FALSE in the function *mlpe_rga*, allowing the calculation of valid AIC scores.

Based on the biology of the target species (e.g. low vagility and territoriality) and on the geographic distribution of sampled populations, separating the effect of geographic distance while correlating landscape resistance and gene flow is an important matter. We performed distance-based Redundancy Analysis (dbRDA: Legendre & Anderson, 1999) to quantify the correlation between the best MLPE model for each environmental variable and Fst/(1-Fst) while controlling the effect of geographic distance. dbRDA was used instead the widely used partial Mantel test because the former analysis seems to be more accurate for species continuously distributed along the landscape and its type II error rates are lower than those of partial Mantel test (Kierepka & Latch, 2015). dbRDA analyses were performed in *vegan* 2.5.1. using Fst/(1-Fst) as response, resistance distance as predictor and log(geographic distance) as condition. The significance of dbRDAs were assessed through an ANOVA-like permutation test using 1000 permutations also performed in *vegan*.

Environmental variables

Distribution of Amazonian anurans have been correlated with environmental variables like forest structure, soil texture, physical-chemical properties of soil, distance of stream, and temperature (Menin, Lima, Magnusson, & Waldez, 2007; Menin, Waldez, & Lima, 2011; Landeiro, Waldez, & Menin, 2014; Jorge, Simões, Magnusson, & Lima, 2016; Ferrão, Fraga, Moravec, Kaefer, & Lima, 2018; Ferreira, Jehle, Stow, & Lima, 2018). Some of these environmental variables may facilitate or impede gene flow. In the present study, four environmental variables were used to detect putatively adaptive SNPs and to estimate the role of environmental gradients on gene flow: temperature seasonality, intensity and duration of dry period, soil structure, and forest structure. (1) The seasonality of temperature has direct effect on immunological system of amphibians (Raffel, Rohr, Kiesecker, & Hudson, 2006) and seasonal environmental can negatively affect the susceptibility of species to disease (and survival). Hence, environments with reasonably stable temperature are expected to facilitate gene flow. (2) Environments with intense and long dry periods — represented herein by the Walsh index (Walsh, 1996) — may affect negatively the suitability of amphibians by maximizing the cutaneous evaporative water loss (Mitchell & Bergman, 2016). As the target species does not inhabit riparian areas that potentially facilitate rehydration during dry periods, environments with shorter and less intense dry periods may be more favorable to occupancy and may favor gene flow. (3) Soil moisture is represented by the silt content. Silty soils are structurally instable, and it increases water retention (Juo & Franzluebbers, 2003), keeping the air close to soil surface and the leaf-litter moister than sandy or clay soils. Eggs of *Phyzelaphryne miriamae* are deposited between the leaf-litter close to soil surface and require favorable moisture conditions to avoid dehydration, due to that silty soils are expected to favor the viability and development of eggs into froglets, facilitating gene flow. (4) We used aboveground live woody biomass density (vegetation biomass hereafter) as proxy of forest structure. The PMI is covered meanly by dense and open lowland rainforest. The leaf area index is known to affect directly the forest’s microclimate (Hardwick et al., 2015). Less dense canopy forests in the tropics (e.g., open lowland rainforest) have lower values of leaf area index that increase the temperature and moisture immediately above the soil due to high values of light and wind incidence (Hardwick et al., 2015). Accordingly, open lowland forests in the southern study area would difficult gene flow by representing less favorable habitat for adults and eggs of the target species.

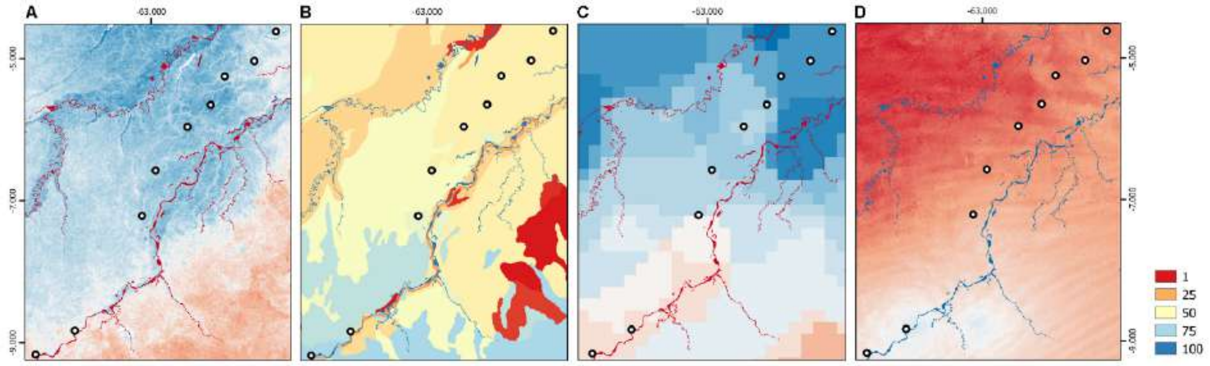

Figure 2. Variables used to test the effect of environmental gradients on gene flow of *P. miriamae* within the interfluve between Purus and Madeira rivers. (A) Silt content. (B) Vegetation biomass. (C) Walsh Index. (D) Temperature seasonality. Black circles: RAPELD sampling sites.

We obtained temperature seasonality (BIO4) of the period 1950–2000 from WorldClim database (Hijmans, Cameron, Parra, Jones, & Jarvis, 2005). Intensity and duration of dry period (Walsh Index) was calculated using monthly precipitation data (WorldClim) and obtained from AMBDATA database (Amaral, Costa, Arasato, Ximenes, & Rennó, 2013). Silt content at 15 cm depth was obtained from SoilGrids database (Hengl et al., 2017) and vegetation biomass (Baccini et al., 2012) was accessed from The Carbon Source database. All raster files were interpolated to 30 arc-sec (~1 km^2) and cropped to the study area using the package *raster*.

Based on the behavior and biology of the target species, large rivers as Purus and Madeira may represent strong physical barriers to migration and gene flow. The absence of the Purus and Madeira rivers in raster files during calculation of resistance distances in *circuitscape* may bias results by considering the pathway the one crossing the river. Due to that, rivers were merged to raster files of all variables before constructions of models combining α and γ to hedge the circuit analysis mainly within PMI. Values assigned to rivers were always higher than the less suitable values to gene flow according to each environmental variable.

RESULTS

Genetic diversity

None of populations deviated from Hardy-Weinberg equilibrium. Approximately 38% of the 4442 putatively neutral SNPs deviated significantly ($p \leq 0.01$) from the HWE of which 1171 SNPs (~ 26%) remained significant after FDR correction. Observed and expected heterozygosity were low in all sampling sites, with H_o ranging from 0.026 ± 0.002 to 0.065 ± 0.002, and H_e ranging from 0.025 ± 0.001 to 0.081 ± 0.002 (Table 1). Expected heterozygosity was lower than H_o in the sampling site M13 ($F_{IS} = -0.0237$). The M06, M10 and M11 showed a positive F_{IS} but the confidence interval encompassed zero (Table 1). F_{IS} Confidence intervals of M03 did not overlap with the intervals of M13 and the highest F_{IS} was estimated for the M11.

Table 1. Genetic diversity indices for all sampling sites. CI, confidence interval; H_e, expected heterozygosity; H_o, observed heterozygosity; F_{is}, fixation index $1-(H_o/H_e)$; N, number of samples; SE, standard error.

	N	H_o ± SE	H_e ± SE	F_{is}	Lower CI	Higher CI
M5	4	0.059 ± 0.003	0.068 ± 0.002	0.1327	0.0776	0.2422
M6	3	0.058 ± 0.003	0.061 ± 0.002	0.0581	-0.0642	0.4464
M7	7	0.065 ± 0.002	0.081 ± 0.002	0.1900	0.0890	0.2473
M8	5	0.064 ± 0.002	0.078 ± 0.002	0.1825	0.0694	0.2767
M9	7	0.065 ± 0.002	0.080 ± 0.002	0.1875	0.0727	0.2532
M10	5	0.065 ± 0.002	0.077 ± 0.002	0.1503	-0.0345	0.2528
HUM	5	0.045 ± 0.002	0.058 ± 0.002	0.2229	-0.0126	0.3861
M12	7	0.044 ± 0.002	0.049 ± 0.002	0.1086	0.0018	0.1738
M13	5	0.026 ± 0.002	0.025 ± 0.001	-0.0237	-0.2125	0.0815

Overall genetic differentiation measured as Fst was high (mean ~0.48), ranging from 0.13 (M6 vs. M7) to 0.80 (M5 vs. M13) (Table 2). The lowest Fst between neighbour sampling sites (less than 100 km) was recovered between M6 and M7 (0.13), while the highest Fst was recovered between M5 and M6 (0.46). Fst was significantly different from zero for each pair of localities (Table 2). Analysis of molecular variance (AMOVA) using sampling site as higher level indicated that 51% of variance was accounted between sampling sites, while 9% was accounted within sampling sites and 40% was accounted between individuals. The higher variance in AMOVA using environmental classes was accounted between classes (44%), followed by variance within samples (35%) and within environmental classes (21%). Statistical significance recovered by permutation tests on both AMOVAs were lower than 0.001.

Table 2. Pairwise genetic differentiation (F_{ST}) across sampling sites (lower diagonal) computed following Weir & Cockerham (1984) and its respective *p*-values (upper diagonal) based on 1000 permutations. Asterisks represent *p* values < 0.01.

	M5	M6	M7	M8	M9	M10	HUM	M12	M13
M5	-	0.03	*	0.01	*	0.03	*	*	*
M6	0.46	-	*	0.02	*	0.03	0.02	*	0.02
M7	0.43	0.13	-	*	*	*	*	*	*
M8	0.49	0.27	0.21	-	*	*	*	*	*
M9	0.53	0.34	0.28	0.14	-	*	*	*	*
M10	0.56	0.40	0.35	0.25	0.19	-	*	*	*
HUM	0.64	0.51	0.45	0.38	0.35	0.22	-	*	*
M12	0.74	0.69	0.64	0.61	0.58	0.54	0.59	-	*
M13	0.80	0.78	0.70	0.69	0.66	0.65	0.69	0.31	-

Genetic structure

The best-fit number of ancestral populations estimated by sNMF was highly concordant with DAPC and both approaches supported five ancestral populations (k = 5). sNMF uncovered high levels of admixture in individuals from sampling sites M08 and M10. However, individuals within the same sampling sites showed similar levels of admixture (Fig. 1). Globally, DAPC recovered high values of posterior membership probabilities for all individuals, except by one individual from sampling site M10 that was attributed to the same population represented by individuals from M6 and M7 (Fig. x).

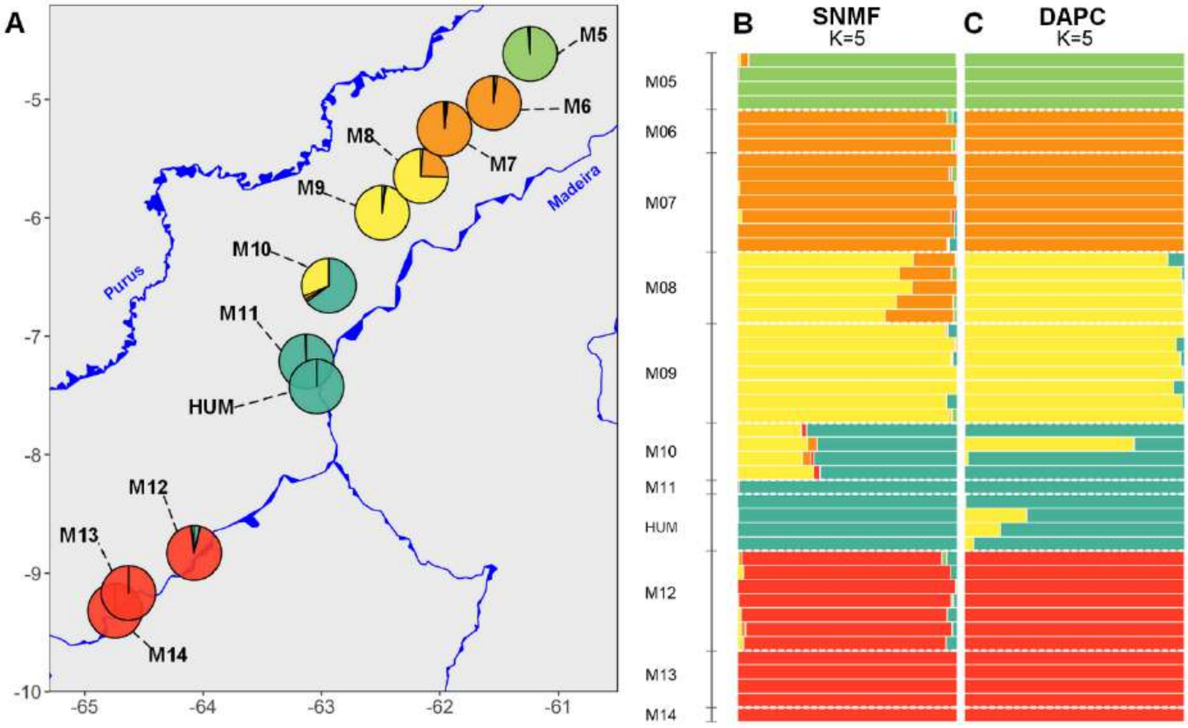

Figure 3. Genetic structure of *Phyzelaphryne miriamae* along the Purus-Madeira Interfluve. (A) Population admixture estimates (k = 5) as recovered by SNMF. (B) Ancestral coefficients of individuals (k = 5) retrieved by SNMF. (C) Posterior membership probabilities of individuals according to DAPC using k = 5.

Isolation by distance

Globally, the pairwise Fst/(1-Fst) in *P. miriamae* increases with larger geographic distances (r = 0.92, p < 0.001) (Fig. 2A). However, the Mantel correlogram using seven classes of geographic distance demonstrated that pairwise Fst/(1-Fst) was spatially autocorrelated within four distance classes (Fig. 2B). Pairwise Fst/(1-Fst) was positively correlated with geographic distances within 60 km (r = 0.34, p = 0.017) and 86 km (r = 0.47, p = 0.004), while negatively correlated within 365 km (r = -0.30, p = 0.05) and 525 km (r = -0.66, p = 0.007). After excluding the effect of temperature seasonality, Walsh Index, and vegetation biomass through dbRDA, the outcome of geographic distance on Fst/(1-Fst) was statistically significant and explained 2.3–3.7%

of gene flow (Table 3). However, the effect of geographic distance was not significant after accounting the effect of silt content ($R^2 < 0.1\%$, $p = 0.71$).

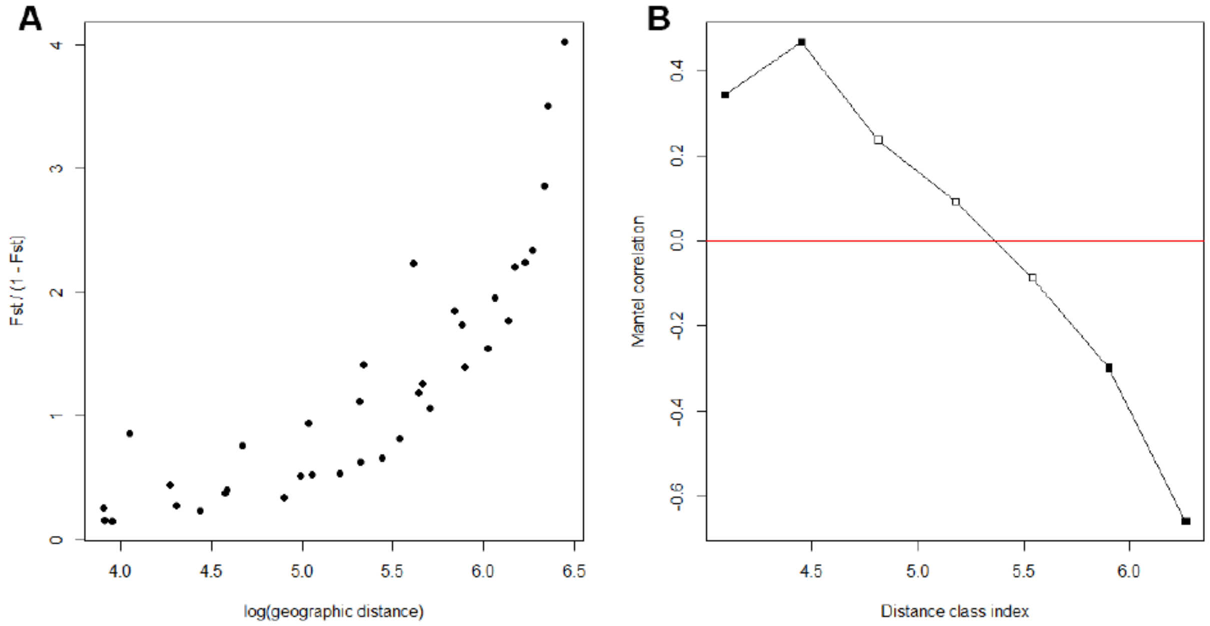

Figure 4. Correlation between Fst/(1-Fst) and log(geographic distance) (**A**) and Mantel correlogram plot depicting the spatial autocorrelation of Fst/(1-Fst) in seven classes of log(geographic distance) (**B**). Filled squares = distance classes with $p \leq 0.05$.

Isolation by resistance

The model with lowest average AICc (11.65) for the effect of silt content on Fst/(1-Fst) in *P. miriamae* was $\alpha = 1000$ and $\gamma = 1$. This model was top-ranked 46.7% of the iterations and explained in average 91.6% of the genetic variation. The Walsh Index explained 91.5% of the variation of Fst/(1-Fst). The best model (average AICc = 10.04) of this environmental variable was $\alpha = 1000$ and $\gamma = 100$ and was top-ranked 48.7% of the time. The top-ranked model (41.1%) explaining the relation between temperature seasonality and Fst/(1-Fst) was $\alpha = 1000$ and $\gamma = 0.1$ (average AICc = 9.35) accounting for 91% of the explanation. Lastly, the best model (average AICc = 10.13) for the effect of forest on Fst/(1-Fst) was $\alpha = 5$ and $\gamma = 0.5$, being top-ranked 35% of the time and explained 91% of the genetic variation. After accounting for the effect of geographic distance through dbRDA analyses, the environmental variable that best explained the genetic variation of *P. miriamae* was temperature seasonality ($R^2 = 0.302$, $p = 0.001$), followed by Walsh Index ($R^2 = 0.295$, $p = 0.001$), vegetation biomass ($R^2 = 0.275$, $p = 0.01$) and silt content ($R^2 = 0.247$, $p = 0.001$).

Table 3. Summary of results of maximum likelihood population effects mixed effects models (MLPE), ecological and geographical distance-based redundancy analyses (dbRDA) depicting the effect of isolation by resistance and distance on gene flow of *P. miriamae* along the Purus-Madeira Interfluve.

Environmental Variable	**MLPE**				**ECO dbRDA**		**GEO dbRDA**	
	α	γ	AICc	r^2	r^2	p	R^2	p
Temperature seasonality	1000	0.1	9.35	0.916	0.302	0.001	0.037	0.001
Walsh Index	1000	100	10.04	0.915	0.295	0.001	0.032	0.001
Vegetation biomass	5	10	10.7	0.918	0.275	0.001	0.023	0.003
Silt content	1000	1	11.65	0.916	0.247	0.001	<0.001	0.716

The *p* values were obtained by analyses of variance (ANOVA) through 1000 permutations.

DISCUSSION

Genetic structure

Genetic clustering analyses in *Phyzelaphryne miriamae* along the PMI revealed high levels of genetic structure at putatively neutral SNPs. Many studies in Amazonia attributed genetic structure of frogs, at least partially, to physical barriers (Fouquet, Ledoux, Dubut, Noonan, & Scotti, 2012; Kaefer, Tsuji-Nishikido, Mota, Farias, & Lima, 2013; Fouquet et al., 2015; Maia, Lima, & Kaefer, 2017; Ortiz, Lima, & Werneck, 2018). However, geographic distribution of genetic clusters in *P. miriamae* cannot be explained by physical barriers due to absence of large rivers or mountains within PMI that match genetic breaks. In this study, five populations in *P. miriamae* distributed along the PMI were recuperated and geographic distribution of populations did not match with abrupt changes in the environment. On the other hand, structure analysis in the large treefrog *Osteocephalus taurinus* recovered three populations occurring in the PMI and genetic breaks coincided well with the ecotonal zone between the open and dense lowland forest (Ortiz, Lima, & Werneck, 2018). Higher levels of genetic structure in *P. miriamae* may be consequence of its life-history features. Small terrestrial anurans with small clutch size and lacking free-living tadpoles are known to be highly structured compared to large arboreal anurans with large clutch size and exotrophic tadpoles in Amazonia (Fouquet, Ledoux, Dubut, Noonan, & Scotti, 2012; Fouquet et al., 2015).

Additionaly, different forest ecotypes explained 73% of the molecular variance of *O. taurinus* within PMI (Ortiz, lima, & Werneck, 2018). In contrast, genetic variation explained by different environmental classes in *P. miriamae* was lower than that explained using sampling sites as factor. It suggests that suddenly environmental changes within PMI are not good proxies of genetic structure and differentiation in *P. miriamae*.

Isolation by distance

Gene flow in *P. miriamae* along landscapes in PMI was affected by geographic distance in our global correlation test. Mantel test detected strong correlation ($r = 0.92$, $p < 0.001$) between genetic differentiation and geographic distance in *P. miriamae*. Using the same test, Funk et al. (2007) recovered moderate ($r = 0.44$) to strong ($r = 0.83$) IBD effect on three populations of the frog *Physalaemus petersi* but no significant effect in a fourth population. Similarly, Mantel correlation (r) varied from 0.40 to 0.55 in the frog *Adenomera andreae* (Fouquet, Ledoux, Dubut, Noonan, & Scotti, 2012). In the frog genus *Allobates*, geographic distance strongly affected gene flow in *A. paleovarzensis* ($r = 0.76$), while moderate ($r = 0.57$) and absence of effect was detected in the *A. nidicola–masniger* complex and *A. tapajos*, respectively (Kaefer, Tsuji-Nishikido, Mota, Farias, & Lima, 2013; Maia, Lima, & Kaefer, 2017). Along the same sampling area in the PMI, gene flow was significantly affected by geographic distance ($r = 0.82$) in *O. taurinus* (Ortiz, Lima, & Werneck, 2018). Although most of these studies have detected IBD, there is no consensus about the role and magnitude of geographic distance on gene flow of Amazonian anurans. Discordances may be consequence of differences in the number and geographic range of sampled localities, habitat configurations, as well as species' dispersal capability and physiology (Jenkins et al., 2010; Paz, Ibáñez, Lips, & Crawford, 2015; van Strien, Holderegger, & van Heck , 2015).

The distribution of our sampling sites along the landscape and the pattern of environmental shift from north to south PMI can bias the detection of IBD. The use of partial tests (e.g. partial Mantel, partial dbRDA) in this scenario would be an alternative approach to detect IBD without competing effects (e.g. IBR). Despite a strong and significant correlation between geographic distance and gene flow in *P. miriamae* demonstrated by Mantel test, this effect decreased substantially ($r^2 = 0.023–0.037$) after removing the effects of environmental resistance through partial dbRDAs. This low IBD effect is supported by Mantel correlogram's results, which showed IBD just on short and very long distances. Recent studies that have also used partial tests to calculate IBD after discounting the effect of environment features in heterogeneous landscapes (Mims, Hauser, Goldberg, & Olden , 2016; Maia, Lima, & Kaefer, 2017). Cushman & Landguth (2010) demonstrated that results of simple correlation tests may be incorrect due to the absence of formal evaluation of competing alternative hypotheses (e.g. environmental features). On the other hand, partial tests are robust in their ability to reject incorrect causal mechanisms and correctly identify the driving process responsible for the observed gene flow across the landscape (Cushman & Landguth, 2010; Shirk, Landguth, & Cushman, 2017).

Isolation by resistance

Our results demonstrated that the ecological gradients are important drivers of genetic differentiation in *P. miriamae*. MLPE models showed strong effect of environmental resistances on gene flow of *P. miriamae*. After removing the effect of IBD through partial dbRDAs, all environmental resistances used to characterize the landscape were statistically significant and explained (r^2) 24.7–30.2% of the variation in gene flow along the PMI. The effect of ecological gradients on genetic differentiation has also been reported through population genetics approach in many organisms, such as invertebrates (Villemey et al., 2016), fishes (Mather, Hanson, Pope, & Riginos, 2018), mammals (Dudaniec et al., 2013; Dudaniec et al., 2016; Ruiz-Lopez et al., 2016), birds (Khimoun et al., 2016), reptiles (Fraga, Lima, Magnusson, Ferrão, & Stow, 2017; Beninde, Feldmeier , Veith, & Hochkirch, 2018; Sánchez-Ramírez et al., 2018), and amphibians (Dudaniec, Spear, Richardson, & Storfer, 2012; Peterman, Connette, Semlitsch, & Eggert , 2014; Burkhart et al., 2017; Ortiz, Lima, & Werneck, 2018). The pronounced effect of ecological gradients on gene flow of *P. miriamae* is similar to those observed in other amphibians. Studying four species of pond-breeding salamanders in North America, Burkhart et al. (2017) showed that genetic differentiation in *Ambystoma annulatum* was best explained by topographic position index ($r^2 = 0.39$) and distance from nearest ravine ($r^2 = 0.54$), while eastness is the best predictor for *Ambystoma opacum* and *Notophthalmus viridescens louisianensis* ($r^2 = 0.30$; in both species) and northness ($r^2 = 0.43$) for *Ambystoma maculatum*. In the Amazonian frog *O. taurinus*, the greatest fraction of genetic variation was observed between forest ecotypes (72.86%) (Ortiz, Lima, & Werneck, 2018).

Temperature seasonality and intensity of dry period (Walsh Index) were the best environmental variables predicting gene flow in *P. miriamae* along the PMI. These variables have a nonlinear relationship with gene flow, explaining 30.2% and 29.5% of its variation, respectively. Landscapes in the PMI with less stable temperature through the year and long dry period prevent gene flow of *P. miriamae*. Extreme environmental conditions are known to difficult suitability in amphibians by acting on their physiology and immunology (Raffel, Rohr, Kiesecker, & Hudson, 2006; Mitchell & Bergman, 2016). Additionally, small amphibians have lower resistances to water loss (Riddell, Apanovitch, Odom, & Sears, 2017). Due to that and the small size of *P. miriamae*, we suggest that long dry periods and strong changes in mean temperature during dry season limit the movement and survival of adults. We do not expect that changes in temperature and intensity of the dry period affect the survival of eggs and froglets because the breeding season of *P. miriamae* coincides with the wet season (more stable temperatures and moisture). This hypothesis is supported by the role of rate water loss in gene flow of adults and juveniles of the salamander *Plethodon albagula* (Peterman, Connette, Semlitsch, & Eggert, 2014). In this species, the rate of water loss predicts genetic differentiation in adults but not in juveniles (Peterman, Connette, Semlitsch, & Eggert, 2014).

Forest structure (vegetation biomass) also explained an important fraction (27.5%) of the gene flow in *P. miriame*. Moreover, the best model showed a nonlinear relationship between vegetation biomass and gene flow, for which high values of vegetation biomass facilitate gene flow between populations. Recently, changes in the structure of forests explained phenotypic differentiation (plumage colour and brightness) in two species of passerine birds (*Gymnopithys salvini* and *Willisornis poecilinotus*) along the PMI (Abreu, Schietti, & Anciães, 2018), and authors argued that more open forests facilitate sexual selection in these species. Differences in forest structure was evoked as the main driver of genetic differentiation in the tree frog. *O. taurinus* across its range in the PMI (Ortiz, Lima, & Werneck, 2018). In our study system, changes in forest structure may drive the gene flow in two different but nonexclusive ways. Firstly, gene flow may be facilitated in denser forests of PMI due to the high production of leaf litter and fallen trees compared to more open forests (Schietti et al., 2016). During field sampling we noted that *P. miriame* seems to prefer habitats with high amount of leaf litter, which are used for reproduction (MF & APL pers. com.). Secondly, the incidence of sunlight and wind is higher in more open forests and result in low moisture, directly affecting the body water balance which may limit movement and survival of adults and egg/embryo survival of *P. miriamae*. The role of forest structure on gene flow in *P. miriamae* is corroborated by ecological studies that correlated the distribution of other terrestrial Amazonian frogs with forest structure (Menin, Lima, Magnusson, & Waldez, 2007; Dias-Terceiro et al., 2014; Ferreira, Jehle, Stow, & Lima, 2018).

Despite the moderate effect of soil structure (silt content) on gene flow of *P. miriamae* compared to other ecological gradients evaluated here, this variable presented a linear correlation and explained 24.7% of the genetic differentiation. In practice, landscapes with silty soils are conductive to gene flow while areas with low percentage of silt are restrictive. High proportion of silt reduces the water drainage capacity of soil (Juo & Franzluebbers ,2003) and has positive effect on moisture of the upper soil layer and leaf litter. As this tiny species inhabits and deposits eggs between dead leaves just above the soil, moisture availability in this layer might affect its survival, reproduction and growth. Such prediction is supported by high rates of hatchling malformations and low rates of embryonic survival in the terrestrial frog *Pseudophryne guentheri* observed in xeric soils against mesic soils (Rudin-Bitterli, Evans, & Mitchell, 2018). In the same study, adults from mesic soils rehydrated faster than those from xeric soils, which was suggested as beneficial to fitness. Moreover, soil structure is correlated with density and composition of terrestrial arthropods in Amazonian forests (Frankling, Magnusson, & Luizão, 2005; Aguiar, Gualberto, & Frankling, 2006; Dambros et al., 2016) and might drive gene flow by enhancing survival and fitness of adults and offspring as result of food resource availability.

Implications for conservation

We revealed high genetic differentiation between populations of *P. miriamae* in the study area. Nevertheless, part of this genetic diversity is threatened by habitat loss and fragmentation as consequence of infrastructure development associated to the reconstruction of the abandoned BR319 highway that intersect the PMI from north to south. A model predicting deforestation as consequence of the reconstruction of this highway revealed that up to 5.4 million hectares of preserved forests will be destroyed until 2050 (Maldonado et al., 2012). The most threatened region according this modelling coincides with the distribution of the three southern populations of *P. miriamae*. Despite the reconstruction of BR319 is delayed due to legal issues, deforestation induced by land speculation already started in the southern PMI, even within conservation units (MF & RF pers. com.). To make it worse, the southern and most differentiated population of *P. miriamae* (M12–M14) is distributed within the impact zone of two giant hydroelectric powerplants and part of the sampled plots in this area is currently submerged. Additionally, intraspecific genetic diversity of other frog species from PMI showed similar geographic pattern of differentiations (Ortiz, Lima, & Werneck, 2018), thus reinforcing the conservation concerns in this part of Amazonia. Unfortunately, intraspecific genetic diversity and evolutionary processes are still not protected by conservation laws in Brazil.

Conclusion

Our results showed that the intraspecific genetic diversity in the terrestrial frog *Phyzelaphryne miriamae* is highly partitioned and geographically structured across its distribution in a wide portion of Amazonia. We found strong evidence for environmental variables predicting gene flow in this species, corroborating the ecological gradient hypothesis. Overall, climatic gradients (seasonal temperature and intensity of dry period) better explained gene flow than edaphic and vegetation variables. Stochastic processes, such as isolation by geographic distance, also drive the evolutionary diversification of our study system but in a less expressive way. Intraspecific genetic diversity of our target species will be threatened by habitat loss and fragmentation if the predicted deforestation becomes real.

ACKNOWLEDGMENTS AND FUNDING INFORMATION

This study was financially supported by Fundação de Amparo à Pesquisa do Estado do Amazonas (FAPEAM) and Brazilian National Council for Scientific and Technological Development (CNPq) through the Program of Support for Excellence Centers (PRONEX) (process number 653/2009), and by Coordenação de Aperfeiçoamento de Pessoal de Nível Superior (CAPES) through Programa de Doutorado-sanduíche no Exterior (PDSE) (process number 88881.131988/2016-01). We thank to Santo Antônio Energia S.A. and Centro de Estudos Integrados da Biodiversidade Amazônica (CENBAM) for logistic support during fieldwork at the Purus-Madeira Interfluve; to Bill Peterman and Rachael Dudaniec for providing and helping with R scripts, and Sonu Yadav and Alex Carey for helping with R scripts; to all members of the Conservation Genetics Lab of Macquarie University for valuable discussion during early stages of this study; to P. Gleeson, Pinduca, Neneco, Rubico, and Joãozinho, for field assistance. MF received PhD scholarship from CAPES and postdoctoral fellowship from CNPq (process 154325/2018-0); AF received PhD scholarship from CNPq. ILK and APL received productivity grants from CNPq.

AUTHOR CONTRIBUTIONS

MF, APL, and AS conceived the study. APL acquired funding for this study. APL, MF, RF, conducted field work. AS, ILK and APL supervised the study. MF conducted bioinformatic analyses and wrote the first draft of this manuscript. MF, APL, RF, ILK, AF, and AS reviewed, edited and approved the final draft of this manuscript.

CONFLICT OF INTEREST

The authors declare there are no competing interests.

DATA ACCESSIBILITY

Raw SNP data (rad file), putatively neutral SNPs (genepop file), raster files of environmental variables, genetic and geographical distance matrices, and R scripts are available at the Dryad Digital Repository (datadryad.org) at the doi:

ORCID

Miquéias Ferrão https://orcid.org/0000-0001-7035-8276

Anthony Ferreira https://orcid.org/0000-0002-3718-8049

Igor L. Kaefer https://orcid.org/0000-0001-6515-0278

Albertina P. Lima https://orcid.org/0000-0003-4586-5633

Adam Stow https://orcid.org/0000-0002-6796-4854

REFERENCES

Abreu, F. H. T., Schietti, J., & Anciães, M. (2018). Spatial and environmental correlates of intraspecific morphological variation in three species of passerine birds from the Purus–Madeira interfluvium, Central Amazonia. *Evolutionary Ecology*, 32, 191–214. doi: 10.1007/s10682-018-9929-4

Aguiar, N. O., Gualberto, T. L., & Franklin, E. (2006). A medium-spatial scale distribution pattern of Pseudoscorpionida (Arachnida) in a gradient of topography (altitude and inclination), soil factors, and litter in a central Amazonia forest reserve, Brazil. *Brazilian Journal of Biology*, 66(3), 791–802. doi: 10.1590/S1519-69842006000500004

Alfaro, J. W. L., Boubli, J. P., Paim, F. P., Ribas, C. C., da Silva, M. N. F., Messias, … Farias, I. P. (2015). Biogeography of squirrel monkeys (genus *Saimiri*): South-central Amazon origin and rapid pan-Amazonian diversification of a lowland primate. *Molecular Phylogenetics and Evolution*, 82: 436–454. doi: 10.1016/j.ympev.2014.09.004

Amaral, S., Costa, C. B., Arasato, L. S., Ximenes, A. C., & Rennó, C. D. (2013). AMBDATA: Variáveis ambientais para Modelos de Distribuição de Espécies (MDEs). Anais do XVI Simpósio Brasileiro de Sensoriamento Remoto (SBSR) 16: 6930–6937.

Antonelli, A., Zizka, A., Carvalho, F. A., Scharn, R., Bacon, C. D., Silvestro, D., & Condamine, F. L. (2018). Amazonia is the primary source of Neotropical biodiversity. *Proceedings of the National Academy of Sciences of the United Sstate of America*, 115(23), 6034–6039. doi: 10.1073/pnas.1713819115

Bates, D., Mächler, M., Bolker, B., & Walker, S. (2015). Fitting Linear Mixed-Effects Models Using lme4. *Journal of Statistical Software*, 67(1), 1–48. doi: 10.18637/jss.v067.i01

Baccini, A., Goetz, S. J., Walker, W. S., Laporte, N. T., Sun, M., Sulla-Menashe, D., … Houghton, R. A. (2012). Estimated carbon dioxide emissions from tropical deforestation improved by carbon-density maps. *Nature Climate Change*, 2, 182–185. doi: 10.1038/NCLIMATE1354

Beninde, J., Feldmeier, S., Veith, M., & Hochkirch, A. (2018). Admixture of hybrid swarms of native and introduced lizards in cities is determined by the cityscape structure and invasion history. *Proceedings of the Royal Society B*, 285(1883), 20180143. doi: 10.1098/rspb.2018.0143

Benjamini, Y., & Yekutieli, D. (2001). The control of the false discovery rate in multiple testing under dependency. *Annals of Statistics*, 29, 1165–1188.

Bivand, R. S., Pebesma, E., & Gomez-Rubio, V. (2013). Applied spatial data analysis with R. Springer.

Bivand, R. S., Keitt, T., & Rowlingson, B. (2017). rgdal: Bindings for the 'Geospatial' Data Abstraction Library. R package version 1.2-16.

Blaustein A. R., Wake, D. B., & Sousa, W. P. (1994). Amphibian declines: judging stability, persistence, and susceptibility of populations to local and global extinctions. *Conservation Biology*, 8(1), 60–71. doi: 10.1046/j.1523-1739.1994.08010060.x

Burkhart, J. J., Peterman, W. E., Brocato, E. R., Romine, K. M., Willis, M. M. S., Ousterhout, B. H., … Eggert, L.S. (2017). The influence of breeding phenology on the genetic structure of four pond-breeding salamanders. *Ecology and Evolution*, 7(13), 4670–4681. doi: 10.1002/ece3.3060

Bush, M. B. (1994). Amazonian speciation: a necessarily complex model. *Journal of Biogeography*, 21, 5–17. doi: 10.2307/2845600

Cintra, B. B. L., Schietti, J., Emillio, T., Martins, D., Moulatlet, G., Souza, P., … Schöngart, J. (2013). Soil physical restrictions and hydrology regulate stand age and wood biomass turnover rates of Purus–Madeira interfluvial wetlands in Amazonia. *Biogeosciences*, 10(11), 7759–7774. doi: 10.5194/bg-10-7759-2013

Clarke, R. T., Rothery, P., & Raybould, A. F. (2002). Confidence limits for regression relationships between distance matrices: Estimating gene flow with distance. *Journal of Agricultural, Biological, and Environmental Statistics*, 7, 361–372. doi: 10.1198/108571102320

Cushman, S. A., & Landguth, E. L. (2010). Spurious correlations and inference in landscape genetics. *Molecular Ecology*, 19(17), 3592–3602. doi: 10.1111/j.1365-294X.2010.04656.x

Dambros, C. S., Morais, J. W., Vasconcellos, A., Souza, J. L., Franklin, E., & Gotelli, N. J. (2016). Association of Ant Predators and Edaphic Conditions with Termite Diversity in an Amazonian Rain Forest. *Biotropica*, 48(2), 237–245. doi: 10.1111/btp.12270

Dias-Terceiro, R. G., Kaefer, I. L., Fraga, R., Araújo, M. C., Simões, P. I., & Lima, A. P. (2015). A Matter of Scale: Historical and Environmental Factors Structure Anuran Assemblages from the Upper Madeira River, Amazonia. *Biotropica*, 47, 259–266. doi: 10.1111/btp.12197

Dudaniec, R. Y., Spear, S. F., Richardson, J. S., & Storfer, A. (2012) Current and historical drivers of landscape genetic structure differ in core and peripheral salamander populations. *PLoS ONE*, 7(5), e36769. doi: 0.1371/journal.pone.0036769

Dudaniec, R. Y., Rhodes, J. R., Worthington Wilmer, J., Lyons, M., Lee, K. E., McAlpine, C. A., & Carrick, F. N. (2013). Using multilevel models to identify drivers of landscape-genetic structure among management areas. *Molecular Ecology*, 22(14), 3752–3765. doi: 10.1111/mec.12359

Dudaniec, R. Y., Worthington Wilmer, J., Hanson, J. O., Warren, M., Bell, S., & Rhodes, J. R. (2016). Dealing with uncertainty in landscape genetic resistance models: a case of three co-occurring marsupials. *Molecular Ecology*, 25(2), 470–486. doi: 10.1111/mec.13482

Dray, S., & Dufour, A. B. (2007). The ade4 package: implementing the duality diagram for ecologists. *Journal of Statistical Software*, 22, 1–20. doi: 10.18637/jss.v022.i04

Endler, J. (1977). Geographic variation, speciation, and clines. Princeton University Press.

Endler, J. (1982). Pleistocene forest refuges: fact or fancy? In *Biological diversification in the Tropics* (pp. 641–657). Columbia University Press, New York, NY, USA.

Excoffier, L., & Lischer, H. E. L. (2010). Arlequin suite ver 3.5: a new series of programs to perform population genetics analyses under Linux and Windows. *Molecular Ecology Resources*, 10(3), 564–567. doi: 10.1111/j.1755-0998.2010.02847.x

Fernandes, A. M., Cohn-Haft, M., Hrbek, T., & Farias, I. P. (2014). Rivers acting as barriers for bird dispersal in the amazon. *Revista Brasileira de Ornitologia*, 22(4), 363–373.

Fernandes, A. M., Wink, M., Sardelli, C. H., & Aleixo, A. (2014). Multiple speciation across the Andes and throughout Amazonia: The case of the spot-backed antbird species complex (*Hylophylax naevius*/*Hylophylax naevioides*). *Journal of Biogeography*, 41(6), 1094–1104. doi: 10.1111/jbi.12277

Ferrão, M., Fraga, R., Moravec, J., Kaefer, I. L., & Lima, A. P. (2018). A new species of Amazonian snouted treefrog (Hylidae: *Scinax*) with description of a novel species-habitat association for an aquatic breeding frog. *PeerJ*, 6, e4321. doi: 10.7717/peerj.4321

Ferreira, M., Aleixo, A., Ribas, C. C., & Santos, M. P. D. (2017). Biogeography of the Neotropical genus *Malacoptila* (Aves: Bucconidae): The influence of the Andean orogeny, Amazonian drainage evolution and palaeoclimate. *Journal of Biogeography*, 44(4), 748–759. Doi: 10.1111/jbi.12888

Ferreira, A. S., Jehle, R., Stow, A. J., & Lima, A. P. (2018). Soil and forest structure predicts large-scale patterns of occurrence and local abundance of a widespread Amazonian frog. *Peerj*, 6, e5424. doi: 10.7717/peerj.5424

Foll, M., & Gaggiotti, O. (2008). A genome-scan method to identify selected loci appropriate for both dominant and codominant markers: a Bayesian perspective. *Genetics*, 180(2), 977–993. doi: 10.1534/genetics.108.092221

Fouquet, A., Ledoux, J. B., Dubut, V., Noonan, B. P., & Scotti, I. (2012) The interplay of dispersal limitation, rivers, and historical events shapes the genetic structure of an Amazonian frog. *Biological Journal of the Linnean Society*, 106(2), 356–373. doi: 10.1111/j.1095-8312.2012.01871.x

Fouquet, A., Loebmann, D., Castroviejo-Fisher, S., Padial, J. M., Orrico, V. G., Lyra, M. L., … Rodrigues, M. T. (2012). From Amazonia to the Atlantic forest: molecular phylogeny of Phyzelaphryninae frogs reveals unexpected diversity and a striking biogeographic pattern emphasizing conservation challenges. *Molecular Phylogenetics and Evolution*, 65(2), 547–561. doi: 10.1016/j.ympev.2012.07.012

Fouquet, A., Courtois, E. A., Baudain, D., Lima, J. D., Souza, S. M., Noonan B. P., & Rodrigues, M. T. (2015). The trans-riverine genetic structure of 28 Amazonian frog species is dependent on life history. *Journal of Tropical Ecology*, 31(4), 361–373. doi: 10.1017/S0266467415000206

Fraga, R., Lima, A. P., Magnusson, W. E., Ferrão, M., & Stow, A. J. (2017). Contrasting patterns of gene flow for Amazonian snakes that actively forage and those that wait in ambush. *Journal of Heredity*, 108(5), 524–534. doi: 10.1093/jhered/esx051

Franklin, E., Magnusson, W. E., & Luizão, F. J. (2005). Relative effects of biotic and abiotic factors on the composition of soil invertebrates communities in an Amazonian savannah. *Applied Soil Ecology*, 29(3), 259–273. doi: 10.1016/j.apsoil.2004.12.004

Frichot, E., Schoville, S. D., Bouchard, G., & Francois, O. (2013). Testing for associations between loci and environmental gradients using latent factor mixed models. *Molecular Biology and Evolution*, 30(7), 1687–1699. doi: 10.1093/molbev/mst063

Frichot, E., Mathieu, F., Trouillon, T., Bouchard, G., & François, O. (2014). Fast and efficient estimation of individual ancestry coefficients. *Genetics*, 196(4), 973–983. doi: 10.1534/genetics.113.160572

Frichot, E., & François, O. (2015). LEA: An R package for landscape and ecological association studies. *Methods in Ecology and Evolution*, 6, 925–929. doi: 10.1111/2041-210X.12382

Funk, W. C., Caldwell, J. P., Peden, C. E., Padial, J. M., De la Riva, I., & Cannatella, D. C. (2007). Tests of biogeographic hypotheses for diversification in the Amazonian forest frog, *Physalaemus petersi*. *Molecular Phylogenetics and Evolution*, 44(2), 825–837. doi: 10.1016/j.ympev.2007.01.012

Gascon, C., Lougheed, S. C., & Bogart, J. P. (1996). Genetic and morphological variation in *Vanzolinius discodactylus*: a test of the river hypothesis of speciation. *Biotropica*, 28, 376–387. doi: 10.2307/2389201

Gascon, C., Malcolm, J. R., Patton, J. L., Silva, M. N. F., Bogart, J. P., Lougheed, S. C., … Boag, P. T. (2000). Riverine barriers and the geographic distribution of Amazonian species. *Proceedings of the National Academy of Sciences of the United States of America*, 97(25), 13673–13677. doi: 10.1073/pnas.230136397

Gosselin, T. (2017). radiator: RADseq Data Exploration, Manipulation and Visualization using R. R package version 0.0.6 https://github.com/thierrygosselin/radiator.

Gower, J. C. (1975). Generalized procrustes analysis. *Psychometrika*, 40(1), 33–51. doi: 10.1007/BF02291478

Haffer, J. (1969). Speciation in Amazonian forest birds. *Science*, 165(3889), 131–137. Doi: 10.1126/science.165.3889.131

Hansen, M. C., Potapov, P. V., Moore, R., Hancher, M., Turubanova, S. A., Tyukavina, A., … Townshend, J. R. G. (2013). High-resolution global maps of 21st-century forest cover change. *Science*, 342(6160), 850-853. doi: 10.1126/science.1244693

Hardwick, S. R., Toumi, R., Pfeifer, M., Turner, E. C., Nilus, R., & Ewers, R. M. (2015). The relationship between leaf area index and microclimate in tropical forest and oil palm plantation: Forest disturbance drives changes in microclimate. *Agricultural and Forest Meteorology*, 201, 187–195. doi: 10.1016/j.agrformet.2014.11.010

Hayakawa, E. H., & Rossetti, D. F. (2015). Late quaternary dynamics in the Madeira river basin, southern Amazonia (Brazil), as revealed by paleomorphological analysis. *Anais da Academia Brasileira de Ciências*, 87(1), 29–49. doi: 10.1590/0001-3765201520130506

Hengl, T., de Jesus, J. M., MacMillan, R. A., Batjes, N. H., Heuvelink, G. B. M., Ribeiro, E., … Gonzales, M. R. (2014). soilGrids1km — Global Soil Information Based on Automated Mapping. PLoS ONE, 9(8), e105992. doi: 10.1371/journal.pone.0105992

Hijmans, R. J. (2017). raster: Geographic Data Analysis and Modeling. R package version 2.6-7.

Hijmans, R. J., Cameron, S. E., Parra, J. L., Jones, P. G., Jarvis, A. (2005). Very high resolution interpolated climate surfaces for global land areas. *International Journal of Climatology*, 25(15), 1965–1978. doi: 10.1002/joc.1276

Hoorn, C., Wesselingh, F. P., ter Steege, H., Bermudez, M. A., Mora, A., Sevink, J., ... Antonelli, A. (2010). Amazonia through time: Andean uplift, climate change, landscape evolution, and biodiversity. *Science*, 330(6006), 927–931. doi: 10.1126/science.1194585

Jaccoud, D., Peng, K., Feinstein, D., & Kilian, A. (2001). Diversity Arrays: a solid state technology for sequence information independent genotyping. *Nucleic Acids Res*, 29(4), e25.

Jenkins, D. G., Carey, M., Czerniewska, J., Fletcher, J., Hether, T., Jones, A., … Tursi, R. (2010). A meta-analysis of isolation by distance: relic or reference standard for landscape genetics? *Ecography*, 33, 315−320. doi: 10.1111/j.1600-0587.2010.06285.x

Jombart, T. (2008). adegenet: a R package for the multivariate analysis of genetic markers. *Bioinformatics*, 24, 1403−1405. doi: 10.1093/bioinformatics/btn129

Jombart, T., Pontier, D., & Dufour, A. B. (2009). Genetic markers in the playground of multivariate analysis. *Heredity*, 102, 330–341. doi: 10.1038/hdy.2008.130.

Jombart, T., Devillard, S., & Balloux, F. (2010). Discriminant analysis of principal components: a new method for the analysis of genetically structured populations. *BMC Genetics*, 11, 94. doi: 10.1186/1471-2156-11-94

Jombart, T., & Ahmed, I. (2011). adegenet 1.3-1: new tools for the analysis of genome-wide SNP data. *Bioinformatics*, 27(21), 3070−3071. doi: doi: 10.1093/bioinformatics/btr521

Jorge, R. F., Simões, P. I., Magnusson, W. E., & Lima, A. P. (2016). Fine-scale habitat heterogeneity explains the local distribution of two Amazonian frog species of concern for conservation. *Biotropica*, 48(5), 694–703. doi: 10.1111/btp.12333

Juo, A. S. R., & Franzluebbers, K. (2003). Tropical soils: properties and management for sustainable agriculture. Oxford University Press, New York, NY, U.S.A.

Kaefer, I. L., Tsuji-Nishikido, B. M., Mota, E. P., Farias, I. P., & Lima, A. P. (2013). The early stages of speciation in Amazonian forest frogs: phenotypic conservatism despite strong genetic structure. Evolutionary Biology, 40(2), 228–245. doi: 10.1007/s11692-012-9205-4

Kamvar, Z. N., Brooks, J. C., & Grünwald, N. J. (2014). *Poppr*: an R package for genetic analysis of populations with clonal, partially clonal, and/or sexual reproduction. *PeerJ*, 2, e281. doi: 10.7717/peerj.281

Keenan, K., McGinnity, P., Cross, T. F., Crozier, W. W., & Prodöhl, P. A. (20113). diveRsity: An R package for the estimation and exploration of population genetics parameters and their associated errors. *Methods in Ecology and Evolution*, 4(8), 782−788. doi: 10.1111/2041-210X.12067

Khimoun, A., Peterman, W., Eraud, C., Faivre, B., Navarro, N., & Garnier, S. (2017). Landscape genetic analyses reveal fine-scale effects of forest fragmentation in an insular tropical bird. Molecular Ecology, 26(19), 4906–4919. doi: 10.1111/mec.14233

Kierepka, E. M., & Latch, E. K. (2015). Performance of partial statistics in individual-based landscape genetics. *Molecular Ecology Resources*, 15(3), 512–525. doi: 10.1111/1755-0998.12332.

Kilian, A., Wenzl, P., Huttner, E., Carling, J., Xia, L., Blois, H., … Uszynski, G. (2012) Diversity Arrays Technology: A Generic Genome Profiling Technology on Open

Platforms. In *Data Production and Analysis in Population Genomics. Methods in Molecular Biology (Methods and Protocols)* (pp. 67–89). Humana Press, Totowa, NJ.

Kueneman, J. G., Woodhams, D. C., Harris, R., Archer, H. M., Knight, R., & Mckenzie, V. J. (2016). Probiotic treatment restores protection against lethal fungal infection lost during amphibian captivity. *Proceedings of the Royal Society B*, 283(1839). doi: 10.1098/rspb.2016.1553

Landeiro, V. L., Waldez, F., & Menin, M. (2014). Spatial and environmental patterns of Amazonian anurans: Differences between assemblages with aquatic and terrestrial reproduction, and implications for conservation management. *Natureza & Conservação*, 12(1), 42–46. doi: 10.4322/natcon.2014.008

Legendre, P., Lapointe, F. J., & Casgrain, P. (1994). Modeling brain evolution from behaviour: a permutational regression approach. *Evolution*, 48 (5), 1487–1499. doi: 10.1111/j.1558-5646.1994.tb02191.x.

Legendre, P., & Anderson, M. J. (1999). Distance-based redundancy analysis: testing multiple species responses in multifactorial ecological experiments. *Ecological Monographs*, 69(1), 1–24. doi: 10.1890/0012-9615(1999)069[0001:DBRATM]2.0.CO;2

Legendre, P., & Legendre, L. (2012) *Numerical Ecology*. Elsevier.

Leite, R. N., & Rogers, D. S. (2013) Revisiting Amazonian phylogeography: insights into diversification hypotheses and novel perspectives. Organisms Diversity & Evolution, 13(4), 639–664. doi: 10.1007/s13127-013-0140-8

Lougheed, S. C., Gascon, C., Jones, D. A., Bogart, J. P., & Boag, P. T. (1999). Ridges and rivers: A test of competing hypotheses of Amazonian diversification using a dart-poison frog (*Epipedobates femoralis*). *Proceedings of the Royal Society of*

London Series B: Biological Sciences, 266(1431), 1829–1835. doi: 10.1098/rspb.1999.0853

Ludwig, D. (1945). The effects of atmospheric humidity on animal life. *Physiological Zoology*, 18, 103–135.

Luu, K., Bazin, E., & Blum, M. G. B. (2017). pcadapt: an R package to perform genome scans for selection based on principal component analysis. *Molecular Ecology Resource*, 17(1), 67–77. doi: 10.1111/1755-0998.12592.

Maia, G. F., Lima, A. P., & Kaefer, I. L. (2017). Not just the river: genes, shapes, and sounds reveal population-structured diversification in the Amazonian frog *Allobates tapajos* (Dendrobatoidea). *Biological Journal of the Linnean Society*, 121(1), 95–108. doi: 10.1093/biolinnean/blw017

Magnusson, W. E, Braga-Neto, R., Pezzini, F., Baccaro, F., Bergallo, H., Penha, J., … Pontes, A. R. M. (2013). *Biodiversidade e monitoramento ambiental integrado: o sistema RAPELD na Amazônia*. Publisher Attema, Santo André, SP, Brazil.

Maldonado, F. D., Keizer, E. W. H., Graça, P. M. L. A., Fearnside, P. M., & Vitel, C. S. (2012). Previsão temporal da distribuição espacial do desmatamento no interflúvio Purus-Madeira até o ano 2050. In *Rio Purus: Água, Território e Sociedade na Amazônia Sul-Ocidental* (pp. 183–196). LibriMundi Press, Ecuador.

Mantel, N. 1967. The detection of disease clustering and a generalized regression approach. *Cancer Research*, 27(2), 209–220.

Martins, D. L., Schietti, J., Feldpausch, T. R., Luizão, F. J., Phillips, O. L., Andrade, A., … Quesada, C. A. (2015). Soil-induced impacts on forest structure drive coarse woody debris stocks across central Amazonia. *Plant Ecology & Diversity*, 8(2), 229–241. doi: 10.1080/17550874.2013.879942

Mather, A. T., Hanson, J. O., Pope, L. C., & Riginos, C. (2018). Comparative phylogeography of two co-distributed but ecologically distinct rainbowfishes of far-northern Australia. *Journal of Biogeography*, 45(1), 127–141. doi: 10.1111/jbi.131170

McRae, B. H., Shah, V. B., & Mohapatra, T. K. (2013). Circuitscape 4 User Guide. The Nature Conservancy. http://www.circuitscape.org.

Menin, M., Lima, A. P., Magnusson, W. E., & Waldez, F. (2007). Topographic and edaphic effects on the distribution of terrestrially reproducing anurans in Central Amazonia: mesoscale spatial patterns. *Journal of Tropical Ecology*, 23(5), 539–547. doi: 10.1017/S0266467407004269

Menin, M., Waldez, F., & Lima, A.P. (2011). Effects of environmental and spatial factors on the distribution of anuran species with aquatic reproduction in central Amazonia. *Herpetological Journal*, 21(4), 255–261.

Mims, M. C., Hauser, L., Goldberg, C. S., & Olden, J. D. (2016). Genetic differentiation, isolation-by-distance, and metapopulation dynamics of the Arizona Treefrog (*Hyla wrightorum*) in an isolated portion of its range. *PLoS ONE*, 11(8), e0160655. doi: 10.1371/journal.pone.0160655

Mitchell, A., & Bergmann, P. J. (2016). Thermal and moisture habitat preferences do not maximize jumping performance in frogs. *Functional Ecology*, 30(5), 733–742. doi: 10.1111/1365-2435.12535

Morin, P. A., Martien, K. K., & Taylor, B. L. (2009). Assessing statistical power of SNPs for population structure and conservation studies. *Molecular Ecology Resources*, 9(1), 66–73. doi: 10.1111/j.1755-0998.2008.02392.x

Moritz, C., Patton, J. L., Schneider, C. J., & Smith, T. B. (2000). Diversification of rainforest faunas: an integrated molecular approach. *Annual Review of Ecology and Systematics*, 31, 533–563. doi: 10.1146/annurev.ecolsys.31.1.533

Nazareno, A. G., Dick, C. W., & Lohmann, L. G. (2017). Wide but not impermeable: Testing the riverine barrier hypothesis for an Amazonian plant species. *Molecular Ecology*, 26(14), 3636–3648. doi: 10.1111/mec.14142.

Oden, N. L., & Sokal, R. R. (1986). Directional autocorrelation: an extension of spatial correlograms to two dimensions. Systematic Biology, 35(4), 608–617. doi: 10.2307/2413120

Oksanen, J., Blanchet, F. G., Friendly, M., Kindt, R., Legendre, P., McGlinn, D., … Wagner, H. (2018). vegan: Community Ecology Package. R package version 2.5-1. https://CRAN.R-project.org/package=vegan

Ortiz, D. A., Lima, A. P., & Werneck, F. P. (2018). Environmental transition zone and rivers shape Intraspecific population structure and genetic diversity of an Amazonian rain forest tree frog. *Evolutionary Ecology*, 32(4), 359–378. doi: 10.1007/s10682-018-9939-2

Paradis, E. (2010). pegas: an R package for population genetics with an integrated-modular approach. *Bioinformatics*, 26(3), 419−420. doi: 10.1093/bioinformatics/btp696

Paz, A., Ibáñez, R., Lips, K. R., & Crawford, A. J. (2015). Testing the role of ecology and life history in structuring genetic variation across a landscape: a trait-based phylogeographic approach. Molecular Ecology, 24(14), 3723−3737. doi:10.1111/mec.13275

Peakall, R., & Smouse, P. E. (2012). Genalex 6.5: Genetic analysis in excel. Population gene software for teaching and research–an update. *Bioinformatics*, 28(19), 2537−2539. doi: 10.1093/bioinformatics/bts460

Peterman, W. E., Connette, G. M., Semlitsch, R. D., & Eggert, L. S. (2014). Ecological resistance surfaces predict fine-scale genetic differentiation in a terrestrial woodland salamander. *Molecular Ecology*, 23(10), 2402–2413. doi:10.1111/mec.12747

Peterman, W. E. (2018). ResistanceGA: An R package for the optimization of resistance surfaces using genetic algorithms. *Methods in Ecology and Evolution*, 9(6),1638–1647. doi: 10.1111/2041-210X.12984

R Core Team (2018). R: A language and environment for statistical com- puting. R Foundation for Statistical Computing.

Raffel, T. R., Rohr, J. R., Kiesecker, J. M., & Hudson, P. J. (2006). Negative effects of changing temperature on amphibian immunity under field conditions. *Functional Ecology*, 20(5), 819–828. doi: 10.1111/j.1365-2435.2006.01159.x

Räsänen, M. E., Salo, J. S., Jungnert, H., & Pittman, L. R. (1990). Evolution of the western Amazon lowland relief: impacts of Andean foreland dynamics. Terra Nova, 2, 320–332. doi: 10.1111/j.1365-3121.1990.tb00084.x

Ribas, C. C., Aleixo, A., Nogueira, A. C. R., Miyaki, C. Y., & Cracraft, J. (2012). A paleobiogeographic model for biotic diversification within Amazonia over the past three million years. *Proceedings of the Royal Society of London Series B*, 279(1729), 681–689. doi: 10.1098/rspb.2011.1120.

Ribas, C. C., Aleixo, A., Gubili, C., d'Horta, F. M., Brumfield, R. T., & Cracraft, J. (2018). Biogeography and diversification of *Rhegmatorhina* (Aves:

Thamnophilidae): Implications for the evolution of Amazonian landscapes during the Quaternary. *Journal of Biogeography*, 45(4), 917–928. doi: 10.1111/jbi.13169

Riddell, E. A., Apanovitch, E. K., Odom, J. P., & Sears, M. W. (2017). Physical calculations of resistance to water loss improve predictions of species range models. Ecol Monogr, 87(1): 21–33. doi:10.1002/ecm.1240

Rossetti, D. F., Gribel, R., Toledo, P. M., Tatumi, S. H., Yee, M., Tudela, … Coelho, L.S. (2018). Unfolding long-term Late Pleistocene–Holocene disturbances of forest communities in the southwestern Amazonian lowlands. *Ecosphere*, 9(10), e02457. doi: 10.1002/ecs2.2457

Rousset, F. (1997). Genetic differentiation and estimation of gene flow from F-statistics under isolation by distance. *Genetics*, 145(4), 1219–1228.

Rudin-Bitterli, T. S., Evans, J. P., & Mitchell, N. J. (2018). Geographic variation in adult and embryonic desiccation tolerance in a terrestrial-breeding frog. *bioRxiv*, 314351. doi: 10.1101/314351

Rudin-Bitterli, T. S., Mitchell, N. J., & Evans, J. P. (2018). Environmental Stress Increases the Magnitude of Nonadditive Genetic Variation in Offspring Fitness in the Frog *Crinia georgiana*. *The American Naturalist*, 192, 461–478. doi: 10.1086/699231

Ruiz-Lopez, M. J., Barelli, C., Rovero, F., Hodges, K., Roos, C., Peterman, W. E., & Ting, N. (2016). A novel landscape genetic approach demonstrates the effects of human disturbance on the Udzungwa red colobus monkey (*Procolobus gordonorum*). *Heredity*, 116(2), 167–176. doi: 10.1038/hdy.2015.82

Ruokolainen, K., Moulatlet, G. M, Zuquim, G., Hoorn, C., & Tuomisto, H. (2018). River Network Rearrangements in Amazonia Shake Biogeography and Civil Security. *Preprints*. doi: 10.20944/preprints201809.0168.v1

Sánchez-Ramírez, S., Rico, Y., Berry, K. H., Edwards, T., Karl, A. E., Henen, B. T., & Murphy, R. W. (2018). Landscape limits gene flow and drives population structure in Agassiz's desert tortoise (*Gopherus agassizii*). *Scientific Rep*ort, 8(1), 11231. doi: 10.1038/s41598-018-29395-6

Sansaloni, C., Petroli, C., Jaccoud, D., Carling, J., Detering, F., Grattapaglia, D., & Kilian, A. (2011). Diversity Arrays Technol- ogy (DArT) and next-generation sequencing combined: genome-wide, high throughput, highly informative genotyping for molecular breeding of *Eucalyptus*. *BMC Proceedings*, 5, 54−55. doi: 10.1186/1753-6561-5-S7-P54

Schietti, J., Martins, D., Emilio, T., Souza, P. F., Levis, C., Baccaro, F. B., … Nardoto, G. B. (2016). Forest structure along a 600 km transect of natural disturbances and seasonality gradients in central-southern Amazonia. *Journal of Ecology*, 104(5), 1335–1346. doi: 10.1111/1365-2745.12596

Shirk, A. J., Landguth, E. L., & Cushman, S. A. (2017). A comparison of regression methods for model selection in individual-based landscape genetic analysis. *Molecular Ecology Resources*, 18(1), 55–67. doi: 10.1111/1755-0998.12709

Sokal, R. R. (1986). Spatial data analysis and historical processes. In *Data analysis and informatics, IV*. (pp. 29–43). North-Holland, Amsterdam.

Sombroek, W. (2000). Amazon landforms and soils relation to biological diversity. *Acta Amazononica*, 30(1), 81–100. doi: 10.1590/1809-43922000301100

Sturges, H. A. (1926). The choice of a class interval. *Journal of the American Statistical Association*, 21(153), 65–66. doi: 10.1080/01621459.1926.10502161

Sun, Y. -B., Xiong, Z. -J., Xiang, X. -Y., Liu, S. -P., Zhou, W. -W., Tu, X. -L., … Zhang, Y. -P. (2015). Whole-genome sequence of the Tibetan frog *Nanorana parkeri* and the comparative evolution of tetrapod genomes. *Proceedings of the*

National Academy of Sciences of the United States of America, 112(11), 1257–1262. doi: 0.1073/pnas.1501764112

Thom, G., & Aleixo, A. (2015). Cryptic speciation in the white-shouldered ant shrike (*Thamnophilus aethiops*, Aves - Thamnophilidae): The tale of a transcontinental radiation across rivers in lowland Amazonia and the northeastern Atlantic Forest. *Molecular Phylogenetics and Evolution*, 82, 95–110. doi: 10.1016/j.ympev.2014.09.023.

van Strien, M. J., Holderegger, R., & van Heck, H. J. (2015). Isolation-by-distance in landscapes: considerations for landscape genetics. *Heredity*, 114, 27–37. doi: 10.1038/hdy.2014.62

Vanzolini, P. E., & Williams, E. E. (1981). The vanishing refuge: a mechanism for ecogeographic speciation. *Papéis Avulsos de Zoologia*, 34:251–55.

Varela, B. J., Lesbarrères, D., Ibáñez, R., & Green, D. M. (2018). Environmental and Host Effects on Skin Bacterial Community Composition in Panamanian Frogs. *Frontiers in Microbiology*, 9, 298. doi: 10.3389/fmicb.2018.00298

Villemey, A., Peterman, W. E., Richard, M., Ouin, A., van Halder, I., Stevens, V. M., … Archaux, F. (2016). Butterfly dispersal in farmland: a replicated landscape genetics study on the meadow brown butterfly (*Maniola jurtina*). *Landscape Ecology*, 31(7), 1629. doi: 10.1007/s10980-016-0348-z

Wallace, A. R. (1852). On the monkeys of the Amazon. *Proceedings of the Zoological Society of London*, 20, 107–110.

Walsh, R. P. D. (1996). Climate. In *The tropical rain forest: an ecological study*. (pp. 159–205). Cambridge University Press, Cambridge.

Weir, B. S., & Cockerham, C. C. (1984) Estimating F-Statistics, for the Analysis of Population Structure. *Evolution*, 38, 1358–1370. doi: 10.1111/j.1558-5646.1984.tb05657.x

Wickham, H. (2017). *dbplyr*: A 'dplyr' Back End for Databases. R package version 1.1.0.

Wright, S. (1943). Isolation by Distance. *Genetics*, 28, 114–138.

Xie, Y. (2016). *DT*: A Wrapper of the JavaScript Library 'DataTables'. R package version 0.2.

Supplemental material S1

METHODS

We calculated pairwise genetic differentiation (F_{ST}) following Weir & Cockerham (1984) between populations in Arlequim v. 3.5.2 (Excoffier &Lischer 2010). Population pairwise F_{ST} and its significance level ($\alpha = 0.05$) were calculated using 1000 permutations. Due to the sampling effort that resulted in just one specimen collected in the sampling site M11 and M15, we included these two samples in the nearby sampling module (HUM and M14, respectively) for population analyses purpose. Sampling site M11 is far ~20 km from HUM and M15 is far ~15 km from M14.

sNMF (Frichot et al. 2014) were used to infer the best-fit number of ancestral populations. The k values (2–10) were tested with 10 replicates for each value of k and 10000 interactions. The best-supported k and the best run were selected by estimation of the lowest error value of ancestry through cross-entropy criterion. sNMF was performed in the R package LEA (Frichot 2015).

Phylogenetic relationship between populations were reconstructed through SNAPP 1.3 (Bryant et al. 2012) implemented in BEAST 2.4.8 (Bouckaert et al.2014). To reduce computational time, we selected 3 representative specimens per population. We ran SNAPP using a chain length of 1,000,000 generations, sampling every 1,000 trees. Two independent runs were executed and combined through TreeAnnotator 2.4.6 after discarding 10% as burn-in.

RESULTS

Genetic differentiation

Table 1. Pairwise genetic differentiation (F_{ST}) across sampling sites (bellow diagonal) computed following Weir & Cockerham (1984) and its respective *p*-values (above diagonal) based on 1000 permutations. Bold values represent nonsignificant *p*-values.

	M01	M02	M03	M05	M06	M07	M08	M09	M10	HUM	M12	M13
M01	-	0.003	0.013	0.003	0.017	0.001	0.006	0.002	0.002	0.003	0.001	0.000
M02	0.212	-	0.022	0.009	0.015	0.000	0.007	0.003	0.009	0.015	0.001	0.007
M03	0.255	0.205	-	0.026	**0.095**	0.005	0.014	0.004	0.021	0.014	0.011	0.021
M05	0.866	0.857	0.846	-	0.032	0.003	0.011	0.007	0.030	0.007	0.004	0.009
M06	0.868	0.858	0.846	0.454	-	0.009	0.015	0.012	0.024	0.027	0.006	0.018
M07	0.848	0.841	0.827	0.417	0.128	-	0.001	0.000	0.002	0.002	0.000	0.002
M08	0.850	0.842	0.827	0.481	0.279	0.212	-	0.002	0.004	0.008	0.001	0.010
M09	0.854	0.847	0.835	0.521	0.349	0.295	0.130	-	0.002	0.003	0.000	0.001
M10	0.859	0.850	0.834	0.555	0.407	0.359	0.260	0.199	-	0.004	0.002	0.006
HUM	0.882	0.876	0.869	0.637	0.528	0.459	0.394	0.354	0.229	-	0.001	0.009

M12	0.902	0.899	0.897	0.742	0.702	0.640	0.603	0.575	0.541	0.588	-	0.001
M13	0.923	0.921	0.925	0.803	0.784	0.697	0.681	0.650	0.643	0.690	0.310	-

Genetic structure

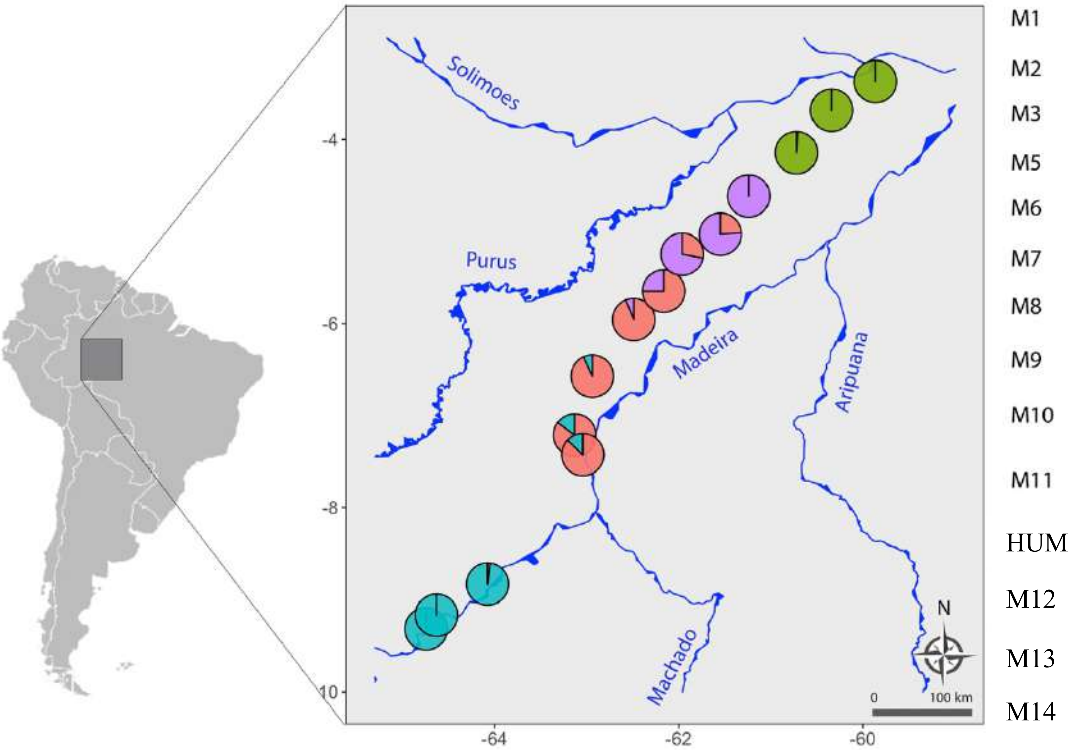

Figure 1. Genetic structure of *Phyzelaphryne miriamae* along the Purus-Madeira Interfluve. Population admixture estimates (k = 4) recovered by SNMF.

Phylogenetic relationships

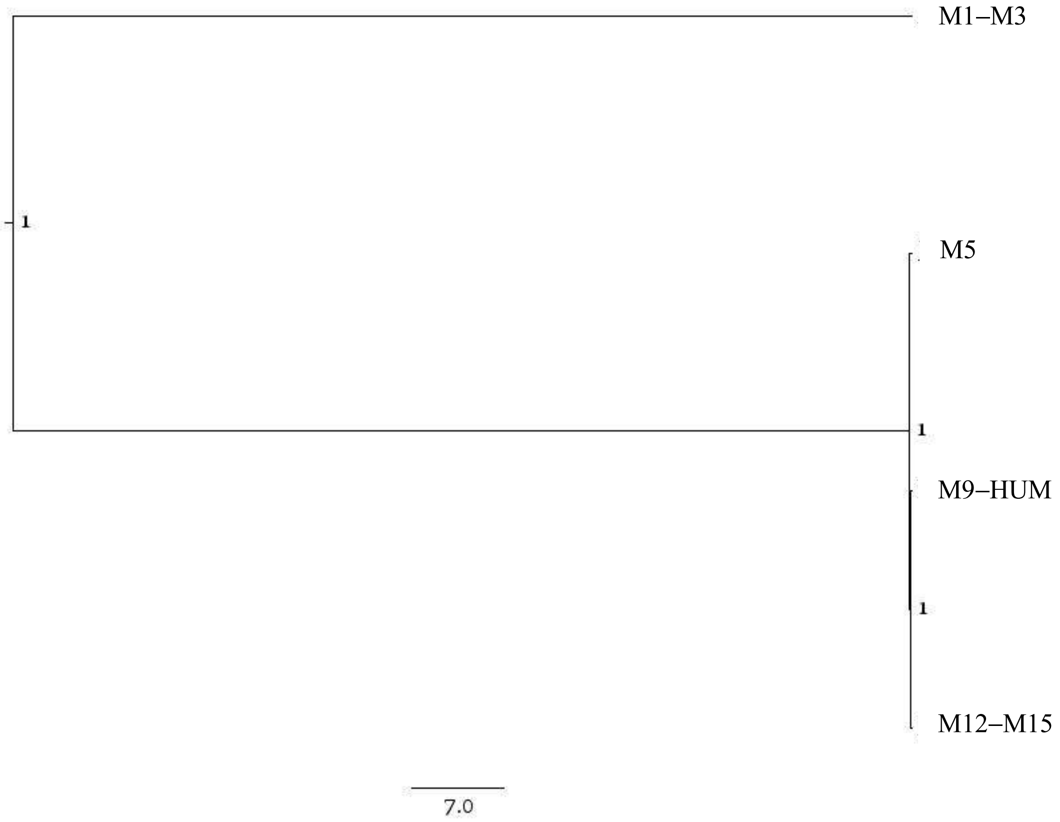

Figure 2. Phylogenetic relationship of populations of *P. miriamae* reconstructed through SNAPP.

SÍNTESE

No primeiro capítulo desta tese, revelamos que o conhecimento a cerca das espécies de *Scinax* que habitam o interflúvio entre os rios Purus e Madeira (IPM) era ínfimo. Além disso, corroboramos a ideia de que áreas pouco exploradas na Amazônia podem estar repletas de espécies desconhecidas para a ciência. No caso do IPM, a diversidade de espécies estava subestimada em 82%. Valor este duas vezes mais alto do que o estimado para a região neotropical.

No segundo capítulo descrevemos formalmente a espécie de *Scinax* mais amplamente distribuída no IPM. Ao utiliza-la como modelo para entender o efeito do ambiente na distribuição de espécies no IPM, revelamos pela primeira vez a associação entre um anuro amazônico de reprodução aquática com uma variável edáfica. Isto demonstra que estudos de associação espécie-habitat conduzidos em áreas menos conhecidas da Amazônia podem revelar resultados inéditos.

No terceiro capítulo descrevemos outra espécie nova de *Scinax*. Só conseguimos registrar a nova espécie em uma pequena área na porção central do IPM, mesmo com inventários intensos em mais de 450 parcelas de amostragem permanente distribuídas por grande parte da Amazônia. Apesar de ocorrer na borda interna do Parque Nacional Nascentes do Lago Jarí, a especulação imobiliária por conta da reconstrução da BR-319 tem feito o desmatamento avançar dentro do parque.

No quarto capítulo descrevemos uma nova espécie de *Scinax* com base em duas populações distribuídas em duas florestas distintas no IPM. Levados pela monofilia recíproca e pelos diferentes padrões de coloração apresentados, hipotetizamos que variações no ambiente podem estar direcionando a diferenciação observada nestas duas populações.

No quinto capítulo testamos a hipótese de gradientes ambientais. Os resultados mostram que tanto gradientes ambientais quanto distância geográfica influenciam o fluxo gênico em *Phyzelaphryne miriame* ao longo das paisagens heterogêneas do IPM. Entretanto, as variáveis ambientais por nós avaliadas explicam melhor o fluxo gênico do que distância geográfica.

Os resultados obtidos nesta tese representam um avanço no conhecimento da diversidade de espécies de anuros do IPM, bem como no entendimento dos fatores e processos responsáveis pela distribuição e diversificação das espécies nesta região pouco explorada da Amazônia. Esta tese compreende apenas o início de uma série de estudos na região. Dezenas de outras novas espécies de anuros ocorrem na região e aguardam descrição formal. Uma vez que espécies distintas reagem de forma diferente as mudanças no ambiente que habitam, estudos futuros descrevendo o papel da heterogeneidade ambiental na distribuição de espécies podem potencialmente revelar novos padrões de associação espécie-habitat. Além dos gradientes ambientais, outros fatores podem também ser responsáveis pela diversificação e manutenção da biodiversidade local, e devem ser investigados de maneira detalhada.

REFERÊNCIAS BIBLIOGRÁFICAS

Abreu, F.H.T., Schiettim, J. e Anciães, M. 2018. Spatial and environmental correlates of intraspecific morphological variation in three species of passerine birds from the Purus–Madeira interfluvium, Central Amazonia. Evolutionary Ecology, 32: 191–214.

Aleixo, A. 2004. Historical diversification of a terra-firme forest bird superspecies: a phylogeographic perspective on the role of different hypotheses of Amazonian diversification. Evolution, 58: 1303–1317.

Allmon, W.D. 1991. A plot study of forest floor litter frogs, central Amazon, Brazil. Journal of Tropical Ecology, 7: 503–522.

Angulo, A. e Icochea, J. 2010. Cryptic species complexes, widespread species and conservation: lessons from Amazonian frogs of the *Leptodactylus marmoratus* group (Anura: Leptodactylidae). Systematics and Biodiversity, 8 (3): 357–370.

Ayres, J.M. e Clutton-Brock, T.H. 1992. River boundaries and species range size in Amazonian Primates. American Naturalist, 140: 531–537.

Bickford, D., Lohman, D.J., Sodhi, N.S., Ng, P.K.L., Meier, R., Winker, K., Ingram, K.K. e Das, I. 2007. Cryptic species as a window on diversity and conservation. Trends in Ecology and Evolution, 22(3): 148–155.

Blaustein A.R., Wake, D.B. e Sousa, W.P. 1994. Amphibian declines: judging stability, persistence, and susceptibility of populations to local and global extinctions. Conservation Biology, 8: 60–71.

Bortolus, A. 2008. Error cascades in the biological sciences: the unwanted consequences of using bad taxonomy in ecology. AMBIO, 37(2): 114–118.

Boubli, J.P., Ribas, C., Lynch Alfaro, J.W., Alfaro, M.E., Silva, M.N.F., Pinho, G.M. e Farias, I.P. 2015. Spatial and temporal patterns of diversification on the Amazon: A test of the riverine hypothesis for all diurnal primates of Rio Negro and Rio Branco in Brazil. Molecular Phylogenetics and Evolution, 82: 400–412.

Brandão, R.A., Caramaschi, U., Vaz-Silva, W. e Campos, L.A. 2013. Three new species of *Proceratophrys* Miranda-Ribeiro 1920 from Brazilian Cerrado (Anura, Odontophrynidae). Zootaxa, 3750: 321–347.

Brown, J.L., Twomey, E., Amézquita, A., Souza, M.B., Caldwell, J.P., Lötters, S., von May, R., Melo-Sampaio, P.R., Mejía-Vargas, D., Pérez-Peña, P.E., Pepper, M., Poelman, E.H., Sanchez-Rodriguez, M. e Summers, K. 2011. A taxonomic revision of the Neotropical poison frog genus *Ranitomeya* (Amphibia: Dendrobatidae). Zootaxa, 3083: 1–120.

Caminer, M.A. e Ron, S.R. 2014. Systematics of treefrogs of the *Hypsiboas calcaratus* and *Hypsiboas fasciatus* species complex (Anura, Hylidae) with the description of four new species. ZooKeys, 370: 1–68.

Caminer, M.A., Milá, B., Jansen, M., Fouquet, A., Venegas, P.J., Chavéz, G., Lougheed, S.C. e Ron, S. 2017. Correction: Systematics of the *Dendropsophus leucophyllatus* species complex (Anura: Hylidae): Cryptic diversity and the description of two new species. PLOS ONE, 12(4): e0176902.

Caramaschi, U. 2010. Notes on the taxonomic status of *Elachistocleis ovalis* (Schneider, 1799) and description of five new species of *Elachistocleis* Parker, 1927 (Amphibia, Anura, Microhylidae). Boletim do Museu Nacional, 527: 1–30.

Carvalho, T.R. e Giaretta, A.A. 2013. Bioacoustics reveals two new syntopic species of *Adenomera* Steindachner (Anura: Leptodactylidae: Leptodactylinae) in the Cerrado of central Brazil. Zootaxa, 3731(3): 533–551.

Cintra, B.B.L., Schietti, J., Emillio, T., Martins, D., Moulatlet, G., Souza, P., Levis, C., Quesada, C.A. e Schöngart, J. 2013 Soil physical restrictions and hydrology regulate stand age and wood biomass turnover rates of Purus–Madeira interfluvial wetlands in Amazonia. Biogeosciences, 10: 7759–7774.

Davey, J.W., Hohenlohe, P.A., Etter, P.D., Boone, J.Q., Catchen, J.M. e Blaxter, M.L. 2011. Genome-wide genetic marker discovery and genotyping using next-generation sequencing**.** Nature Reviews Genetics, 12: 499–510.

Duellman, W.E. 1999. Distribution patterns of amphibians in South America. In: W.E. Duellman (ed.). Patterns of distribution of amphibians: a global perspective. The Johns Hopkins University Press, Baltimore, USA. p. 255–328.

Duellman, W.E. e Trueb, L. 1994. Biology of Amphibians.The Johns Hopkins University Press, USA, 670p.

Duellman, W.E. e Thompson, R. 1996. Anuran Amphibians from a seasonally dry forest in southeastern Peru and comparisons of the anurans among sites in the upper amazon basin. Occasional Papers of the Natural History Museum the University of Kansas Lawrence, 180: 1–34.

Endler, J. 1977. Geographic variation, speciation, and clines. Princeton: Princeton University Press.

Endler, J. 1982. Pleistocene forest refuges: fact or fancy? In G. T. Prance (Ed.), Biological diversification in the Tropics (pp. 641–657). New York: Columbia University Press.

Ernst, R. e Rödel, M.-O. 2006. Community assembly and structure of tropical leaf-litter anurans. Ecotropica, 12: 113–129.

Eterovick, P.C. e Barata, I.M. 2006. Distribution of tadpoles within and among Brazilian streams: the influence of predators, habitat size and heterogeneity. Herpetologica, 62: 365–377.

Fernandes, A.M., Wink, M. e Aleixo, A. 2012. Phylogeography of the Chestnut-tailed Antbird (*Myrmeciza hemimelaena*) clarifies the role of rivers in Amazonian biogeography. Journal of Biogeography, 39: 1524–1535.

Ferreira, M., Aleixo, A., Ribas, C.C. e Santos, M.P.D. 2017. Biogeography of the Neotropical genus *Malacoptila* (Aves: Bucconidae): The influence of the Andean orogeny, Amazonian drainage evolution and palaeoclimate. Journal of Biogeography, 4: 748–759.

Ferreira, A.S., Jehle, R., Stow, A.J. e Lima, A.P. 2018. Soil and forest structure predict large-scale patterns of occurrence and local abundance of a widespread Amazonian frog. PeerJ, 6: e5424.

Fouquet, A., Gilles, A., Vences, M., Marty, C., Blanc, M. e Gemmell, N.J., 2007a. Underestimation of species richness in neotropical frogs revealed by mtDNA analyses. PLoS ONE 2(10): e1109.

Fouquet, A., Gaucher, P., Blanc, M. e Velez-Rodriguez. 2007b. Description of two new species of *Rhinella* (Anura: Bufonidae) from the lowlands of the Guiana shield. Zootaxa, 1663: 17–32.

Fouquet, A., Cassini, C.S., Haddad, C.F.B., Pech, N., Rodrigues, M.T. e Emerson, B. 2014. Species delimitation, patterns of diversification and historical biogeography of the Neotropical frog genus *Adenomera* (Anura, Leptodactylidae). Journal of Biogeography, 41: 855–870.

Fouquet, A., Courtois, E.A., Baudain, D., Lima, J.D., Souza, S.M., Noonan B.P., Rodrigues, M.T. 2015. The trans-riverine genetic structure of 28 Amazonian frog species is dependent on life history. Journal of Tropical Ecology, 31: 361–373.

Funk, W.C., Caldwell, J.P., Peden, C.E., Padial, J.M., De la Riva, I. e Cannatella, D.C. 2007. Tests of biogeographic hypotheses for diversification in the Amazonian forest frog, *Physalaemus petersi*. Molecular Phylogenetics and Evolution, 44: 825–837.

Funk, W.C., Caminer, M. e Ron, S.R. 2011. High levels of cryptic species diversity uncovered in Amazonian frogs. Proc. Roy. Soc. Lond. B. 279 (1734): 1806–1814.

Gascon, C., Lougheed, S. C. e Bogart, J. P. 1996. Genetic and morphological variation in *Vanzolinius discodactylus*: a test of the river hypothesis of speciation. Biotropica, 28: 376–387.

Gascon, C., Lougheed, S.C. e Bogart, J.P. 1998. Patterns of genetic population differentiation in four species of Amazonian frogs: a test of the riverine barrier hypothesis. Biotropica, 30, 104–119.

Gascon, C., Malcolm, J.R., Patton, J.L., Silva, M.N.F., Bogart, J.P., Lougheed, S.C., Peres, C.A., Neckel, S. e Boag, P.T. 2000. Riverine barriers and the geographic distribution of Amazonian species. Proceedings of the National Academy of Sciences of the United States of America, 97: 13673–13677.

Gaston, K.J. e Blackburn, T. M. 2003. Macroecology and conservation biology. In T. M. Blackburn, & K. J. Gaston (Eds.), Macroecology: Concepts and consequences. Oxford: Blackwell Science.

Gotelli, N.J. 2004. A taxonomic wish-list for community ecology. Philosophical Transactions of the Royal Society B: Biological Science, 359: 585–597.

Haffer, J. 1969. Speciation in Amazonian forest birds. Science, 165: 131–137.

Houlahan, J.E., Findlay, C.S., Schmidt, B.R., Meyer, A.H. e Kuzmin, S.L. 2000. Quantitative evidence for global amphibian population declines. Nature, 404: 752–755.

Isaac, N.J.B., Mallet, J. e Mace, G.M. 2004. Taxonomic inflation: its influence on macroecology and conservation. Trends in Ecology & Evolution, 19(9): 464–469.

Jorge, R.F., Simões, P.I., Magnusson, W.E. e Lima, A.P. 2016. Fine-scale habitat heterogeneity explains the local distribution of two Amazonian frog species of concern for conservation. Biotropica, 48: 694–703.

Jungfer, K.-H., Faivovich, J., Padial, J.M., Castroviejo-Fisher, S., Lyra, M.L., Berneck, B.V.M., Iglesias, P.P., Kok, P. J. R., MacCulloch, R. D., Rodrigues, M. T., Verdade, V.K., Torres Gastello, C.P., Chaparro, J.C., Valdujo, P.H., Reichle, S., Moravec, J., Gvoždík, V., Gagliardi-Urrutia, G., Ernst, R., De la Riva, I., Means, D.B., Lima, A.P., Señaris, J.C., Wheeler, W.C., Haddad, C.F.B. (2013). Systematics of spiny-backed treefrogs (Hylidae: *Osteocephalus*): an Amazonian puzzle. Zoologica Scripta, 42: 351–380.

Jungfer, K.-H., Verdade, V.K., Faivovich, J. e Rodrigues, M.T. 2016. A new species of spiny-backed treefrog (*Osteocephalus*) from Central Amazonian Brazil (Amphibia: Anura: Hylidae). Zootaxa, 4114: 171–181.

Keller, A., Rödel, M.O., Linsenmair, K.E. e Grafe, T.U. 2009. The importance of environmental heterogeneity for species diversity and assemblage structure in Bornean stream frogs. Journal of Animal Ecology, 78(2): 305–314.

Lima, A.P., Simões, P.I. e Kaefer, I.L. 2015. A new species of *Allobates* (Anura: Aromobatidae) from Parque Nacional da Amazônia, Pará State, Brazil. Zootaxa, 3980(4): 501–525.

Lougheed, S.C., Gascon, C., Jones, D.A., Bogart, J.P. e Boag, P.T. 1999. Ridges and rivers: A test of competing hypotheses of Amazonian diversification using a dart-poison frog (*Epipedobates femoralis*). Proceedings of the Royal Society of London Series B-Biological Sciences, 266: 1829–1835.

Ludwig, D. 1945 The effects of atmospheric humidity on animal life. Physiological Zoology, 18: 103–135.

Lynch Alfaro, J.W., Boubli, J.P., Paim, F.P., Ribas, C.C., da Silva, M.N.F., Messias, M.R., Röhe, F., Mercês, M.P., Silva Júnior, J.S., Silva, C.R., Pinho, G.M., Koshkarian, G., Nguyen, M.T.T., Harada, M.L., Rabelo, R.M., Queiroz, H.L., Alfaro, M.E. e Farias, I.P. 2015. Biogeography of squirrel monkeys (genus *Saimiri*): South-central Amazon origin and rapid pan-Amazonian diversification of a lowland primate. Molecular Phylogenetics and Evolution, 82: 436–454.

Maia, G.F., Lima, A.P. e Kaefer, I.L. 2017. Not just the river: genes, shapes, and sounds reveal population-structured diversification in the Amazonian frog *Allobates tapajos* (Dendrobatoidea). Biological Journal of the Linnean Society, 121(1): 95–108.

Mardis, E.R. 2008. The impact of next-generation sequencing technology on genetics. Trends in Genetics, 24: 133–141.

Martins, D.L., Schietti, J., Feldpausch, T.R., Luizão, F.J., Oliver, L., Andrade, A., Castilho, C.V., Laurance, S.G., Oliveira, Á., Ieda, L. e Quesada, C.A. 2015. Soil-induced impacts on forest structure drive coarse woody debris stocks across central Amazonia. Plant Ecology and Diversity, 8: 229–241.

McCormack, J.E., Hird, S.M., Zellmer, A.J., Carstens, B.C. e Brumfield, R.T. 2003. Applications of next-generation sequencing to phylogeography and phylogenetics. Molecular Phylogenetics and Evolution, 66: 526–538.

Melo-Sampaio, PR, Oliveira, R.M. e Prates, I. 2018. A New Nurse Frog from Brazil (Aromobatidae: *Allobates*), with Data on the Distribution and Phenotypic Variation of Western Amazonian Species. South American Journal of Herpetology, 13(2): 131–149.

Menin, M., Lima, A.P., Magnusson, W.E. e Waldez, F. 2007. Topographic and edaphic effects on the distribution of terrestrially reproducing anurans in Central Amazonia: mesoscale spatial patterns. Journal of Tropical Ecology, 17(2): 86–91.

Menin, M., Waldez, F. e Lima, A.P. 2011. Effects of environmental and spatial factors on the distribution of anuran species with aquatic reproduction in central Amazonia. Herpetological Journal, 21: 255–261.

Mittermeier, R.A., Mittermeier, C.G., Brooks, T.M., Pilgrim, J.D., Konstant, W.R., Fonseca, G.A.B. e Kormos, C. 2003. Wilderness and biodiversity conservation. Proceedings of the National Academy of Sciences of the United States of America, 100(18): 10309–10313.

Moritz, C., Patton, J.L., Schneider, C.J. e Smith, T.B. 2000. Diversification of rainforest faunas: an integrated molecular approach. Annual Review of Ecology and Systematics, 31: 533–563.

Nair, A., Gopalan, S.V., George, S., Kumar, K.S., Teacher, A.G.F. e Merilä, J. 2012. High cryptic diversity of endemic Indirana frogs in the Western Ghats biodiversity hotspot. Animal Conservation, 15: 489–498.

Naka, L.N. e Brumfield, R.T. 2018. The dual role of Amazonian rivers in the generation and maintenance of avian diversity. Science Advances, 4(8): eaar8575.

Nazareno, A.G., Dick, C.W. e Lohmann, L.G. 2017. Wide but not impermeable: Testing the riverine barrier hypothesis for an Amazonian plant species. Molecular Ecology, 26: 3636–3648.

Nores, M. 1999. An alternative hypothesis for the origin of Amazonian bird diversity. Journal of Biogeography, 26: 475–485.

Ortiz, D.A., Lima, A.P. e Werneck, F.P. 2018. Environmental transition zone and rivers shape Intraspecific population structure and genetic diversity of an Amazonian rain forest tree frog. Evolutionary Ecology, 32(4): 359–378.

Padial, J.M., Miralles, A., De la Riva, I. e Vences, M. 2010. The integrative future of taxonomy. Frontiers in Zoology, 7: 16.

Padial, J.M., Chaparro, J.C., Castroviejo-Fisher, S.J., Guayasamin, J.M., Lehr, E., Delgado, A.J., Vaira, M., Teixeira, M.Jr., Aguayo, R. e De La Riva, I. 2012 A Revision of Species Diversity in the Neotropical Genus *Oreobates* (Anura: Strabomantidae), with the Description of Three New Species from the Amazonian Slopes of the Andes. American Museum Novitates, 3752: 1–55.

Parris, K.M. e McCarthy, M.A. 1999. What influences the structure of frog assemblages at forest streams? Australian Journal of Ecology, 24: 495–502.

Pearman, P.B. 1997. Correlates of Amphibian Diversity in an Altered Landscape of Amazonian Ecuador. Conservation Biology, 11: 1211–1225.

Peloso, P.L., Sturaro, M.J., Forlani, M.C., Gaucher, P., Motta, A.P. e Wheeler, W.C. 2014. Phylogeny, taxonomic revision, and character evolution of the genera *Chiasmocleis* and *Syncope* (Anura: Microhylidae) in the Amazonia, with descriptions of three new species. Bulletin of American Museum of Natural History, 386(1): 1–112.

Pinheiro, L.C., Bitar, Y.O.C., Galatti, U.,Neckel- Oliveira, S. e Santos-Costa, M.C. 2012. Amphibians from southeastern state of Pará: Carajás Region, northern Brazil. CheckList, 8(4): 693–702.

Rakotoarison, A., Scherz, M.D., Glaw, F., Köhler, J., Andreone, F., Franzen, M., Glos, J., Hawlitschek, O., Jono, T., Mori, A., Ndriantsoa, S.H., Rasoamampionona Raminosoa, N., Riemann, J.C., Rödel, M.O., Rosa, G.M., Vieites, D.R., Crottini, A. e Vences, M. 2017. Describing the smaller majority: integrative taxonomy reveals twenty-six new species of tiny microhylid frogs (genus *Stumpffia*) from Madagascar. Vertebrate Zoology, 67: 271–398.

Räsänen, M.E., Linna, A.M., Santos, J.C.R. e Negri, F.R. 1995. Late Miocene tidal deposits in the Amazonian foreland basin. Science, 269: 386–390.

Rašić, G., Filipović, I., Weeks, A.R. e Hoffmann, A.A. 2014. Genome-wide SNPs lead to strong signals of geographic structure and relatedness patterns in the major arbovirus vector, *Aedes aegypti*. BMC Genomics, 15: 275.

Ribas, C.C., Aleixo, A., Nogueira, A.C.R., Miyaki, C.Y. e Cracraft, J. 2012. A paleobiogeographic model for biotic diversification within Amazonia over the past three million years. Proceedings of the Royal Society of London Series B, 279: 681–689.

Ribas, C.C., Aleixo, A., Gubili, C., d'Horta, F.M., Brumfield, R.T. e Cracraft, J. 2018. Biogeography and diversification of *Rhegmatorhina* (Aves: Thamnophilidae): Implications for the evolution of Amazonian landscapes during the Quaternary. Journal of Biogeography, 45: 917–928.

Ribeiro, J.W., Lima, A.P. e Magnusson, W.E. 2012. The effect of riparian zones on species diversity of frogs in Amazonian forest. Copeia, 2012(3): 375–381.

Ricklefs, R.E. 2004. A comprehensive framework for global patterns in biodiversity. Ecology Letters, 7: 1–15.

Rojas, R.R., Fouquet, A., Ron, S.R., Hernández-Ruz, E.J., Melo-Sampaio, P.R., Chaparro, J.C., Vogt, R.C., Carvalho, V.T., Pinheiro, L.C., Avila, R.W., Farias, I.P., Gordo, M. e Hrbek, T. 2018. A Pan-Amazonian species delimitation: high species diversity within the genus *Amazophrynella* (Anura: Bufonidae). PeerJ 6: e4941.

Rojas-Ahumada, D.P., Landeiro, V.L. e Menin, M. 2012. Role of environmental and spatial processes in structuring anuran communities across a tropical rain forest. Austral Ecology, 37: 865–873.

Schietti, J. , Martins, D. , Emilio, T. , Souza, P.F., Levis, C. , Baccaro, F.B., Pinto, J.L., Moulatlet, G.M., Stark, S.C., Sarmento, K. , Araújo, R.N., Costa, F.R., Schöngart, J. , Quesada, C.A., Saleska, S.R., Tomasella, J. , Magnusson, W.E. e Nardoto, G.B. 2016. Forest structure along a 600 km transect of natural disturbances and seasonality gradients in central-southern Amazonia. Journal of Ecology, 104: 1335–1346.

Simões, P.I., Lima, A.P. e Farias, I.P. 2010. The description of a cryptic species related to the pan-Amazonian frog *Allobates femoralis* (Boulenger 1883) (Anura: Aromobatidae). Zootaxa, 2406: 1–28.

Silva, F.R., Almeida-Neto, M., Prado, V.H.M., Haddad, C.F.B. e Rossa-Feres, D.C. 2012. Humidity levels drive reproductive modes and phylogenetic diversity of amphibians in the Brazilian Atlantic Forest. Journal of Biogeography, 39: 1720–1732.

Symula, R., Schulte, R. e Summers, K. 2003. Molecular systematics and phylogeography of Amazonian poison frogs of the genus *Dendrobates*. Molecular Phylogenetics and Evolution, 26: 452–475.

Stuart, S.N., Chanson, J.S., Cox, N.A., Young, B.E., Rodrigues, A.S., Fischman, D.L. e Waller, R.W. 2004. Status and trends of amphibian declines and extinctions worldwide. Science, 306: 1783–1785.

Teixeira, M., Dal Vechio, F., Recoder, R.S., Carnaval, A.C., Strangas, M., Damasceno, R.P., Sena, M.A. e Rodrigues, M.T. 2012. Two new species of marsupial tree-frogs genus *Gastrotheca* Fitzinger, 1843 (Anura, Hemiphractidae) from the Brazilian Atlantic Forest. Zootaxa, 3437: 1–23.

Tsuji-Nishikido, B.M. e Menin, M. 2011. Distribution of frogs in riparian areas of an urban forest fragment in Central Amazonia. Biota Neotropica, 11(2): 63–70.

Venegas, P.J. e Duellman, W.E. 2012. Two syntopic new species of the *Pristimantis orestes* Group (Anura: Strabomantidae) from northwestern Peru. Zootaxa, 3249: 47–59.

Wallace, A.R. 1852. On the monkeys of the Amazon. Proceedings of the Zoological Society of London, 20: 107–110.

Webb, S.D. 1995. Biological implications of the middle Miocene Amazon seaway. Science, 269: 361–362.

Zimmerman, B.L. e Bierregaard, R.O. 1986. Relevance of the equilibrium theory of island biogeography and species area relations to conservation with a case from Amazonia. Journal of Biogeography, 13: 133–143.